Decomposition of Novel Diazosugars:

Effects on Regioselectivity

by

Ashley Marie Malich

Submitted in Partial Fulfillment of the Requirements

for the Degree of

Masters in Science

in the

Chemistry

Program

YOUNGSTOWN STATE UNIVERSITY

August 2008

Decomposition of Novel Diazosugars:
Effects on Regioselectivity

Ashley Marie Malich

I hereby release this thesis to the public. I understand that this thesis will be made available from the OhioLINK ETD Center and the Maag Library Circulation Desk for public access. I also authorize the University or other individuals to make copies of this thesis as needed for scholarly research.

Signature:

_____

Ashley Marie Malich, Student Date

Approvals:

_____

Dr. Peter Norris, Thesis Advisor Date

_____

Dr. John A. Jackson, Committee Member Date

_____

Dr. Michael A. Serra, Committee Member Date

_____

Dr. Peter J. Kasvinsky, Dean of School of Graduate Studies & Research Date

Thesis Abstract

The following work describes the construction and decomposition of azidodeoxy sugars with diazoesters attached. The fate of the projected carbeniod intermediate formed in the presence of a rhodium(II) catalyst resulted in the products of inter- and intramolecular imine formation however, no C-H insertion onto the furanose platform was observed. This research also led to the formation of ketone derivatives and dimeric ethers.

Acknowledgements

I would like to thank Youngstown State University and the School of Graduate Studies for giving me the opportunity to pursue my master's degree in Chemistry. I would like to express my gratitude and appreciation to the entire YSU Chemistry Department, especially Dr. Matthias Zeller, for all of your time and help throughout my years here at YSU.

I would also like to thank Dr. Peter Norris for being my research advisor over the past few years. Your guidance throughout my academic career is greatly appreciated. For being on my thesis committee and also for all your help, I would like to extend a thank you to Dr. John Jackson and Dr. Michael Serra.

My friends and colleagues at YSU, I would like to thank you for making the past two years an experience to remember. You have helped me out so much and made some memories along the way, I can not thank you enough.

A special thank you goes out to my family and friends, especially my mother and grandparents, for everything you have provided me throughout my life. It is because of your constant support, encouragement, and love that I have become the person I am today.

Table of Contents

Title Page……..i

Signature Page…….ii

Abstract……...iii

Acknowledgements…….iv

Table of Contents…….v

List of Figures……vii

Introduction

Natural Products……...……1

Carbohydrates…….…….……4

Glycosides and Branched-chain Sugars……...5

Diazocarbonyl Compounds……..7

Transition Metal-Catalyzed Reactions…….8

Imines…….16

Azides……19

Statement of Problem…….23

Results and Discussion

Furanose Platform……..24

Phenacyl Ester-Substituted Sugars……28

Diazoester-Substituted Sugars……...29

Attempted Decomposition of Diazoester-Substituted Sugars……31

Rhodium(II)-Catalyzed Decomposition of Diazoester Sugars……..32

Experimental……..45

References……..67

Appendix A……73

Appendix B……..129

List of Figures

Figure 1 A chimeric or hybrid benzodiazepine……..2

Figure 2 Naturally occurring α-methylenebis-γ-butyrolactones……2

Figure 3 Plakortones A, B, C, and D……..3

Figure 4 Secosyrin 1 and 2…….3

Figure 5 Mono- and disubstituted xylofuranose…….6

Figure 6 A generic diazo compound……..7

Figure 7 Xylose-derived diazoester……8

Figure 8 Generic carboxamidate and carboxylate dirhodium(II) catalysts……..10

Figure 9 Benzylic insertion product…….15

Figure 10 Carbene dimers……..15

Figure 11 Depiction of a generic imine…….16

Figure 12 Imine-Enamine Tautomerism……16

Figure 13 Depiction of a generic azide……..19

Figure 14 X-Ray crystal structure of **3**……..26

Figure 15 Structure of $Rh_2(OAc)_4$ and $Rh_2(OCCF_3)_4$……33

Figure 16 X-Ray crystal structure of macrocycle **9**……...37

Figure 17 Alternate x-ray crystal structure of macrocycle **9**……..38

Figure 18 X-Ray crystal structure of oxazepine **10**……41

Figure 19 ^{1}H NMR spectrum of **1**……..74

Figure 20 COSY NMR spectrum of **1**……75

Figure 21 ^{13}C NMR spectrum of **1**…….76

Figure 22 HSQC NMR spectrum of **1**……77

Figure 23 Mass spectrum of **1**……78

Figure 24 ^{1}H NMR spectrum of **2**……..79

Figure 25 COSY NMR spectrum of **2**……80

Figure 26 ^{13}C NMR spectrum of **2**……81

Figure 27 HSQC NMR spectrum of **2**……82

Figure 28 Mass spectrum of **2**……83

Figure 29 ^{1}H NMR spectrum of **3**……..84

Figure 30 COSY NMR spectrum of **3**……85

Figure 31 ^{13}C NMR spectrum of **3**……86

Figure 32 HSQC NMR spectrum of **3**……87

Figure 33 Mass spectrum of **3**……88

Figure 34 ^{1}H NMR spectrum of **4**……..89

Figure 35 COSY NMR spectrum of **4**……90

Figure 36 ^{13}C NMR spectrum of **4**……....91

Figure 37 HSQC NMR spectrum of **4**……92

Figure 38 Mass spectrum of **4**……93

Figure 39 ^{1}H NMR spectrum of **5**……..94

Figure 40 COSY NMR spectrum of **5**……95

Figure 41 ^{13}C NMR spectrum of **5**……96

Figure 42 HSQC NMR spectrum of **5**……97

Figure 43 Mass spectrum of **5**……98

Figure 44 ^{1}H NMR spectrum of **6**……..99

Figure 45 COSY NMR spectrum of **6**……..100

Figure 46 ^{13}C NMR spectrum of **6**……...101

Figure 47 HSQC NMR spectrum of **6**……..102

Figure 48 Mass spectrum of **6**……..103

Figure 49 IR spectrum of **6**……...104

Figure 50 ^{1}H NMR spectrum of **7**……105

Figure 51 COSY NMR spectrum of **7**……..106

Figure 52 ^{13}C NMR spectrum of **7**……...107

Figure 53 HSQC NMR spectrum of **7**……..108

Figure 54 Mass spectrum of **7**……..109

Figure 55 ^{1}H NMR spectrum of **8**……110

Figure 56 COSY NMR spectrum of **8**……..111

Figure 57 ^{13}C NMR spectrum of **8**……...112

Figure 58 HSQC NMR spectrum of **8**……..113

Figure 59 Mass spectrum of **8**……..114

Figure 60 ^{1}H NMR spectrum of **9** (original)……115

Figure 61 COSY NMR spectrum of **9** (original)……..116

Figure 62 ^{13}C NMR spectrum of **9** (original)……...117

Figure 63 HSQC NMR spectrum of **9** (original)……..118

Figure 64 Mass spectrum of **9** (original)……..119

Figure 65 ^{1}H NMR spectrum of **9** (possible)……...120

Figure 66 COSY NMR spectrum of **9** (possible)……121

Figure 67 ^{13}C NMR spectrum of **9** (possible)……..122

Figure 68 Mass spectrum of **9** (possible)……123

Figure 69 ^{1}H NMR spectrum of **10**……..124

Figure 70 COSY NMR spectrum of **10**……125

Figure 71 ^{13}C NMR spectrum of **10**……126

Figure 72 HSQC NMR spectrum of **10**……127

Figure 73 Mass spectrum of **10**……128

Figure 74 X-Ray crystal structure of **3**……130

Figure 75 X-Ray crystal structure of **9**……137

Figure 76 Alternate x-ray crystal structure of **9**……...147

Figure 77 X-Ray crystal structure of **10**……...157

Introduction

Natural Products

An ancient science in itself, natural products chemistry encompasses any substance that is created by nature that has some pharmaceutical or biological significance. These structures can be found anywhere from the mold that grows on a tree to the insect that lives in it. Most of these chemical compounds have a complex structure and the intricacies of that structure may not be known. The unknown has sparked the exploration of the total synthesis of these structures harvested from nature.

The structures of interest are usually secondary metabolites but primary metabolites are also important in the synthesis of pharmacologically and biologically significant molecules. Primary metabolites are small molecules involved directly in the growth, development and reproduction of an organism. These small molecules include fats, amino acids, proteins and carbohydrates. Secondary metabolites are more complex structures not directly involved, but act "…as non-nutritional chemicals controlling the biology of other species in the environment."[1]

Macrocycles are often found very often in natural products. These structures are comprised of many functional groups allowing for the investigation into substructures that may be more potent. A chimeric or hybrid benzodiazepine, shown in Figure 1, is one of many macrocyclic scaffolds derived from carbohydrates. Benzodiazepines are a class of medications that depress the central nervous system to slow it down in order to treat conditions such as anxiety, insomnia and other related psychological disorders. Variations of this structure allow for investigation into the active receptor space in the central nervous system. [2]

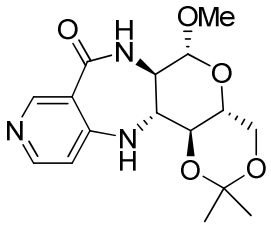

Figure 1: A chimeric or hybrid benzodiazepine.

One characteristic structure of interest is that of two fused furan rings. This type of structure can be found in α-methylenebis-γ-butyrolactones. Found in *Xylaria obovata*, *Penicillium canadense*, and *Sporothrix*, examples of such molecules are shown in Figure 2. The three natural products xylobovide, canadensolide and sporothriolide are sought after because of their phytotoxic, antifungal, and antibacterial properties. Used as a synthetic platform, dimethyl itaconate-anthracene lead to the construction of the two fused furan rings found in this class of natural products.[3] Synthesis of canadensolide has been extensively investigated. The structure was achieved using methods such as radical cyclisation,[4,5] $Cu(TBS)_2$-catalyzed intramolecular cyclopropanation of glycols,[6] iodolactonization followed by treatment with SiO_2/xylene,[7] and a process utilizing an imino-Claisen reaction.[8]

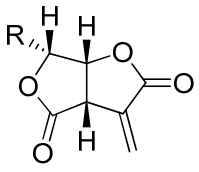

R = C_2H_5 ; Xylobovide
R = *n*-C_4H_9 ; Canadensolide
R = *n*-C_6H_{13} ; Sporothriolide

Figure 2: Naturally occurring α-methylenebis-γ-butyrolactones.

Another class of compounds with two fused furan rings is the plakortones (Figure 3). These secondary metabolites can be isolated from the Caribbean sponges *Plakortis*

halichondrioides and *P. simplex* and contain the 2,6-dioxabicyclo[3.3.0]octan-3-one structural motif. They are of particular interest because of their activating effect on cardiac SR-Ca^{2+}-pumping ATPase which can correct irregularities during cardiac muscle relaxation. The fused furan rings were constructed utilizing a Pd(II)-mediated lactone forming cascade.[9,10]

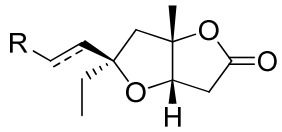

R = Et ; plakortone A/C
R = Me ; plakortone B/D

Figure 3: Plakortones A, B, C, and D.

Secosyrins 1 and 2 are a class of molecules that also contain two furan rings but which are oriented in a *spiro* bicyclic structure as seen in Figure 4. Co-produced with the syringolides, both classes of compounds can be isolated from *Pseudomonas syringae* pv. *tomato*. The biological activity of the secosyrins is unknown, however, they are of interest because of their structural similarities to syringolides, which have a known effect on the hypersensitive response. Synthetic strategies explored for secosyrin formation include the use of $RuCl_3$ catalysis on a protected furan followed by a one-pot deprotection and lactonization with trifluoroacetic anhydride/trifluoroacetic acid. [11,12]

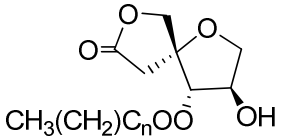

n = 4 ; Secosyrin 1
n = 6 ; Secosyrin 2

Figure 4: Secosyrin 1 and 2.

Years of synthetic investigation into all the above compounds and other natural products has not only "…lead to a better understanding of specific architectural domains but also how the reactive features of a natural product can be harnessed to deliver new classes of therapeutic agents with real-world applicability."[13] Whether or not the desired molecules were constructed, a vast amount of new chemistry has been discovered that inevitably can be used in future natural product syntheses.[13] In order for these natural products to be medically useful, they need to be constructed in a realistic time period at reasonable cost.

Carbohydrates are a useful way to begin synthesizing natural products from an inexpensive source of chirality. Many synthetic methods developed for natural product synthesis from carbohydrates involve cheap protocols that are flexible allowing for further investigation.[14] Retrosynthetic strategies are important when working with carbohydrates because the "sugar" portion is sometimes highly modified. Once evaluated, chiral synthetic intermediates can be built from a sugar.[15]

Carbohydrates

Carbohydrates can be classified into one of three different groups: monosaccharides, oligosaccharides, and polysaccharides. These three groups of organic structures are used to store and transport energy. Carbohydrates are actually the most abundant organic molecules and they are found in nature in everything from plants to human blood. The three main groups of carbohydrates are based on the number of carbohydrate units present.[16]

A simple carbohydrate has the empirical formula $C_n(H_2O)_n$. A monosaccharide is a single carbohydrate unit and the single units can either form an aldose or a ketose; an aldose contains an aldehyde functional group and a ketose has a ketone functional group. These chiral molecules can also take on either a D or L configuration; in a Fischer projection the second to last OH in the chain is either to the right or left, respectively. Depending on the situation, a monosaccharide unit can take on a cyclic or acyclic structure and protecting groups can be used to lock the configuration of the unit in a specific orientation. When these single units are linked together, an oligosaccharide (2-10 units) or a polysaccharide (10 or more units) is formed.[16]

Glycosides and Branched-chain Sugars

Two carbohydrate derivatives found in nature are branched-chain sugars and glycosides. Branched-chain sugars occur when a carbohydrate has a carbon substituent attached at a non-terminal carbon; glycosides are formed when a non-carbohydrate group is attached to the anomeric carbon. Depending on whether a –CR, –OR, –NR, or –SR group is attached the structure is named a *C*-, *O*-, *N*-, or *S*-glycoside.[17]

Branched-chain sugars can be constructed through many methods. The most commonly used methods involve Grignard reagents, opening of epoxides, 1,4-conjugate addition, radical chemistry, and the Wittig reaction. While synthesizing these structures, other reactive sites on the sugar must be blocked with protecting groups. Two frequently used protecting groups are the acetate and isopropylidene groups; the latter being very useful because they can protect two hydroxyls at once.[18]

D-Xylose can potentially be used as a starting material to form a branched-chain sugar. In order to utilize its structural features, some of the alcohols must be protected with the protecting group of choice being the isopropylidene group. Two locations exist on the xylose structure for an isopropylidene group to be attached and the acid-catalyzed reaction with acetone tends to give either a mono or a disubstituted product (Figure 5); the disubstituted product is protected at the 1,2-OH groups and the 5,6-OH groups whereas the monosubstituted product only has the 1,2-OH groups protected. [18]

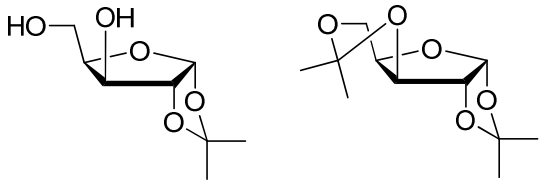

Figure 5: mono- and disubstituted xylofuranose

Isopropylidene groups have been found to be efficiently introduced into carbohydrates structures using acetone and sulfuric acid. D-Glucofuranose is protected with isopropylidene groups in a procedure beginning with the addition of a small amount of sulfuric acid to D-glucose in acetone solution. After reaction for about 5 hours, the solution was neutralized by the addition of 50% sodium hydroxide solution followed by addition of solid sodium hydrogen carbonate. After filtration, solvent removal, and an extraction with water, the mono and disubstituted products were isolated. It was also found that the disubstituted product could then be converted to the mono substituted product by using fractional distillation. [18]

During protection of xylose at the 1,2-OH groups complications arise using a similar procedure as described for D-glucose. After working through the problems, a one-

pot synthesis of 1,2-*O*-isopropylidene-α-D-xylofuranose was devised that resulted in high yields. It was found that by using finely ground xylose and only letting the mixture of acetone and sulfuric acid stir for roughly 30 mintues before neutralization the reaction was more successful. Neutralization was done in a two-step procedure to allow for the hydrolysis of the unwanted O5-O6 protecting group. First a 1.1 M solution of sodium carbonate was added and after 2.5 hours of vigorous stirring in an ice bath, the solution was neutralized completely with solid sodium carbonate and left to stir overnight. The monosubstituted product was successfully recrystallized from ethyl acetate-light petroleum but only after gravity filtration, purification through a silica gel filter, and crystallization from a 30:1 chloroform-methanol solution.[19]

Diazocarbonyl Compounds

A diazo compound consists of two nitrogen atoms double bonded to each other with one nitrogen also double bonded to a carbon (Figure 6). The generic formula of this structure is $R_2C{=}N_2$. The central nitrogen possesses a positive charge while a negative charge is distributed between the carbon and the terminal nitrogen. Two compounds more stable than a simple diazo group are α-diazoketones and α-diazoesters because of their ability to delocalize the negative charge into the carbonyl.[20]

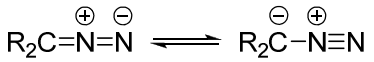

Figure 6: A generic diazo compound.

Diazo compounds can be synthesized in a two-step procedure. The first step involves the introduction of a carbonyl group to the starting material, which can be done

using benzoic acid, for example, and DCC (dicyclohexylcarboimide). Next, the diazo group can be transferred to the structure using TsN_3/MsN_3[21] or *p*-acetamido-benzenesulfonyl azide[22] and a base such as triethylamine. Beginning with a protected D-xylose, the resulting structure would be that in Figure 7.

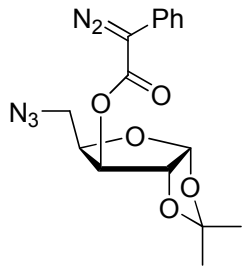

Figure 7: Xylose-derived diazoester.

Transition Metal-Catalyzed Reactions

Decomposition of diazo compounds can be accomplished using transition metal catalysts. These reactions form a metal-stabilized carbene after the displacement of N_2 and regeneration of the catalyst; the electrophilic carbene can be transferred to an electron-rich substrate (S:) (Scheme 1).[23] This substrate can be either a double bond, single bond C-H, N-H, O-H, carbonyl group, etc.[23,24] Carbenoid insertion reactions can either be intermolecular or intramolecular, however, the current research is more concerned with intramolecular reactions following decomposition of diazo compounds.

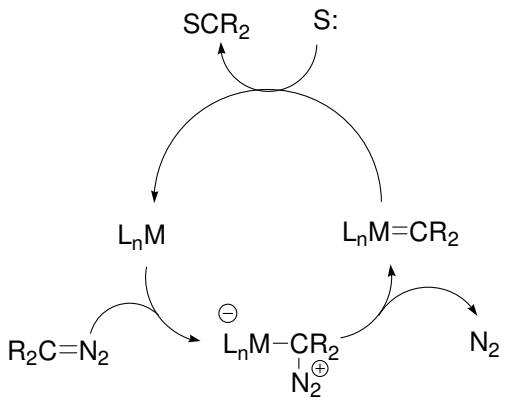

Scheme 1: Metal-catalyzed diazo decomposition cycle.[23]

Different transition metals can be used to catalyze decomposition reactions of diazo compounds. Copper, palladium, zinc, and rhodium catalysts are among the transition metals commonly used in decomposition reactions. Our research focuses on the use of the rhodium(II)-catalyzed reactions. The most common form of rhodium(II) is the diamagnetic dimers of Rh-Rh.[25,26] A large variety of bridging ligands can be attached to the central Rh-Rh to form numerous dirhodium species and these dirhodium catalysts are of interest because of their ability to better control the reactivity and selectivity of the decomposition of the diazo compounds. The reactions mediated by these structures are also able to proceed under mild conditions compared to those of other transition metal catalysts. Overall, the Rh catalyst, the substrate structure, and the functional group in the α position play a role in the regio- and stereoselectivites of the decomposition of a diazo compound.[26,27]

Two major groups of dirhodium(II) catalyst complexes exist depending on the ligands to which they are bridged, namely carboxylate or carboxamidate ligands (Figure 8). Dirhodium(II) tetraacetate, $Rh_2(OAc)_4$, is the parent catalyst of all the others. This structure leaves one vacant site on each metal for carbene attachment after the four

bridging acetate ligands are attached. When the four bridging acetates are replaced with various carboxylate or carboxamidate ligands, a wide range of unique catalysts can be formed. The carboxamidates have a higher degree of asymmetric induction because of the closer proximity of the axial carbene centrer due to the nitrogen's adjacent stereogenic center. By varying these ligands, the dirhodium catalyst systems can be designed to promote a specific reactivity and selectivity.[26,28]

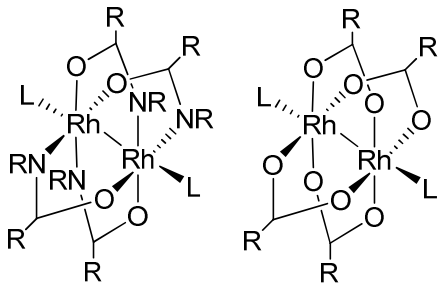

Figure 8: Generic carboxamidate and carboxylate dirhodium(II) catalysts.

Reports describing reactivity and stereoselectivity in catalytic cyclopropanation were also expected to apply to C-H insertion reactions. A trend observed showed decreased reactivity and increased selectivity as electron withdrawal by the dirhodium (II) ligands decreased. This was supported by research focusing on just those characteristics using rhodium perfluorobutyrate, rhodium acetate, and either rhodium acetamide or rhodium prolactam. Rhodium perfluorobutyrate has the greatest electron withdrawal ability then rhodium acetate followed by rhodium acetamide and rhodium prolactam. Diazoacetoacetates were decomposed using all of these rhodium catalysts in CH_2Cl_2 and the said trend was observed. A mechanism was presented depicting the rationale behind these C-H insertion processes (Scheme 2).[29]

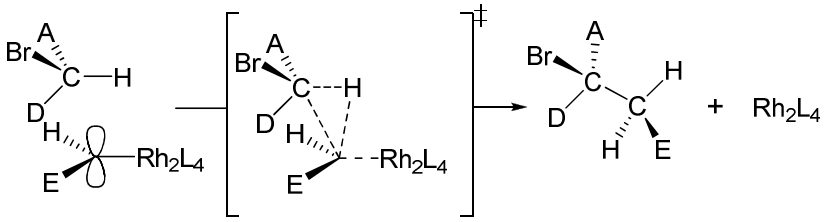

Scheme 2: Interaction between metal catalyst and substrate.

The effect caused by electron-withdrawing ligands is attributed to the simultaneous changing of the Rh-Rh bond length. If a ligand is more electron-donating the Rh-Rh bond shortens; electron-withdrawal by ligands increases the bond length. Axial ligands also affect this specific bond length. When water was attached axially, the bond length was longer than when methanol was in that position.[23] It has been seen that the more electron-deficient ligands of the rhodium carboxylates showed higher activity and therefore higher yields.[30]

Steric factors in the ligands can also influence the selectivity and reactivity of the decomposition. The usual trend for reactivity in a C-H insertion site is methane > methylene > methyl, however, when different catalysts are employed, the insertion site differs accordingly because of the steric environment of the ligands. In the reaction of a diazoester with rhodium tetraacetate, insertion led to the formation of a five-membered ring or a four-membered ring in a 2:1 ratio. When the same substrate was decomposed in the presence of rhodium triphenylacetate, the insertion lead mainly to the four-membered ring. The reaction can be seen in Equation 1.[23]

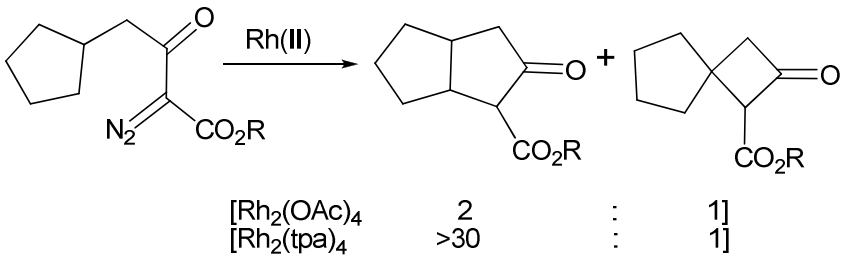

Equation 1.

When a diazo ester was decomposed in the presence of 2-propanol, different Rh(II) catalysts and different transition metal catalysts were used to determine if there was an effect on the reaction. The highest yields were obtained when rhodium(II) acetate was used as the catalyst. Some of the other catalysts needed heat to aid in formation of any product at all. This was key evidence that the metal was involved in the stage of O-H insertion. When trying to proceed with intermolecular O-H insertions it was found that using anything other than dichloromethane as a solvent led to an increase in side reactions and no improvement of the reaction. Temperature was also varied and this actually decreased the diastereoselectivity. [28]

In more of a "green" approach, a decomposition reaction of a diazo compound was performed using water or a wet solvent system. The results were also compared to a reaction done without a catalyst in water. The outcomes were quite different. It was found that N-H insertion occurred in the presence of a Rh(II) catalyst in water with heat while the reaction in only water with heat provided the alcohol product (Scheme 3). When the Rh(II)-catalyzed reaction was done in the presence of dry $CDCl_3$ and THF, the substrate and catalyst were not completely dissolved at room temperature which could eventually limit the reaction. At room temperature, the substrate and catalyst were soluble

in water. The fastest reaction turned out to be in wet $CDCl_3$. It is thought that the water molecules are involved in a step of the mechanism where the labile axial ligand of $Rh_2(OAc)_4$ is replaced by the water. This interaction makes the catalyst more reactive due to either the more labile Rh-ligand bond or the increased stability of an intermediate during the diazo attack.[27]

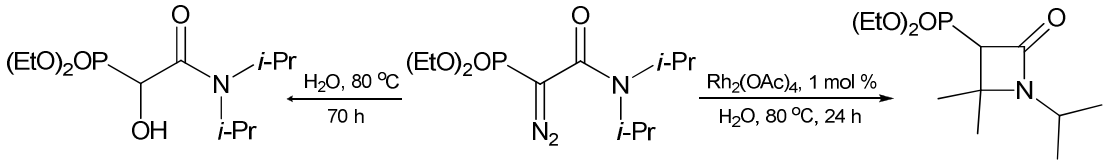

Scheme 3.

In the presence of water, if the alcohol product predominates, changing the catalyst to one with more hydrophobic character increases C-H insertion instead of the O-H insertion. When this was done to prevent the presence of water near the reacting metallocarbenoid, C-H insertion did predominate when the substrate was hydrophobic also. Water not only is more a environmentally friendly solvent but allows for the recovery of the Rh(II) catalyst used. It has been found that once recovered the catalyst can be used in subsequent reactions.[27]

The solvent does have a significant effect on the reaction products and this will vary in each reaction. Solvent choice goes along with Rh(II) ligand choice. It was observed that more polar solvents were needed for product formation if polar intermediates occurred. Equation 2 shows the product formation from the reaction of the two substrates in the presence of a rhodium(II) catalyst in a polar solvent. When the solvent was changed to a nonpolar solvent, product formation was suppressed completely.[23]

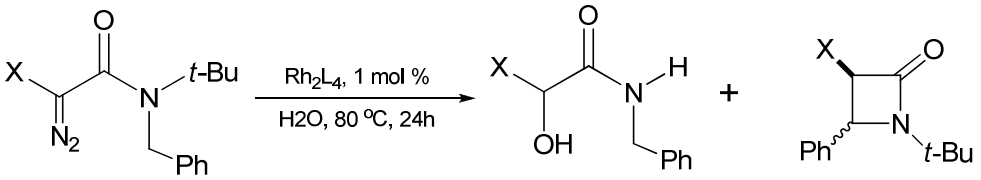

Equation 2.

Overall, any structural changes to a substrate will induce some type of effect on the chemistry that follows a decomposition reaction involving a Rh(II) catalyst. The structural changes could range from chirality to substituent characteristics. Substituent characteristics that have been seen to affect the insertion sites of these decompositions include their electron-donation or withdrawal and their size.[29,31,32]

During the decomposition of diazoamides, the *N*-bis(trimethylsilyl)methyl group was able to guide the site of insertion. The stereochemistry directed the carbene C-H insertion to form a five-membered ring instead of a four-membered ring by inserting β to the N instead of α. If a hexyl ring was attached to the *N*-BTMM group, insertion was favored at the secondary C-H of the cyclohexyl ring instead of the tertiary C-H of the cyclohexyl ring. It was further seen that if an electron-withdrawing carbalkoxy group with the original insertion site α, the site is deactivated and insertion occurs at the β position.[31]

When a D-glucopyranose structure was used in a diazo decomposition unexpected results occurred. The glucose was protected at the anomeric carbon by a (trimethylsilyl)ethyl group and all but the OH on C6 were benzyl-protected. In the presence of $Rh_2(OAc)_4$ catalyst benzylic insertion occurred (Figure 9). The reaction was tried again but instead of benzyl protection of the hydroxyls, methoxy protecting groups were used. Again using $Rh_2(OAc)_4$, diazo decomposition was attempted but resulted in carbene dimers (Figure 10). Results of this nature show that the structure of the substrate

did not favor C-H insertion because of geometrical constraints. In most cases C-H insertion takes place into a tertiary C-H bond and at a C-H bond activated by an oxygen substituent while favoring the formation of a five-membered ring.[29,32]

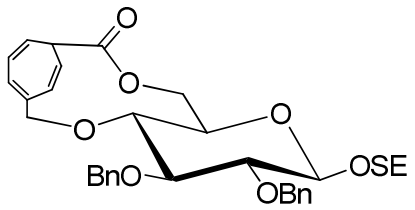

Figure 9: Benzylic insertion product.

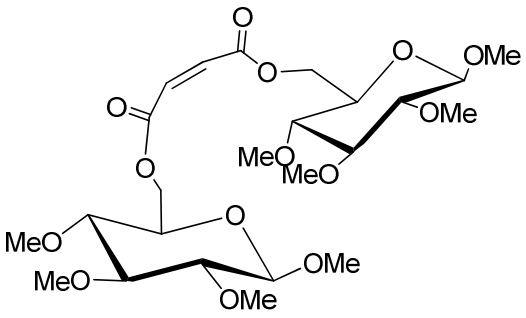

Figure 10: Carbene dimers.

In another case, when decomposing the diazoester of 1,2;5,6-di-*O*-isopropylidene-D-glucofuranose, formation of a five-membered ring was the favorable process. The reaction was done with a $Rh_2(OAc)_4$ catalyst in CH_2Cl_2 solution. Dissolved in CH_2Cl_2, the diazoester was added to the catalyst solution slowly and, upon completion of the reaction, insertion proved (by NMR) to be at the C-2-H bond forming a five-membered ring (Equation 3).[33]

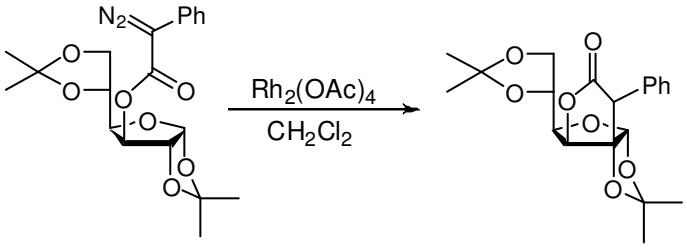

Equation 3.

Imines

An imine is a functional group used frequently in biological chemistry as a means of association between two species, aiding in the transformation of substrates during biological processes. Imines are characterized by the chemical formula $R_2C{=}NR$ and a generic depiction can be seen in Figure 11. This reactive group can exist as either a primary/secondary ketimine or a primary/secondary aldimine.[34]

$$R_2CH{-}CR{=}NR$$

Figure 11: Depiction of a generic imine.

One of the distinct characteristics that make imines important in synthetic chemistry is its participation in the phenomenon of tautomerism, which is essentially a proton shift from one atom to another thereby changing the structure. Imines tautomerize to the enamine form, (Figure 12), with the equilibrium usually lying in favor of the imine form. The basic structure of the imine fundamentally decides the equilibrium because enamines need hydrogen present on the nitrogen for the actual proton shift to occur. [35,36]

$$R_2CH{-}CR{=}NR \rightleftharpoons R_2C{=}CR{-}NHR$$

Figure 12: Imine-Enamine Tautomerism.

One of the traditional methods for synthesizing imines is the addition of a primary amine to an aldehyde or a ketone. Through this basic reaction one equivalent of water is lost after the formation of a hemiaminal (Scheme 4). Aldehydes usually react faster under lower temperature conditions while ketones usually require higher temperatures and longer reaction times. The results of imination starting with aldehydes also gives less byproducts than a ketone. Side reactions such as 1,4-additions and aldol condensations are contingent on the prolonged time period and/or the presence of water. Another factor affecting the outcome of imine formation is whether the amine is aliphatic or aromatic.[34,37]

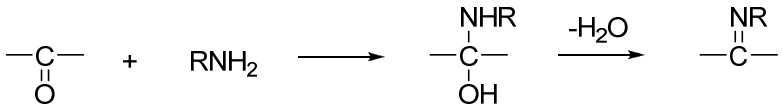

Scheme 4.

Stable imines are formed when the amine is aromatic, resulting in a structure usually referred to as a Schiff base. Love presented an efficient way to produce some of these imines that are sterically hindered (Equation 4).[38] The amine was added in slight excess to benzophenone, then a catalytic amount of concentrated sulfuric acid was also added. After the addition of tetraethyl orthosillicate ($Si(OEt)_4$), the mixture was then heated at 160 °C overnight.[38]

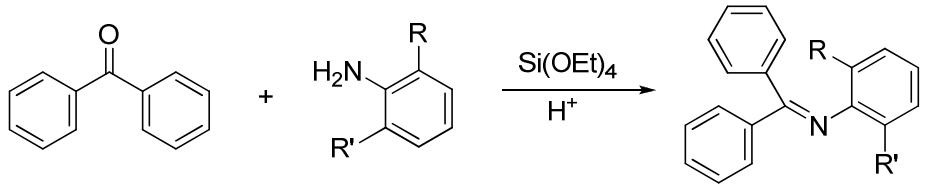

Equation 4.

When the two functionalities needed to form an imine are found on the same structure, a cycle is formed. Similar to that of sugars, ring-chain tautomerism is seen in molecules that contain both an aldehyde and an amine (Equation 5). This type of proton shift requires much more vigourous conditions than normal. Catalysis is usually applied by means of strong acid/base and thermal or photochemical energy. The oxidation state of the amine in effect determines whether an imine can be formed.[39,40]

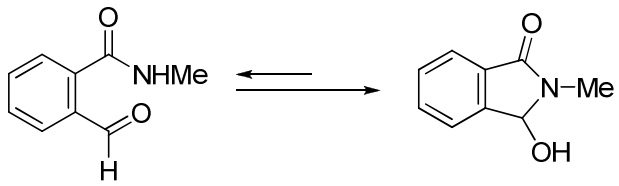

Equation 5.

In the Friedlander Quinolone Synthesis, another bicyclic structure is formed from a slightly different starting materials. Shown in Equation 6, Varala *et al.* found that the most efficient catalysis employs 5 mol-% $Nd(NO_3)_3 \cdot 6\ H_20$ in ethanol. After reacting at room temperature for 10 hours, a quinoline resulted. Quinolines have a wide use as scaffolds in medicinal chemistry.[41]

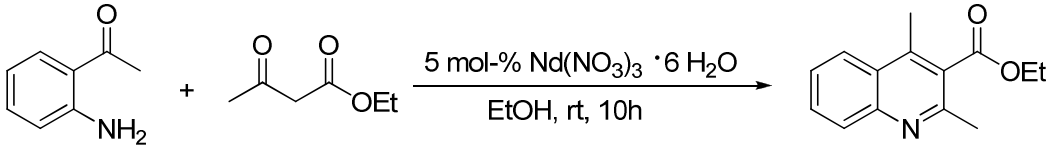

Equation 6 .

Imines can also be formed from the thermolysis of alkyl azides (Scheme 5). It is not certain that the intermediate is formed in all cases, but it has been concluded that in a large number of cases a nitrene is generated from the loss of nitrogen gas. Another

proposal suggested that the R-group migration and nitrogen elimination is a concerted process. Essentially, this reaction proceeds by the loss of nitrogen followed by a rearrangement to form the corresponding imine.[42]

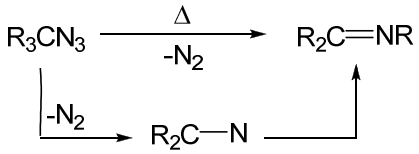

Scheme 5.

Azides

Azides have been used in organic chemistry for numerous reasons from linkage sites to inducing regio-effects. The general chemical formula is R-N_3 where the central nitrogen atom has a formal positive charge and the first and third nitrogen atoms have a negative charge distributed between them (Figure 13).[43]

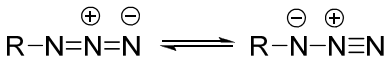

Figure 13: Depiction of a generic azide.

Applications of azides include use as protecting groups, as substrates within biologically active compounds, and as intermediates in natural product synthesis. Using azides as protecting groups is beneficial because of their stability towards organometallic catalysts. Azide derivatives of certain medications, such as COX-2 inhibitors, tend to exhibit similar behavior but are more potent than the original structure.[44]

The dipolar character makes the azido group capable of reacting in numerous ways. At the azide terminus, nucleophiles can attack whereas electrophiles can attack at the α-nitrogen atom. When there is a polarophile, azides can participate in 1,3-dipolar

cycloadditions. Decomposition of this functional group can produce nitrenes, while reduction of an azide can lead to an amine.[44]

One of the principle methods for synthesizing azides involves an S_N2 reaction. During the reaction, a halide or sulfonate group is replaced by the azide functional group. In one example of azide synthesis, 2,3,4-tri-*O*-acetyl-α-D-glucopyranosyl bromide is reacted with sodium azide in a solution of acetone/water to form a glycosyl azide (Equation 7).[24]

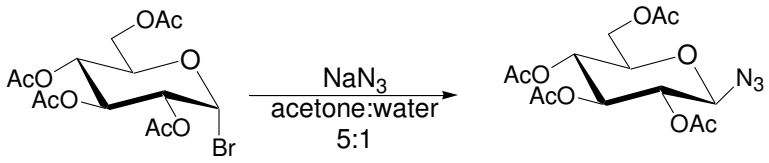

Equation 7.

A related method of preparation of an azide also utilizes an S_N2 reaction. Beginning with xylofuranosyl diol, OH-5 was tosylated with TsCl in pyridine at 0 °C. The carbohydrate was further reacted in DMF at 90 °C with sodium azide. This reaction, which resulted in an overall yield of 86%, is seen in Equation 8.[45]

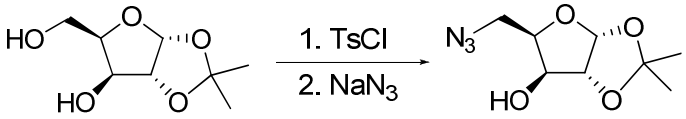

Equation 8.

Once the azide functionality has beed added to a structure, it can be further reacted. The structural properties of the azido group enable it to have some directing and activating effects in substitution, addition, and elimination reactions. Azido groups tend to exhibit a polarizability effect, either electron-donating or electron-withdrawing, depending on the

type of reagent used. Aromatic substitution reactions show a preference for the *ortho* or *para* positions when an azide is present. During nucleophilic addition reactions, the electron-withdrawal by the group tends to predominate thereby activating the attack. When an azido group is present in elimination reactions, there is usually no effect on the product formed.[43]

Decomposition reactions also can be influenced by the substituents attached to the reacting component. An experiment was designed to test the competing effects of a methoxy group and an azido group in a $Rh_2(OAc)_4$ catalyzed decomposition of 1-methyl-1-(diazoacetyl)-cyclohexane. An insertion product α- to the azido group and a related product for insertion α- to the methoxy group were formed in an 8:1 ratio. This ratio was even increased when a $Rh_2(Cap)_4$ catalyst was used to a 30:1 ratio in favor of the insertion site α to the azido group. The outcome in Equation 9 was thought to be to due the electron-withdrawing characteristic of the azide functional group.[46]

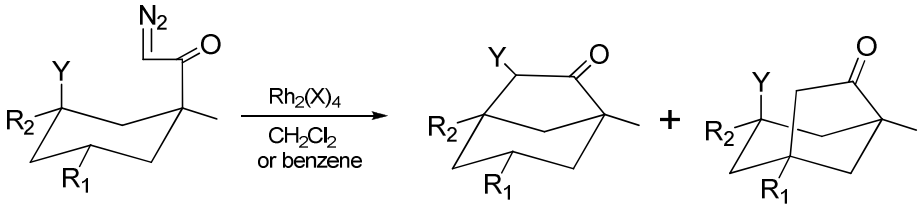

Equation 9.

In the absence of a diazo group, it has been observed that the azide functionality will actually associate with the rhodium catalyst for an intramolecular C-H amination to occur. Different catalysts were explored for use and resulted in yields from 9% to >95%. Among the catalysts used were $Rh_2(OAc)_4$, $Rh_2(O_2CCF_3)_4$, and $Rh_2(O_2CC_3F_7)_4$. Scheme 6

depicts this process and the optimum conditions using a rhodium(II) perfluorobutyrate catalyst at 30-60 °C resulting in >95% yield.[30]

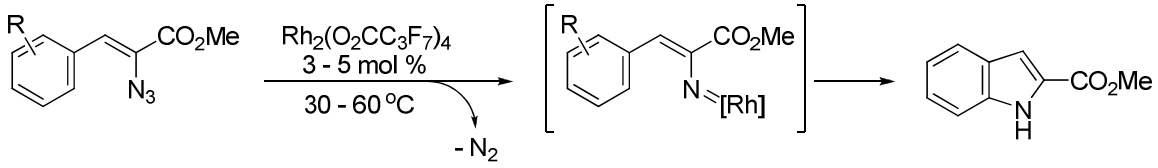

Scheme 6.

Our research focus is on the effects of N_3 on a projected carbenoid intermediate formed in the presence of a rhodium(II) catalyst, including any effects on regioselectivity of C-H insertion chemistry during insertion on a D-xylofuranose platform. Two possible ring structures can be formed but the preference for either site is not yet known. The two insertion sites exist at the carbon α- to the azido group, C5, and the carbon at the second position in the furanose platform, C2. Different catalysts will also be used to further clarify the results.

Statement of Problem

Synthesizing structures that are commonly found in natural products chemistry is a major goal in organic chemistry. Carbohydrates will be used to produce azidodeoxy sugars that potentially can be used to make some of these structures. Azidodeoxy sugars with diazoesters attached will be constructed and then decomposed. The decomposition reaction will be studied to determine the fate of the projected carbenoid intermediate formed in the presence of a rhodium(II) catalyst, including any effects on regioselectivity that the azide group might have on C-H insertion chemistry. NMR and X-ray crystallography will be used extensively to determine product structures.

Results and Discussion

Furanose Platform

Carbohydrates are a good source of synthetic intermediates rich in chirality. These structures contain many hydroxyl groups that tend to be reactive, and in order to better control reactivity later in a reaction scheme, this functionality is protected. The protecting group of choice in this research is the isopropylidene group because it not only protects two hydroxyls at once but does not interfere with subsequent reactions. Often times the protocol for attaching this type of protecting group is fairly easy, involving use of an excess amount of acetone and a catalytic amount of acid.

Beginning with D-(+)-xylose, 1,2-*O*-isopropylidene-α-D-xylofuranose (**1**) was synthesized instead of being purchased from Aldrich since the method used is inexpensive. Once the D-(+)-xylose was fully dissolved in a solution of acetone and concentrated sulfuric acid, it was neutralized first with a 1.1 M Na_2CO_3 solution and then with solid sodium carbonate. After neutralization, TLC indicated the presence of two products, a mono- (**1**) and diacetone-D-xylose (**2**) structure (Equation 10). It was observed that the longer the solution stayed at a lower pH, the more time the reaction has to form the mono-protected xylose structure. Column chromatography (30:1 / $CHCl_3$: MeOH) was used to purify the product mixture and rid it of any unreacted xylose.[19] Extraction of a methylene chloride solution with water was used to separate the two different protected sugars; the more polar monoacetone D-xylose (**1**) was found in the water layer whereas the diacetone-D-xylose (**2**) remained in the organic phase.

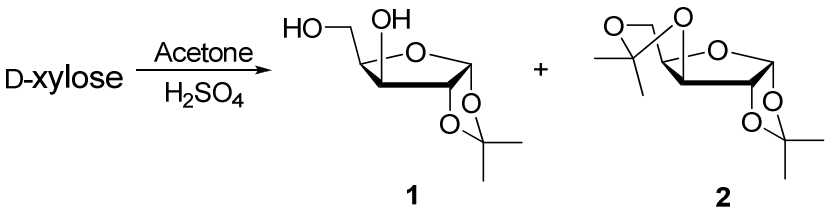

Equation 10.

After a number of successful reactions to obtain 1,2-*O*-isopropylidene-α-D-xylofuranose (**1**), several grams of 1,2;5,6-di-*O*-isopropylidene-α-D-xylofuranose (**2**) accumulated. In order to obtain as much of monoacetone-D-xylose (**1**) as possible, the diacetone-D-xylose (**2**) was reacted in the same conditions to yield more of the desired singly protected sugar (Equation 11). NMR spectra proved that both reactions to form monoacetone-D-xylose were successful. Diacetone-D-xylose showed four singlets, 3 hydrogens per signal, between 1.33 and 1.50 ppm whereas monoacetone-D-xylose only had two singlets, with 3 hydrogens per signal, representing the isopropylidene group now in place at O-1 and O-2.

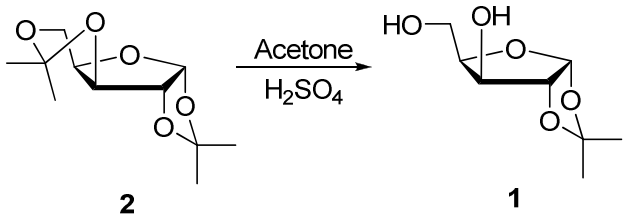

Equation 11.

Once the hydroxyl groups were protected it was time to attach an azido group to C-5. The successful completion of this task was first approached by the introduction of a better leaving group to the primary hydroxyl group. *p*-Toluenesulfonyl chloride was used

in the presence of pyridine to attach a good leaving group, methylbenzenesulfonyl ester, to 1,2-*O*-isopropylidene-α-D-xylofuranose (Equation 12).[45] The presence of two reacting hydroxyls required the use of the lower reaction temperatures of an acetone/ice bath to ensure attachment at only OH-5. Once the reaction was determined complete by TLC, NMR and MS were used to verify the structure. A distinct singlet at 2.45 ppm (3H) and doublets at 7.36 (2H) and 7.80 ppm (2H) corresponded to the tosyl structure in place at C-5; mass spectrometry resulted in a signal at 367.2 corresponding to **3** plus one sodium. A crystal structure was also acquired after crystallization of the white solid during slow evaporation of the compound in $CDCl_3$ resulted in a colorless block, orthorhombic crystal class (Figure 14).

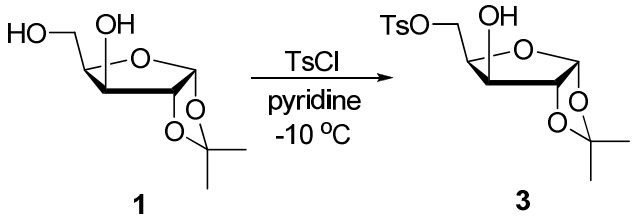

Equation 12.

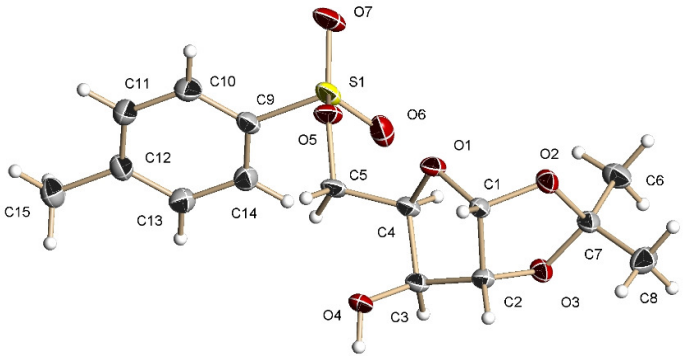

Figure 14: X-Ray crystal structure of 5-*O*-(4-methylbenzenesulfonyl)-1,2-*O*-isopropylidene-α-D-xylofuranose (**3**).

After an aqueous workup, 5-*O*-(4-methylbenzenesulfonyl)-1,2-*O*-isopropylidene-α-D-xylofuranose (**3**) was used without further purification to construct the azide, 5-azidodeoxy-1,2-*O*-isopropylidene-α-D-xylofuranose (**4**).[45] Execution of this S_N2 reaction used an excess of sodium azide in dimethylformamide at 72 °C (Equation 13). Originally 6:1 equivalents of sodium azide were used, however after reaction over night presence of the tosylated sugar was still observed in the NMR and MS spectra. In order to ensure completion overnight, the reaction employed 10:1 equivalents of sodium azide. Further purification via flash column chromatography (3:1 / hexane: ethyl acetate) was still required for retrieval of the pure azidodeoxy sugar (**4**). Mass spectrometry analysis was a little difficult due to the decreased stability of the structure under electron spray ionization; when compound stability was lowered to 30% an accurate signal was observed at 238.3 corresponding to the azidodeoxy sugar (**4**) plus one sodium atom. NMR spectroscopy not only showed the disappearance of the signals corresponding to the methylbenzenesulfonyl ester but now a distinct doublet can be seen at 3.59 ppm for H-5, the α-azido position. A broad singlet at 3.05 ppm is evidence of the single hydroxyl left at C-3 of this furanose platform. Recrystallization of the white solid was attempted but only resulted in the formation of a fibrous solid.

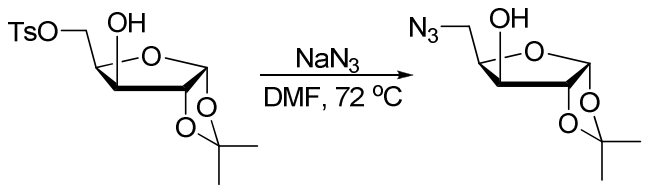

3 **4**

Equation 13.

Phenacyl Ester-Substituted Sugars

With only one reactive hydroxyl left, 5-azidodeoxy-1,2-*O*-isopropylidene-α-D-xylofuranose (**4**) can undergo a Steglich esterification (Equation 14). Generally a Steglich esterification involves reaction of an alcohol with a carboxylic acid in the presence of a catalytic amount of 4-(dimethylamino)pyridine (DMAP) and 1,3-dicyclohexylcarbodiimide (DCC).[24] In order to construct the desired ester, compound (**4**) was reacted with 1.3 equivalents of phenylacetic acid while slowing adding a 1.0 M DCC solution. After completion was determined by TLC, filtration was used to remove the DCC byproduct. Despite these efforts, not all of the byproduct was removed so further purification was required. Flash column chromatography (3:1 / hexane: ethyl acetate) resulted in a pure colorless syrup that was shown to be 3-*O*-(2-phenylacetyl)-5-azidodeoxy-1,2-*O*-isopropylidene-α-D-xylofuranose (**5**).

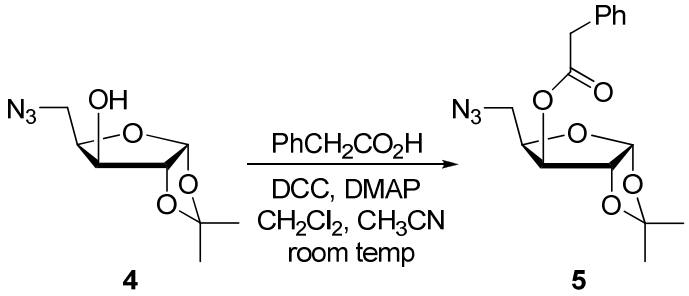

4 **5**

Equation 14.

Despite unsuccessful attempts to crystallize this phenacyl ester, the ^{1}H NMR spectrum substantiated this method for esterification of 5-azidodeoxy-1,2-*O*-isopropylidene-α-D-xylofuranose (**4**). The characteristic singlet at 3.64 ppm corresponds to the two protons of the $–CH_2–$ *alpha* to the carbonyl of the newly formed ester. Esterification at O-3 is also exhibited by the disappearance of the broad singlet belonging

to the OH group that once was previously on the furanose structure. A multiplet in accord with five protons at 7.30 ppm belongs to the hydrogens of the phenyl group of the now attached phenacyl ester.

The carbon-13 spectrum of 3-*O*-(2-phenylacetyl)-5-azidodeoxy-1,2-*O*-isopropylidene-α-D-xylofuranose (**5**) supported the evidence gained from the ^{1}H NMR spectrum. Four signals in the aromatic region, 127-134 ppm, worth a total of 6 carbons agrees with a symmetrical benzene ring. At 41.16 ppm, a single carbon signal appears belonging to the carbon *alpha* to the ester attached at C-3. Downfield at 170.18 ppm, a signal of significantly less intensity is seen for the carbonyl carbon of the phenacyl ester thus constructed.

Diazoester-Substituted Sugars

The next step in our reaction scheme was the transformation of the phenacyl ester (**5**) into a diazocarbonyl compound by utilizing a diazotransfer reaction (Equation 15). Successful execution of diazotransfer was done implementing 1,8-diazobicyclo-[5.4.0]undec-7-ene (DBU) as the base and *p*-acetamidobenzenesulfonyl azide (*p*-ABSA).[22] Upon completion, TLC (3:1 /hexane: ethyl acetate) depicted the presence of several products. The desired diazoester was subsequently found to be the least polar of the products. Purification was accomplished through flash column chromatography using chloroform as the solvent system. This was possible because, although very similar separation was seen compared to that in a 3:1 /hexane: ethyl acetate solution, the reaction mixture was slightly more soluble in chloroform. Formation and purification of the reaction mixture resulted in an orange syrup that could not be crystallized, but which was

identified as, 3-*O*-(2-diazo-2-phenylacetyl)-5-azidodeoxy-1,2-*O*-isopropylidene-α-D-xylofuranose (**6**).

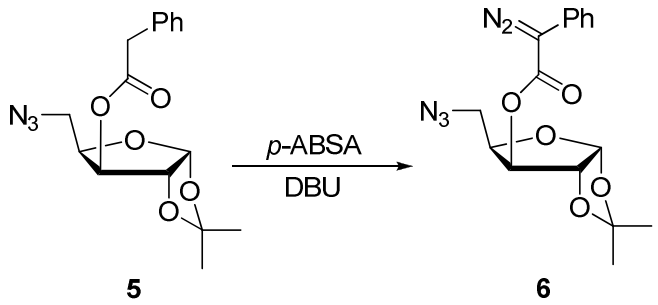

5 **6**

Equation 15.

Proton and carbon spectra of the thick orange syrup deemed the reaction to be successful. The most distinct sign of diazo formation was the disappearance of the 2-H singlet at 3.64 ppm for the position *alpha* the carbonyl where C-N=N now resides. With this reactive group present *alpha* also to the phenyl group, those proton signals are now split into two multiplets at 7.23 and 7.42 ppm accounting for one and four hydrogens, respectively. In the carbon spectrum, diazo formation was indicated by the complete disappearance of the carbon signal originally at 41.16 ppm, that is now the carbon attached to N=N; it has been seen in other diazo compounds that the introduction of a diazo group can correspond with the disappearance of the carbon signal altogether. The structure is still intact with all other signals still at the representative shifts with only a slight shift in the carbonyl signal, which is now more downfield also due to the diazo structure's electronic effect.

The mass spectrum of this diazoester was not as helpful in alluding to successful diazo formation. After careful consideration of the signal corresponding to an *m/z* of

341.3, it was determined that even though compound stability was lowered to 30 % the structure of the diazoester was not stable enough to withstand electron spray ionization. The calculated *m/z* is 588.33, so 341.3 would represent the diazoester without three nitrogen molecules but plus one sodium atom. This is a logical explanation due to the very reactive, unstable nature of both the diazo- and azido- group present on this sugar structure. IR spectroscopy is also proof that both functionalities are present with bands at 2094 and 2254 cm^{-1} corresponding to an azide and diazo, respectively.

Attempted Decomposition of Diazoester-Substituted Sugars

3-*O*-(2-Diazo-2-phenylacetyl)-5-azidodeoxy-1,2-*O*-isopropylidene-α-D-xylofuranose (**6**) is unique in that its overall structure contains not only one nitrogen functionality but two. With both an azido- and diazo-group present, there is the possibility of decomposition in the absence of any catalyst but heat activated. Dissolved in a minimal amount of toluene, the solution of **6** was heated until bubbles/gas evolution was observed. In the first attempt at decomposition the vessel was heated to 105 °C and monitored periodically over 19 hours. The second attempt was only reacted for 2 hours at 90 °C. Both attempts resulted in TLC plates exhibiting five different products. When purified using flash column chromatography with gradient elution (3:1 / hexane: ethyl acetate; ethyl acetate; methanol), the compounds were separated and analyzed *via* NMR spectroscopy, to show no distinguishable product but possible fragments of the diazoester.

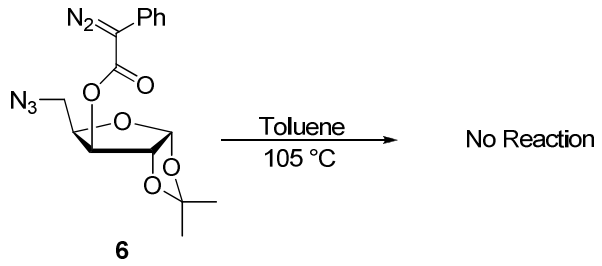

Equation 16.

Another attempt at diazoester decomposition was performed using an inexpensive transition metal catalyst, copper (II) acetylacetonate (Equation 17). Following the slow addition of $Cu(C_5H_7O_2)_2$ solution to a solution of **6** *via* addition funnel over a period of 2.5 hours, TLC (3:1/hexane: ethyl acetate) showed no real sign of reaction after stirring over night. Filtration through a column of Celite removed most of the copper catalyst but still left a crude mixure, which was examined by ^1H NMR to conclude that only unreacted starting material was present.

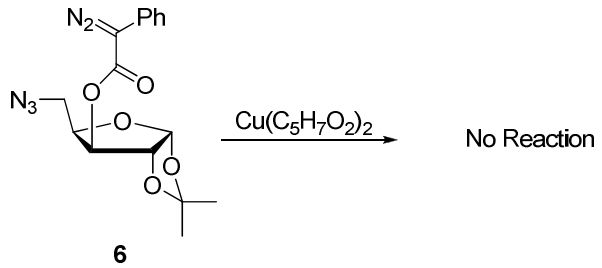

Equation 17.

Rhodium(II)-Catalyzed Decomposition of Diazoester Sugars

Rhodium catalysts are known for aiding in the decomposition reactions of diazoester sugars therefore this area was investigated. Two separate catalysts were used in this investigation: rhodium (II) tetraacetate ($Rh_2(OAc)_4$) and rhodium (II)

tetratriflouroacetate, ($Rh_2(OCCF_3)_4$). Figure 15 illustrates the different ligands present in both catalysts that may play a role in the outcome of the decomposition of 3-*O*-(2-diazo-2-phenylacetyl)-5-azidodeoxy-1,2-*O*-isopropylidene-α-D-xylofuranose (**6**).[23,30]

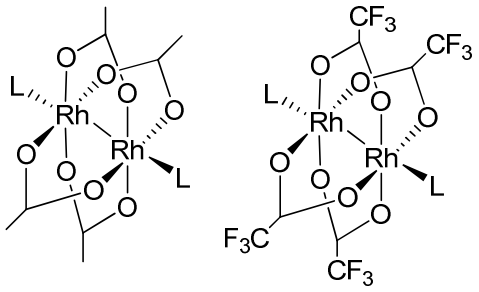

Figure 15: Structure of $Rh_2(OAc)_4$ and $Rh_2(OCCF_3)_4$.

The first attempt at decomposition of 3-*O*-(2-diazo-2-phenylacetyl)-5-azidodeoxy-1,2-*O*-isopropylidene-α-D-xylofuranose (**6**) was in the presence of rhodium (II) tetraacetate under inert conditions (Equation 18). Inert conditions included the use of anhydrous, degassed solvents, flame-dried glassware, solid materials dried on a vacuum pump for at least three days and a nitrogen atmosphere. The rhodium catalyst was dried using a drying pistol on a vacuum pump and P_2O_5 as the dessicant. Despite attempts to rid the reaction vessels of water and oxygen, both played a role in this reaction.

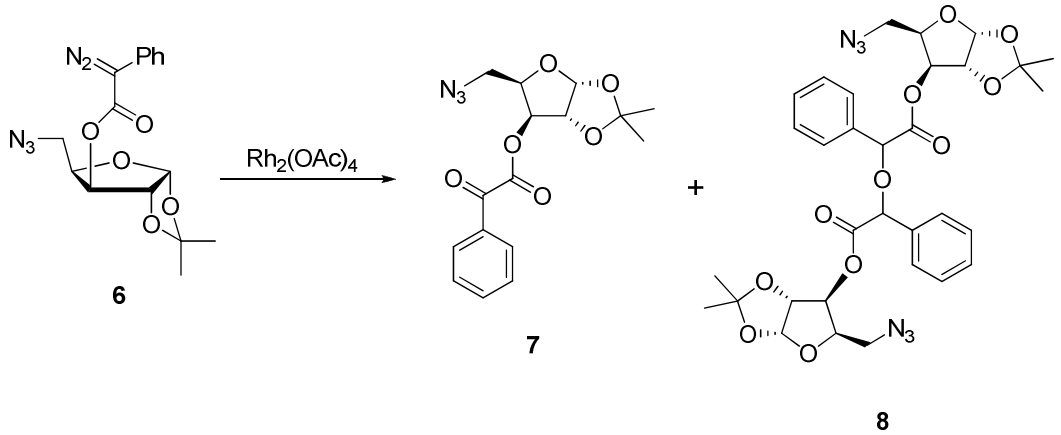

Equation 18.

Reaction setup began by making up two separate dichloromethane solutions of the diazoester (**6**) and the rhodium catalyst, $Rh_2(OAc)_4$. Once prepared, the diazoester (**6**) was added dropwise *via* syringe pump to the vessel under nitrogen atmosphere containing the catalyst. After complete addition, reaction progress was monitored by TLC (3:1 / hexane: ethyl acetate) until the disappearance of starting material. Seven products appeared to be present upon consumption of the diazoester (**6**). Following Celite filtration and flash column chromatography purification with gradient elution (3:1 / hexane: ethyl acetate; ethyl acetate; methanol) only two pure products were isolated cleanly enough for thorough analysis.

The major products isolated were not those resulting from an anticipated insertion reaction (Equation 18). A dimeric ether was formed through the presence of water from the solvent, diazoester, or rhodium (II) catalyst. Oxygen present in the reaction caused the formation of a keto-ester.[24] Niether of these products were crystallized however careful NMR and MS analysis proved the composition of both structures.

The dimeric ether's structure was not immediately obvious from the ^{1}H NMR spectrum, but was determined after mass spectrometry evaluation of the signal 703.6 *m/z*. Along with a mass about twice that of the diazoester, accounts of water interaction to form dimeric ethers seen during previous work in this area alluded to this possibility. The proton spectrum was very similar to that of the diazoester (**6**) but the ^{13}C NMR spectrum displayed two fewer signals than expected. This could be explained by the newly formed ether linkage between two molecules of diazoester-derived carbnoid. The two signals that appear to be absent from the spectra correspond to the carbonyl and the carbon *alpha* to the ester and ether.

Previous work in this area also found interaction of oxygen with the intermediate carbenoid to form a keto-ester.[24] The first sign of ketone formation was the appearance of more resolved and split multiplets corresponding to the phenyl ring protons; these signals now appeared as three separate multiplets at 7.55, 7.70, and 8.02 ppm, representing 2, 1, and 2 hydrogens, respectively. Carbon spectral analysis was very useful in supporting the structure of this product. There were now two signals downfield with significantly lower intensity than the rest; the signal at 162.30 ppm is typical of an ester carbonyl carbon and 184.87 ppm is representative of a ketone carbonyl carbon.

With side reactions occurring because of the presence of water and oxygen, a more controlled, inert atmosphere was desired. This controlled inert atmosphere was achieved by using a fully automated glove box. All solvents placed in the glovebox were anhydrous from the supplier and degassed before transferred to an appropriate container. Any solid material introduced to this environment was dried on a vacuum pump for at least five days as previously done unless sealed at the supplier. Oxygen and water levels were recorded at the start of each new reaction. Reaction setup was the same as previously done and still included the dropwise addition of the diazoester (**6**) solution at a rate of 1.00 mL/hour *via* syringe pump to the solution of rhodium (II) catalyst. The use of TLC to monitor reaction progress was used only when the reaction vessel was removed from this contained environment after adequate reaction time.

The first reaction performed in the inert atmosphere of the glove box was the decomposition of 3-*O*-(2-diazo-2-phenylacetyl)-5-azidodeoxy-1,2-*O*-isopropylidene-α-D-xylofuranose (**6**) in the presence of rhodium (II) tetraacetate catalyst (Equation 19). Overall it was determined that three products, a macrocycle (**9**), an oxazepine (**10**), and a

keto-ester (**7**), can be formed from this reaction however this was not the original observation.

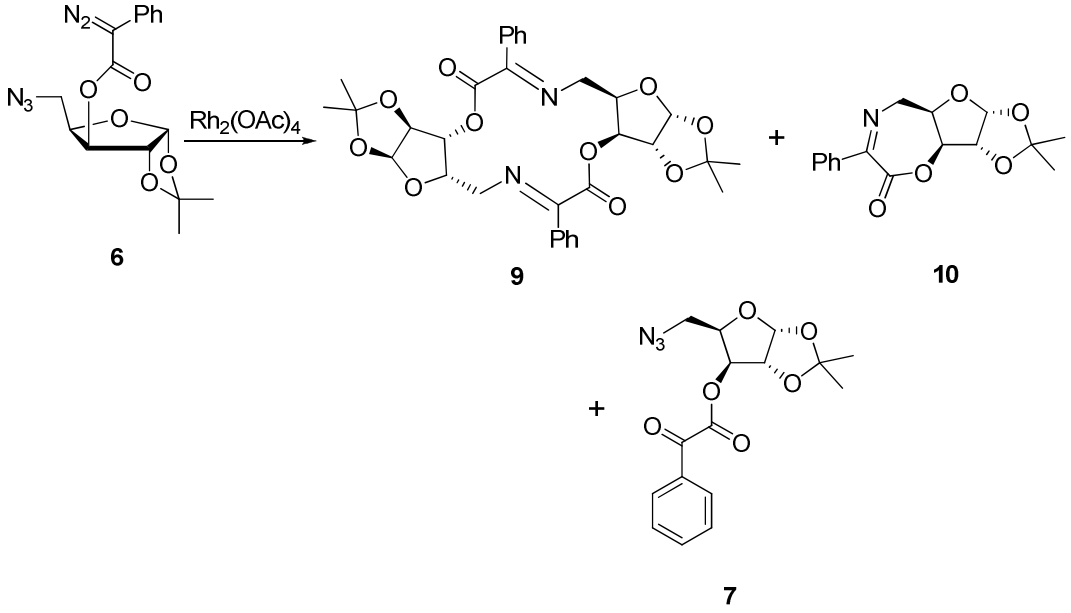

Equation 19.

Macrocycle **9** was the first product isolated from the reaction mixture in yields up to 2.68% due to crystallization during slow evaporation of a hexane/ethyl acetate solution. Different attempts at this reaction produced two slightly different packing patterns for the macrocycle structure. The first crystal structure was obtained from a colorless plate that belonged to the monoclinic crystal system (Figure 15). Unit cell dimensions were as follows: a = 12.2470(16) Å, $\alpha = 90°$; b = 8.9617(12) Å, $\beta = 92.672(2)°$; c = 13.4118(17) Å, $\gamma = 90°$. A second crystal structure was obtained from a colourless block of the same crystal system (Figure 16). This time the unit cell dimensions varied slightly but only in the *y* direction: a = 12.4039(12) Å, $\alpha = 90°$; b = 9.5046(9) Å, $\beta = 95.238(2)°$; c = 12.4401(11) Å, $\gamma = 90°$. Regardless of the packing pattern, this 14-membered macrocycle

is actually observed to be symmetrical possessing a C_2v axis and belongs to space group $P2_1$.

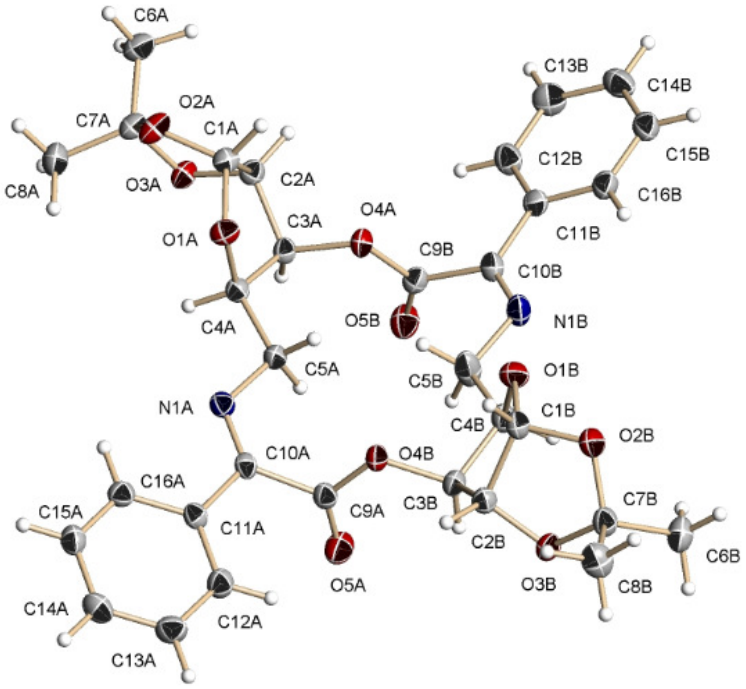

Figure 16: X-Ray crystal structure of macrocycle **9**.

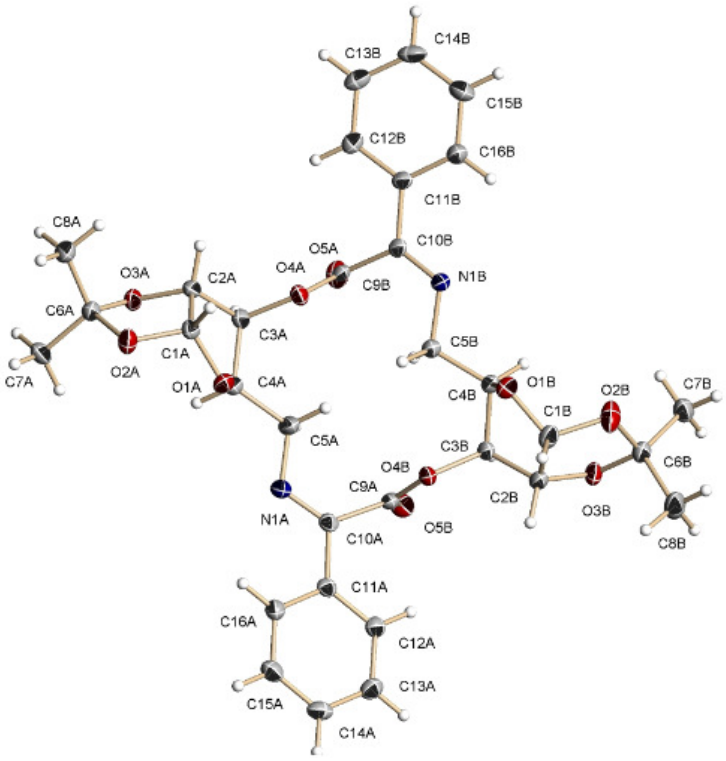

Figure 17: Alternate x-ray crystal structure of macrocycle **9**.

The ^{1}H NMR spectrum of this macrocycle was not very conclusive by itself in the structural identification of **9**. Overall the signals were very similar to that of the diazoester just shifted downfield about 0.5 ppm on average. The most distinct differences in the proton spectrum of the macrocycle were the more resolved diastereotopic protons attached to C-5 and the downfield shifted signals for H-3. Two doublet of doublets at 3.87 and 3.96 ppm pertain to the two H-5 protons. The proton signal for H-3 was now shifted to 5.73 ppm while the H-4 doublet of doublet of doublets proton signal was more downfield at 4.97 ppm.

It was discovered later on in this investigation that a second conformational isomer may exist for macrocycle **9**. The ^{1}H spectrum showed some significant differences not

only with the spectrum originally obtained for the macrocycle but also with that belonging to diazoester **6**. Diastereotopic protons on C-5 now possessed quite different shifts at 3.48 and 3.92 ppm and H-3 was found shifted upfield to 4.11 ppm. The proton on C-4 was also found in a new location at 4.18 ppm but was still observed as a doublet of doublet of doublets.

The difference in the two ^{1}H NMR spectra for the same compound is not yet fully understood but two different orientations of the large ring structure is believed to be a contributing factor. A lot of times structures can take on quite different orientations in solution compared to solid state, and with two different crystal patterns known, a second orientation is thought to exist with a large energy barrier to go back to the original orientation. Mass spectral analysis agree suggesting both samples are the same compound, 606.1 and 677.3 for the original macrocycle and the alternate macrocycle plus 3 sodium atoms, respectively. The possibility of sample decomposition was considered but with no actual melting point, it is unlikely that a structure that only decomposes at 158 °C would degrade over a few months.

Despite distinct differences in the two proton spectra of this macrocycle (**9**), ^{13}C NMR spectra show an additional carbon signal in accord with the –C=N– carbon. As might be expected, the shifts for –COO were different in both samples. In the first sample's spectrum, 161.66 and 164.37 ppm were the locations for of –COO and –C=N–, respectively. The alternate macrocycle sample displayed signals for –COO at 186.66 ppm and –C=N–at 163.36 ppm. These peaks are of characteristicly lower intensity than the rest, a trend observed with structures of this nature.

The oxazepine **10** formed during decomposition was only isolated in pure form after reaction of 3-*O*-(2-diazo-2-phenylacetyl)-5-azido-1,2-*O*-isopropylidene-α-D-xylofuranose in the presence of a different catalyst, $Rh_2(OCCF_3)_4$ (Equation 20). This catalyst also allowed the formation of the macrocycle **9**, oxazepine **10**, and keto-ester **7**. Pure crystals of oxazepine **10** were collected after crystallization by slow evaporation from a solution of hexane / ethyl acetate (Figure 17). The yellow block belongs to the monoclinic crystal system and possesses P1 space group characteristics. Somewhat similar in structure to the macrocycle **9** by NMR, this intramolecular product is not as symmetrical and appears to be structurally more strained than the macrocycle.

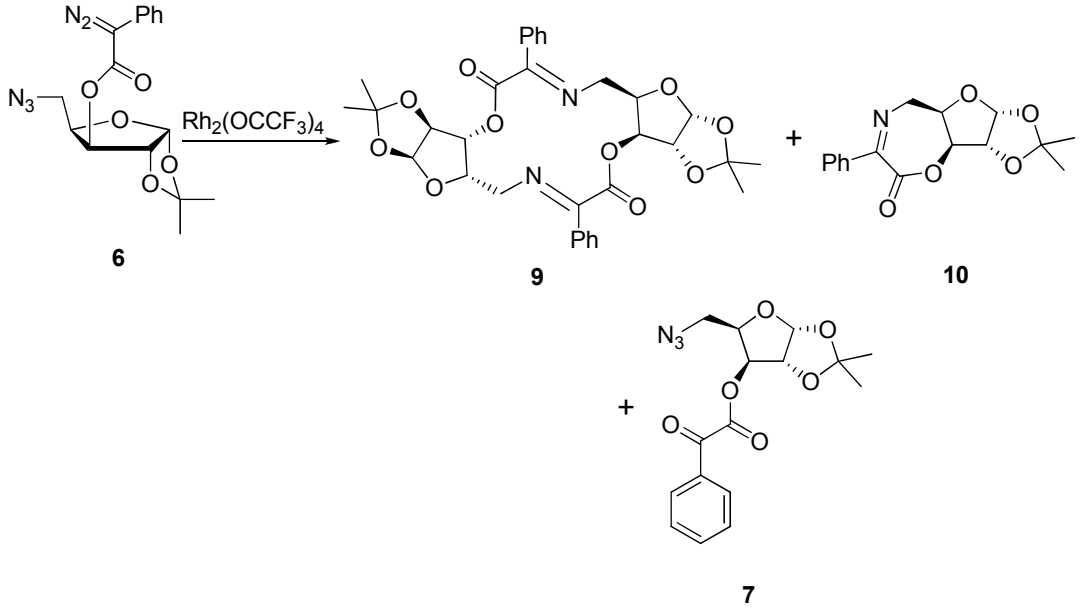

Equation 20.

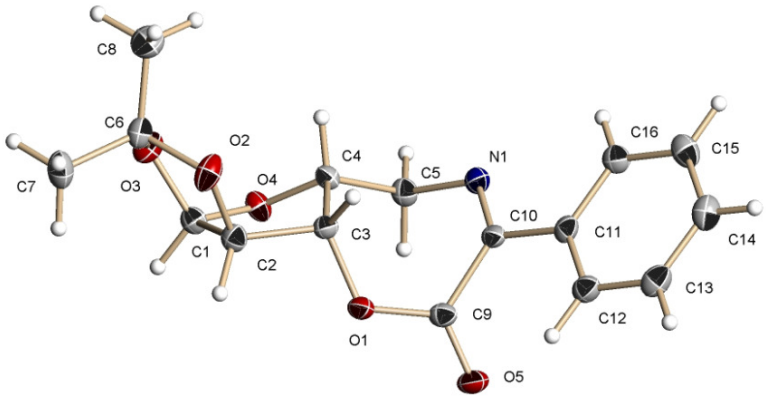

Figure 18: X-Ray crystal structure of oxazepine **10**.

Structural strain may be a contributing factor to the different ^{1}H NMR spectrum that this structure represents. The most unique signal, at 3.42 ppm, represents one of the protons on C-5 as a clear doublet of doublets with $J_1 = J_2$. At 4.58 ppm, the other diastereotopic proton on C-5 is also represented by a doublet of doublets. The single proton on C-4 still appears as a doublet of doublet of doublets at 4.85 ppm. The proton signal for H-3 has also shifted upfield to 4.51 ppm. The only two signals that did not shift to a drastically different region were those corresponding to H-1 and H-2.

Carbon spectral analysis of oxazepine **10** resulted in very few changes compared to that of diazoester **6**. Most of the carbon signals still possessed the same shift value except C-4 and C-5. Carbon 4 was now located at 79.16 ppm, downfield from its original position. The same trend was seen for C-5, now positioned at 52.02 ppm. Ring structure could be a contributing to the change in these carbon shifts. At less intensity than the rest, a peak at 162.81 ppm was now representing the –C=N– carbon.

After isolation of macrocycle **9** and oxazepine **7**, investigation of the mechanistic route of formation was carried out. In recent literature, azides were found to actually

associate with rhodium (II) catalysts and form a nitrenoid instead of a carbenoid. These reactive species are thought to behave very similarly but result in nitrogen insertion reactions to from structures such as amines, imines, etc. With this in mind, the schematic investigation was taken one step back to determine which structure was responsible for imine formation, the azide or the diazo.

Decomposition of 3-*O*-(2-phenylacetyl)-5-azidodeoxy-1,2-*O*-isopropylidene-α-D-xylofuranose (**5**) was then attempted to see if reaction would still occur in the absence of a diazo functional group. Reaction conditions and procedures followed those used in previous decomposition reactions of the diazoester **6**. Both the rhodium (II) tetraacetate and rhodium (II) tetratriflouroacetate catalysts were used in this investigation (Equation 21, Equation 22). Crude reaction mixtures were analyzed using TLC (3:1 / hexane: ethyl acetate) and ^{1}H NMR spectroscopy following initial purification through a column of Celite. Both trials showed some evidence of reaction on a TLC plate however, ^{1}H NMR spectra displayed mainly unreacted starting material.

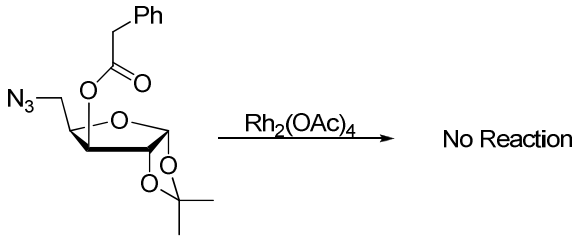

5

Equation 21.

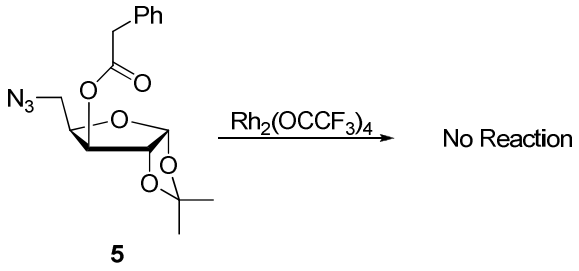

5

Equation 22.

With no evidence that the diazo group decomposition likely initiated the formation of these new compounds, a mechanistic explanation was proposed. The intermolecular mechanism can be seen in Scheme 7 however, the intramolecular reaction is believed to occur in the same manner. Beginning with formation of a metal stabilized carbene, the diazo compound interacts with the rhodium catalyst as previously believed with evolution of N_2. Possessing a formal negative charge, the internal nitrogen of the azido group is thought to attack at the carbenoid carbon. Then through an elimination type reaction, another molecule of N_2 is released and the catalyst dissociates from the reacting species. Intermolecular imine formation results in the macrocycle **9** and an intramolecular reaction gives the oxazepine **10.**

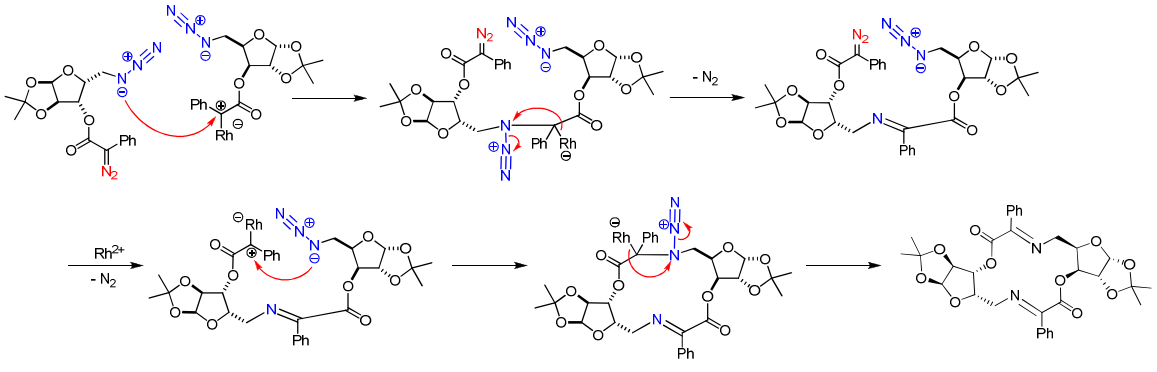

Scheme 7.

Other products formed during decomposition of 3-*O*-(2-diazo-2-phenylacetyl)-5-azidodeoxy-1,2-*O*-isopropylidene-α-D-xylofuranose (**6**) were only identified by careful analysis of impure spectra. Therefore accurate yields were not able to be calculated unless further purification is successfully done. Crude yields do show the tendency of one catalyst to aid in formation of one product over another. This is very important to know in the further investigation of this process as a means to produce imines.

Reaction conditions, including solvent amount and catalyst, are among the factors that may affect this type of imine formation. Formation of complex reaction mixtures requires the development and use of efficient purification methods. Further investigation of the chemistry induced by the presence of an azido group during decomposition of diazoesters is needed to determine how applicable this process may be in other research areas.

Experimental

General Procedure

All reactions were monitored using Thin Layer Chromatography (TLC) and ultraviolet light detection with the reaction materials that are UV-active. Indication of a carbohydrate product was done by treating the TLC plates with a 5% sulfuric acid/methanol solution in order to char the material. Product isolation was done using flash column chromatography performed with 32-63 μm, 60-Å silica gel. Bruker Avance II/III 400 MHz NMR instruments with TOPSPIN software were used for ^{1}H and ^{13}C spectroscopy using $CDCl_3$ as solvent. Proton and carbon chemical shifts (δ) are recorded in parts per million (ppm). Splitting patterns of multiplets are labeled s (singlet), d (doublet), dd (doublet of doublets), ddd (doublet of doublet of doublets), t (triplet), q (quartet), and m (multiplet) with coupling constants measured in Hertz (Hz). Thermo Electron Corporation IR 200 Infrared spectrometer was also used for additional analysis of product structure. A Bruker Daltonics Liquid Chromatography-Mass Spectrometer was used for low resolution mass spectrometry. The solid-state crystal structures of select compounds were determined by x-ray diffraction using Bruker-Nonius SMART APEX CCD Diffractometer.

Preparation of 1,2-*O*-isopropylidene-α-D-xylofuranose (1) and 1,2;5,6-di-*O*-isopropylidene-α-D-xylofuranose from D-(+)-xylose (2).

In a 1000 mL round-bottom flask with a magnetic stir bar, 20.00 mL of concentrated H_2SO_4 was added carefully to 520 mL of acetone. Finely ground D-(+)-xylose (20.00 g, 133.26 mmol) was added and left to stir for about 30 minutes until

completely dissolved. A 1.1 M solution of Na_2CO_3 (224.00 mL, 246.40 mmol) was added slowly while cooled in an ice bath and vigorously stirred. After 2.5 hours of vigorously stirring, 14.00 g of solid Na_2CO_3 was added while being cooled in an ice bath and left to vigorously stir overnight (~26 hours). Since the solution was still acidic by litmus paper, another 14.00 g of solid Na_2CO_3 was added in the same manner and left to stir overnight, for about 24 hours. Once the reaction's pH was checked and completion was determined using TLC, the solution was rid of the salts formed using gravity filtration. The mixture was reduced, dissolved in chloroform and extracted three times with 75.00 mL of dI H_2O. Both the organic and aqueous layers were checked for product using TLC and concentrated under reduced pressure. The products were then purified using flash column chromatography (30:1 / chloroform:methanol). The organic layer contained 1.71 g of 1,2;5,6-di-*O*-isopropylidene-α-D-xylofuranose (5.57%) as an almost colorless syrup. The aqueous layer contained 18.8 g of 1,2-*O*-isopropylidene-α-D-xylofuranose (74.16%) as a colorless syrup, which then crystallized to a white solid by scratching of the vessel.

1,2-*O*-isopropylidene-α-D-xylofuranose (1):

^{1}H NMR ($CDCl_3$): δ 1.40 (s, 3H, -$OCCH_3$), 1.49 (s, 3H, -$OCCH_3$), 4.00 (m, 2H, H-5), 4.18 (dd, 1H, H-4, *J* = 4.06, 7.02 Hz), 4.29 (s, 1H, H-2), 4.52 (d, 1H, H-3, *J* = 3.62 Hz), 5.97 (d, 1H, *J* = 3.68 Hz).

^{13}C NMR ($CDCl_3$): δ 26.17 (1C, -$OCCH_3$), 26.72 (1C, -$OCCH_3$), 60.68 (1C, C-5), 76.31 (1C, C-2), 79.31 (1C, C-4), 85.52 (1C, C-3), 104.79 (1C, C-1), 111.80 (1C, O-C-O).

m/z calculated: 190.19 *m/z* found (ESI): 213.1 (+Na)

M.P. = 66-67 °C

R_f = 0.35 (ethyl acetate).

1,2;5,6-di-*O*-isopropylidene-α-D-xylofuranose (2):

^{1}H NMR: δ 1.33 (s, 3H, -OCCH$_3$), 1.39 (s, 3H, -OCCH$_3$), 1.45 (s, 3H, -OCCH$_3$), 1.50 (s, 3H, -OCCH$_3$), 4.03 (dd, 1H, H-4, *J* = 2.34, 3.74 Hz), 4.09 (m, 2H, H-5), 4.13 (d, 1H, H-O, *J* = 2.51 Hz), 4.30 (d, 1H, H-3, *J* = 2.16 Hz), 4.52 (d, 1H, H-2, *J* = 3.72 Hz), 6.01 (d, 1H, H-1, *J* = 3.72 Hz).

^{13}C NMR: δ 18.72 (1C, -OCCH$_3$), 26.16 (1C, -OCCH$_3$), 26.74 (1C, -OCCH$_3$), 28.91 (1C, -OCCH$_3$), 60.17 (1C, C-5), 71.61 (1C, C-2), 73.20 (1C, C-4), 84.66 (1C, C-3), 97.48 (1C, O-C-O), 105.21 (1C, C-1), 111.62 (1C, O-C-O).

m/z calculated:230.26 *m/z* found (ESI): 253.1 (+Na)

M.P. = N/A (light yellow syrup)

R_f = 0.68 (ethyl acetate).

Preparation of 1,2-*O*-isopropylidene-α-D-xylofuranose (1) from 1,2;5,6-di-*O*-isopropylidene-α-D-xylofuranose (2).

Dissolved in 60.00 mL of acetone, 10.11 g (43.91 mmol) of 1,2;5,6-di-*O*-isopropylidene-α-D-xylofuranose (2) is transfered to a 500 mL round bottom flask. An additional 200 mL acetone is added then 10.00 mL concentrated sulfuric acid is added

while cooled in an ice bath and vigorously stirred with a magnetic stir bar. Subsequent to complete addition of the sulfuric acid, neutralization was started by slow addition of 113.00 mL 1.1 M Na_2CO_3 solution (124.3 mmol) while cooled in an ice bath. The reaction flask was left to stir for three hours when 11.8 g Na_2CO_3 was added to the ice bath cooled and vigorously stirred solution. After 24 hours, the salts were filtered off using gravity filtration and the solution concentrated under reduced pressure. The mixture was reduced, dissolved in chloroform and extracted three times with 75.00 mL of dI H_2O. Both the organic and aqueous layers were checked for product using TLC and concentrated under reduced pressure. Product purification was done using flash column chromatography (30:1 / chloroform:methanol). The aqueous layer contained 5.84 g (30.71 mmol, 69.93%) of 1,2-*O*-isopropylidene-α-D-xylofuranose (1).

^{1}H NMR ($CDCl_3$): δ 1.40 (s, 3H, -$OCCH_3$), 1.49 (s, 3H, -$OCCH_3$), 3.40 (m, 2H, H-5), 4.18 (dd, 1H, H-4, *J* = 4.06, 7.01 Hz), 4.29 (s, 1H, H-2), 4.52 (d, 1H, H-3, *J* = 3.62 Hz), 5.97 (d, 1H, *J* = 3.68 Hz).

^{13}C NMR ($CDCl_3$): δ 26.17 (1C, -$OCCH_3$), 26.72 (1C, -$OCCH_3$), 60.68 (1C, C-5), 76.31 (1C, C-2), 79.31 (1C, C-4), 85.52 (1C, C-3), 104.79 (1C, C-1), 111.80 (1C, O-C-O).

m/z calculated: 190.19 *m/z* found (ESI): 213.1 (+Na)

M.P. = 66-67 °C

R_f = 0.35 (ethyl acetate).

Preparation of 5-*O*-(4-methylbenzenesulfonyl)-1,2-*O*-isopropylidene-α-D-xylofuranose (3) from 1,2-*O*-isopropylidene-α-D-xylofuranose (1).

In a flame-dried 250 mL round bottom flask equipped with a septum and magnetic stir bar, 5.027 g (26.43 mmol) of 1,2-*O*-isopropylidene-α-D-xylofuranose (1) and 5.556 g (29.14 mmol) of *p*-toluenesulfonyl chloride were placed under nitrogen atmosphere. Anhydrous pyridine (30.00 mL) was added *via* syringe. The reaction was stirred for 2.5 hours in an acetone/ice bath until the reaction was determined complete by TLC (ethyl acetate). The reaction mixture was transferred to a 250 mL separatory funnel using 40.00 mL of methylene chloride, the organic phase was washed with 5% H_2SO_4 (3 x 40.00 mL) followed by dI H_2O (3 x 40.00 mL). The remaining organic layer was dried with anhydrous magnesium sulfate that was removed using gravity filtration. Concentration of the organic layer under reduced pressure resulted in 8.04 g of compound **3** as a white solid (88.35%). The solid state crystal structure was obtained by crystallization in $CDCl_3$ (NMR sample).

^{1}H NMR: δ 1.29 (s, 3H, -OCCH_3), 1.46 (s, 3H, -OCCH_3), 2.45 (s, 3H, CH_3-Ph), 2.56 (d, 1H, H-O, *J* = 5.27 Hz), 4.14 (m, 1H, H-4), 4.28 (m, 1H, H-2), 4.34 (m, 2H, H-5), 4.50 (d, 1H, H-3, *J* = 3.60 Hz), 5.87 (d, 1H, H-1, *J* = 3.60 Hz), 7.36 (d, 2H, H-Ph, *J* = 7.96 Hz), 7.80 (d, 2H, H-Ph, *J* = 8.36 Hz).

^{13}C NMR: δ 21.67 (1C, CH_3-Ph), 26.20 (1C, -OCCH_3), 26.78 (1C, -OCCH_3), 66.49 (1C, C-4), 74.30 (1C, C-2), 7.67 (1C, C-5), 85.07 (1C, C-3), 104.98 (1C, C-1), 112.12 (1C, O-C-O), 128.03 (2C, Ph), 130.02 (2C, Ph), 132.34 (1C, Ph) 145.31 (1C, S-Ph).

m/z calculated: 344.38 *m/z* found (ESI): 367.2 (+Na)

M.P. = decomposes at 72-74 °C

R_f = 0.45 (1:1 / hexane: ethyl acetate).

Preparation of 5-azidodeoxy-1,2-*O*-isopropylidene-α-D-xylofuranose (4) from 5-*O*-(4-methylbenzenesulfonate)-1,2-*O*-isopropylidene-α-D-xylofuranose (3).

In a three-neck 100 mL round bottom flask containing a magnetic stir bar, 6.01 g (17.45 mmol) of 5-*O*-(4-methylbenzenesulfonate)-1,2-*O*-isopropylidene-α-D-xylofuranose (3) was dissolved in 25.00 mL of dimethylformamide (DMF). Sodium azide (11.57 g, 178.05 mmol) was added and the reaction was heated to 73 °C using a heating mantle. The mixture was stirred overnight (26 hours) while a reflux condenser was atop the flask. Transferred to a 250 mL round bottom flask, the reaction was concentrated under reduced pressure using high vacuum. The mixture was transferred to a 250 mL separatory funnel using 25.00 mL dI H_2O and 25.00 mL of $CHCl_3$. After extraction of with dI H_2O (2 x 25.00 mL), the organic layer was dried over magnesium sulfate and reduced to a colorless syrup. The syrup was purified using flash column chromatography (3:1 / hexane: ethyl acetate) and resulted in 3.21 g (14.92 mmol, 85.48%) of a white solid, **4**.

^{1}H NMR: δ 1.32 (s, 3H, -OCCH_3), 1.50 (s, 3H, -OCCH_3), 3.59 (d, 2H, H-5, *J* = 6.24 Hz), 4.23 (d, 1H, H-2, *J* = 2.80 Hz), 4.28 (ddd, 1H, H-4, *J* = 2.84, 6.24, 6.24 Hz), 4.52 (d, 1H, H-3, *J* = 3.72 Hz), 5.95 (d, 1H, H-1, *J* = 3.68 Hz).

^{13}C NMR: δ 26.17 (1C, -$OCCH_3$), 26.71 (1C, -$OCCH_3$), 49.19 (1C, C-5), 74.92 (1C, C-2), 78.63 (1C, C-4), 85.36 (1C C-3), 104.81 (1C, C-1), 112.08 (1C, O-C-O).

m/z calculated: 215.21 *m/z* found (ESI): 238.3 (+Na)

M.P. = 66-68 °C

R_f = 0.51 (1:1 / hexane: ethyl acetate).

Preparation of 3-*O*-(2-phenylacetyl)-5-azidodeoxy-1,2-*O*-isopropylidene-α-D-xylofuranose (5) from 5-azidodeoxy-1,2-*O*-isopropylidene-α-D-xylofuranose (4).

An oven-dried addition funnel was attached to a flame dried 250 mL round bottom flask equipped with a magnetic stir bar and containing 2.25 g (10.46 mmol) of 5-azidodeoxy-1,2-*O*-isopropylidene-α-D-xylofuranose (**4**), 1.745 g (12.82 mmol) of phenylacetic acid, and 0.2260 g (1.85 mmol) of DMAP. Once the apparatus was placed under nitrogen atmosphere, 20.00 mL methylene chloride (anhydrous) and 20.00 mL acetonitrile (anhydrous) were added *via* syringe. Into the addition funnel, 12.50 mL of dicyclohexylcarbodiimide (DCC, 1 M in CH_2Cl_2) was placed and added dropwise over two hours to the solution. After 19 hours of stirring and completion, as determined by TLC, the mixture was gravity filtered and concentrated under reduced pressure. The syrup/solid mixture was dissolved in 40.00 mL of methylene chloride and transferred to a 250 mL separatory funnel where it was washed with 5% H_2SO_4 (3 x 40.00 mL) and dI H_2O (3 x 40.00 mL). Once the organic layer was dried over anhydrous magnesium sulfate, it was filtered and concentrated under reduced pressure. Further purification was

done using a column of silica gel with the solvent system 3:1 / hexane: ethyl acetate. A colorless syrup of 2.97 g (8.94 mmol, 85.44%) resulted as compound **5**.

^{1}H NMR: δ 1.28 (s, 3H, -OCCH$_3$), 1.49 (s, 3H, -OCCH$_3$), 3.24 (dd, 1H, H-5, *J* = 5.52, 12.80 Hz), 3.32 (dd, 1H, H-5, *J* = 7.02, 12.80 Hz), 3.64 (s, 2H, H-CHPh), 4.34 (ddd, 1H, H-4, *J* = 3.02, 5.62, 6.96 Hz), 4.46 (d, 1H, H-2, *J* = 3.72 Hz), 5.19 (d, 1H, H-3, *J* = 3.00 Hz), 5.87 (d, 1H, H-1, *J* = 3.72 Hz), 7.30 (m, 5H, Ph).

^{13}C NMR: δ 26.18 (1C, -OCCH$_3$), 26.66 (1C, -OCCH$_3$), 41.16 (1C, -CH$_2$Ph), 48.96 (1C, C-5), 76.42 (1C, C-3), 77.66 (1C, C-4), 83.31 (1C, C-2), 104.76 (1C, C-1), 112.32 (1C, O-C-O), 127.45 (1C, Ph), 128.74 (2C, Ph), 129.20 (2C, Ph), 133.24 (1C, Ph), 170.18 (1C, -COO).

m/z calculated: 332.33 *m/z* found (ESI): 356.2 (+Na)

M.P. = N/A (colorless syrup)

R_f = 0.66 (ethyl acetate).

Preparation of 3-*O*-(2-Diazo-2-phenylacetyl)-5-azidodeoxy-1,2-*O*-isopropylidene-α-D-xylofuranose (6) from 3-*O*-(2-phenylacetyl)-5-azidodeoxy-1,2-*O*-isopropylidene-α-D-xylofuranose (5).

Containing 3-*O*-(2-phenylacetyl)-5-azidodeoxy-1,2-*O*-isopropylidene-α-D-xylofuranose (4.51 g, 13.53 mmol) and *p*-acetamidobenzenesulfonyl azide (4.236 g, 17.63 mmol), a flame-dried 250 mL round bottom flask equipped with a septum and a magnetic stir bar was placed under nitrogen atmosphere. After the addition of 40.00 mL of

anhydrous acetonitrile and 40.00 mL of anhydrous dichloromethane *via* syringe, 2.60 mL (17.40 mmol) of DBU was added dropwise over 2.5 hours. The reaction was established to be complete after stirring overnight for 18 hours. Subsequent to concentration of the reaction mixture under reduced pressure, it was diluted with 80.00 mL of dichloromethane and transferred to a 250 mL separatory funnel to perform an aqueous workup; the organic phase was washed with 5% H_2SO_4 (3 x 80.00 mL), dI H_2O (3 x 80.00 mL), and then dried over anhydrous magnesium sulfate. The filtered solution was concentrated and the orange syrup was purified on a silica gel column (chloroform as eluent). Diazo-transfer product 3-*O*-(2-Diazo-2-phenylacetyl)-5-azidodeoxy-1,2-*O*-isopropylidene-α-D-xylofuranose (**6**), resided as 3.36 g (9.35 mmol, 69.11%) of an orange syrup.

^{1}H NMR: δ 1.33 (s, 3H, -OCCH_3), 1.54 (s, 3H, -OCCH_3), 3.46 (dd, 1H, H-5, *J* = 5.52, 12.80 Hz), 3.52 (dd, 1H, H-5, *J* = 7.03, 12.80 Hz), 4.48 (ddd, 1H, H-4, *J* = 4.64, 7.65, 2.13 Hz), 4.66 (d, 1H, H-2, *J* = 3.76 Hz), 5.37 (d, 1H, H-3, *J* = 3.26 Hz), 5.97 (d, 1H, H-1, *J* = 3.76 Hz), 7.23 (m, 5H, Ph).

^{13}C NMR: δ 26.23 (1C, -OCCH_3), 26.71 (1C, -OCCH_3), 49.31 (1C, C-5), 76.87 (1C, C-3), 77.73 (1C, C-4), 83.50 (1C, C-2), 104.79 (1C, C-1), 112.47 (1C, O-C-O), 124.10 (2C, Ph), 124.55 (1C, Ph), 126.39 (1C, Ph), 129.12 (2C, Ph), 163.65 (1C, -COO).

m/z calculated: 358.33 *m/z* found (ESI): 341.3

M.P. = N/A (orange syrup)

R_f = 0.49 (3:1 / hexane:ethyl acetate).

Attempted decomposition of 3-*O*-(2-Diazo-2-phenylacetyl)-5-azidodeoxy-1,2-*O*-isopropylidene-α-D-xylofuranose (6) in refluxing toluene.

3-*O*-(2-Diazo-2-phenylacetyl)-5-azidodeoxy-1,2-*O*-isopropylidene-α-D-xylofuranose (0.34 g, 0.95 mmol) was dissolved in 9.00 mL of toluene and transferred to a 3-neck 50 mL round bottom flask. The solution was stirred with a magnetic stir bar and gradually heated to boiling using a heating mantle in the apparatus that was topped with a reflux condenser. After 19 hours Thin Layer Chromatography (3:1 / hexane:ethyl acetate) showed 5 possible products. After concentration and purification *via* flash column chromatography with gradient elution (3:1 / hexane: ethyl acetate; ethyl acetate; methanol), purification was inadequate such that no verifiable product was recovered.

Attempted decomposition of 3-*O*-(2-Diazo-2-phenylacetyl)-5-azidodeoxy-1,2-*O*-isopropylidene-α-D-xylofuranose (6) in the presence of copper (II) acetylacetonate catalyst.

Copper (II) acetylacetonate (0.015 g, 0.0573 mmol) in 20.00 mL of dichloromethane was added dropwise over 2.5 hours *via* an addition funnel to a 250 mL round bottom flask containing a solution of 3-*O*-(2-diazo-2-phenylacetyl)-5-azidodeoxy-1,2-*O*-isopropylidene-α-D-xylofuranose (0.47 g, 1.31 mmol) in 30.00 mL dichloromethane. Once the addition of the catalyst was complete, the mixture was stirred with a magnetic stir bar for 18 hours. Celite was used to filter off the copper (II) acetylacetonate before concentration under reduced pressure was done. NMR of the crude mixture (0.51 g) showed the presence of mostly unreacted starting material.

Decomposition of 3-*O*-(2-Diazo-2-phenylacetyl)-5-azidodeoxy-1,2-*O*-isopropylidene-α-D-xylofuranose (6) in the presence of dirhodium (II) tetraacetate under inert conditions.

The dirhodium (II) tetraacetate catalyst was dried for 5 days using a drying gun and a high vacuum pump. 3-*O*-(2-Diazo-2-phenylacetyl)-5-azidodeoxy-1,2-*O*-isopropylidene-α-D-xylofuranose was also dried for 5 days on a high vacuum pump prior to decomposition. In 20.00 mL of anhydrous dichloromethane, 0.85 g (2.37 mmol) of the diazoester was dissolved under nitrogen atmosphere and degassed for 20 minutes. Next, 0.034 g (0.0769 mmol) of $Rh_2(OAc)_4$ was placed in a flame-dried 250 mL round bottom flask containing a magnetic stir bar. The vessel was placed under nitrogen atmosphere and 40.00 mL of dichloromethane was added *via* syringe to make the $Rh_2(OAc)_4$ solution. Once the catalyst was dissolved, the solution was degassed for 15 minutes leaving only 38 mL of $Rh_2(OAc)_4$ solution. The remaining 18 mL of diazoester solution was placed in a 20 mL syringe and added to the $Rh_2(OAc)_4$ solution 1.00 mL/hr *via* syringe pump. After complete addition of the diazoester to the $Rh_2(OAc)_4$ solution, the reaction was monitored using TLC (3:1 / hexane:ethyl acetate) which showed a complex reaction mixture containing at least 5 distinct products. Purification was done using flash column chromatography with gradient elution (3:1 / hexane: ethyl acetate; ethyl acetate; methanol). Two products obtained from this reaction were a ketoester **7** (0.14 g, 0.4031 mmol, 17.04%) and an ether-linked dimer **8** (0.13 g, 0.1910 mmol, 8.08%).

Keto-ester (7)

^{1}H NMR: δ 1.35 (s, 3H, -OCCH_3), 1.57 (s, 3H, -OCCH_3), 3.49 (dd, 1H, H-5, *J* = 6.33, 12.64 Hz), 6.64 (dd, 1H, H-5, *J* = 6.70, 12.64 Hz), 4.52 (ddd, 1H, H-4, *J* =

2.99, 6.60, 6.60 Hz), 4.69 (d, 1H, H-2, *J* = 3.76 Hz), 5.51 (d, 1H, H-3, *J* = 2.96 Hz), 5.99 (d, 1H, H-1, *J* = 3.76 Hz), 7.55 (m, 2H, Ph), 7.70 (m, 1H, Ph), 8.02 (m, 1H, Ph).

^{13}C NMR: δ 26.24 (1C, -OCCH$_3$), 26.66 (1C, -OCCH$_3$), 48.71 (1C, C-5), 77.43 (1C, C-4), 77.51 (1C, C-3), 83.19 (1C, C-2), 104.87 (1C, C-1), 112.70 (1C, O-C-O), 129.14 (2C, Ph), 130.05 (2C, Ph), 132.00 (1C, Ph), 135.40 (1C, Ph), 162.30 (1C, -COO), 184.87 (1C, -C=O).

m/z calculated: 347.32 *m/z* found (ESI): 370.2 (+Na)

M.P. = N/A (light yellow syrup)

R_f = 0.48 (3:1 / hexane: ethyl acetate).

Ether-linked dimer (8)

^{1}H NMR: δ 1.23 (s, 6H, -OCCH$_3$), 1.48 (s, 6H, -OCCH$_3$), 3.45 (dd, 1H, H-5, *J* = 6.78, 12.80 Hz), 4.13 (d, 2H, H-2, *J* = 3.72 Hz), 4.40 (ddd, 2H, H-4, *J* = 2.99, 6.09, 6.35 Hz), 5.25 (d, 2H, H-3, *J* = 2.96 Hz), 5.66 (d, 2H, H-1, *J* = 3.51 Hz), 7.38 (m, 10H, Ph).

^{13}C NMR: δ 26.18 (2C, -OCCH$_3$), 26.67 (2C, -OCCH$_3$), 49.01 (2C, C-5), 72.87 (2C, C-3), 77.53 (2C, C-4), 82.84 (2C, C-2), 104.65 (2C, C-1), 112.61 (2C, O-C-O), 126.34 (4C, Ph), 128.83 (4C, Ph), 137.61 (2C, Ph), 172.55 (2C, Ph).

m/z calculated: 680.66 *m/z* found (ESI): 703.6 (+Na)

M.P. = N/A (light yellow syrup)

R_f = 0.20 (3:1 / hexane: ethyl acetate).

Decomposition of 3-*O*-(2-Diazo-2-phenylacetyl)-5-azidodeoxy-1,2-*O*-isopropylidene-α-D-xylofuranose (6) in the presence of dirhodium (II) tetraacetate under inert conditions of a glovebox.

3-*O*-(2-Diazo-2-phenylacetyl)-5-azido-1,2-*O*-isopropylidene-α-D-xylofuranose (1.47 g, 4.09 mmol) was dried for 5 days on a high vacuum pump before being placed inside the glovebox. Once the orange syrup was dry and placed inside the glovebox, it was dissolved in 30.00 mL of dichlormethane then transferred to a 20.00 mL syringe and the remainder placed in a scintillation vial. Fifty milliliters of methylene chloride was poured into the original 250 mL round bottom flask, where 0.052 g (0.12 mmol) of $Rh_2(OAc)_4$ was added and dissolved with an additional 48.00 mL of methylene chloride. The diazoester solution was added at a rate of 1.00 mL/hr to the catalyst solution *via* syringe pump. Following complete addition of diazoester to the reaction flask, the mixture was left to stir overnight (26 hours) before being removed from the glovebox (T = 26 °C; H_2O = 24.0 ppm; O_2 = 647.6 ppm). Subsequent to removal of the reaction flask, the reaction was analyzed using TLC and the catalyst removed by filtration through a column of Celite. Further purification of the complex reaction mixture was done using flash column chromatography with gradient elution (3:1 / hexane: ethyl acetate; ethyl acetate; methanol); product was loaded onto the column as a dry silica mixture. The

decomposition resulted in the formation of a keto-ester (**7**), a 14-membered macrocycle (**9**), and oxazepine (**10**).

Keto-ester (7)

^{1}H NMR: δ 1.35 (s, 3H, -OCCH$_3$), 1.57 (s, 3H, -OCCH$_3$), 3.49 (dd, 1H, H-5, *J* = 6.33, 12.64 Hz), 6.64 (dd, 1H, H-5, *J* = 6.70, 12.64 Hz), 4.52 (ddd, 1H, H-4, *J* = 2.99, 6.60, 6.60 Hz), 4.69 (d, 1H, H-2, *J* = 3.76 Hz), 5.51 (d, 1H, H-3, *J* = 2.96 Hz), 5.99 (d, 1H, H-1, *J* = 3.76 Hz), 7.55 (m, 2H, Ph), 7.70 (m, 1H, Ph), 8.02 (m, 1H, Ph).

^{13}C NMR: δ 26.24 (1C, -OCCH$_3$), 26.66 (1C, -OCCH$_3$), 48.71 (1C, C-5), 77.43 (1C, C-4), 77.51 (1C, C-3), 83.19 (1C, C-2), 104.87 (1C, C-1), 112.70 (1C, O-C-O), 129.14 (2C, Ph), 130.05 (2C, Ph), 132.00 (1C, Ph), 135.40 (1C, Ph), 162.30 (1C, -COO), 184.87 (1C, -C=O).

m/z calculated: 347.32 *m/z* found (ESI): 370.2 (+Na)

M.P. = N/A (light yellow syrup)

R_f = 0.48 (3:1 / hexane: ethyl acetate).

14-Membered Macrocycle (original) (9)

^{1}H NMR: δ 1.35 (s, 6H, -OCCH$_3$), 1.61 (s, 6H, -OCCH$_3$), 3.87 (dd, 2H, H-5, *J* = 3.00, 15.37 Hz), 3.96 (dd, 2H, H-5, *J* = 9.52, 15.41 Hz), 4.64 (d, 2H, H-2, *J* = 3.96 Hz), 4.97 (ddd, 2H, H-4, *J* = 2.87, 2.87, 9.47 Hz), 5.73 (d, 2H, H-3, *J* = 2.76 Hz), 6.00 (d, 2H, H-1, *J* = 3.84 Hz), 7.45 (m, 6H, Ph), 7.75 (m, 4H, Ph).

^{13}C NMR: δ 26.37 (2C, -OCCH$_3$), 26.74 ((2C, -OCCH$_3$), 55.06 (2C, C-5), 78.52 (2C, C-3), 78.65 (2C, C-4), 83.46 (2C, C-2), 105.24 (2C, C-1), 112.49 (2C, O-C-O), 127.37 (4C, Ph), 128.69 (4C, Ph), 131.59 (2C, Ph), 133.37 (2C, Ph), 161.66 (2C, C=N), 164.3741 (2C, -COO).

m/z calculated: 606.62 *m/z* found (ESI): 629.7 (+Na)

M.P. = decomposes at 158 °C

R_f = 0.30 (3:1 / hexane: ethyl acetate).

14-Membered Macrocycle (possible) (9)

^{1}H NMR: δ 1.32 (s, 6H, -OCCH$_3$), 1.50 (s, 6H, -OCCH$_3$), 3.48 (m, 2H, H-5), 3.92 (m, 2H, H-5), 4.11 (d, 2H, H-3, *J* = 2.28 Hz), 4.18 (ddd, 2H, H-4, *J* = 2.40, 4.40, 9.56 Hz), 4.61 (d, 2H, H-2, *J* = 3.64 Hz), 5.95 (d, 2H, H-1, *J* = 3.60 Hz), 7.49 (m, 4H, Ph), 7.65 (m, 2H, Ph), 8.31 (m, 4H, Ph).

^{13}C NMR: δ 26.09 (2C, -OCCH$_3$), 26.78 (2C, -OCCH$_3$), 37.22 (2C, C-5), 74.17 (2C, C-3), 79.37 (2C, C-4), 84.93 (2C, C-2), 104.81 (2C, C-1), 111.73 (2C, O-C-O), 128.66 (4C, Ph), 131.22 (4C, Ph), 132.92 (2C, Ph), 134.82 (2C, Ph), 163.36 (2C, C=N), 186.66 (2C, -COO).

m/z calculated: 606.62 *m/z* found (ESI): 677.3 (+ 3Na)

M.P. = decomposes at 158 °C

R_f = 0.30 (3:1 / hexane: ethyl acetate).

Oxazepine (10)

^{1}H NMR: δ 1.33 (s, 3H, -$OCCH_3$), 1.48 (s, 3H, -$OCCH_3$), 3.41 (dd, 1H, H-5, *J* = 10.58, 10.58 Hz), 4.51 (d, 1H, H-3, J = 3.0812 Hz), 4.58 (dd, 1H, H-5, *J* = 6.10, 10.66 Hz), 4.80 (d, 1H, H-2, *J* = 4.73 Hz), 4.85 (ddd, 1H, H-4, *J* = 3.17, 6.16, 10.49 Hz), 6.10 (d, 1H, H-1, *J*= 3.76), 7.44 (m, 2H, Ph), 7.52 (m, 1H, Ph), 7.85 (m, 2H, Ph).

^{13}C NMR: δ 26.33 (1C, -$OCCH_3$), 26.79 (1C, -$OCCH_3$), 52.02 (1C, C-5), 79.16 (1C, C-4), 81.44 (1C, C-3), 82.12 (1C, C-2), 106.72 (1C, C-1), 112.58 (1C, O-C-O), 127.82(1C, Ph), 128.84 (2C, Ph), 132.20 (1C, Ph), 133.00 (1C, Ph), 162.81 (1C, C=N), 164.43 (1C, -COO).

m/z calculated: 303.31 *m/z* found (ESI): 304.2

M.P. = 136-140 °C

R_f = 0.50 (3:1 / hexane: ethyl acetate).

Decomposition of 3-*O*-(2-Diazo-2-phenylacetyl)-5-azidodeoxy-1,2-*O*-isopropylidene-α-D-xylofuranose (6) in the presence of dirhodium (II) trifluoroacetate under inert conditions of a glove box.

3-*O*-(2-Diazo-2-phenylacetyl)-5-azidodeoxy-1,2-*O*-isopropylidene-α-D-xylofuranose (1.21 g, 3.37 mmol) was transferred to the glove box after being dried on a

high vacuum pump for 5 days. In the glove box (T = 28 °C; H_2O = 12.7 ppm; O_2 = 120.9 ppm), the orange syrup was dissolved in 30.00 mL of dichloromethane, then drawn into a 20.00 mL syringe with the remainder placed in a scintillation vial. The dirhodium (II) trifluoroacetate (0.062 g, 0.094 mmol) was placed into the original 250 mL round bottom flask containing 50.00 mL of dichloromethane and dissolved with an additional 40.00 mL dicholormethane. Once the catalyst was dissolved with a magnetic stir bar, continuously the diazoester solution was added continuously dropwise at a rate of 1.00 mL/hr *via* syringe pump. Subsequent to complete addition of the diazoester the reaction was left to stir in the glove box over night (23 hours). Removed from the inert atmosphere a complex crude reaction mixture was verified by TLC and NMR even after removal of some rhodium catalyst by filtration through a column containing Celite. Further purification of the complex reaction mixture was done using flash column chromatography with gradient elution (3:1 / hexane: ethyl acetate; ethyl acetate; methanol); product was loaded onto the column as a dry silica mixture. The decomposition resulted in the formation of a keto-ester (**7**), a 14-membered macrocycle (**9**), and an oxazepine (**10**).

Keto-ester (7)

^{1}H NMR: δ 1.35 (s, 3H, -$OCCH_3$), 1.57 (s, 3H, -$OCCH_3$), 3.49 (dd, 1H, H-5, *J* = 6.33, 12.64 Hz), 6.64 (dd, 1H, H-5, *J* = 6.70, 12.64 Hz), 4.52 (ddd, 1H, H-4, *J* = 2.99, 6.60, 6.60 Hz), 4.69 (d, 1H, H-2, *J* = 3.76 Hz), 5.51 (d, 1H, H-3, *J* = 2.96 Hz), 5.99 (d, 1H, H-1, *J* = 3.76 Hz), 7.55 (m, 2H, Ph), 7.70 (m, 1H, Ph), 8.02 (m, 1H, Ph).

^{13}C NMR: δ 26.24 (1C, -$OCCH_3$), 26.66 (1C, -$OCCH_3$), 48.71 (1C, C-5), 77.43 (1C, C-4), 77.51 (1C, C-3), 83.19 (1C, C-2), 104.87 (1C, C-1), 112.70 (1C, O-

C-O), 129.14 (2C, Ph), 130.05 (2C, Ph), 132.00 (1C, Ph), 135.40 (1C, Ph), 162.30 (1C, -COO), 184.87 (1C, -C=O).

m/z calculated: 347.32 *m/z* found (ESI): 370.2 (+Na)

M.P. = N/A (light yellow syrup)

R_f = 0.48 (3:1 / hexane: ethyl acetate).

14-Membered Macrocycle (original) (9)

^{1}H NMR: δ 1.35 (s, 6H, -OCCH$_3$), 1.61 (s, 6H, -OCCH$_3$), 3.87 (dd, 2H, H-5, *J* = 3.00, 15.37 Hz), 3.96 (dd, 2H, H-5, *J* = 9.52, 15.41 Hz), 4.64 (d, 2H, H-2, *J* = 3.96 Hz), 4.97 (ddd, 2H, H-4, *J* = 2.87, 2.87, 9.47 Hz), 5.73 (d, 2H, H-3, *J* = 2.76 Hz), 6.00 (d, 2H, H-1, *J* = 3.84 Hz), 7.45 (m, 6H, Ph), 7.75 (m, 4H, Ph).

^{13}C NMR: δ 26.37 (2C, -OCCH$_3$), 26.74 ((2C, -OCCH$_3$), 55.06 (2C, C-5), 78.52 (2C, C-3), 78.65 (2C, C-4), 83.46 (2C, C-2), 105.24 (2C, C-1), 112.49 (2C, O-C-O), 127.37 (4C, Ph), 128.69 (4C, Ph), 131.59 (2C, Ph), 133.37 (2C, Ph), 161.66 (2C, C=N), 164.3741 (2C, -COO).

m/z calculated: 606.62 *m/z* found (ESI): 629.7 (+Na)

M.P. = decomposes at 158 °C

R_f = 0.30 (3:1 / hexane: ethyl acetate).

14-Membered Macrocycle (possible) (9)

^{1}H NMR: δ 1.32 (s, 6H, -OCCH$_3$), 1.50 (s, 6H, -OCCH$_3$), 3.48 (m, 2H, H-5), 3.92 (m, 2H, H-5), 4.11 (d, 2H, H-3, *J* = 2.28 Hz), 4.18 (ddd, 2H, H-4, *J* = 2.40, 4.40, 9.56 Hz), 4.61 (d, 2H, H-2, *J* = 3.64 Hz), 5.95 (d, 2H, H-1, *J* = 3.60 Hz), 7.49 (m, 4H, Ph), 7.65 (m, 2H, Ph), 8.31 (m, 4H, Ph).

^{13}C NMR: δ 26.09 (2C, -OCCH$_3$), 26.78 (2C, -OCCH$_3$), 37.22 (2C, C-5), 74.17 (2C, C-3), 79.37 (2C, C-4), 84.93 (2C, C-2), 104.81 (2C, C-1), 111.73 (2C, O-C-O), 128.66 (4C, Ph), 131.22 (4C, Ph), 132.92 (2C, Ph), 134.82 (2C, Ph), 163.36 (2C, C=N), 186.66 (2C, -COO).

m/z calculated: 606.62 *m/z* found (ESI): 677.3 (+ 3Na)

M.P. = decomposes at 158 °C

R_f = 0.30 (3:1 / hexane: ethyl acetate).

Oxazepine (10)

^{1}H NMR: δ 1.33 (s, 3H, -OCCH$_3$), 1.48 (s, 3H, -OCCH$_3$), 3.41 (dd, 1H, H-5, *J* = 10.58, 10.58 Hz), 4.51 (d, 1H, H-3, J = 3.0812 Hz), 4.58 (dd, 1H, H-5, *J* = 6.10, 10.66 Hz), 4.80 (d, 1H, H-2, *J* = 4.73 Hz), 4.85 (ddd, 1H, H-4, *J* = 3.17, 6.16, 10.49 Hz), 6.10 (d, 1H, H-1, *J*= 3.76), 7.44 (m, 2H, Ph), 7.52 (m, 1H, Ph), 7.85 (m, 2H, Ph).

^{13}C NMR: δ 26.33 (1C, -OCCH$_3$), 26.79 (1C, -OCCH$_3$), 52.02 (1C, C-5),

79.16 (1C, C-4), 81.44 (1C, C-3), 82.12 (1C, C-2), 106.72 (1C, C-1), 112.58 (1C, O-C-O), 127.82(1C, Ph), 128.84 (2C, Ph), 132.20 (1C, Ph), 133.00 (1C, Ph), 162.81 (1C, C=N), 164.43 (1C, -COO).

m/z calculated: 303.31 *m/z* found (ESI): 304.2

M.P. = 136-140 °C

R_f = 0.50 (3:1 / hexane: ethyl acetate).

Attempted decomposition of 3-*O*-(2-phenylacetyl)-5-azidodeoxy-1,2-*O*-isopropylidene-α-D-xylofuranose (6) in the presence of dirhodium (II) tetraacetate under inert conditions of a glove box.

3-*O*-(2-Phenylacetyl)-5-azidodeoxy-1,2-*O*-isopropylidene-α-D-xylofuranose (1.18 g, 3.54 mmol) was dried for 5 days on a high vacuum pump before placed inside the glovebox. Once placed inside the glovebox, the colorless syrup was dissolved in 30.00 mL of dichloromethane then transferred to a 20.00 mL syringe and the remainder placed in a scintillation vial. Methylene chloride (50.00 mL) was poured into the original 250 mL round bottom flask, where 0.044 g (0.1030 mmol) of $Rh_2(OAc)_4$ was added and dissolved with an additional 40.00 mL of methylene chloride. The phenylacetyl ester solution was continuously added at a rate of 1.00 mL/hr to the catalyst solution *via* syringe pump. Following complete addition of phenylacetyl ester to the reaction flask, the mixture was left to stir overnight (25 hours) before being removed from the glovebox (T = 28 °C; H_2O = 33.0 ppm; O_2 = 304.4 ppm). Subsequent to removal of the reaction flask, the reaction was analyzed using TLC and the catalyst removed by filtration through a

column of Celite. Analysis of the reaction mixture using NMR concluded that no significant reaction occurred but unreacted starting material remained.

Attempted decomposition of 3-*O*-(2-phenylacetyl)-5-azidodeoxy-1,2-*O*-isopropylidene-α-D-xylofuranose (6) in the presence of dirhodium (II) trifluoroacetate under inert conditions of a glove box.

3-*O*-(2-Phenylacetyl)-5-azidodeoxy-1,2-*O*-isopropylidene-α-D-xylofuranose (1.13 g, 3.39 mmol) was transferred to the glove box after being dried on a high vacuum pump for 5 days. In the glove box (T = 28 °C; H_2O = 14.8 ppm; O_2 = 163.8 ppm), the colorless syrup was dissolved in 30.00 mL of dichloromethane, then drawn into a 20.00 mL syringe with the remainder placed in a scintillation vial. The dirhodium (II) trifluoroacetate (0.062 g, 0.094 mmol) was placed into the original 250 mL round bottom flask containing 50.00 mL of dichloromethane and dissolved with an additional 40.00 mL of dicholoromethane. Once the catalyst was dissolved with a magnetic stir bar, continuously the phenylacetyl ester solution was added dropwise at a rate of 1.00 mL/hr *via* syringe pump. Subsequent to complete addition of the phenylacetyl ester the reaction was left to stir in the glove box over night (23 hours). Removed from the inert atmosphere a complex crude reaction mixture was verified by TLC and NMR even after removal of some rhodium catalyst by filtration through a column containing Celite. Analysis of the reaction mixture using NMR concluded that no significant reaction occurred with only unreacted starting material remaining.

References

1. Torssell, K. B. G. *Natural Product Chemistry: A Mechanistic and Biosynthetic Approach to Secondary Metabolism.* John Wiley & Sons Limited: Chichester, England, 1983.
2. Murphy, P. V., "Peptidomimetics, glycomimetics and scaffolds from carbohydrate building blocks," *Eur. J. Org. Chem.* **2007**, 4177-4187.
3. Lertvorachon, J.; Thebtaranorith, Y.; Thongpanchang, T.; Thongyoo, P., "Stereoslective synthesis of naturally occurring α-methylenebis-γ-butyrolactones; an application of novel oxiranyl "remote" anions," *J. Org. Chem.* **2001**, *66*, 4692-4694.
4. Sharma, G. V. M.; Gopinath, T., "Radical cyclisation approach for the synthesis of (+)-dihydrocanadensolide, (+)-dihydrosporothriolide and their C-3 epimers from D-xylose," *Tetrahedron* **2003**, *59*, 6521-6530.
5. Sharma, G. V. M.; Gopinath, T., "Radical-mediated stereoselective synthesis of (+)-dihydrocanadensolide and (-)-3-*epi*-dihydrocanadensolide from D-xylose," *Tetrahedron Lett.* **2001**, *42*, 6183-6186.
6. Yu, M.; Lynch, V.; Pagenkopf, B. L., "Intramolecular cyclopropanation of glycals: Studies toward the synthesis of canadensolide, sporothriolide, and xylobovide," *Organic Lett.* **2001**, *3*, 2563-2566.
7. Tsuboi, S.; Muranaka, K.; Sakai, T.; Takeda, A., "Highly stereo- and regioselective alkylation of alkylidenemalonates. Its application to the synthesis of (±)-canadensolide," *J. Org. Chem.* **1986**, *51*, 4944-4946.

8. Nubbemeyer, U., "Synthesis of (+)-canadensolide, (-)-santolinolide A and (-)-santolinolide B: The imino-Claisen reaction in natural products synthesis," *Synthesis* **1993**, 1120-1128.
9. Hayes, P. Y.; Kitching, W., "Total synthesis and absolute stereochemistry of plakortone D," *J. Am. Chem. Soc.* **2002**, *124*, 9718-9719.
10. Semmelhack, M. F.; Shanmugam, P., "Development of an approach to the synthesis of plakortones," *Tetrahedron Lett.* **2000**, *41*, 3567-3571.
11. Donohoe, T. J.; Fisher, J. W.; Edwards, P. J., "Synthesis of (±)-secosyrin 1 and a formal synthesis of (-)-secocyrin 1," *Organic Lett.* **2004**, *6*, 465-467.
12. Midland, S. L.; Keen, N. T.; Sims, J. J., "Secosyrins 1 and 2 and syributins 1 and 2: Novel structures produced by bacteria expressing the *avrD* Gene," *J. Org. Chem*. **1995**, *60*, 1118-1119.
13. Nicolaou, K. C.; Snyder, S. A., "The essence of total synthesis," *PNAS* **2004**, *101*, 11929-11936.
14. Tauss, A.; Wrodnigg, T. M.; Stutz, A. E., "Sophisticated products from cheap renewable sources: Simple carbohydrates in natural products synthesis," *Recent Res. Develop. Org. Chem.* **1999**, *3*, 319-342.
15. Hanessian, S., "Approaches to the total synthesis of natural products using "chiral templates" derived from carbohydrates," *Acc. Chem. Res.* **1979**, *12*, 159-165.
16. Stick, R.V. *Carbohydrates: The Sweet Molecules of Life.* Academic Press: San Diego, 2001.
17. Collins, P. M.; Ferrier, R. J. *Monosacharides: Their Chemistry and Their Roles in Natural Products.* John Wiley & Sons: Chichester, England, 1995.

18. Hanessian, S. *Preparative Carbohydrate Chemistry.* Marcel Dekker Inc.: New York, 1997.

19. Moravcova, J.; Capkova, J.; Stanek, J., "One-pot synthesis of 1,2-*O*-isopropylidene-α-D-xylofuranose," *Carbohydr. Res.* **1994**, *263*, 61-66.

20. Patai, S. *The Chemistry of the Diazonium and Diazo Groups.* John Wiley & Sons: Chichester, England, 1978.

21. Taber, D. F.; Ruckle, R. E., Jr.; Hennessy, M. J., "Mesyl azide: A superior reagent for diazo transfer," *J. Org. Chem.* **1986**, *51*, 4077-4078.

22. Padwa, A.; Sheehan, S. M.; Straub, C. S., "An isomunchnone-based method for the synthesis of highly substituted 2(1*H*)-pyridones," *J. Org. Chem.* **1999**, *64*, 8648-8659.

23. Padwa, A.; Austin, D. J., "Ligand effects on the chemoselectivity of transition metal catalyzed reactions of α-diazo carbonyl compounds," *Angew. Chem. Int. Ed. Engl.* **1994**, *33*, 1797-1815.

24. Sacui, I. A., "Synthesis and decomposition of novel diazosugars," Youngstown State University MS Thesis, 2006.

25. DeWit, D. G., "Reactivity of mononuclear rhodium(II) compounds," *Coord. Chem. Rev.* **1996**, *147*, 209-246.

26. Roos, G. H.; Raab, C. E., "Dirhodium(II) carbenes: A rich source of chiral products," *S. Afr. J. Chem.* **2001**, *54*, 1-40.

27. Candeias, N. R.; Gois, P. M. P.; Afonso, C. A. M., "Rh(II)-catalyzed intramolecular C-H insertion of diazo substrates in water: Scope and limitations," *J. Org. Chem.* **2006**, *71*, 5489-5497.

28. Aller, E.; Brown, D. S.; Cox, G. G.; Miller, D. J.; Moody, C. J., "Diasteroselectivity in the O-H insertion reactions of rhodium carbenoids derived from phenyldiazoacetates of chiral alcohols. Preparation of α-hydroxy and α-alkoxy esters," *J. Org. Chem.* **1995**, *60*, 4449-4460.

29. Doyle, M. P.; Westrum, L. J.; Wolthuis, W. N. E.; See. M. M.; Boone, W. P.; Bagheri, V.; Pearson, M. M., "Electronic and steric control in carbon-hydrogen insertion reactions of diazoacetoacetates catalyzed by dirhodium(II) carboxylates and carboxamides," *J. Am. Chem. Soc.* **1993**, *115*, 958-964.

30. Stokes, B. J.; Dong, H.; Leslie, B. E.; Pumphrey, A. L.; Driver, T. G., "Intramolecular C-H amination reactions: Exploitation of the Rh_2(II)-catalyzed decomposition of azidoacrylates," *J. Am. Chem. Soc.* **2007**, *129*, 7500-7501.

31. Wee, A. G. H.; Duncan, S. C., "The bis(trimethylsilyl)methyl group as an effective N-protecting group and site-selective control element in rhodium(II)-catalyzed reaction of diazoamides," *J. Org. Chem.* **2005**, *70*, 8372-8380.

32. Branderhorst, H. M.; Kemmink, J.; Liskamp, R. M. J.; Pieters, R. J., "Catalytic conversion of diazosugars," *Tetrahedron Lett.* **2002**, *43*, 9601-9603.

33. Berndt, D. F.; Norris, P., "Intramolecular carbene and nitrene insertion at C-2 of diacetone-D-glucose," *Tetrahedron Lett.* **2002**, *43*, 3961-3962.

34. Patai, S. *The Chemistry of the carbon-nitrogen double bond.* Interscience Publishers: London, 1970.

35. Lammertsma, K.; Prasad, B., "Imine-enamine tautomerism," *J. Am. Chem. Soc.* **1994**, *116*, 642-650.

36. Chuang, C.; Lien, M., "Computational study on the effects of substituents and functional groups in the isomerization of 1- and 2-substituted propenes, acetaldimines and aldehydes," *Eur. J. Org. Chem.* **2004**, 1432-1443.

37. Eisch, J. J.; Sanchez, R., "Selective oxophilic imination of ketones with bis(dichloroaluminum) phenylimide," *J. Org. Chem.* **1986**, *51*, 1848-1852.

38. Love, B. E.; Ren, J., "Synthesis of sterically hindered imines," *J. Org. Chem.* **1993**, *58*, 5556-5557.

39. Bowden, K.; Hiscocks, S. P.; Perjessy, A., "Ring-chain tautomerism. Part 9. 2-Acylbenzamides, 8-acyl-1-naphthalamides and 5-acyl-4-phenanthramides," *J. Chem. Soc., Perkin Trans. 2* **1998**, 291-295.

40. Valters, R.E.; Flitsch, W. *Ring-Chain Tautomerism.* Plenum Press, New York, 1985.

41. Varal, R.; Enugala, R.; Adapa, S. R., "Efficient and rapid friedlander synthesis of functionalized quinolines catalyzed by neodymium(III) nitrate hexahydrate," *Synthesis* **2006**, *22*, 3825-3830.

42. Abramovitch, R. A.; Kyba, E. P., "Thermolysis of tertiary alkyl azides," *J. Am. Chem. Soc.* **1974**, *96*, 480-488.

43. Patai, S. *The Chemistry of the Azido Group*. Interscience Publishers: London, 1971.

44. Brase, S.; Gil, C.; Knepper, K.; Zimmerman, V., "Organic azides: An exploding diversity of a unique class of compounds," *Angew. Chem. Int. Ed.* **2005**, *44*, 5188-5240.

45. Hotha, S.; Anegundi, R. I.; Natu, A., "Expedient synthesis of 1,2,3-triazole-fused tetracyclic compounds by intramolecular Huisgen ('click') reactions on carbohydrate-derived azido-alkynes," *Tetrahedron Lett.* **2005**, *46*, 4585-4588.

46. Wang, P.; Adams, J., " Model studies of the stereoelectronic effect in Rh(II) mediated carbenoid C-H insertion reactions," *J. Am. Chem. Soc.* **1994**, *116*, 3296-3305.

Appendix A

NMR, IR and Mass Spectra

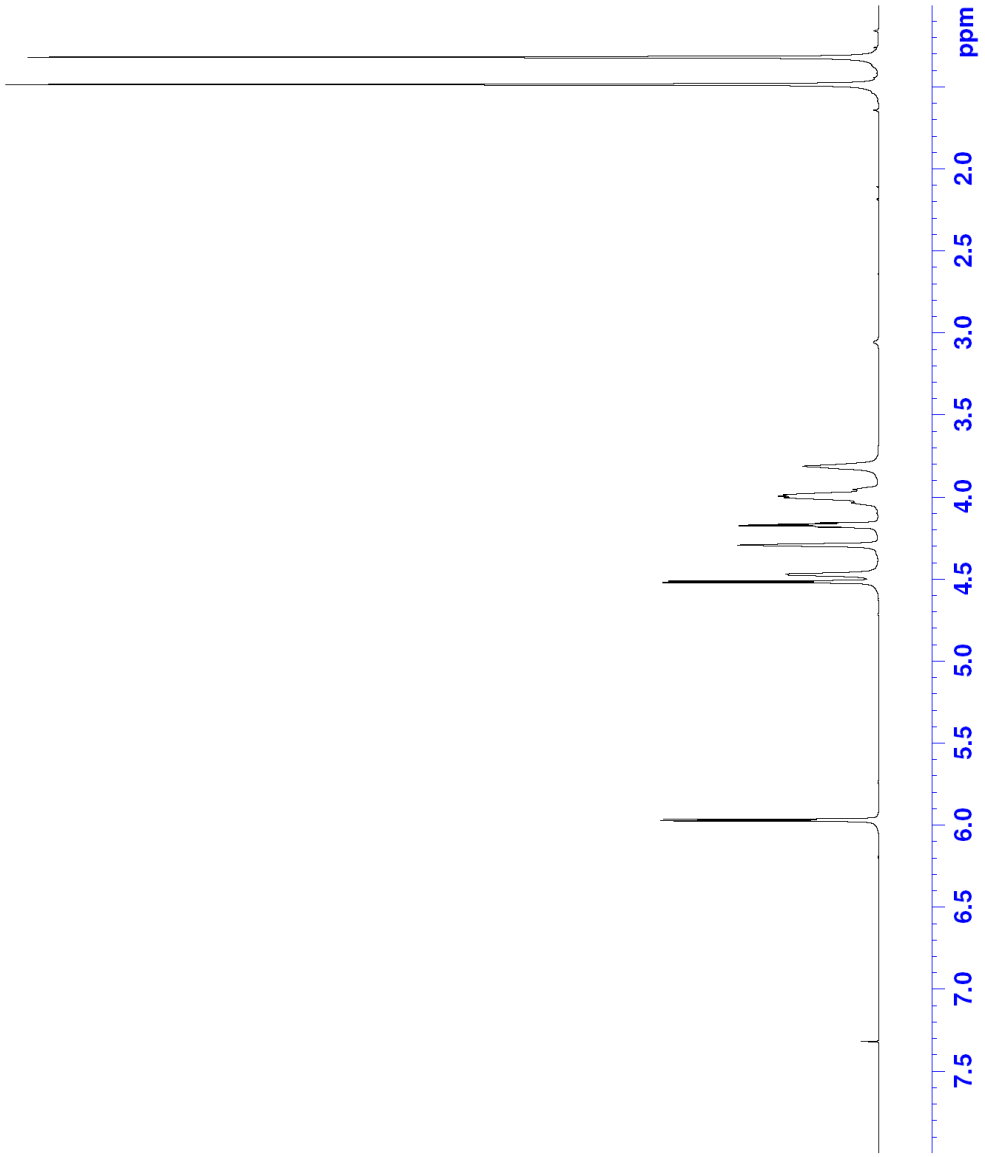

Figure 19: ^{1}H NMR spectrum of 1,2-*O*-isopropylidene-α-D-xylofuranose (**1**).

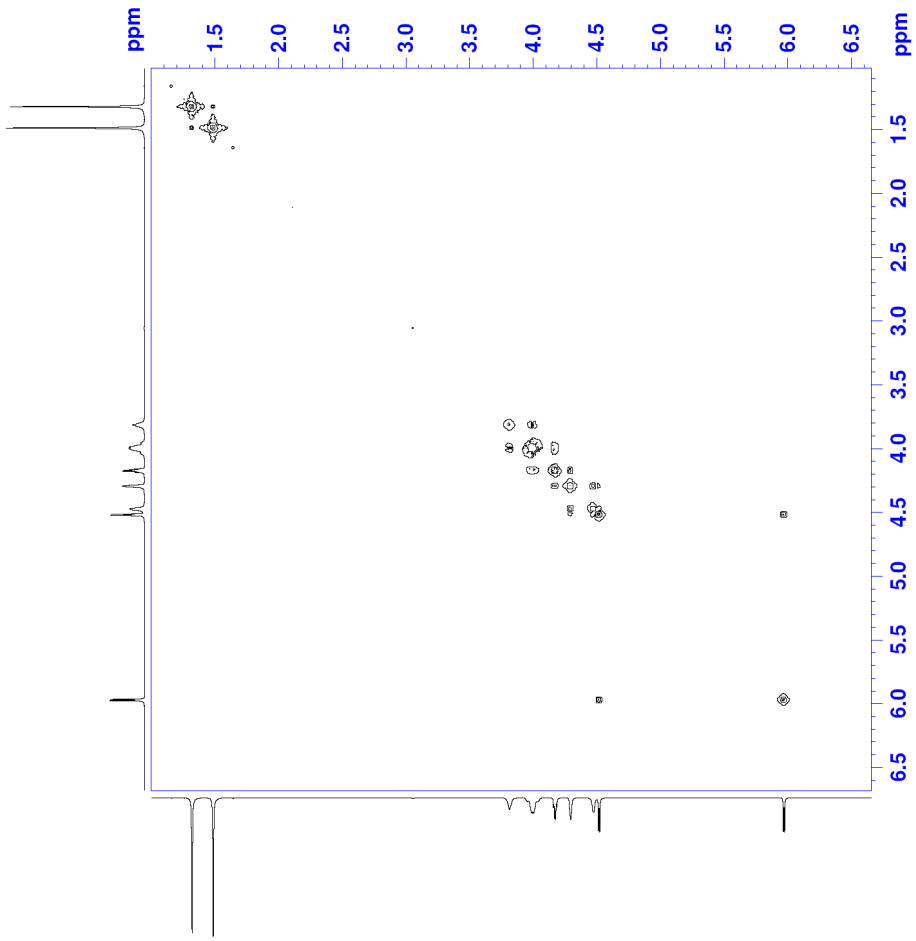

Figure 20: COSY NMR spectrum of 1,2-*O*-isopropylidene-α-D-xylofuranose (**1**).

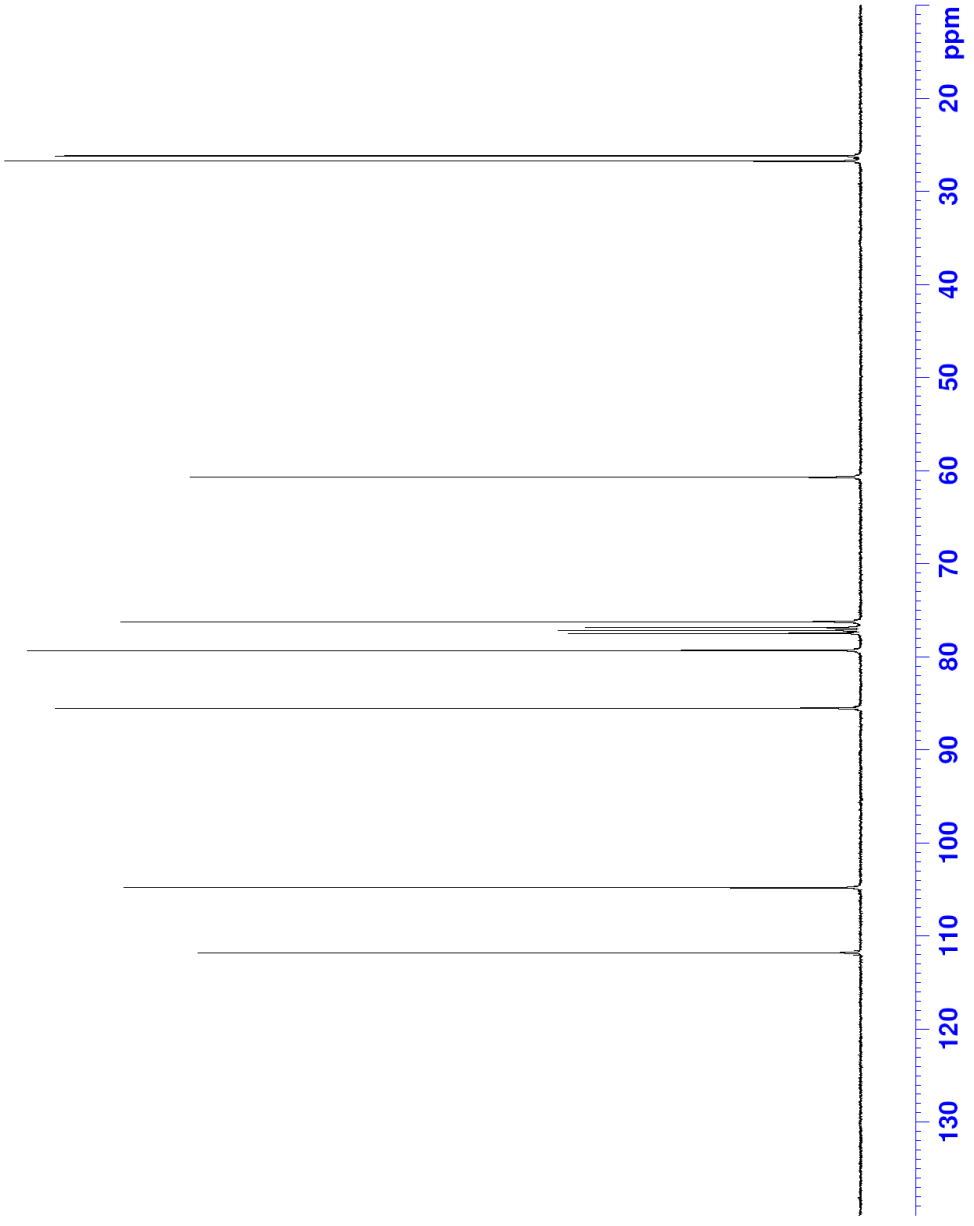

Figure 21: ^{13}C NMR spectrum of 1,2-*O*-isopropylidene-α-D-xylofuranose (**1**).

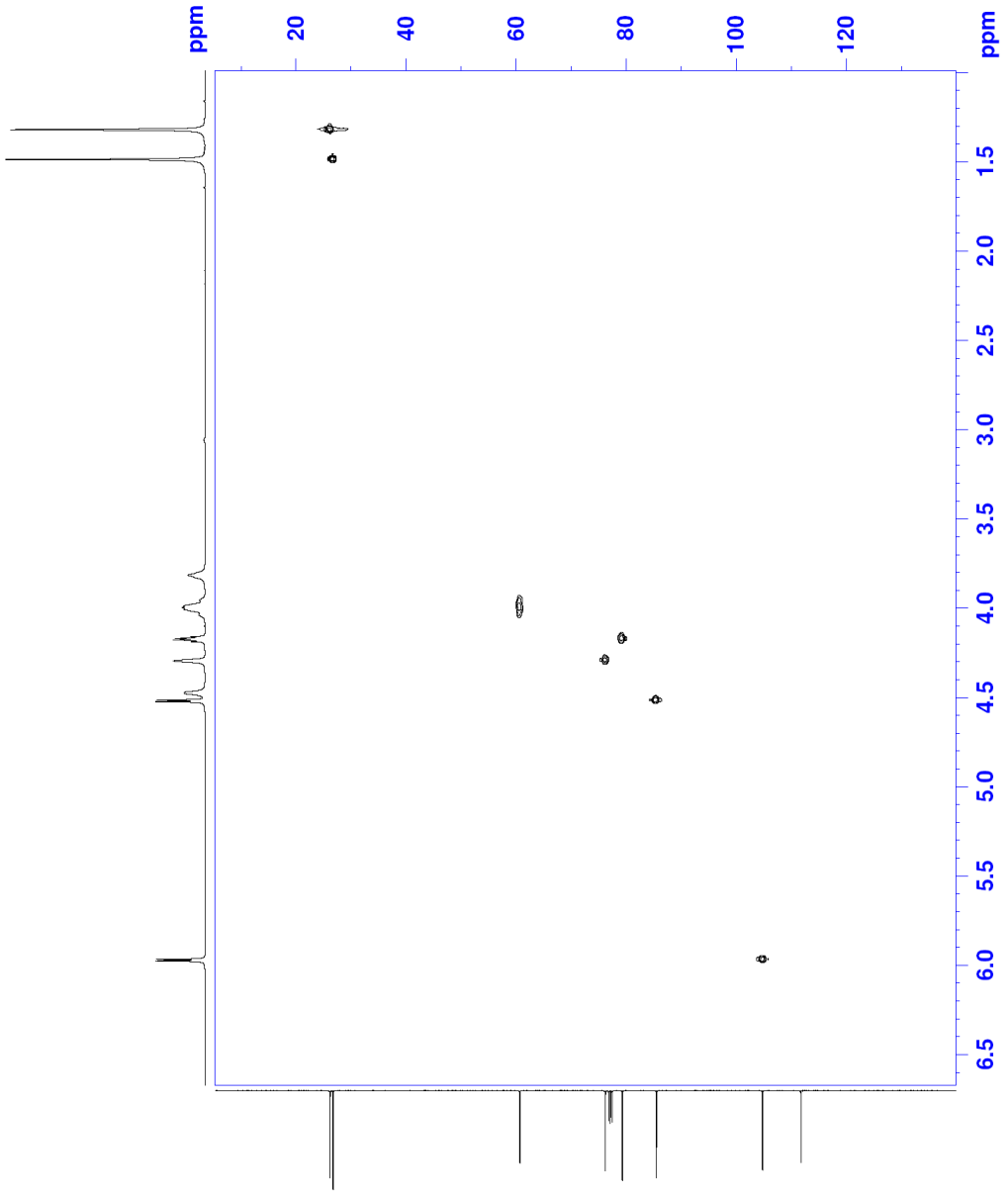

Figure 22: HSQC NMR spectrum of 1,2-*O*-isopropylidene-α-D-xylofuranose (**1**).

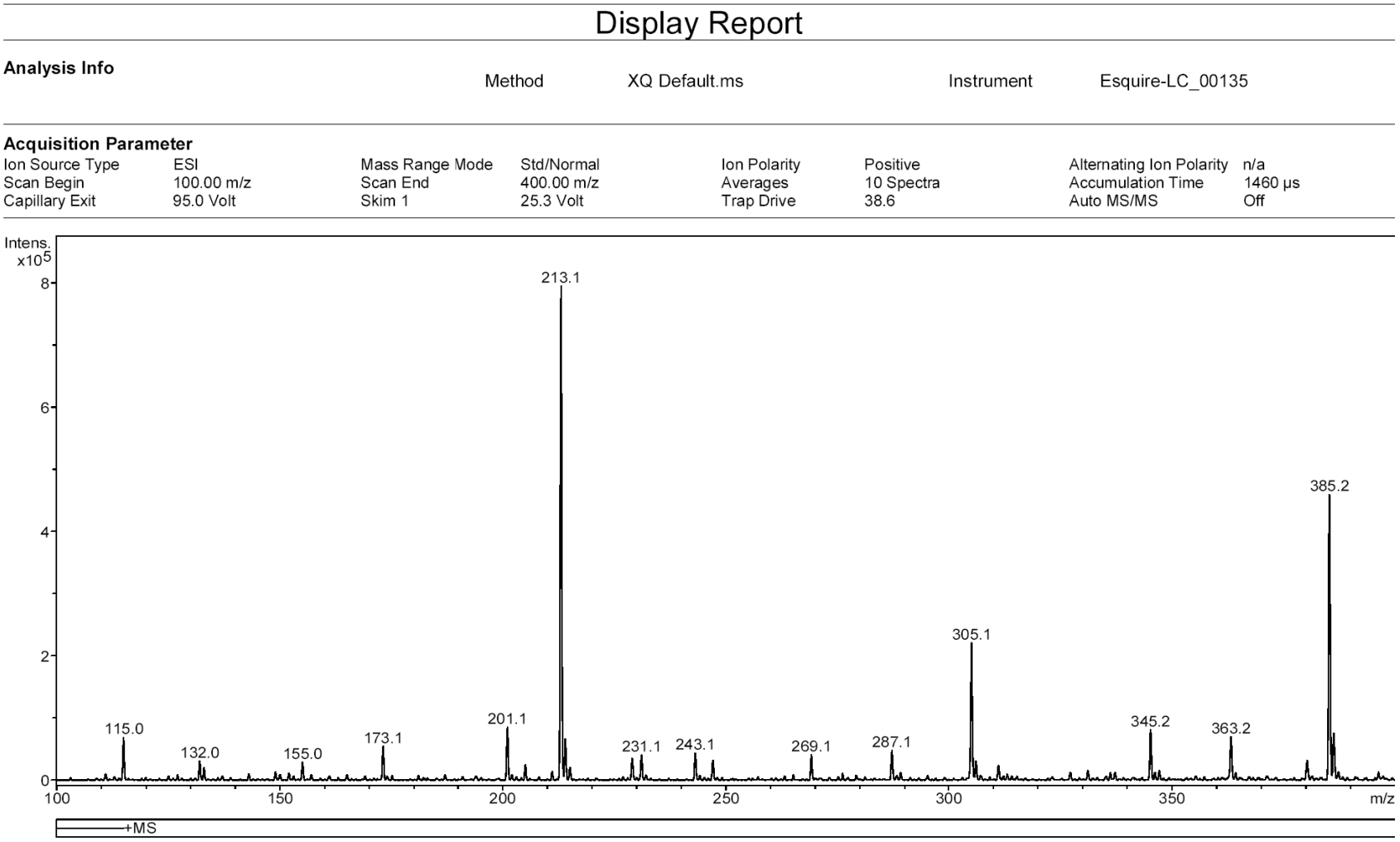

Figure 23: Mass spectrum of 1,2-*O*-isopropylidene-α-D-xylofuranose (**1**).

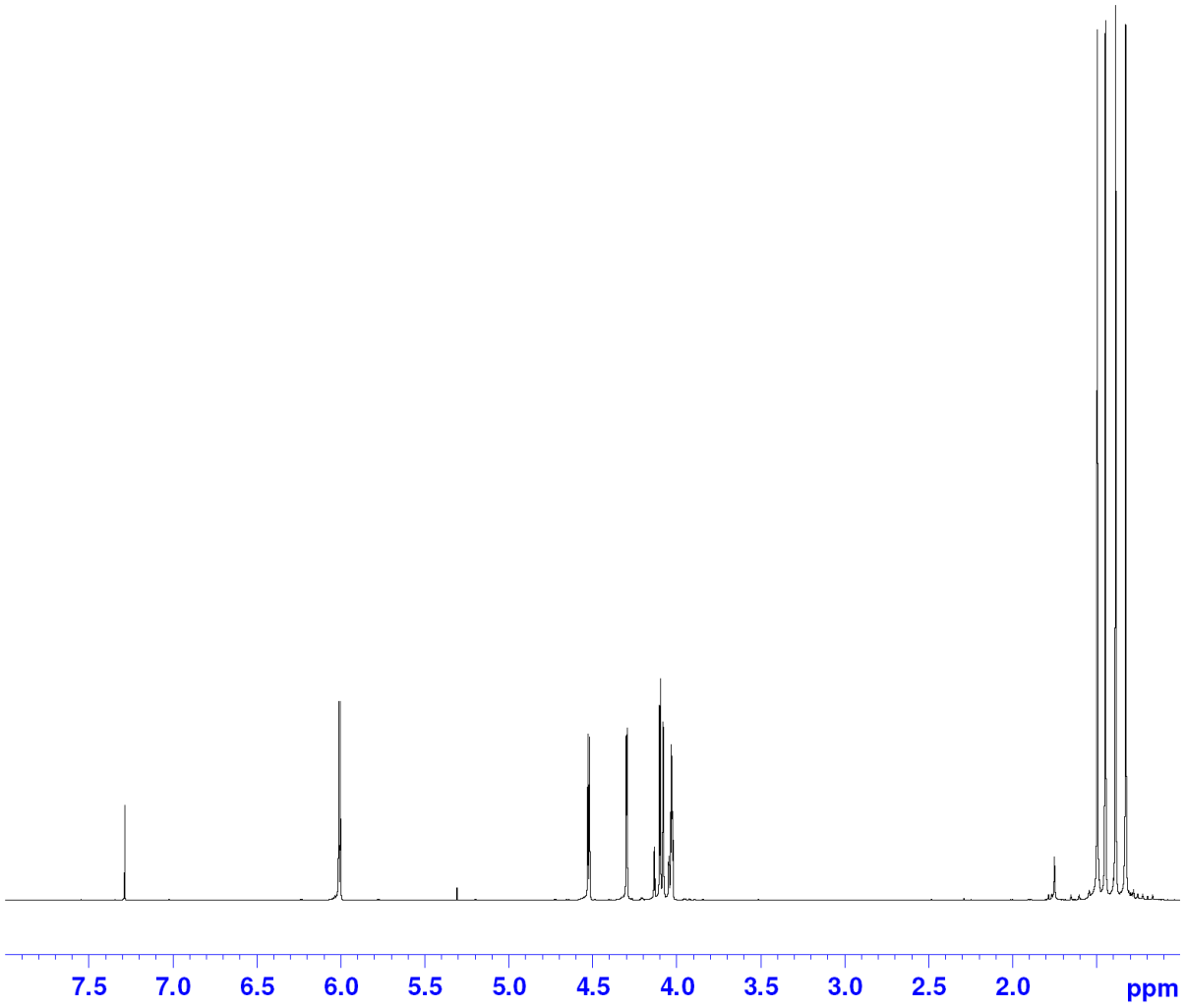

Figure 24: ^{1}H NMR spectrum of 1,2;5,6-di-*O*-isopropylidene-α-D-xylofuranose (**2**).

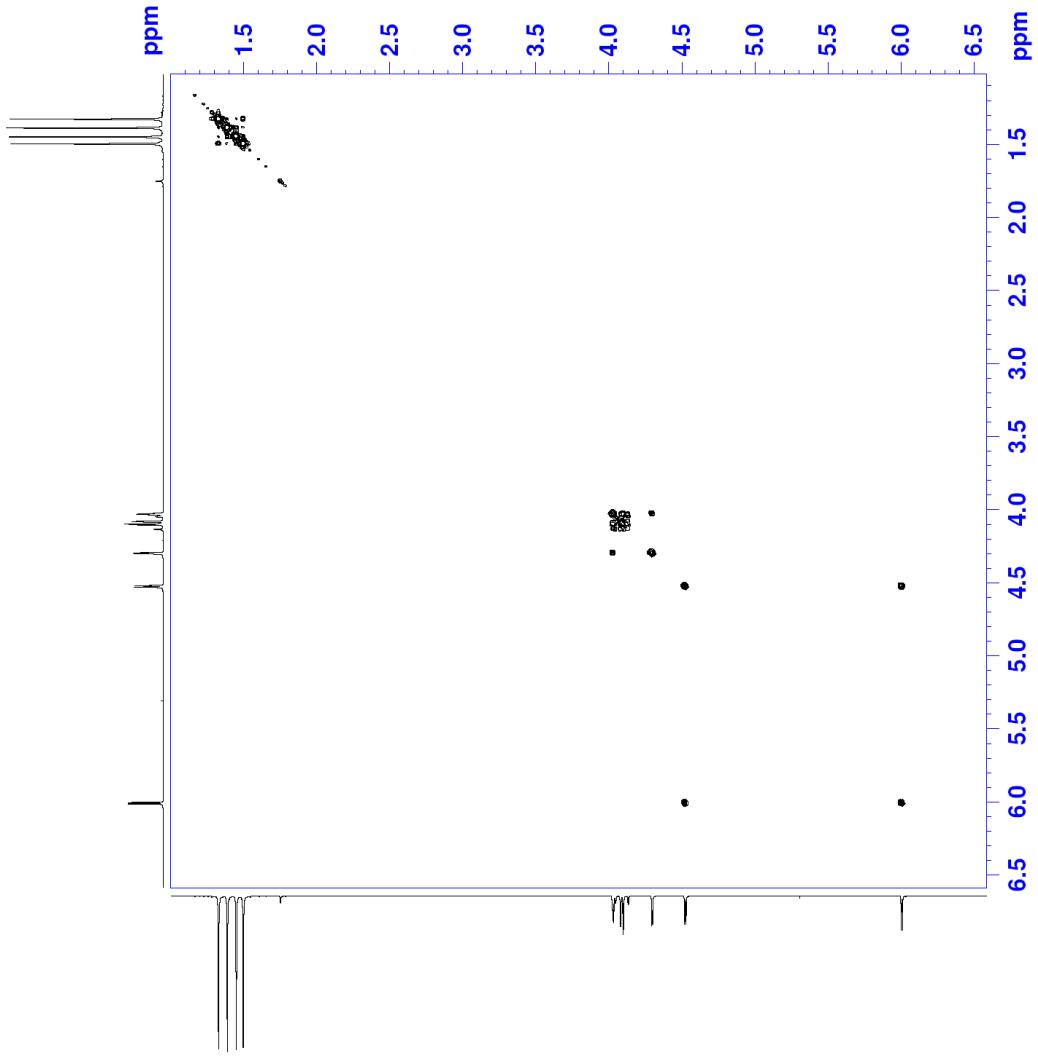

Figure 25: COSY NMR spectrum of 1,2;5,6-di-*O*-isopropylidene-α-D-xylofuranose (**2**).

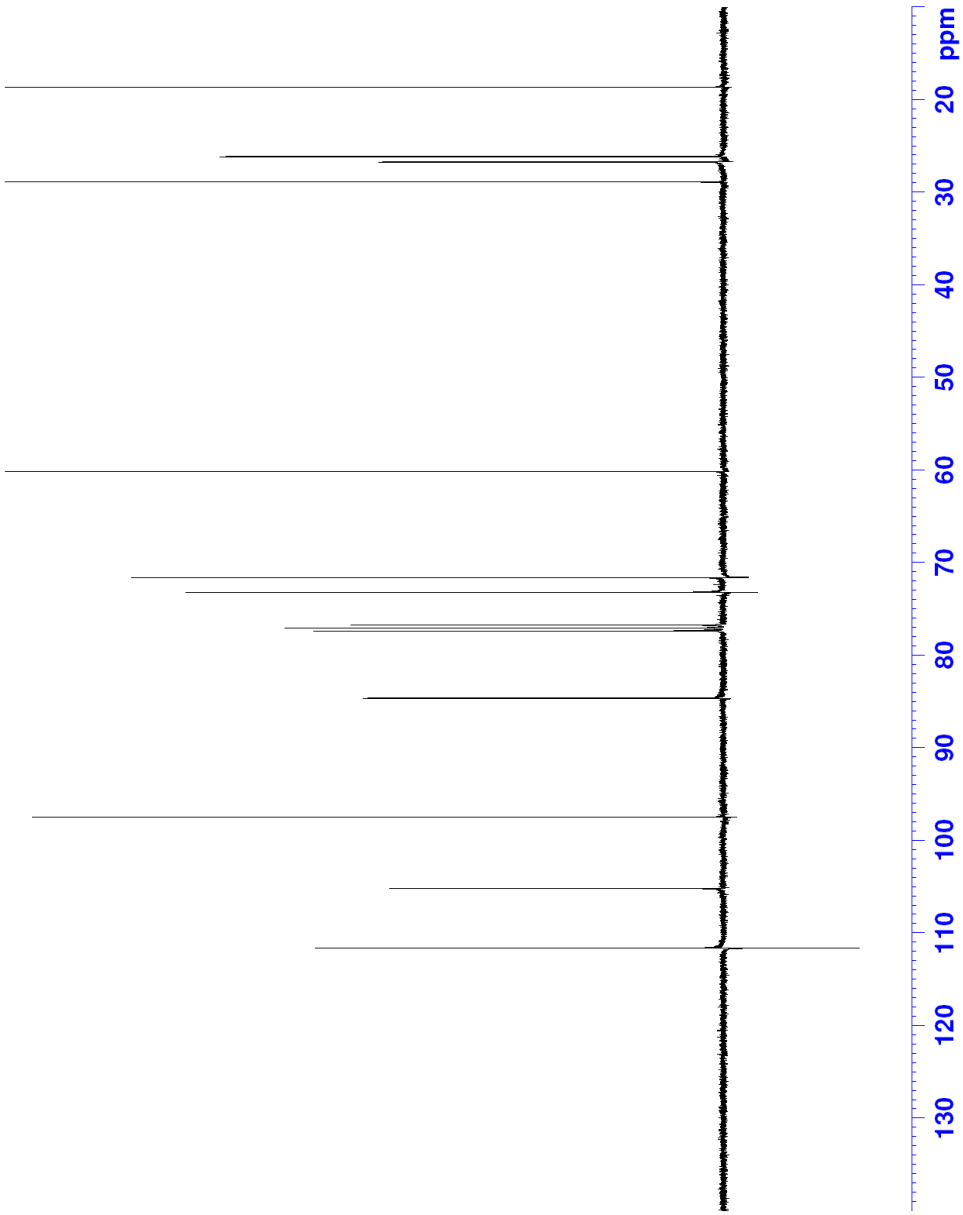

Figure 26: ^{13}C NMR spectrum of 1,2;5,6-di-*O*-isopropylidene-α-D-xylofuranose (**2**).

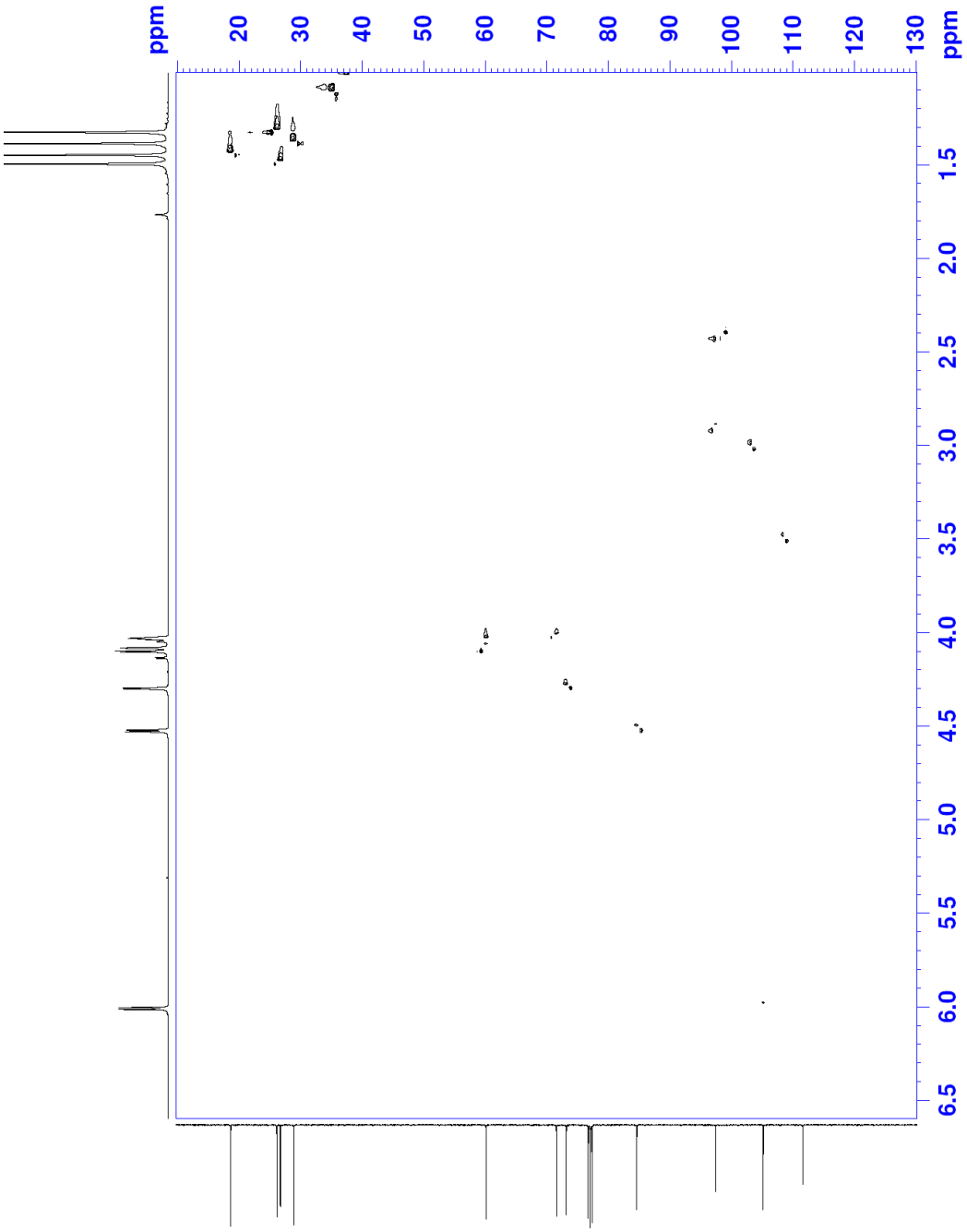

Figure 27: HSQC NMR spectrum of 1,2;5,6-di-*O*-isopropylidene-α-D-xylofuranose (**2**).

Display Report

Analysis Info

Method XQ Default.ms Instrument Esquire-LC_00135

Acquisition Parameter

Ion Source Type	ESI	Mass Range Mode	Std/Normal	Ion Polarity	Positive	Alternating Ion Polarity	n/a
Scan Begin	100.00 m/z	Scan End	500.00 m/z	Averages	10 Spectra	Accumulation Time	8786 µs
Capillary Exit	94.4 Volt	Skim 1	24.9 Volt	Trap Drive	43.7	Auto MS/MS	Off

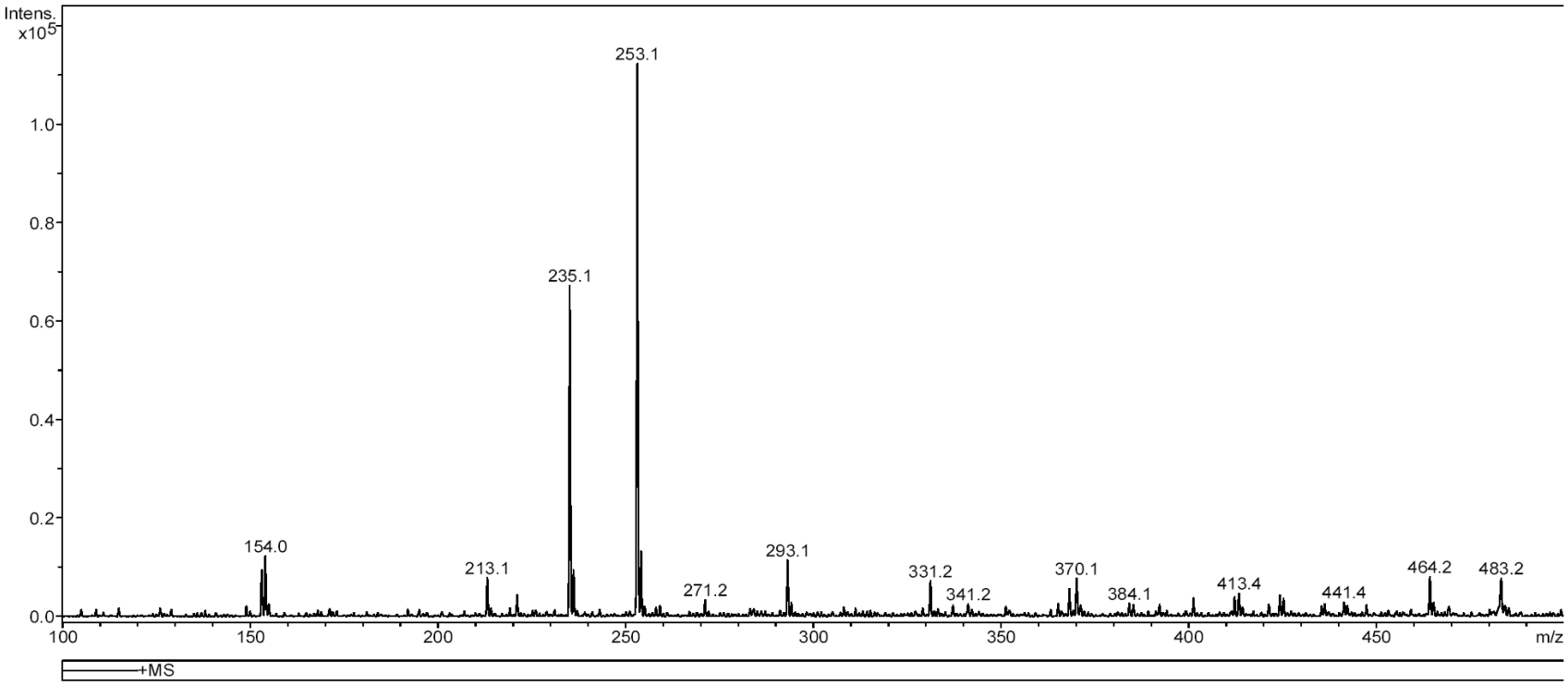

Figure 28: Mass spectrum of 1,2;5,6-di-*O*-isopropylidene-α-D-xylofuranose (**2**).

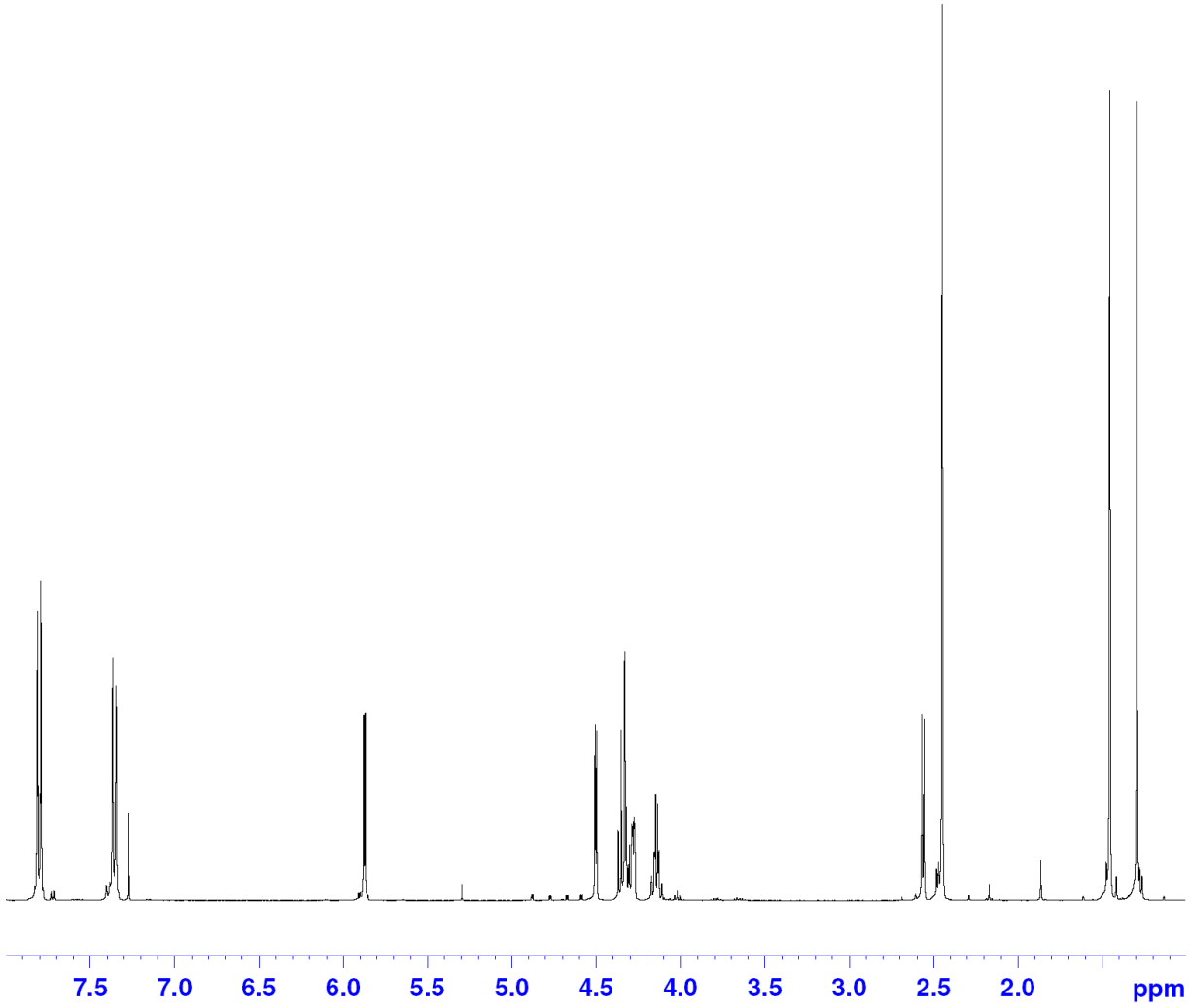

Figure 29: [1]H NMR spectrum of 5-*O*-(4-methylbenzenesulfonyl)-1,2-*O*-isopropylidene-α-D-xylofuranose (**3**).

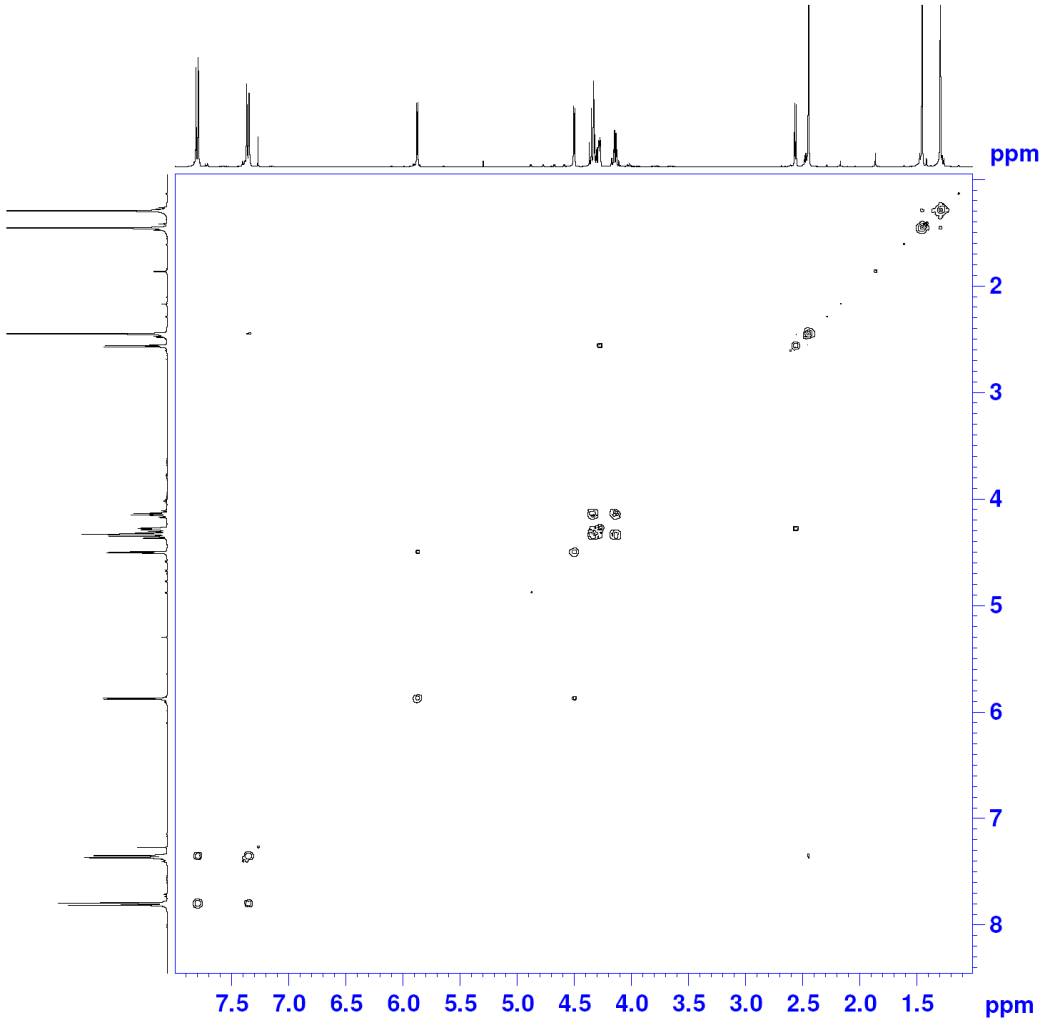

Figure 30: COSY NMR spectrum of 5-*O*-(4-methylbenzenesulfonyl)-1,2-*O*-isopropylidene-α-D-xylofuranose (**3**).

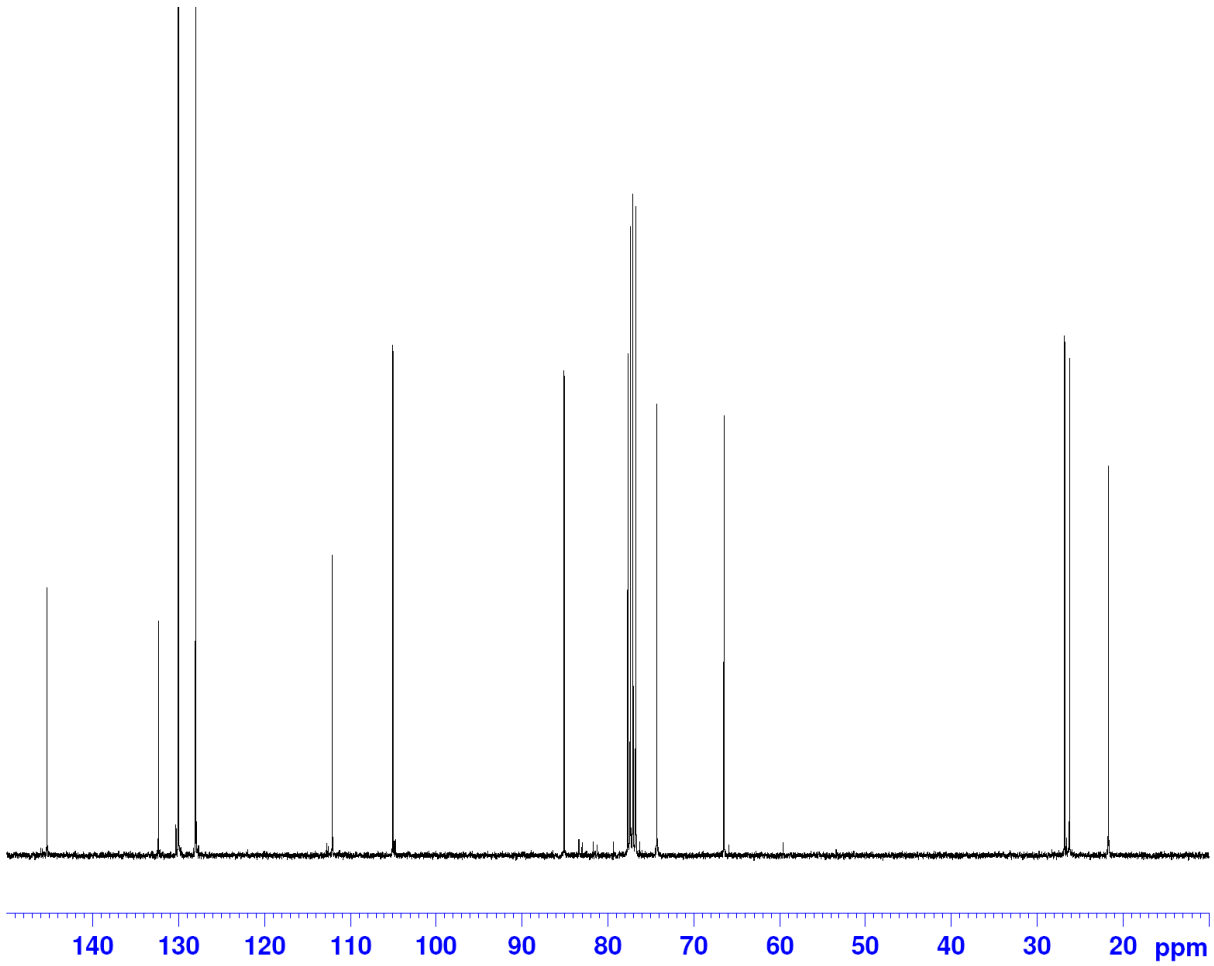

Figure 31: ^{13}C NMR spectrum of 5-*O*-(4-methylbenzenesulfonyl)-1,2-*O*-isopropylidene-α-D-xylofuranose (**3**).

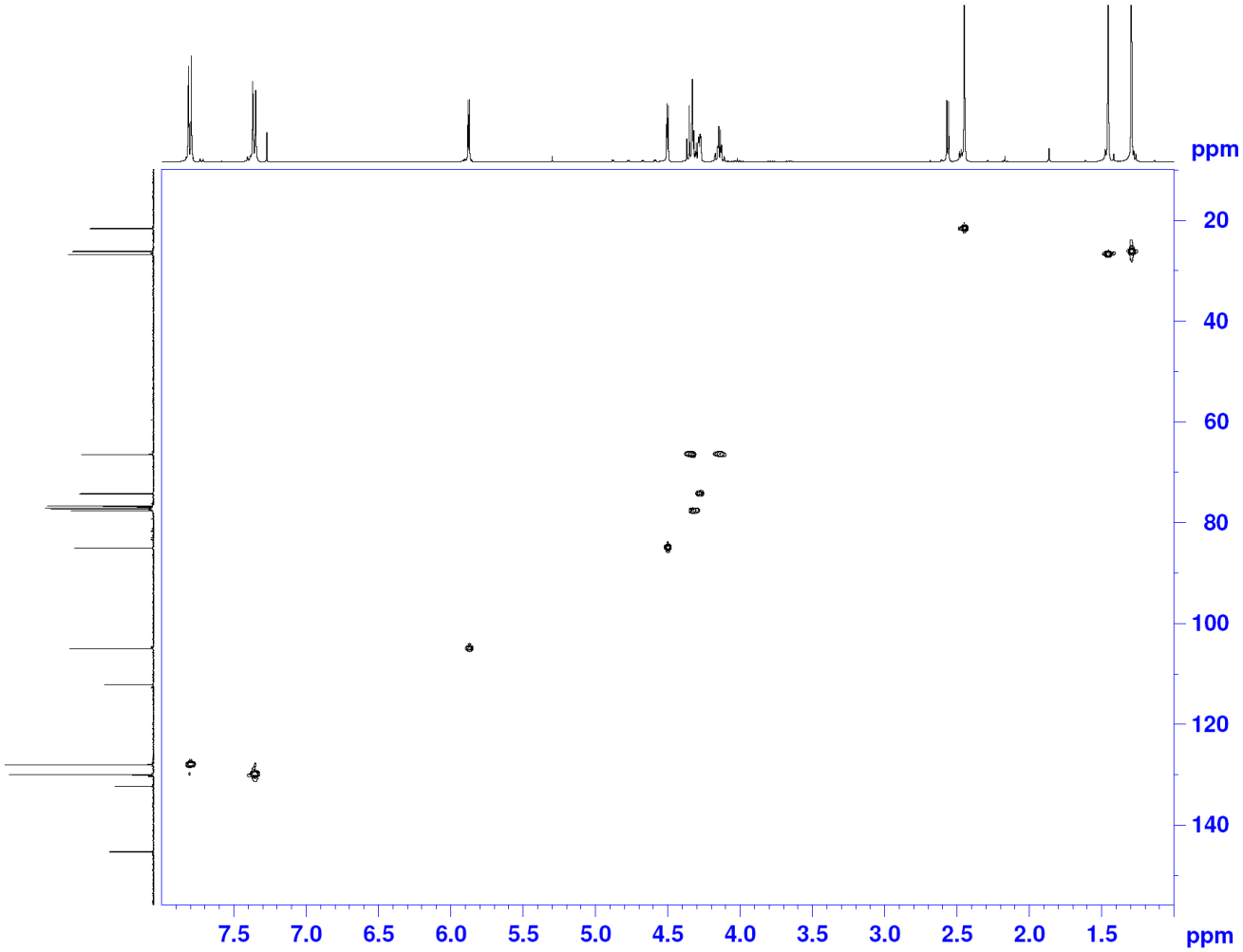

Figure 32: HSQC NMR spectrum of 5-*O*-(4-methylbenzenesulfonyl)-1,2-*O*-isopropylidene-α-D-xylofuranose (**3**).

Display Report

Analysis Info

Method XQ Default.ms Instrument Esquire-LC_00135

Acquisition Parameter

Ion Source Type	ESI	Mass Range Mode	Std/Normal	Ion Polarity	Positive	Alternating Ion Polarity	n/a
Scan Begin	200.00 m/z	Scan End	500.00 m/z	Averages	10 Spectra	Accumulation Time	873 µs
Capillary Exit	108.6 Volt	Skim 1	35.3 Volt	Trap Drive	41.5	Auto MS/MS	Off

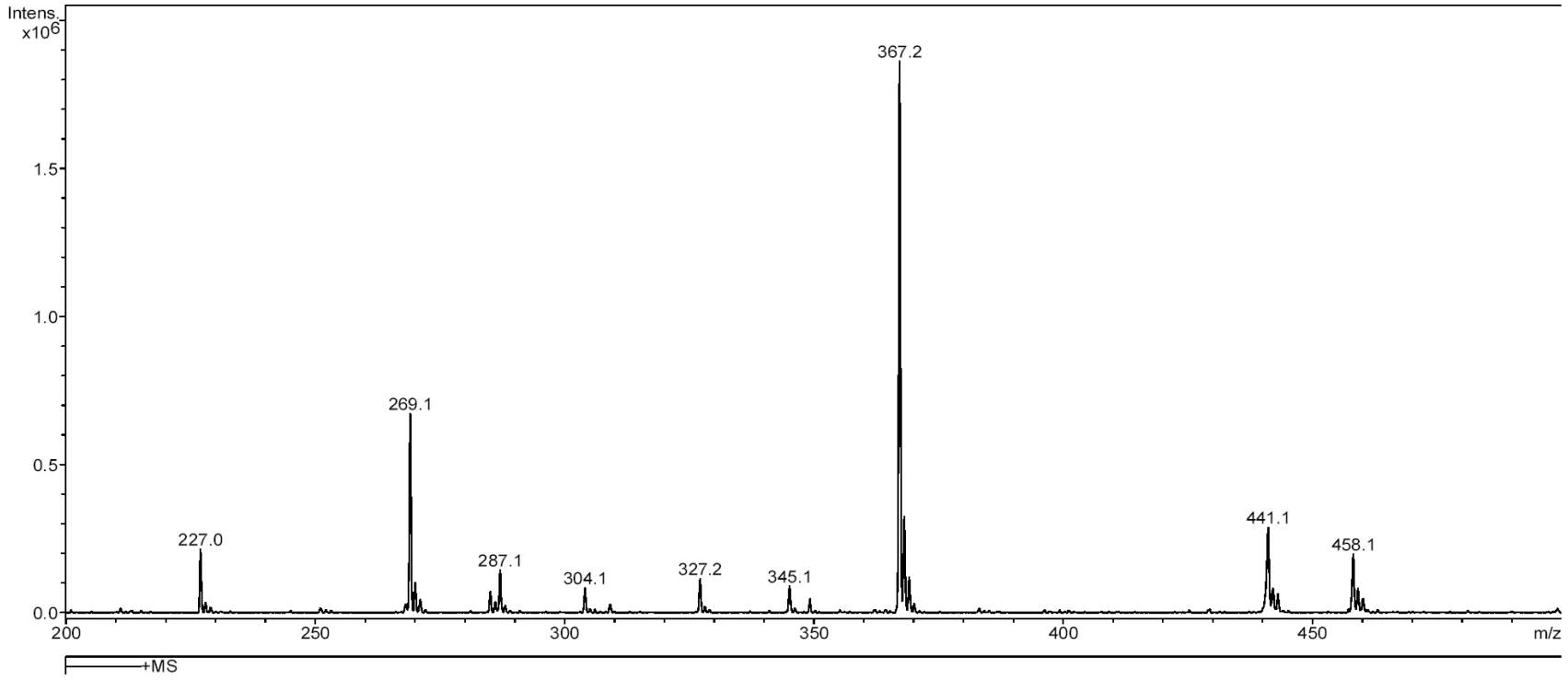

Figure 33: Mass spectrum of 5-*O*-(4-methylbenzenesulfonyl)-1,2-*O*-isopropylidene-α-D-xylofuranose (**3**).

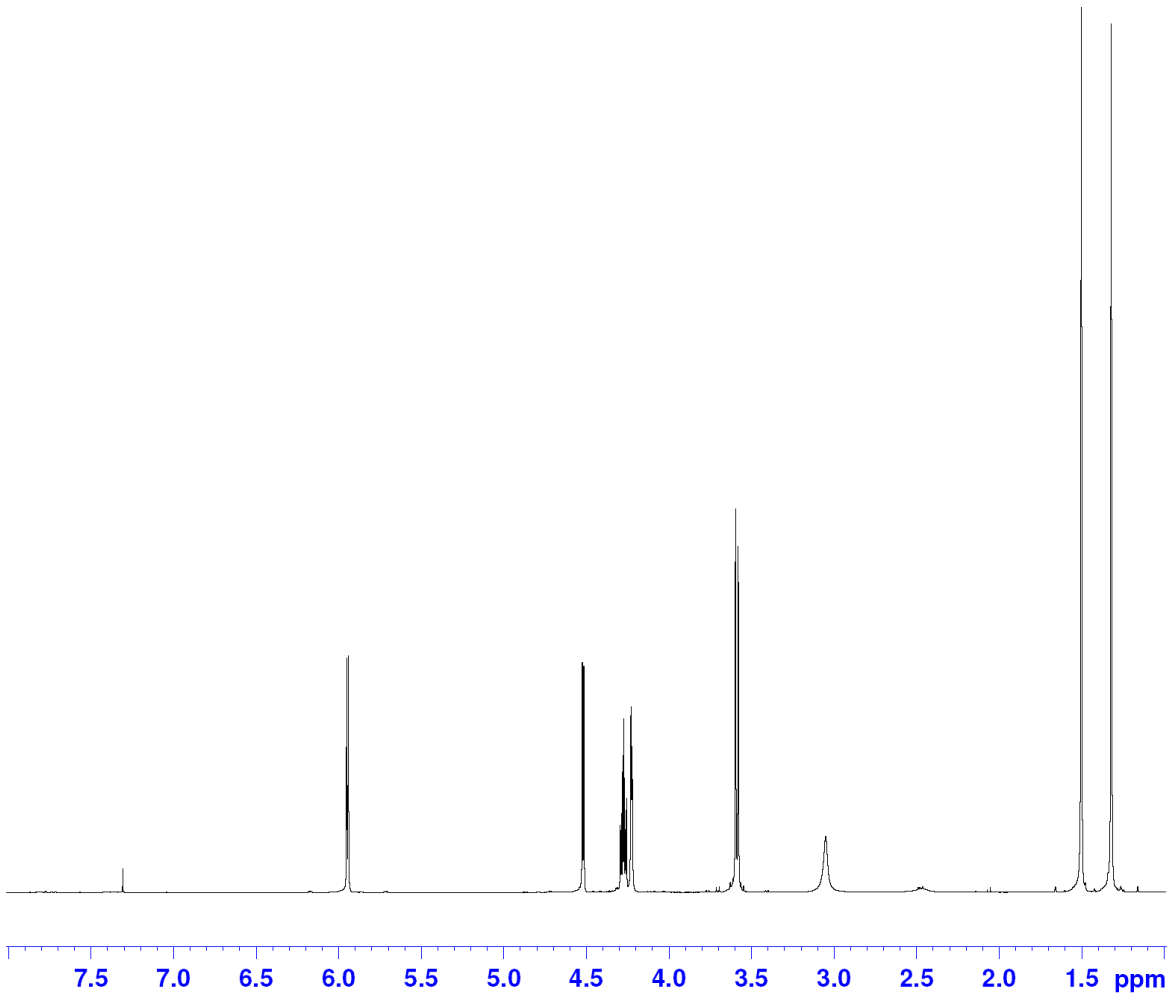

Figure 34: ^{1}H NMR spectrum of 5-azidodeoxy-1,2-*O*-isopropylidene-α-D-xylofuranose (**4**).

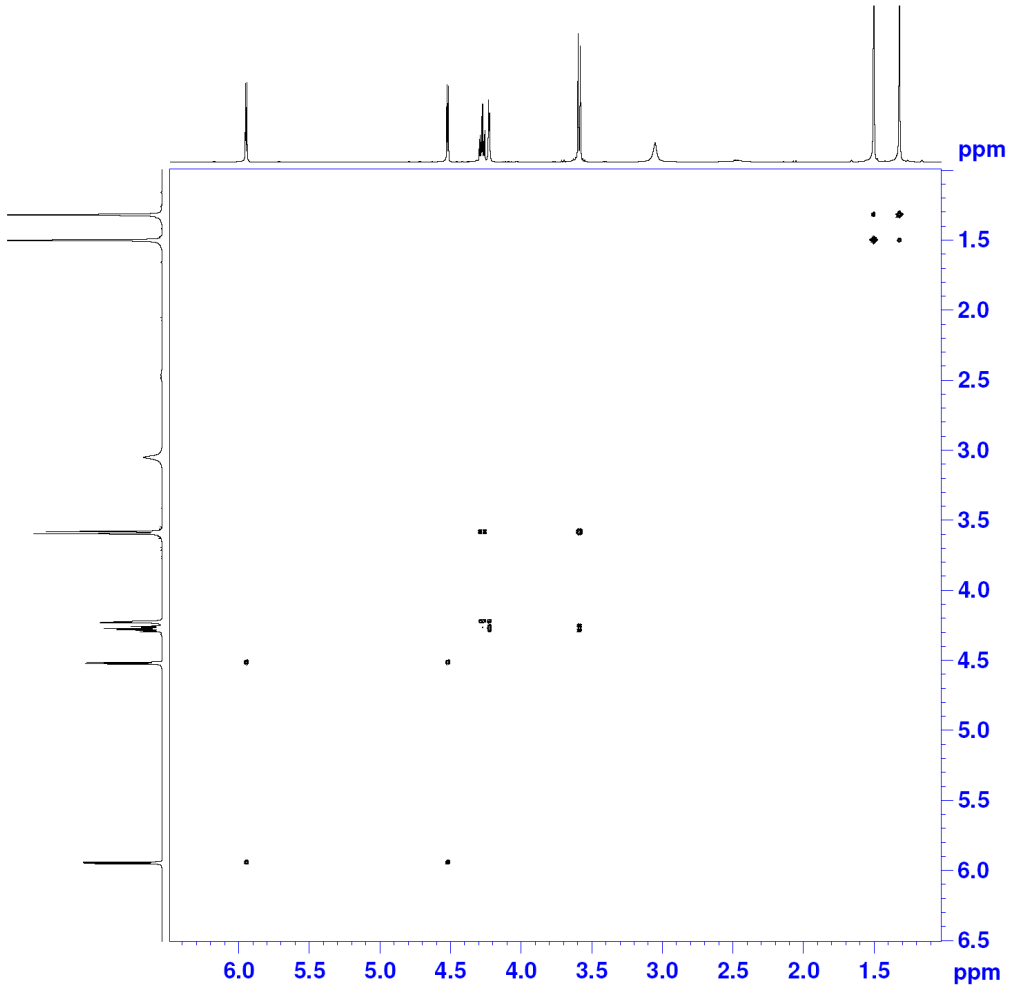

Figure 35: COSY NMR spectrum of 5-azidodeoxy-1,2-*O*-isopropylidene-α-D-xylofuranose (**4**).

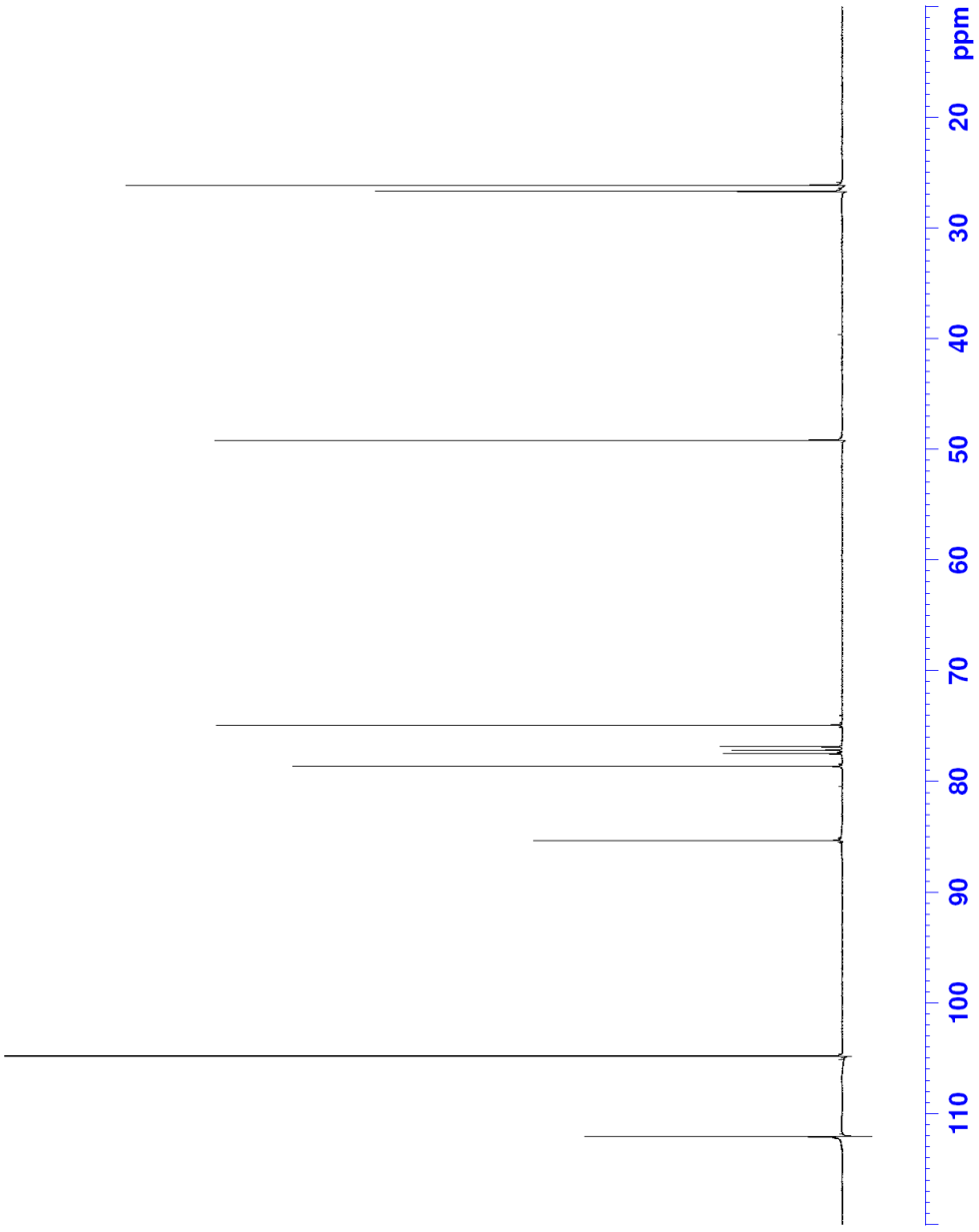

Figure 36: ^{13}C NMR spectrum of 5-azidodeoxy-1,2-*O*-isopropylidene-α-D-xylofuranose (**4**).

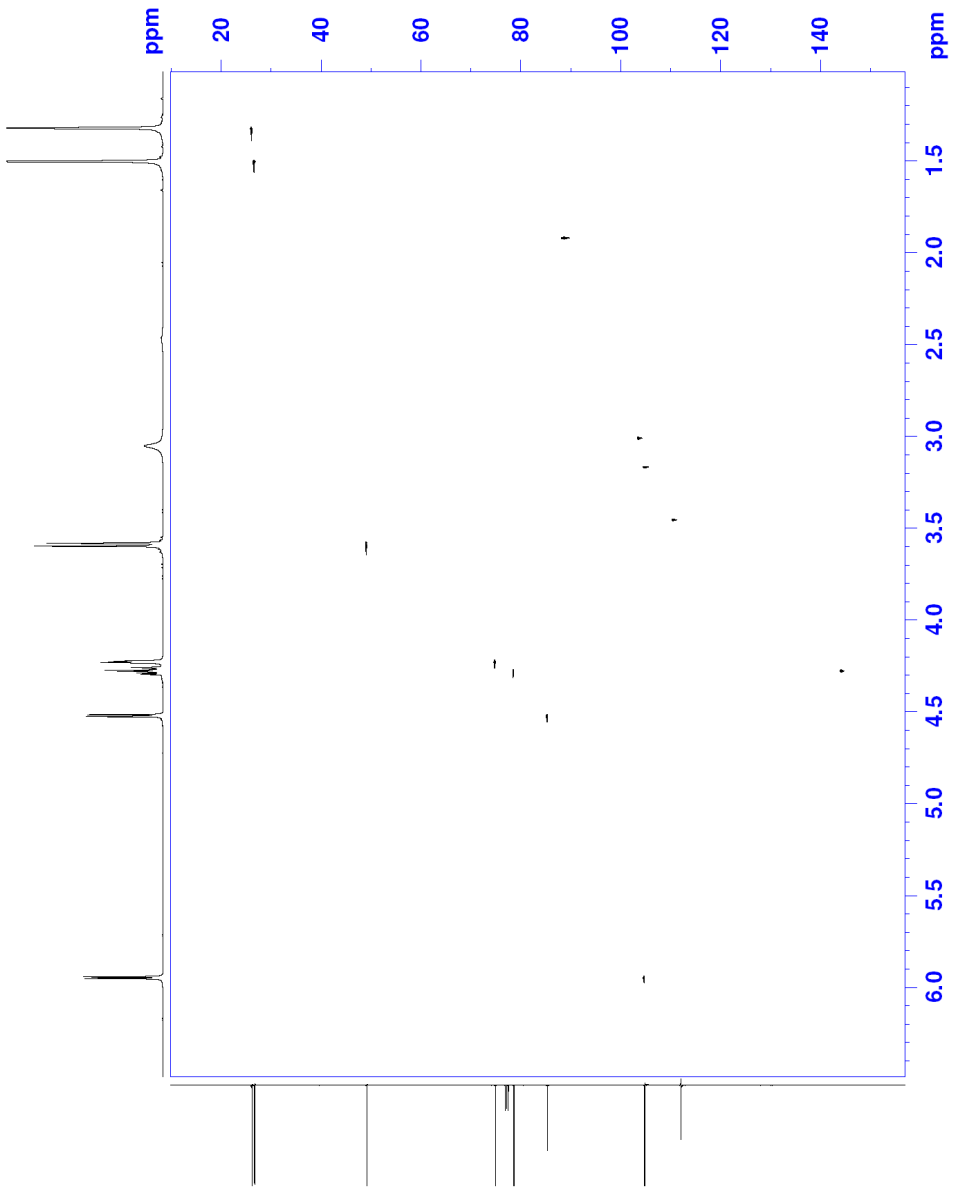

Figure 37: HSQC NMR spectrum of 5-azidodeoxy-1,2-*O*-isopropylidene-α-D-xylofuranose (**4**).

Display Report

Analysis Info

Method XQ Default.ms Instrument Esquire-LC_00135

Acquisition Parameter

Ion Source Type	ESI	Mass Range Mode	Std/Normal	Ion Polarity	Positive	Alternating Ion Polarity	n/a
Scan Begin	100.00 m/z	Scan End	340.00 m/z	Averages	5 Spectra	Accumulation Time	31865 µs
Capillary Exit	76.3 Volt	Skim 1	10.2 Volt	Trap Drive	43.2	Auto MS/MS	Off

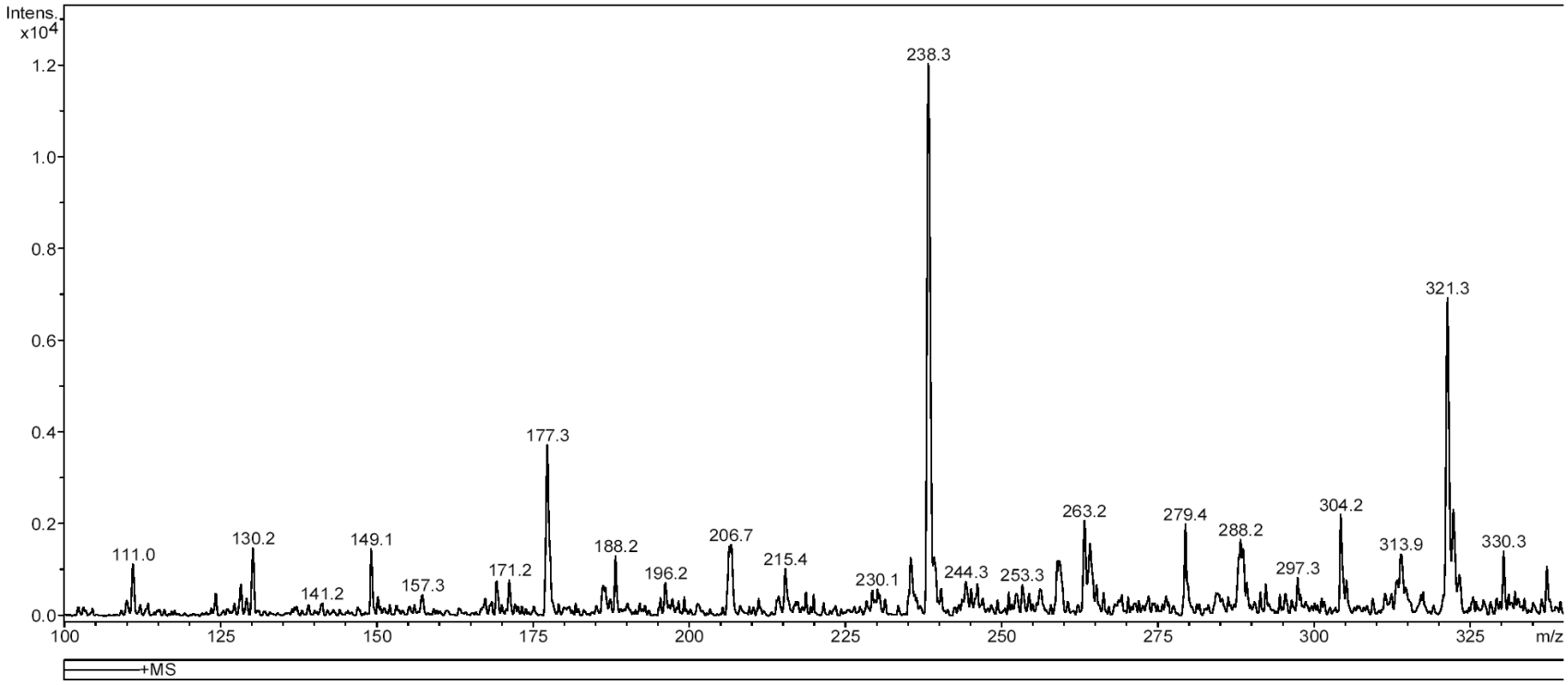

Figure 38: Mass spectrum of 5-azidodeoxy-1,2-*O*-isopropylidene-α-D-xylofuranose (**4**).

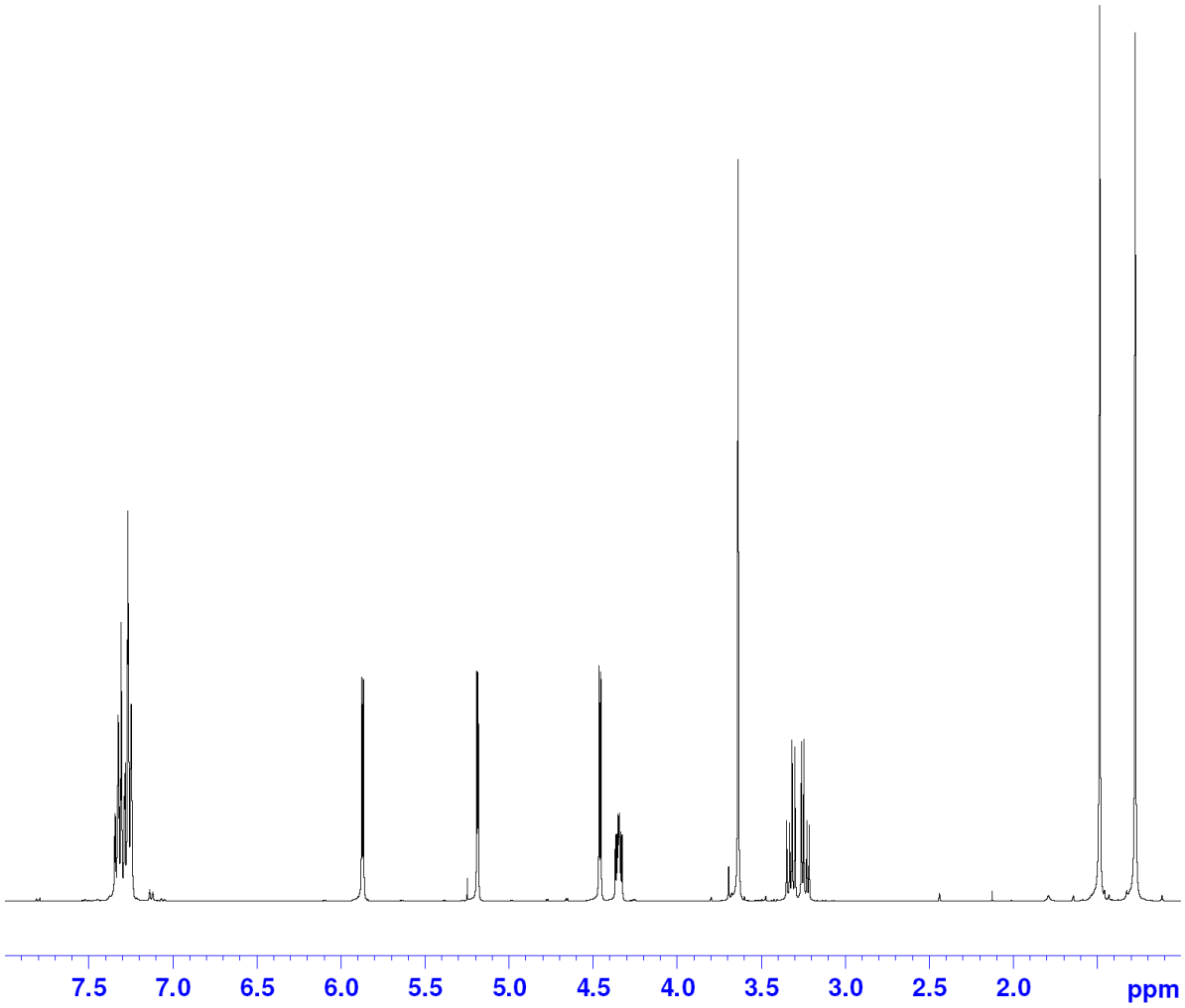

Figure 39: ^{1}H NMR spectrum of 3-*O*-(2-phenylacetyl)-5-azidodeoxy-1,2-*O*-isopropylidene-α-D-xylofuranose (**5**).

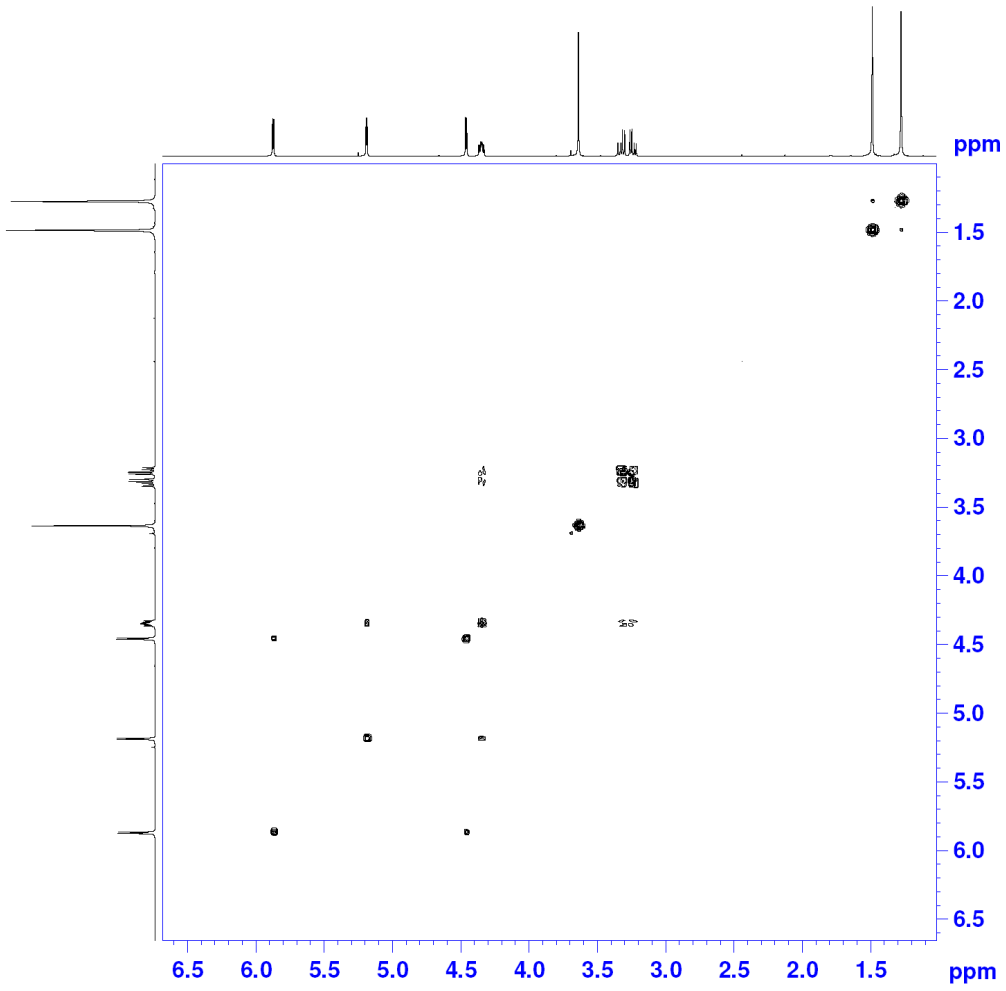

Figure 40: COSY NMR spectrum of 3-*O*-(2-phenylacetyl)-5-azidodeoxy-1,2-*O*-isopropylidene-α-D-xylofuranose (**5**).

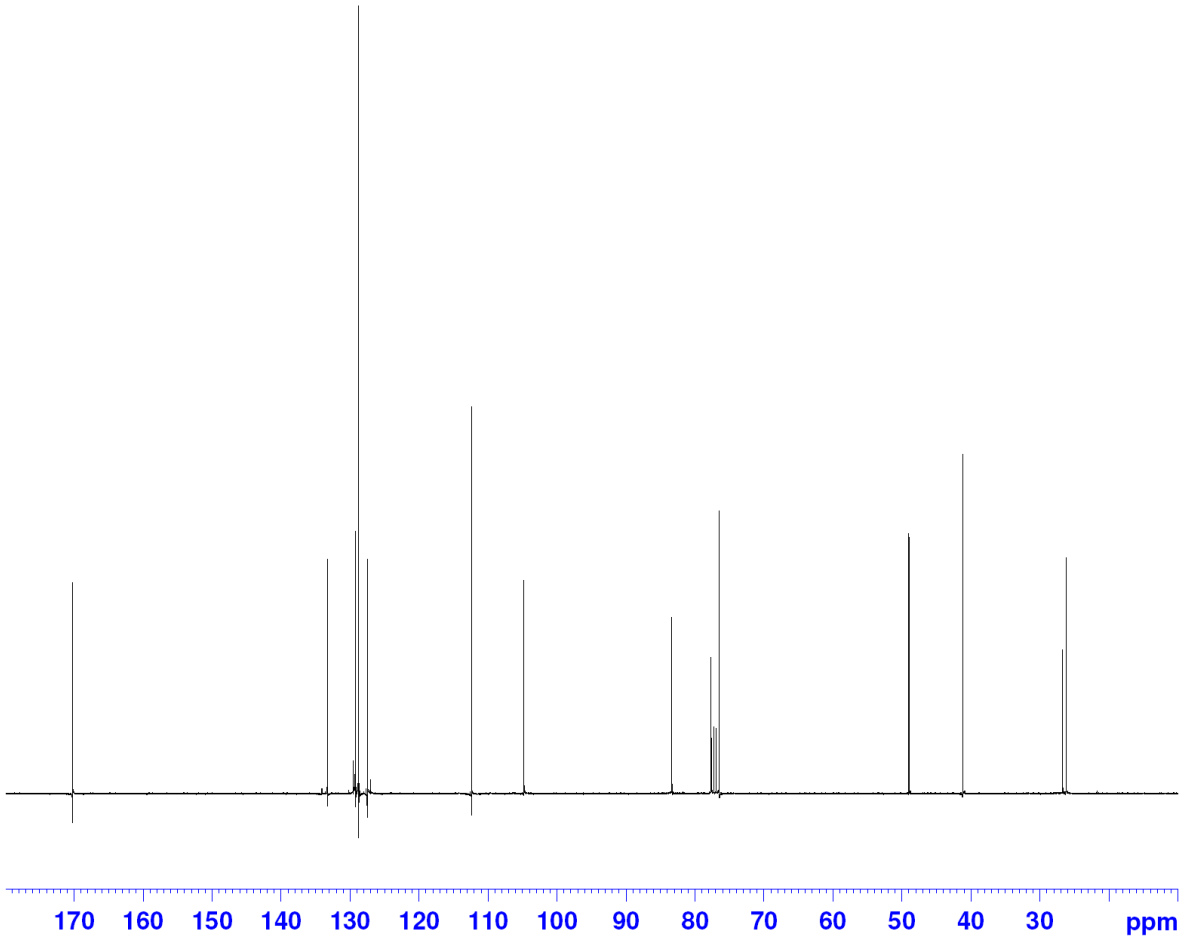

Figure 41: ^{13}C NMR spectrum of 3-*O*-(2-phenylacetyl)-5-azidodeoxy-1,2-*O*-isopropylidene-α-D-xylofuranose (**5**).

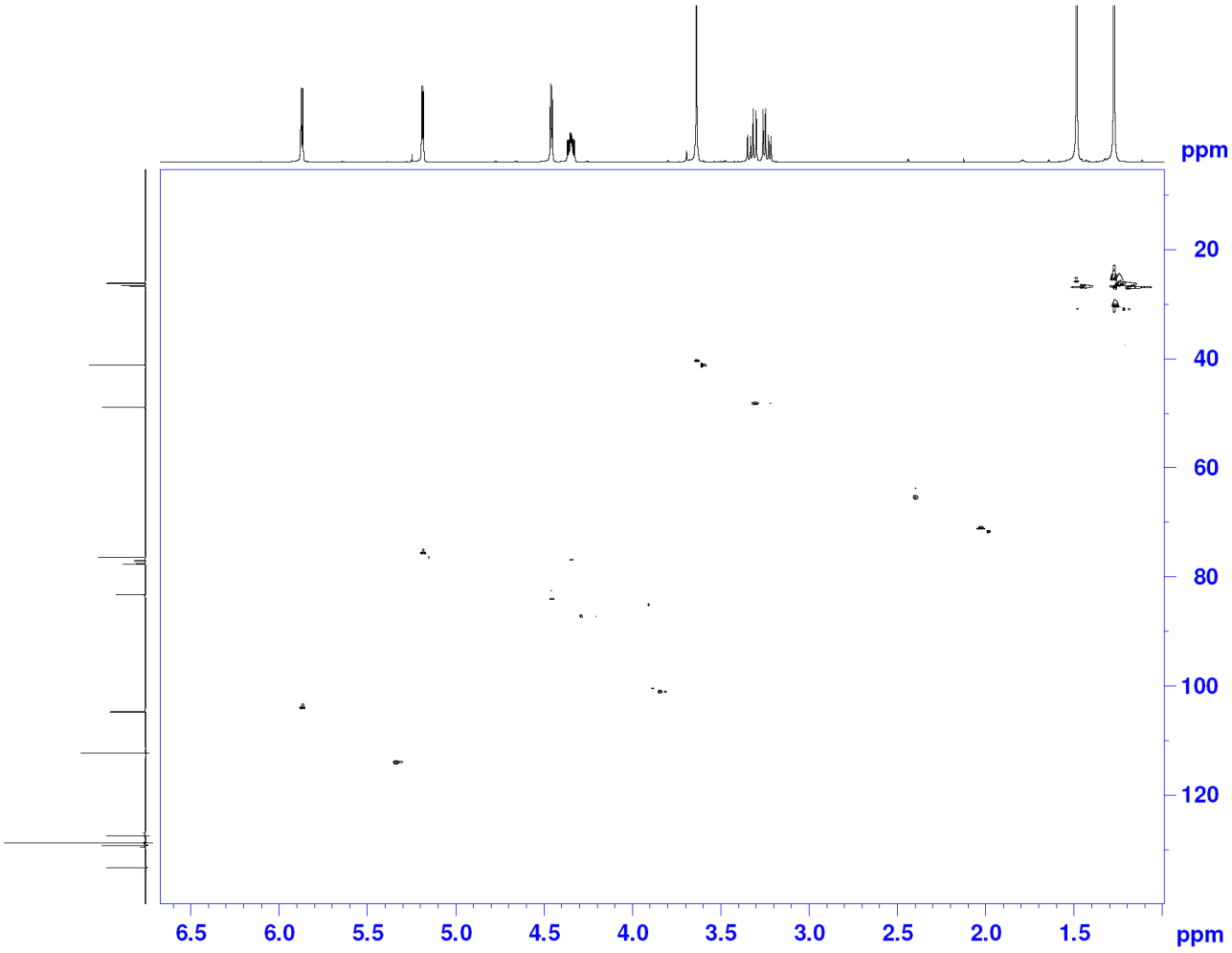

Figure 42: HSQC NMR spectrum of -*O*-(2-phenylacetyl)-5-azidodeoxy-1,2-*O*-isopropylidene-α-D-xylofuranose (**5**).

Display Report

Analysis Info

Method	XQ Default.ms	Instrument	Esquire-LC_00135

Acquisition Parameter

Ion Source Type	ESI	Mass Range Mode	Std/Normal	Ion Polarity	Positive	Alternating Ion Polarity	n/a
Scan Begin	100.00 m/z	Scan End	400.00 m/z	Averages	5 Spectra	Accumulation Time	5341 µs
Capillary Exit	107.7 Volt	Skim 1	34.6 Volt	Trap Drive	47.7	Auto MS/MS	Off

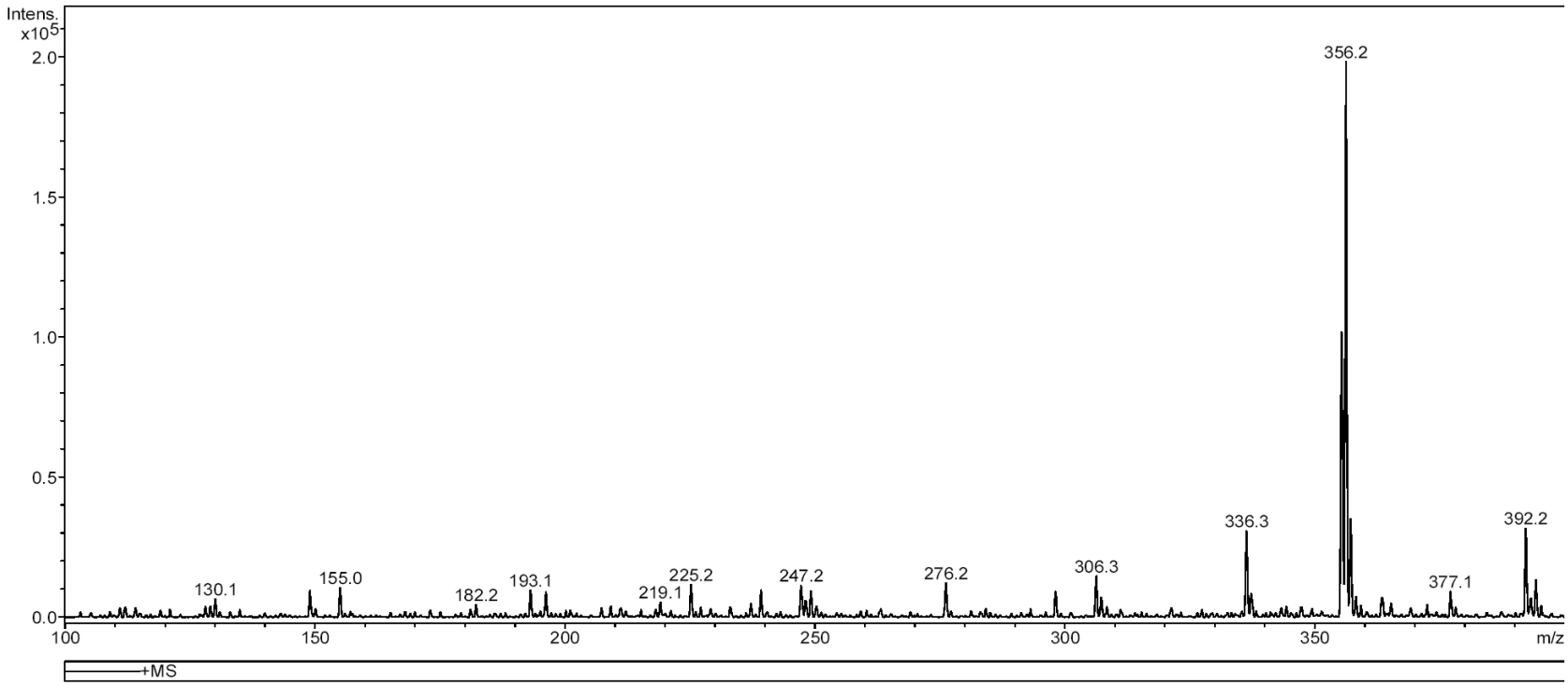

Figure 43: Mass spectrum of -*O*-(2-phenylacetyl)-5-azidodeoxy-1,2-*O*-isopropylidene-α-D-xylofuranose (**5**).

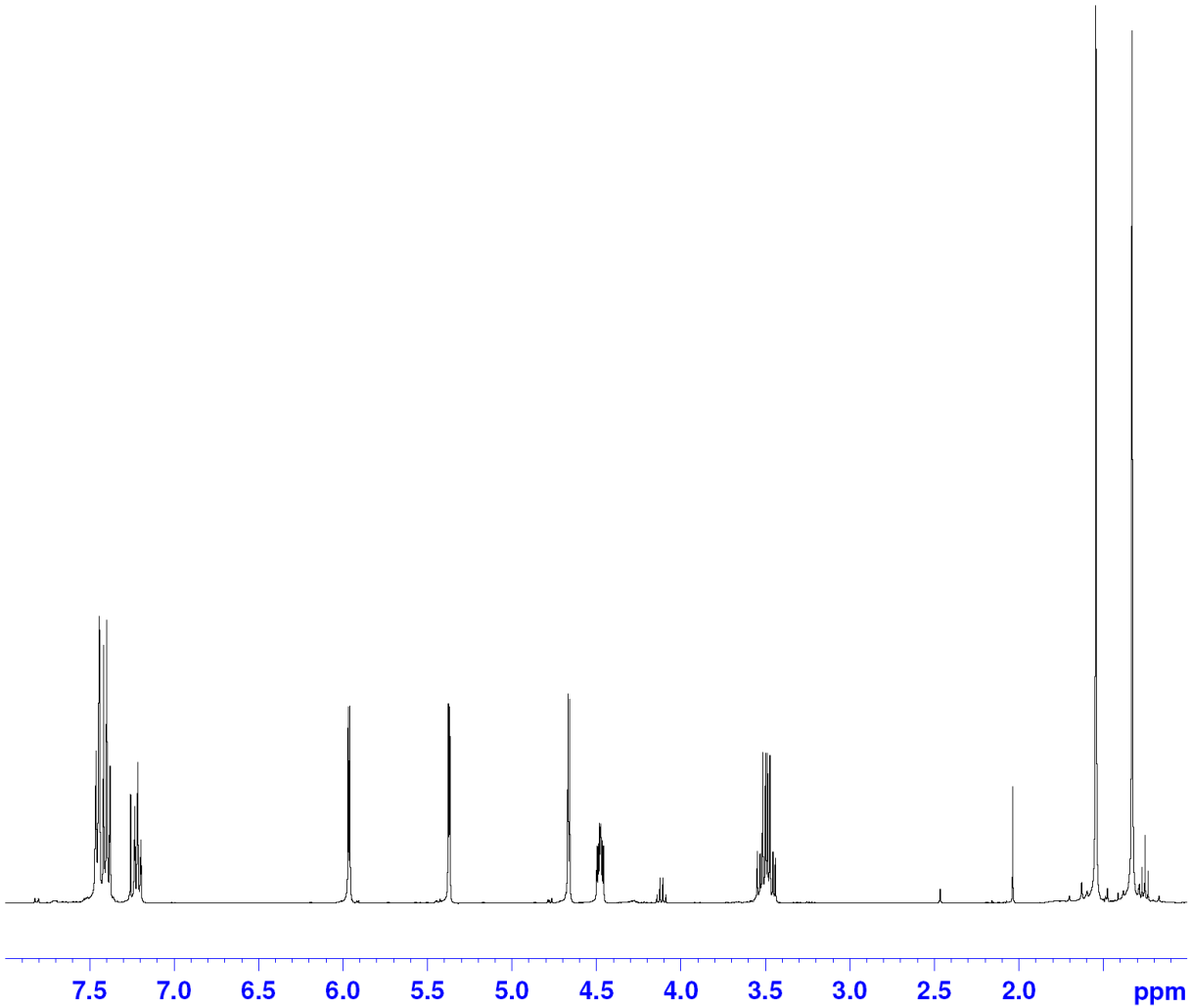

Figure 44: ^{1}H NMR spectrum of 3-*O*-(2-Diazo-2-phenylacetyl)-5-azidodeoxy-1,2-*O*-isopropylidene-α-D-xylofuranose (**6**).

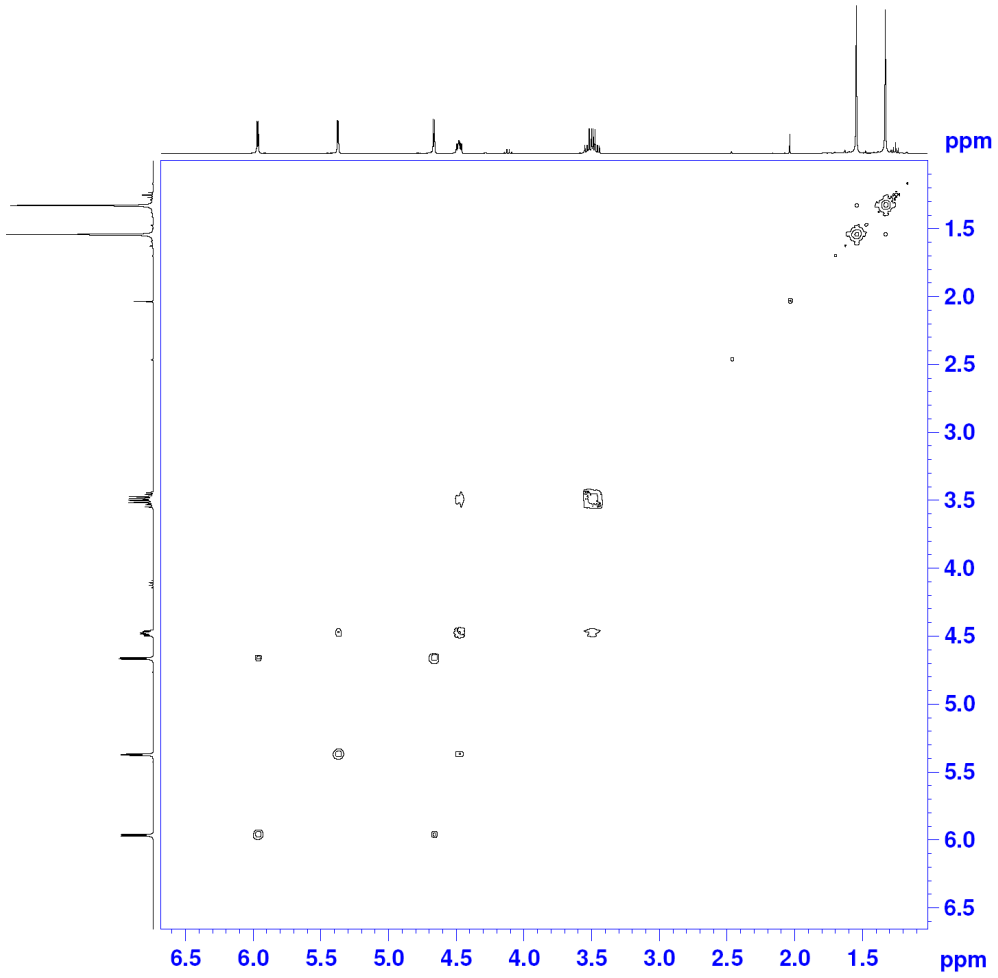

Figure 45: COSY NMR spectrum of 3-*O*-(2-Diazo-2-phenylacetyl)-5-azidodeoxy-1,2-*O*-isopropylidene-α-D-xylofuranose (**6**).

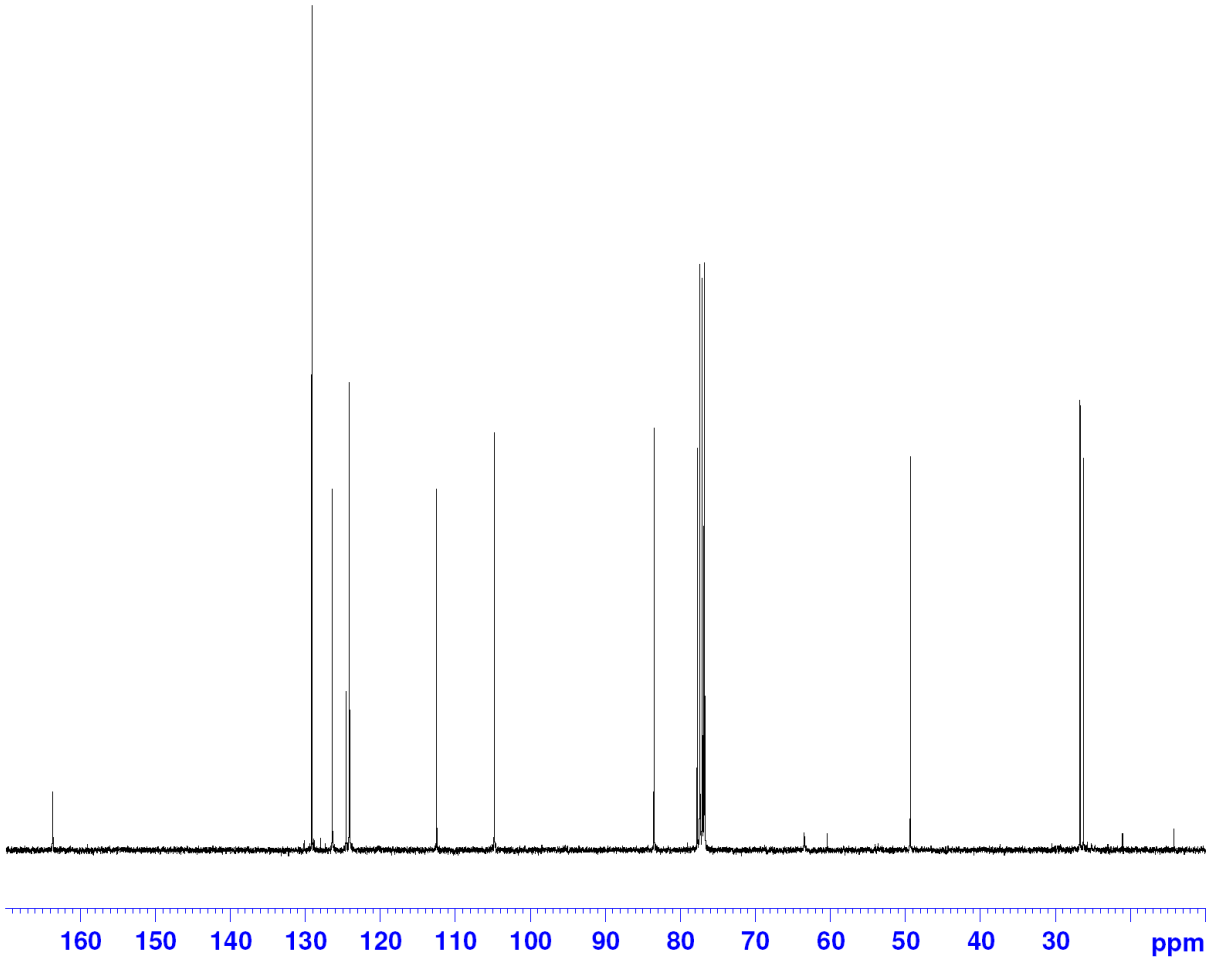

Figure 46: ^{13}C NMR spectrum of 3-*O*-(2-Diazo-2-phenylacetyl)-5-azidodeoxy-1,2-*O*-isopropylidene-α-D-xylofuranose (**6**).

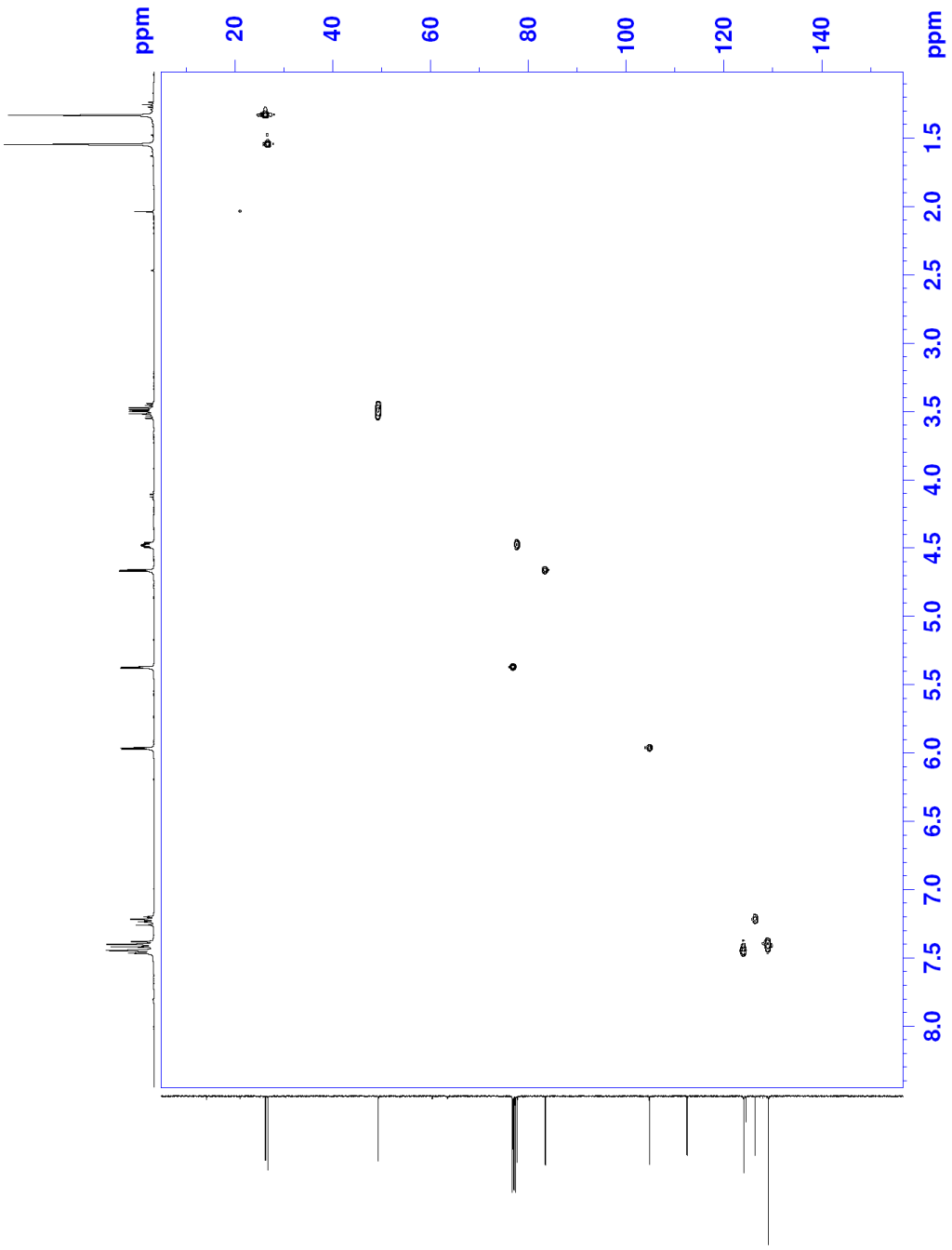

Figure 47: COSY NMR spectrum of 3-*O*-(2-Diazo-2-phenylacetyl)-5-azidodeoxy-1,2-*O*-isopropylidene-α-D-xylofuranose (**6**).

Display Report

Analysis Info

Method XQ Default.ms Instrument Esquire-LC_00135

Acquisition Parameter

Ion Source Type	ESI	Mass Range Mode	Std/Normal	Ion Polarity	Positive	Alternating Ion Polarity	n/a
Scan Begin	200.00 m/z	Scan End	500.00 m/z	Averages	10 Spectra	Accumulation Time	5974 µs
Capillary Exit	85.8 Volt	Skim 1	18.2 Volt	Trap Drive	48.7	Auto MS/MS	Off

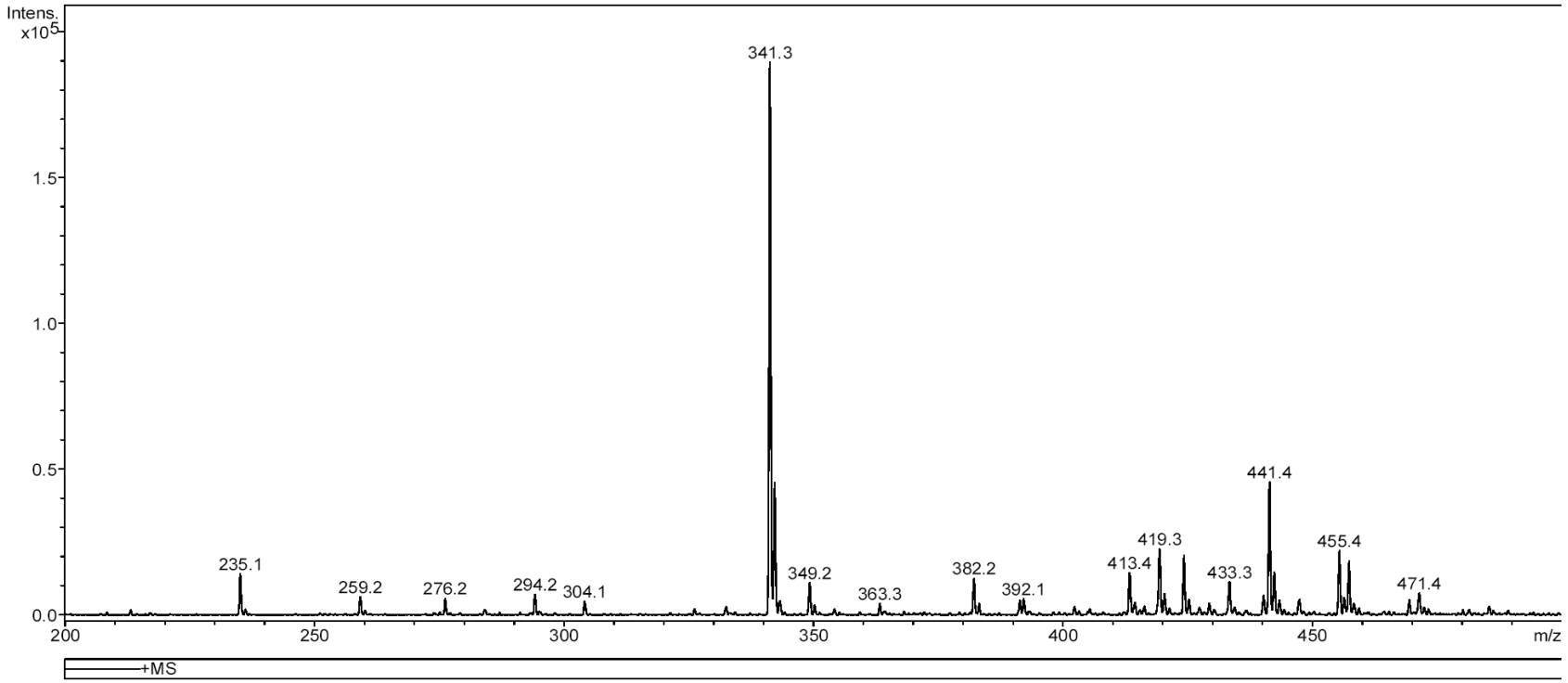

Figure 48: Mass spectrum of 3-*O*-(2-Diazo-2-phenylacetyl)-5-azidodeoxy-1,2-*O*-isopropylidene-α-D-xylofuranose (**6**).

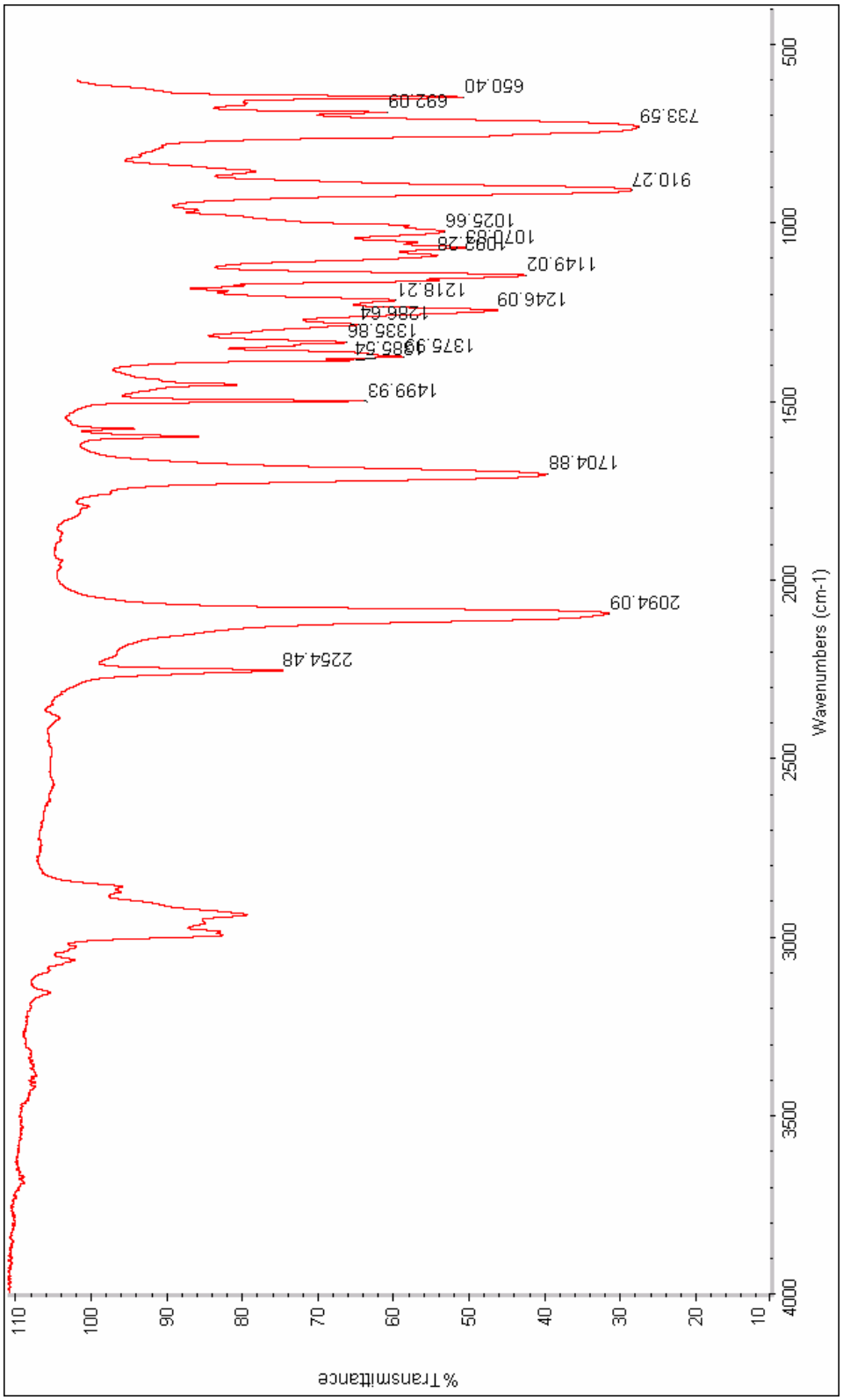

Figure 49: IR spectrum of 3-*O*-(2-Diazo-2-phenylacetyl)-5-azidodeoxy-1,2-*O*-isopropylidene-α-D-xylofuranose (**6**).

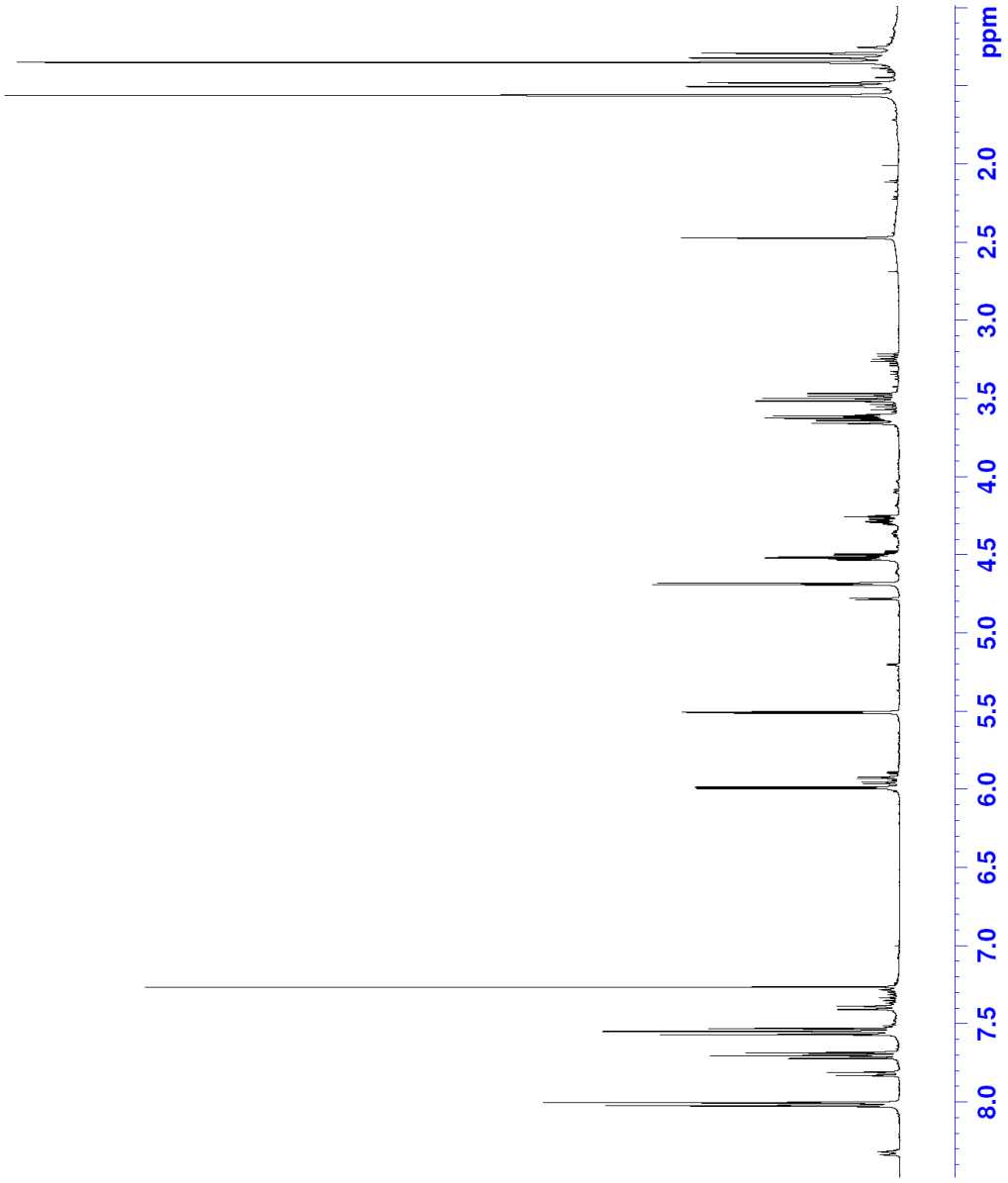

Figure 50: ^{1}H NMR spectrum of keto-ester (**7**).

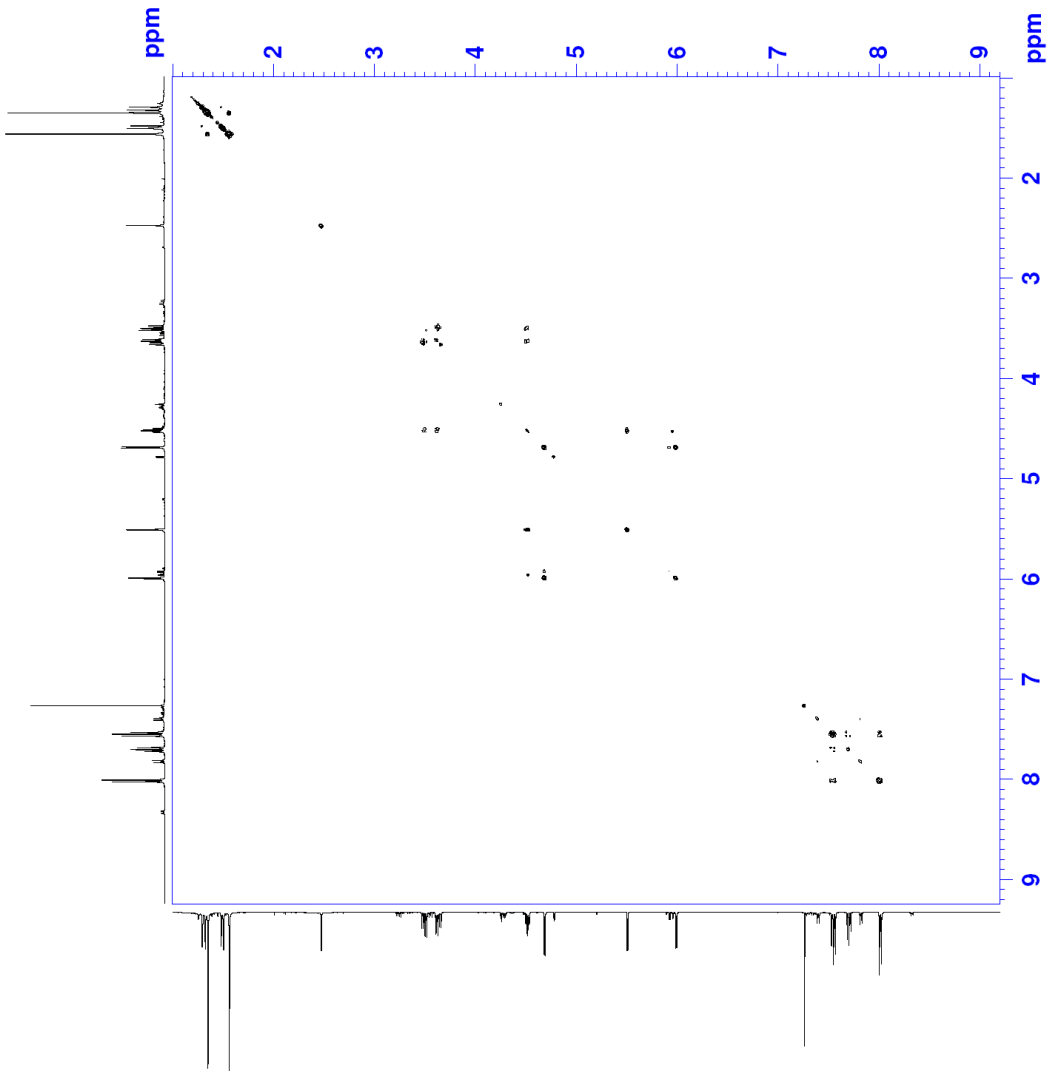

Figure 51: COSY NMR spectrum of keto-ester (**7**).

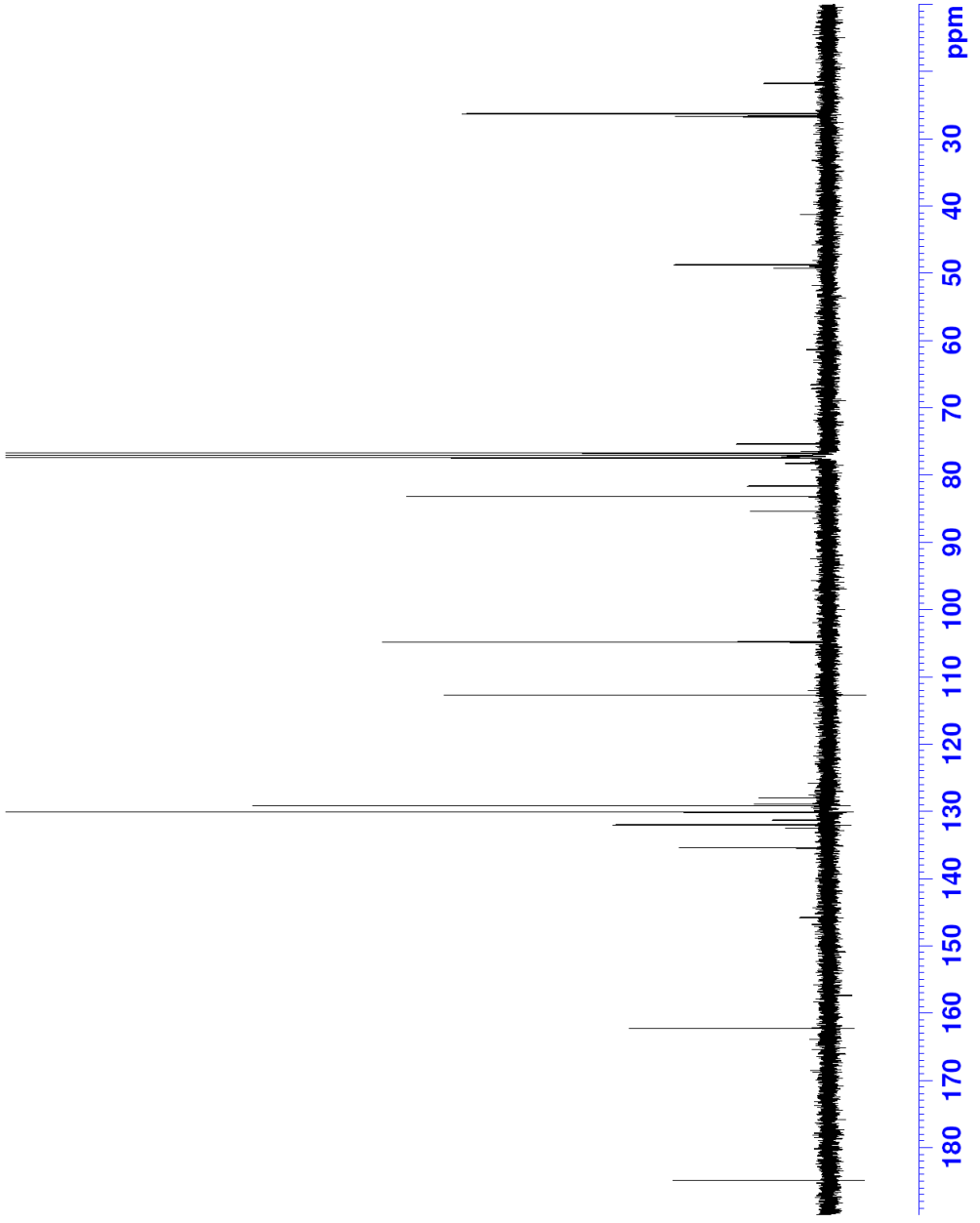

Figure 52: ^{13}C NMR spectrum of keto-ester (**7**).

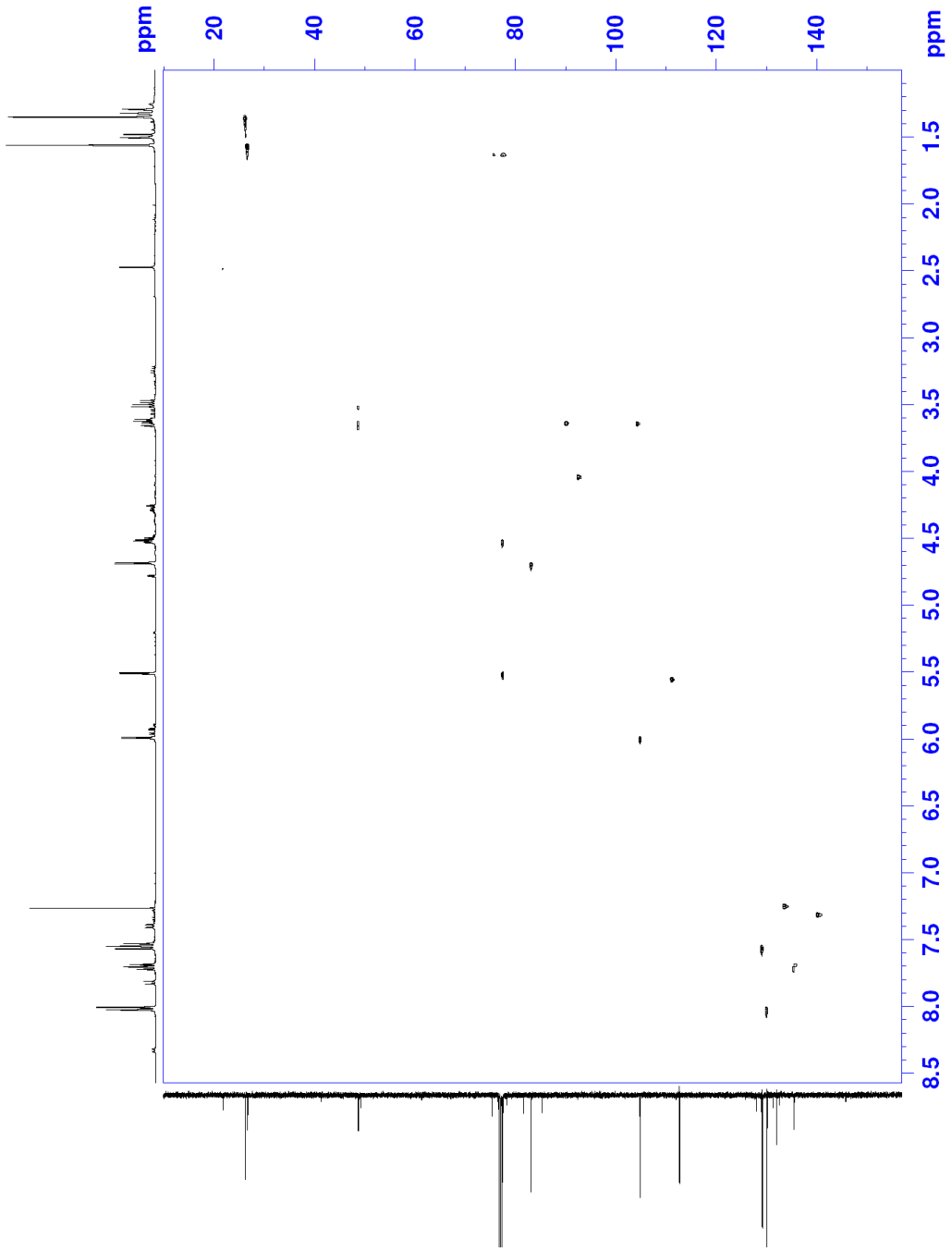

Figure 53: HSQC NMR spectrum of keto-ester (**7**).

Display Report

Analysis Info

Method XQ Default.ms Instrument Esquire-LC_00135

Acquisition Parameter

Ion Source Type	ESI	Mass Range Mode	Std/Normal	Ion Polarity	Positive	Alternating Ion Polarity	n/a
Scan Begin	250.00 m/z	Scan End	450.00 m/z	Averages	10 Spectra	Accumulation Time	3280 µs
Capillary Exit	96.8 Volt	Skim 1	26.7 Volt	Trap Drive	48.2	Auto MS/MS	Off

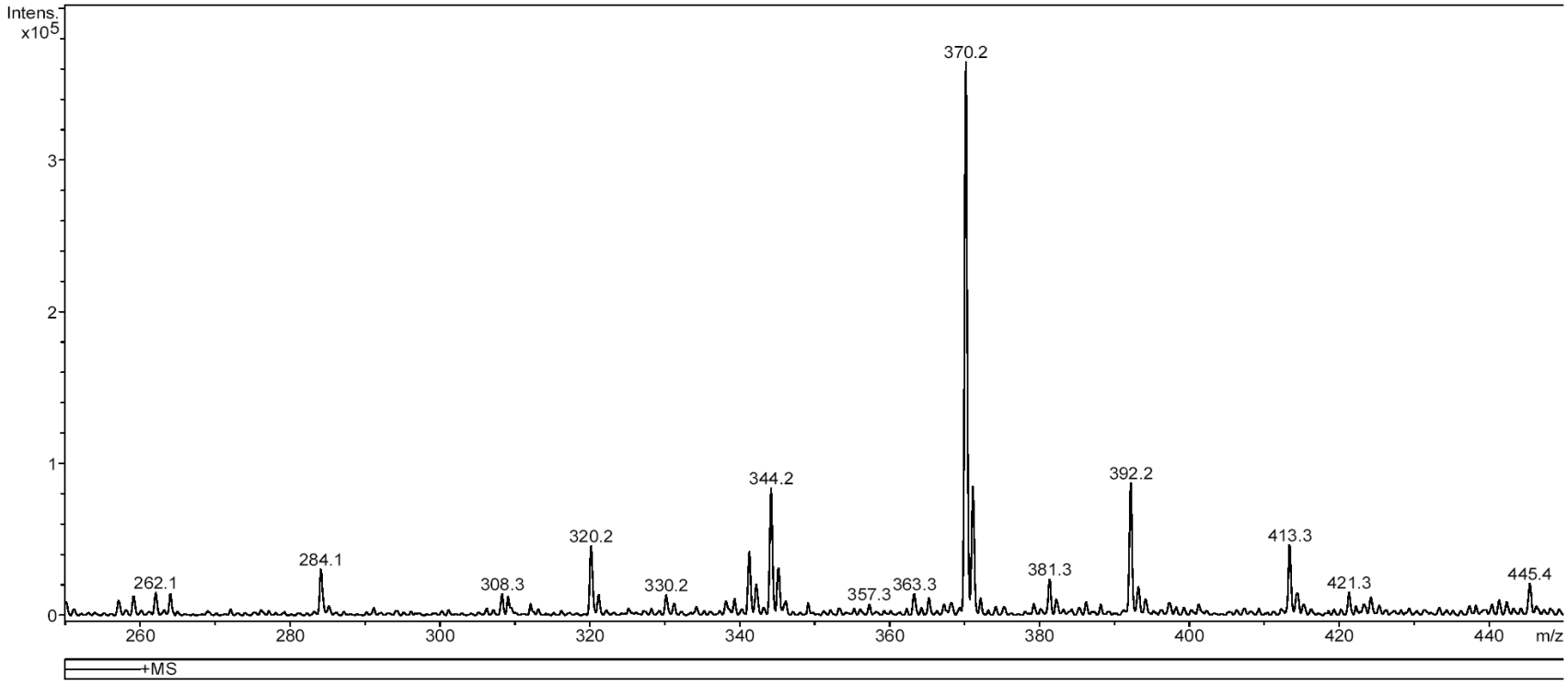

Figure 54: Mass spectrum of keto-ester (**7**).

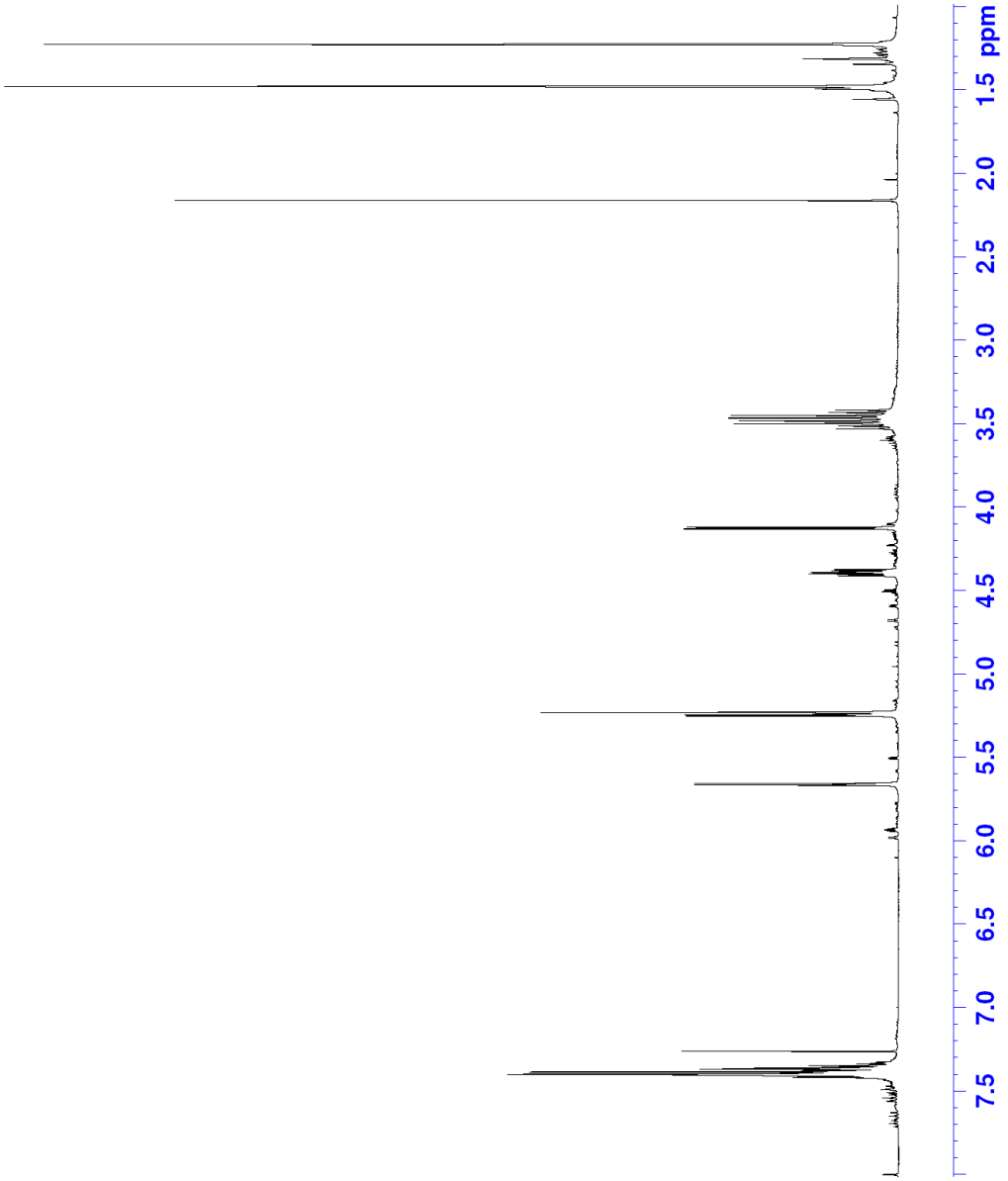

Figure 55: ^{1}H NMR spectrum of ether-linked dimer (**8**).

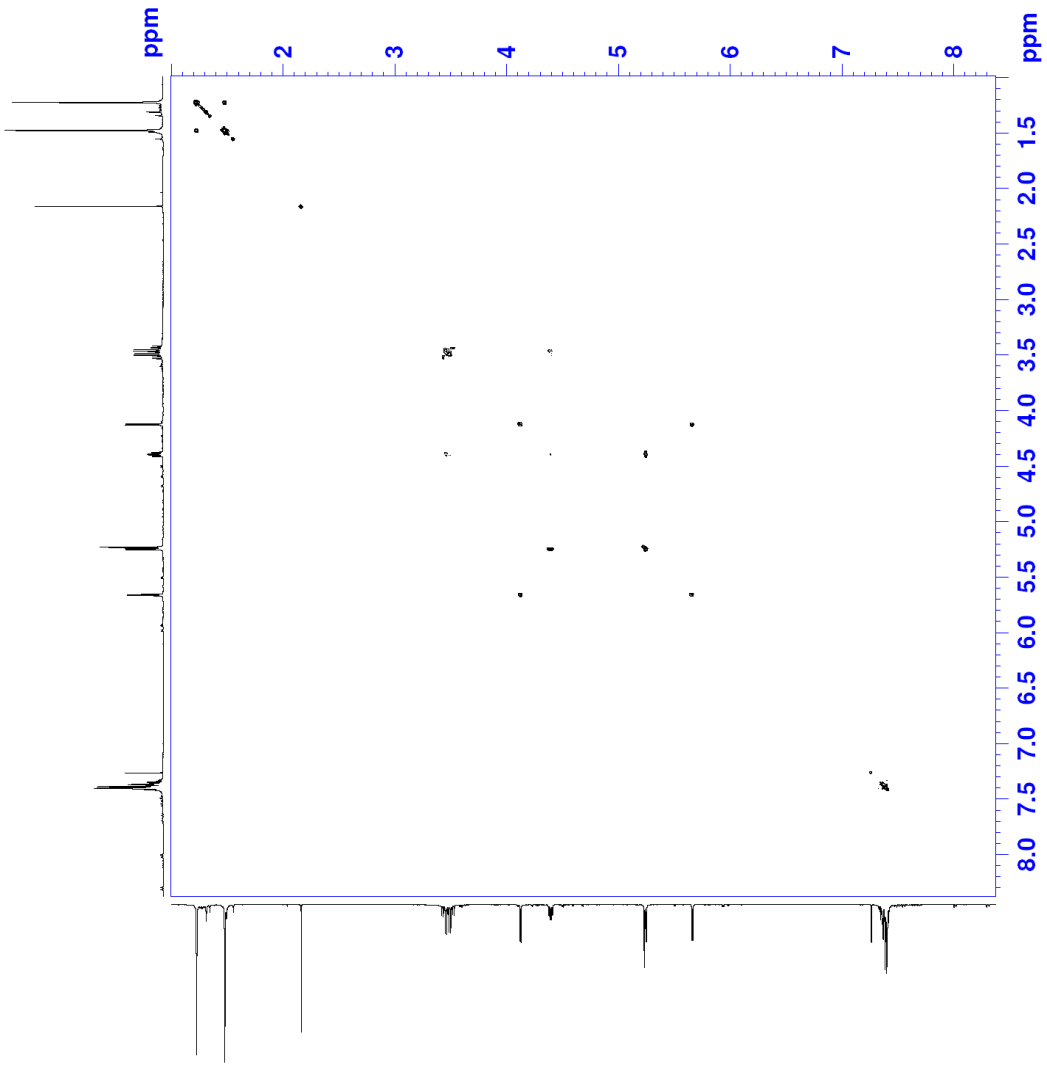

Figure 56: COSY NMR spectrum of ether-linked dimer (**8**).

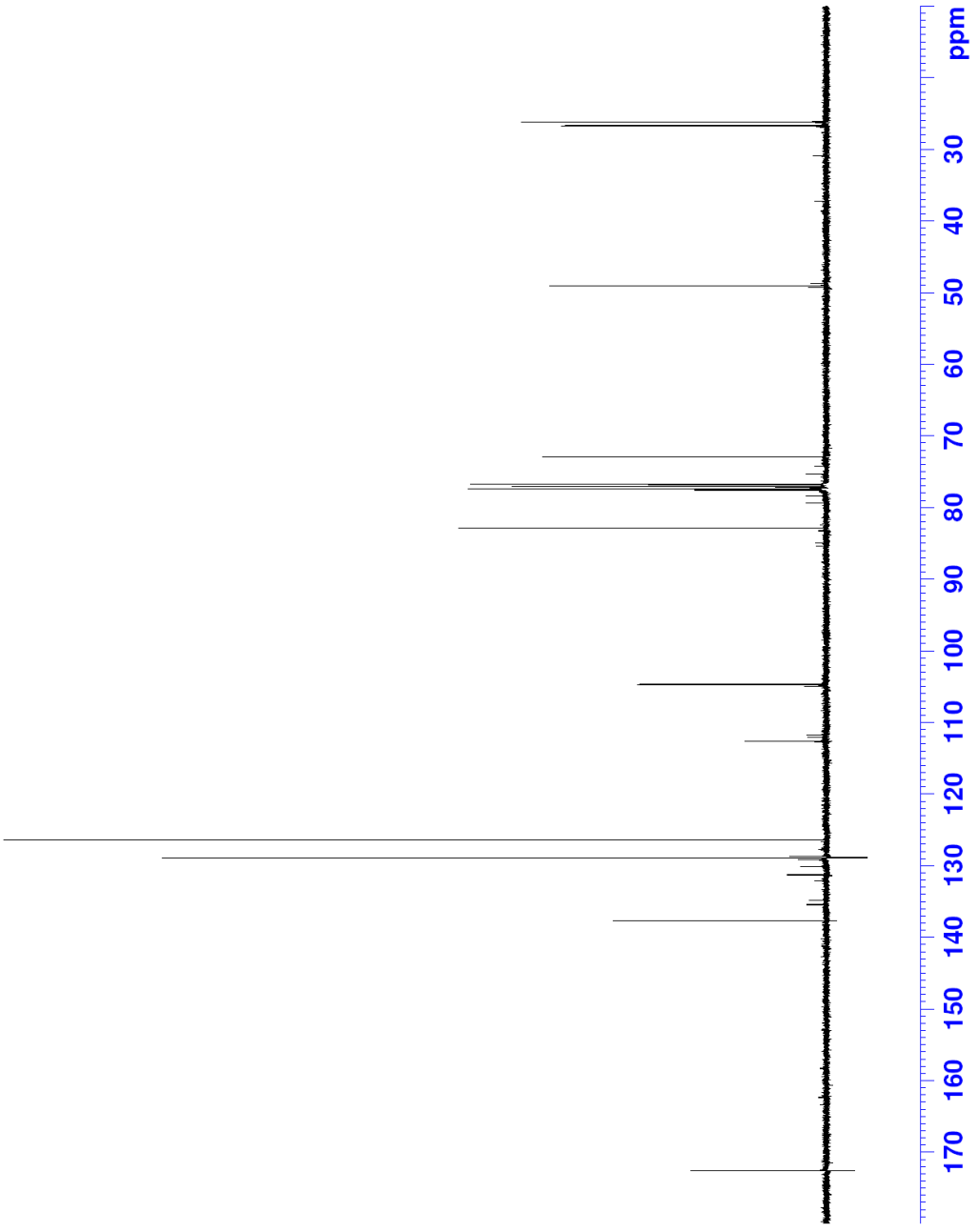

Figure 57: ^{13}C NMR spectrum of ether-linked dimer (**8**).

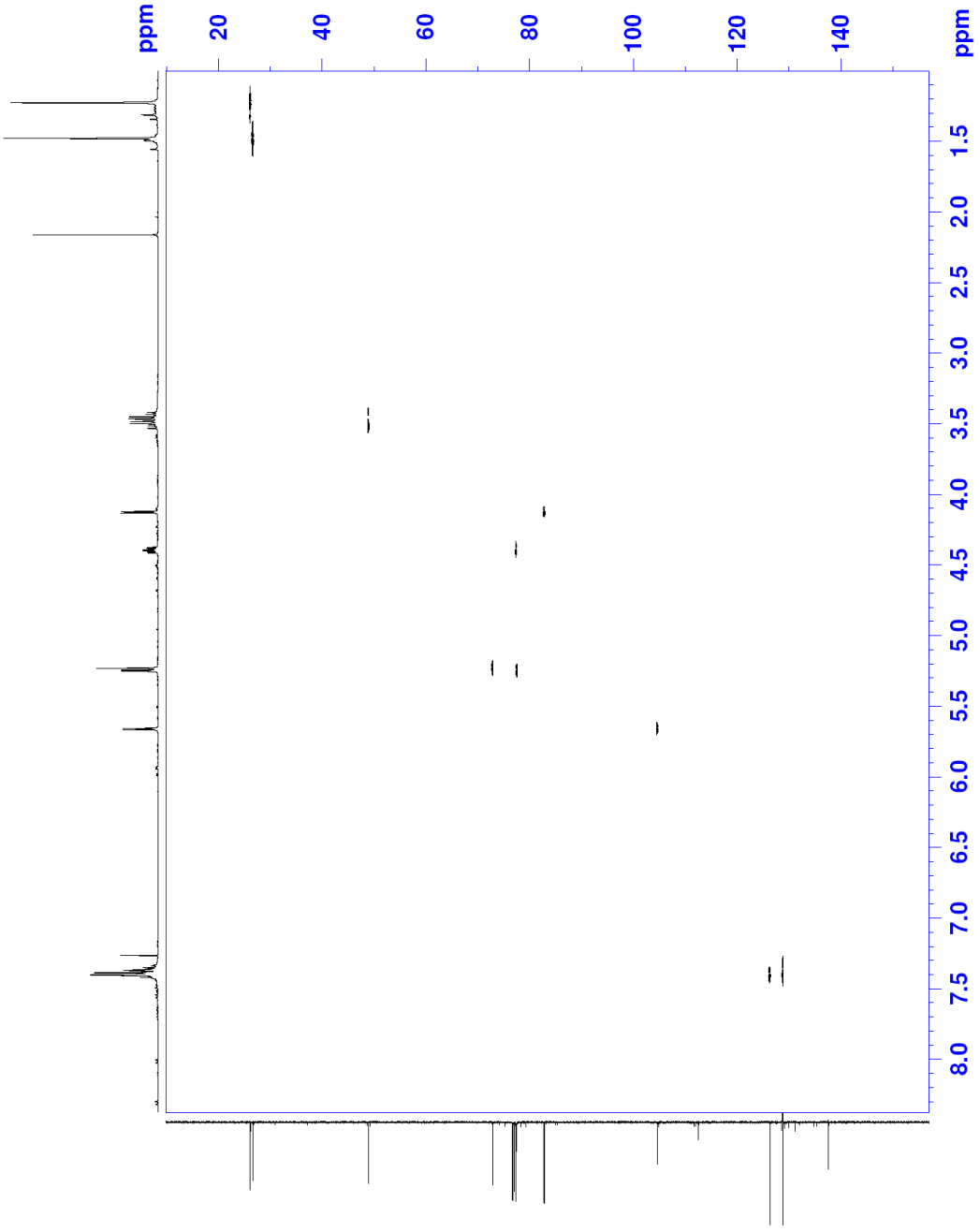

Figure 58: HSQC NMR spectrum of ether-linked dimer (**8**).

Display Report

Analysis Info

Method XQ Default.ms Instrument Esquire-LC_00135

Acquisition Parameter

Ion Source Type	ESI	Mass Range Mode	Std/Normal	Ion Polarity	Positive	Alternating Ion Polarity	n/a
Scan Begin	15.00 m/z	Scan End	1000.00 m/z	Averages	5 Spectra	Accumulation Time	1111 µs
Capillary Exit	107.6 Volt	Skim 1	34.5 Volt	Trap Drive	47.6	Auto MS/MS	Off

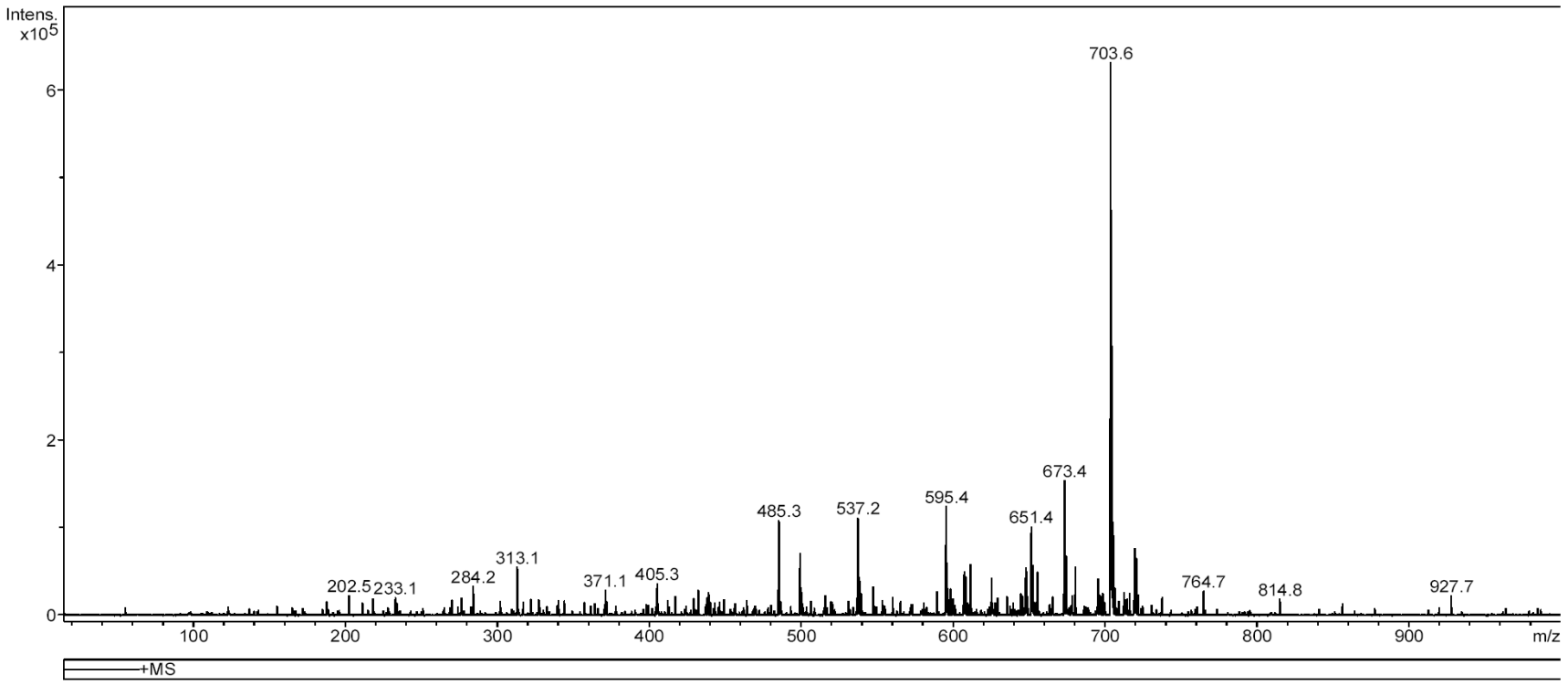

Figure 59: Mass spectrum of ether-linked dimer (**8**).

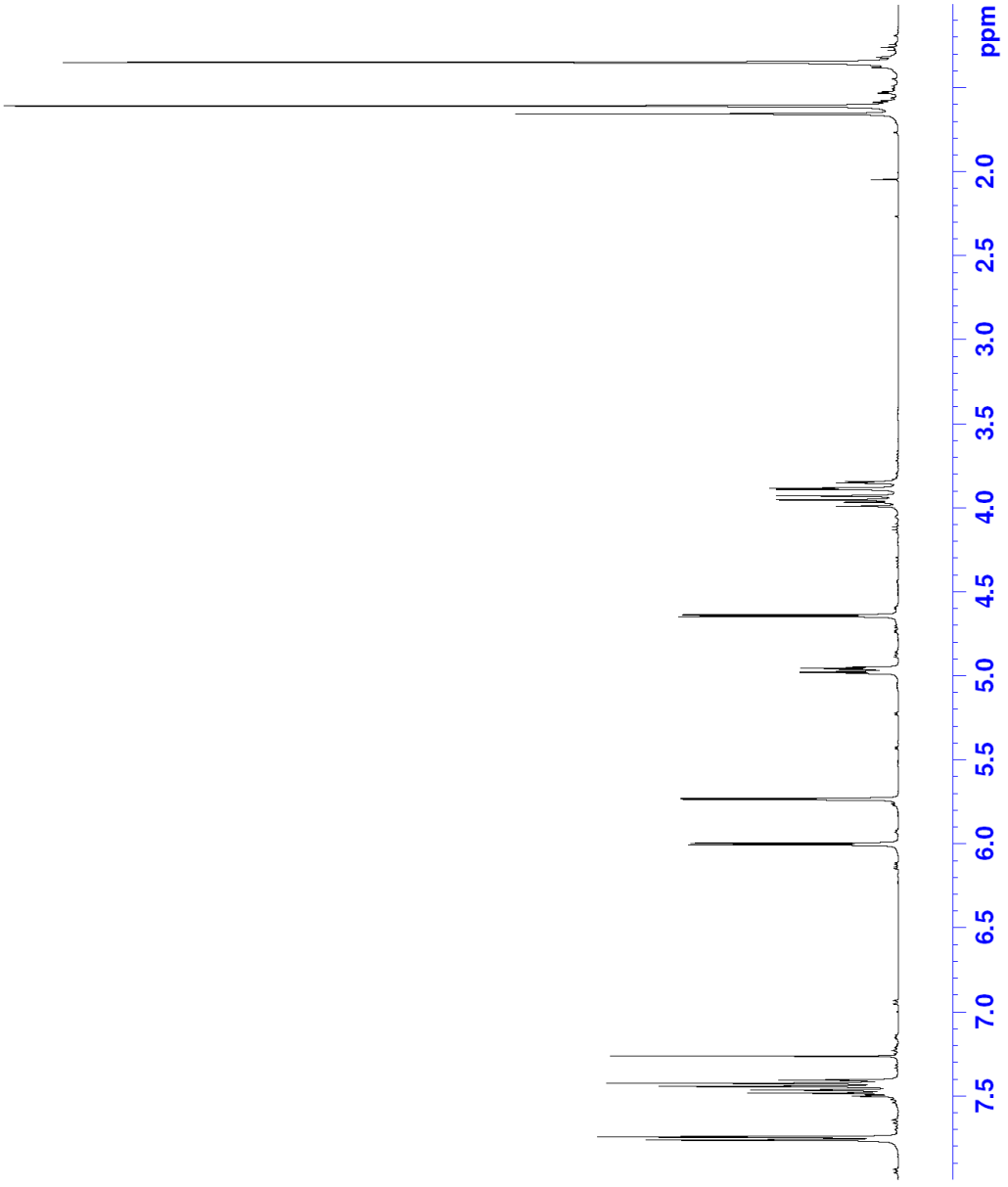

Figure 60: ^{1}H NMR spectrum of 14-membered macrocycle (original) (**9**).

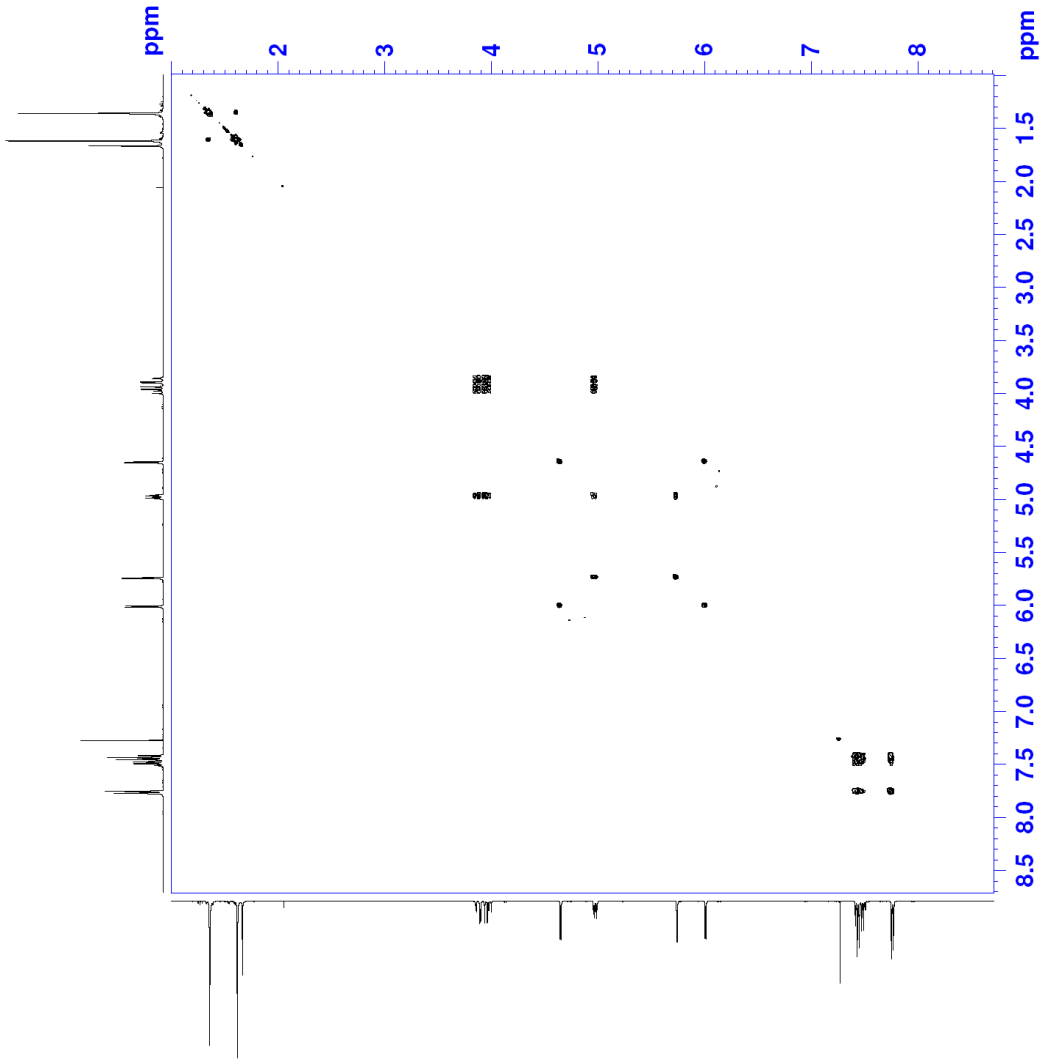

Figure 61: COSY NMR spectrum of 14-membered macrocycle (original) (**9**).

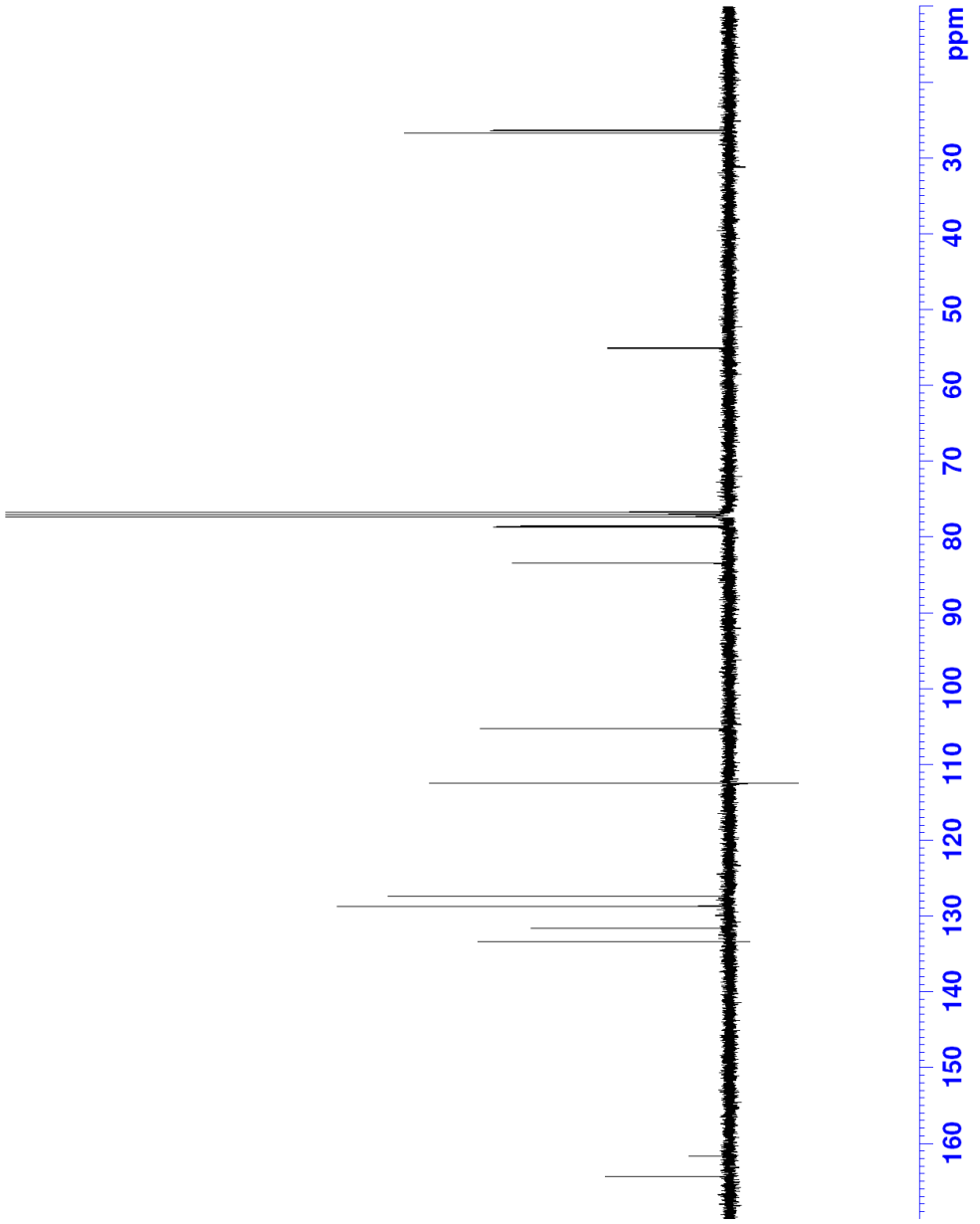

Figure 62: ^{13}C NMR spectrum of 14-membered macrocycle (original) (**9**).

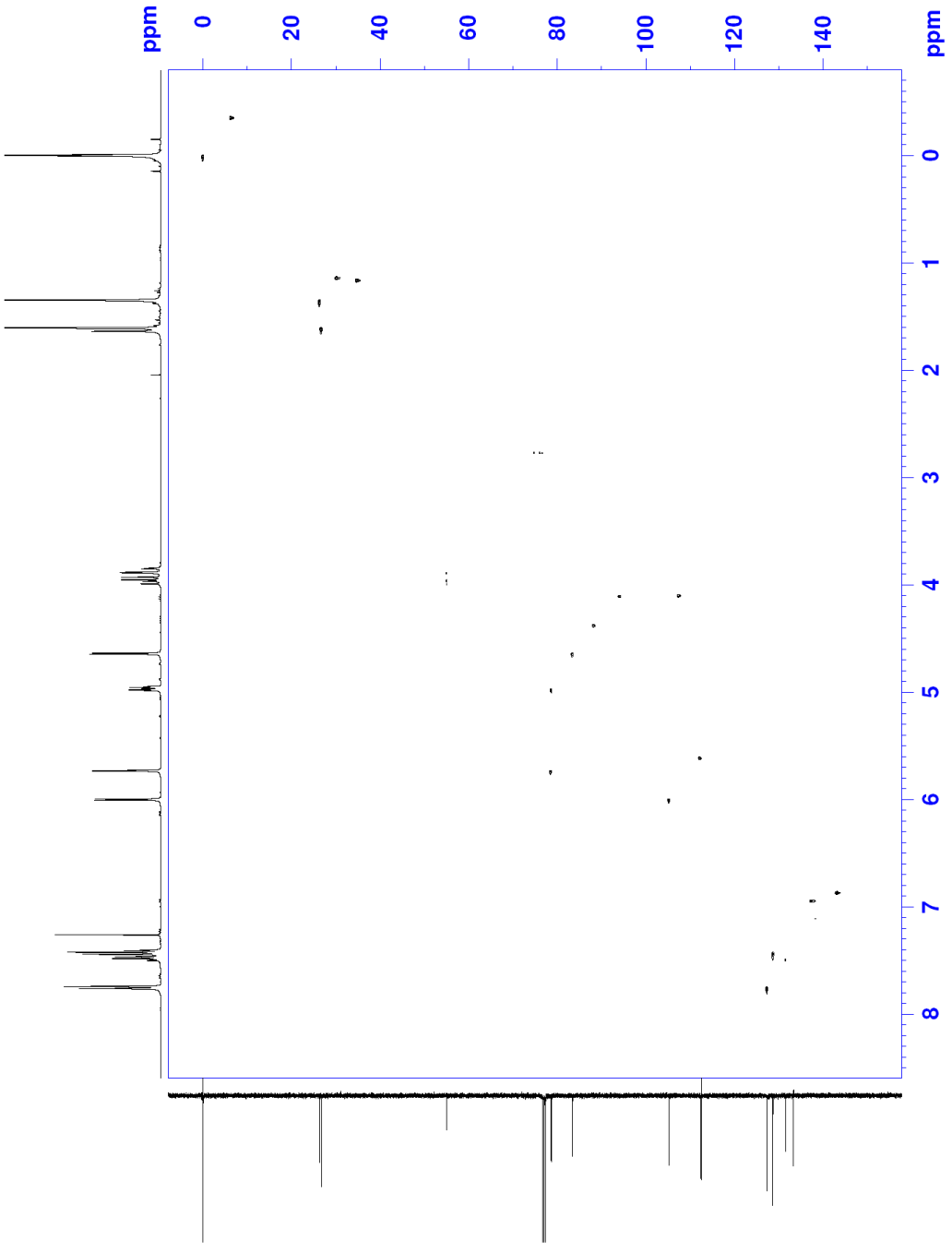

Figure 63: HSQC NMR spectrum of 14-membered macrocycle (original) (**9**).

Display Report

Analysis Info

Method XQ Default.ms Instrument Esquire-LC_00135

Acquisition Parameter

Ion Source Type	ESI	Mass Range Mode	Std/Normal	Ion Polarity	Positive	Alternating Ion Polarity	n/a
Scan Begin	450.00 m/z	Scan End	750.00 m/z	Averages	10 Spectra	Accumulation Time	5922 µs
Capillary Exit	105.3 Volt	Skim 1	32.9 Volt	Trap Drive	58.2	Auto MS/MS	Off

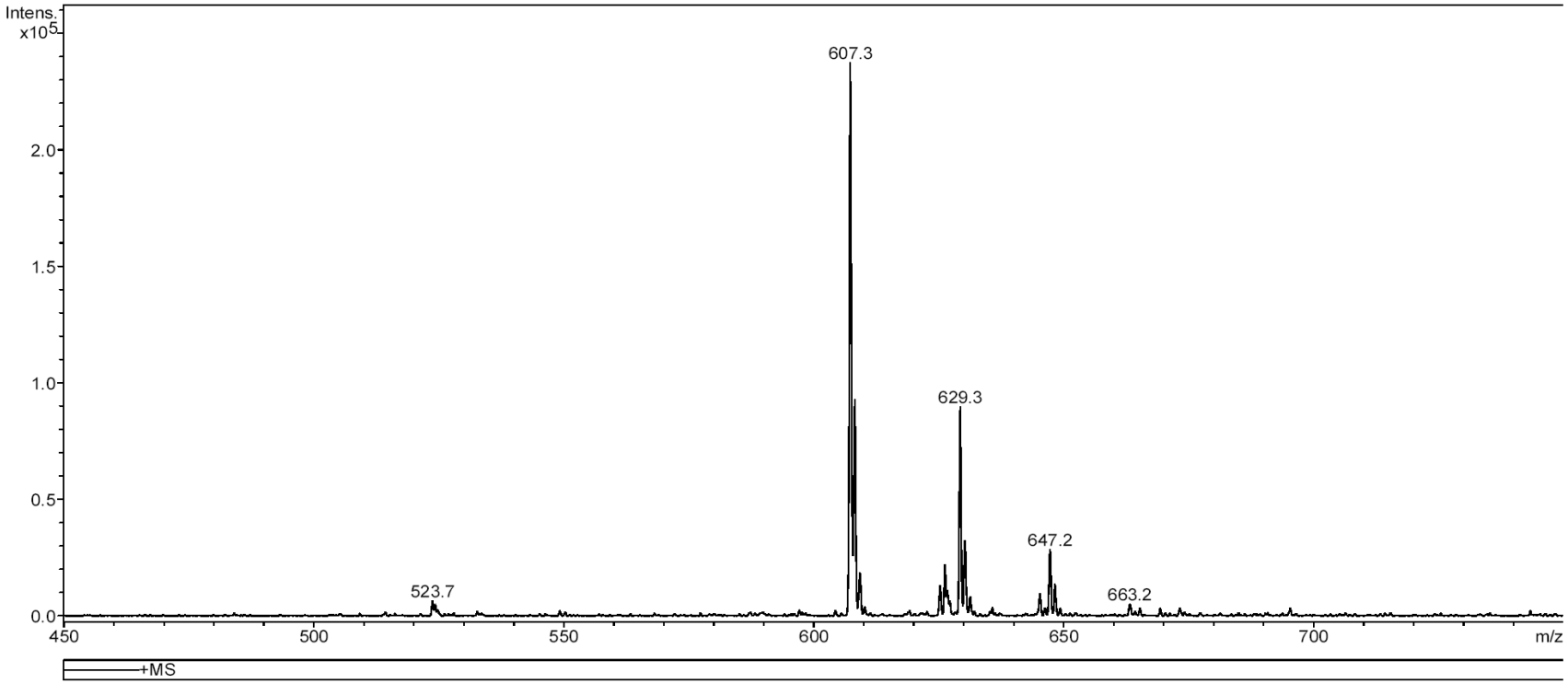

Figure 64: Mass spectrum of 14-membered macrocycle (original) (**9**).

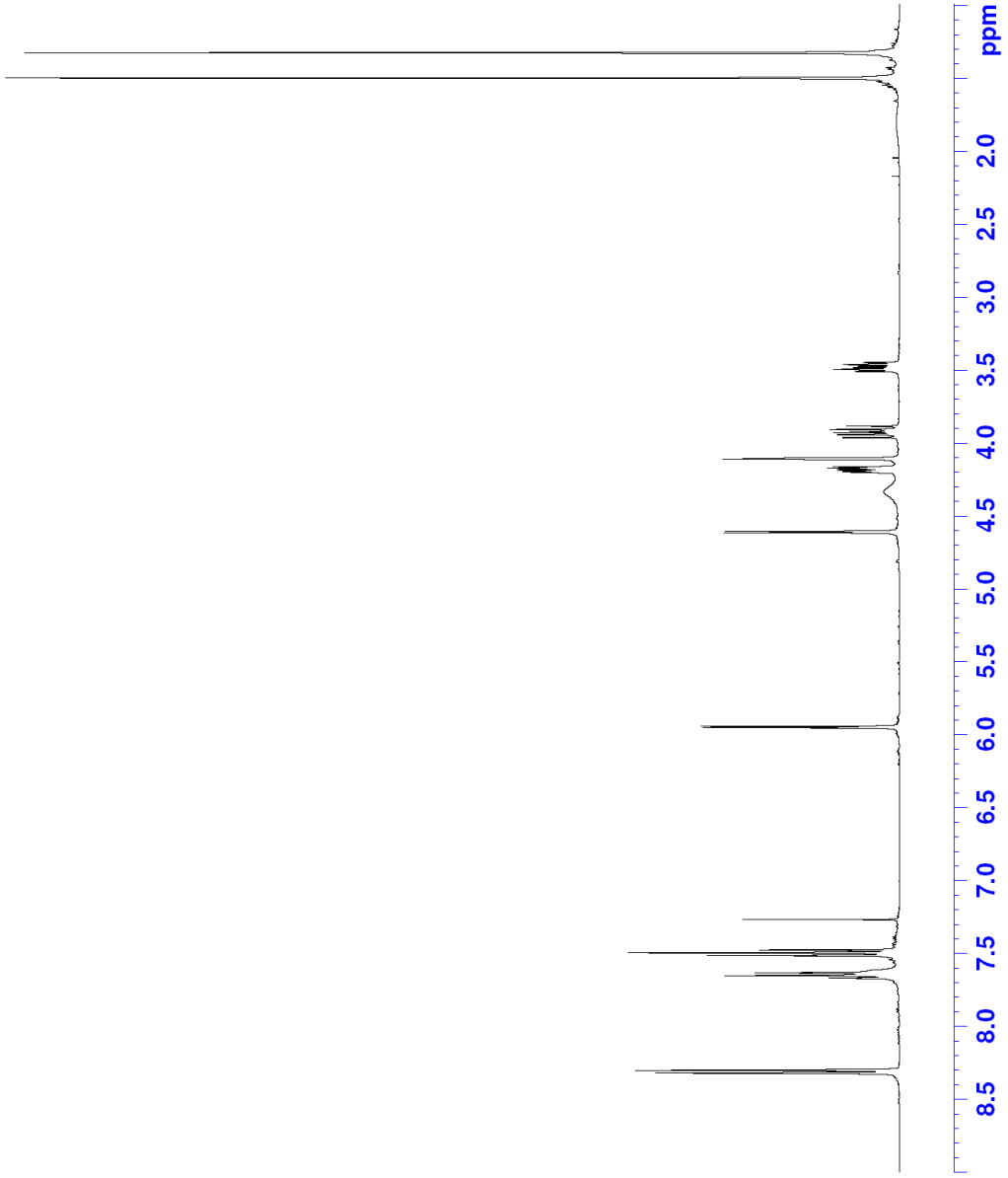

Figure 65: ^{1}H NMR spectrum of 14-membered macrocycle (possible) (**9**).

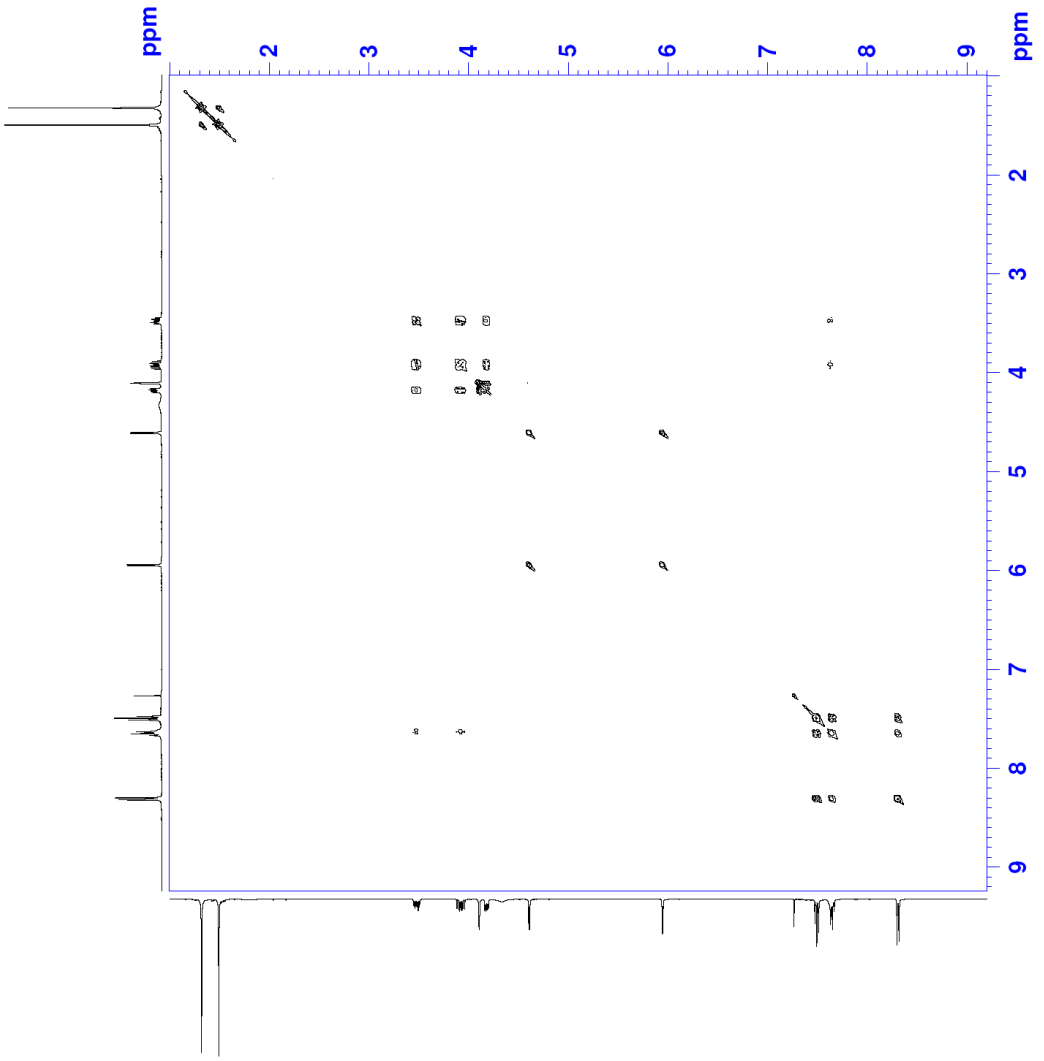

Figure 66: COSY NMR spectrum of 14-membered macrocycle (possible) (**9**).

Figure 67: ^{13}C NMR spectrum of 14-membered macrocycle (possible) (**9**).

Display Report

Analysis Info

Method XQ Default.ms Instrument Esquire-LC_00135

Acquisition Parameter

Ion Source Type	ESI	Mass Range Mode	Std/Normal	Ion Polarity	Positive	Alternating Ion Polarity	n/a
Scan Begin	500.00 m/z	Scan End	750.00 m/z	Averages	5 Spectra	Accumulation Time	763 µs
Capillary Exit	100.0 Volt	Skim 1	29.0 Volt	Trap Drive	58.2	Auto MS/MS	Off

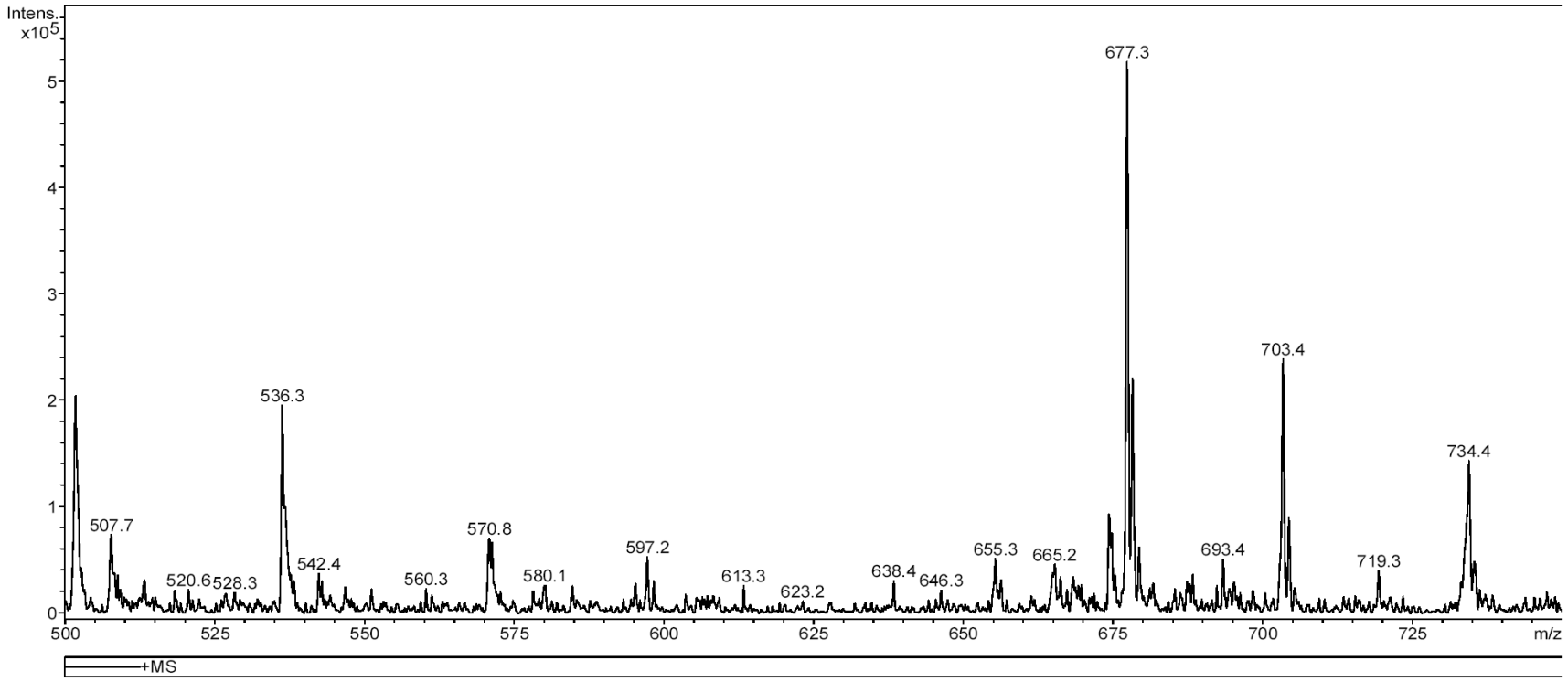

Figure 68: Mass spectrum of 14-membered macrocycle (possible) (**9**).

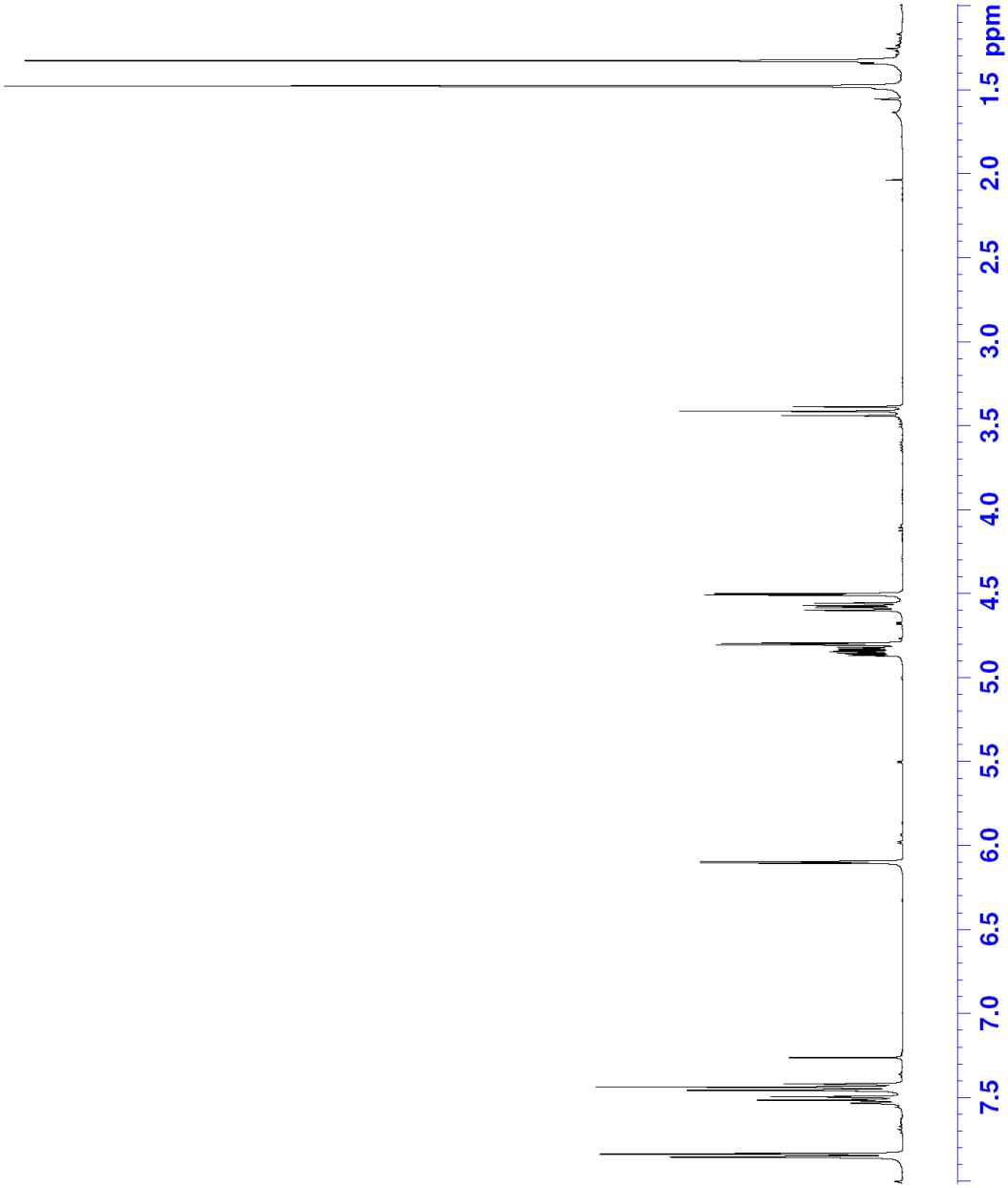

Figure 69: ^{1}H NMR spectrum of oxazepine (**10**).

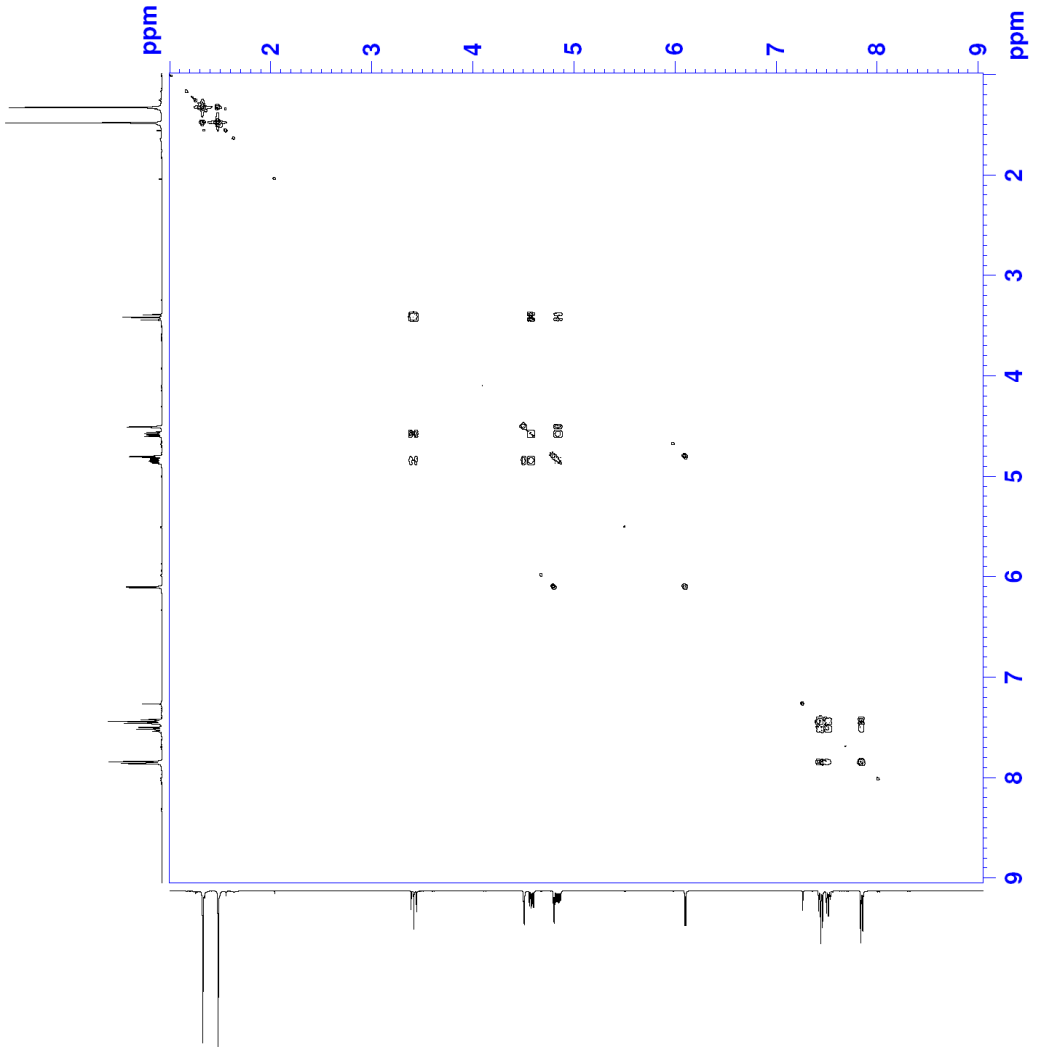

Figure 70: COSY NMR spectrum of oxazepine (**10**).

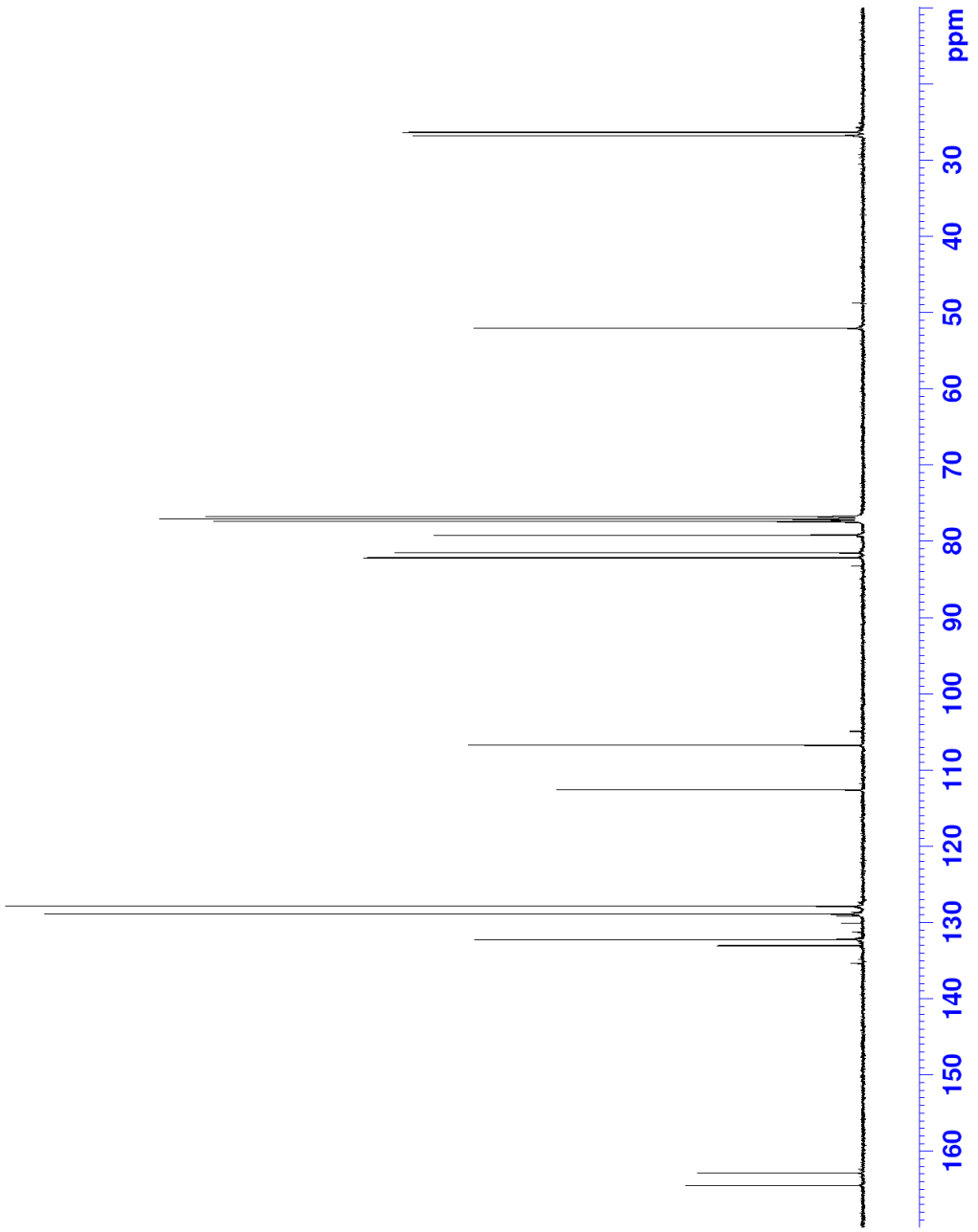

Figure 71: ^{13}C NMR spectrum of oxazepine (**10**).

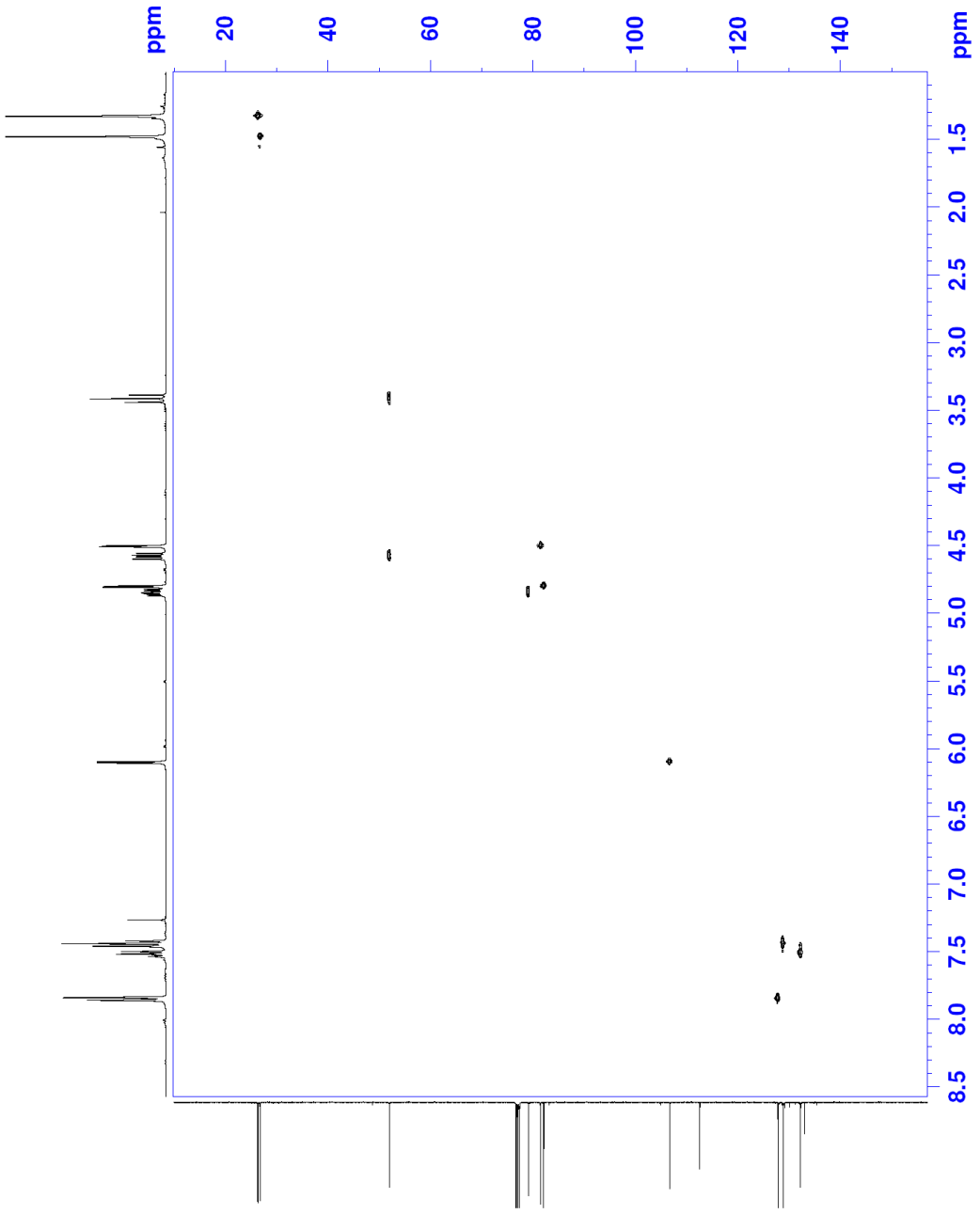

Figure 72: HSQC NMR spectrum of oxazepine (**10**).

Display Report

Analysis Info

Method XQ Default.ms Instrument Esquire-LC_00135

Acquisition Parameter

Ion Source Type	ESI	Mass Range Mode	Std/Normal	Ion Polarity	Positive	Alternating Ion Polarity	n/a
Scan Begin	150.00 m/z	Scan End	350.00 m/z	Averages	5 Spectra	Accumulation Time	12778 µs
Capillary Exit	79.3 Volt	Skim 1	12.8 Volt	Trap Drive	46.5	Auto MS/MS	Off

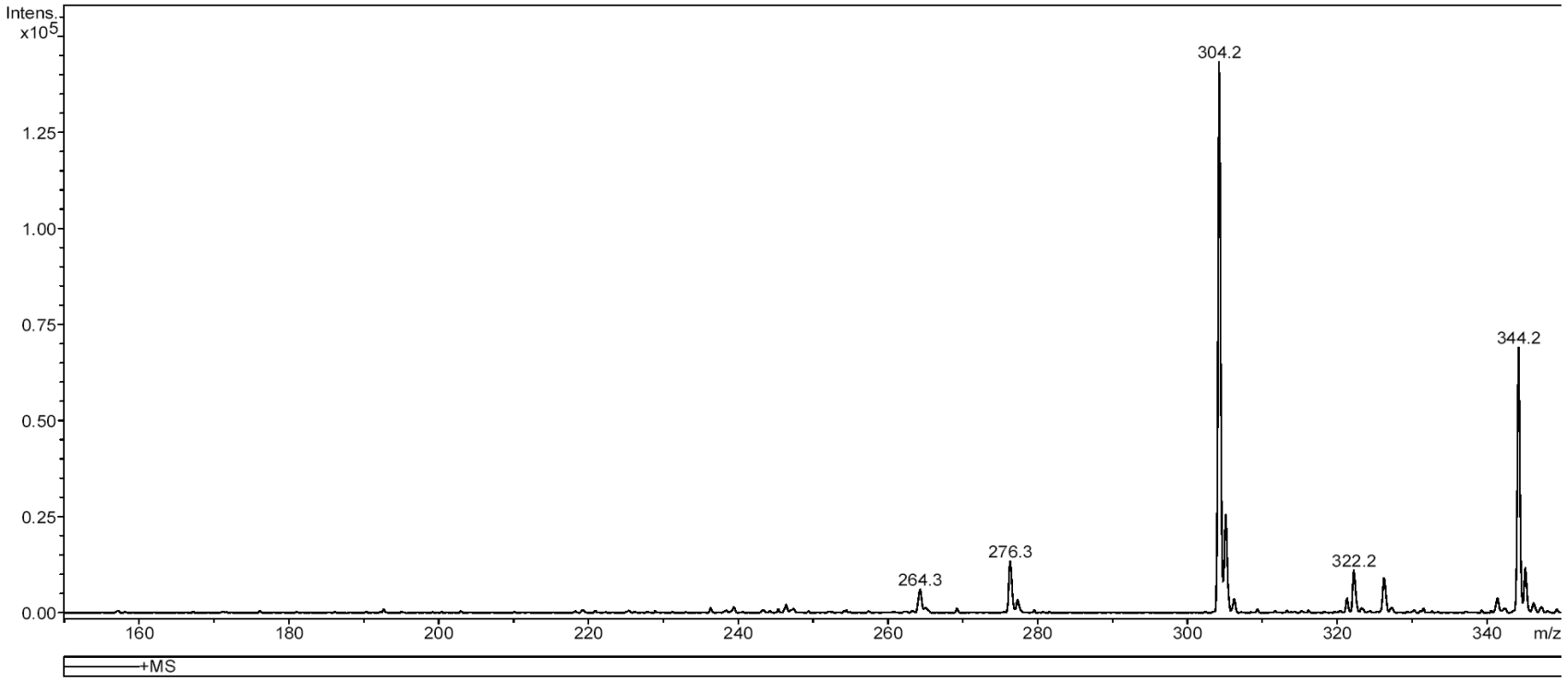

Figure 73: Mass spectrum of oxazepine (**10**).

Appendix B

X-Ray Crystallography

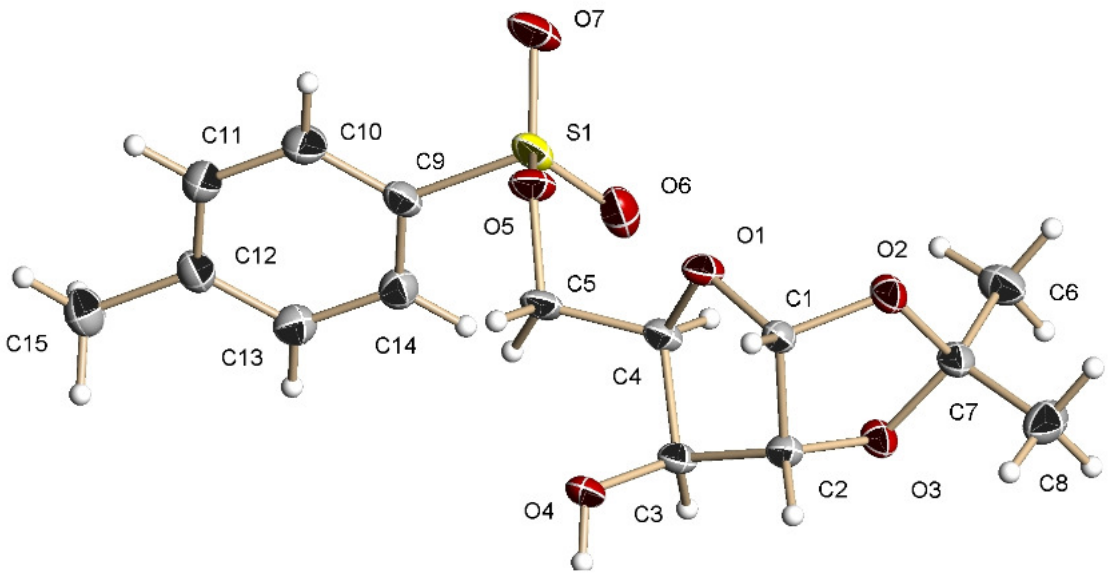

Figure 74: X-Ray crystal structure of 5-*O*-(4-methylbenzenesulfonyl)-1,2-*O*-isopropylidene-α-D-xylofuranose (**3**).

Table 1. Crystal data and structure refinement for 08mz206_0m:

Identification code: 08mz206_0m
Empirical formula: C16 H17 O5
Formula weight: 303.31
Temperature: 100(2) K
Wavelength: 0.71073 Å
Crystal system: Monoclinic
Space group: P1
Unit cell dimensions:
a = 5.7348(5) Å, α = 90°
b = 11.3363(10) Å, β = 101.8530(10)°
c = 11.1977(10) Å, γ = 90°
Volume, *Z*: 712.46(11) Å^3, 2
Density (calculated): 1.414 Mg/m^3
Absorption coefficient: 0.106 mm^{-1}
F(000): 320
Crystal size: 0.55 × 0.40 × 0.24 mm
Crystal shape, colour: block, colourless
θ range for data collection: 1.86 to 28.28°
Limiting indices: $-7 \le h \le 7$, $-15 \le k \le 14$, $-11 \le l \le 14$
Reflections collected: 5290
Independent reflections: 1826 (*R*(int) = 0.0156)
Completeness to θ = 28.28°: 98.4 %
Absorption correction: multi-scan
Max. and min. transmission: 0.975 and 0.876
Refinement method: Full-matrix least-squares on F^2
Data / restraints / parameters: 1826 / 1 / 201
Goodness-of-fit on F^2: 1.098
Final *R* indices [$I>2\sigma(I)$]: R1 = 0.0270, wR2 = 0.0727
R indices (all data): R1 = 0.0278, wR2 = 0.0734
Largest diff. peak and hole: 0.228 and −0.184 e × Å^{-3}

Refinement of F^2 against ALL reflections. The weighted R-factor wR and goodness of fit are based on F^2, conventional R-factors R are based on *F*, with *F* set to zero for negative F^2. The threshold expression of $F^2 > 2\sigma(F^2)$ is used only for calculating R-factors

Treatment of hydrogen atoms:
All hydrogen atoms were placed in calculated positions and were refined with an isotropic displacement parameter 1.5 (methyl) or 1.2 times (all

others) that of the adjacent carbon or nitrogen atom.

Table 2. Atomic coordinates [× 10^4] and equivalent isotropic displacement parameters [$Å^2$ × 10^3] for 08mz206_0m. U(eq) is defined as one third of the trace of the orthogonalized U_{ij} tensor.

	x	y	z	U(eq)
C(1)	4299(3)	8887(1)	8479(1)	20(1)
C(2)	6864(3)	8381(1)	8841(2)	20(1)
C(3)	6882(3)	7328(1)	8001(1)	17(1)
C(4)	4717(3)	7567(1)	6979(1)	17(1)
C(5)	3589(3)	6448(2)	6370(1)	21(1)
C(6)	7060(3)	10341(2)	8293(2)	22(1)
C(7)	7543(3)	11071(2)	9453(2)	30(1)
C(8)	7748(4)	10951(2)	7222(2)	33(1)
C(9)	6631(3)	5214(2)	8148(1)	20(1)
C(10)	6885(3)	5182(1)	6817(1)	18(1)
C(11)	8777(3)	4427(1)	6500(1)	19(1)
C(12)	10390(3)	3814(2)	7380(2)	23(1)
C(13)	12107(3)	3094(2)	7045(2)	26(1)
C(14)	12239(3)	2986(2)	5829(2)	27(1)
C(15)	10672(3)	3623(2)	4943(2)	26(1)
C(16)	8948(3)	4334(2)	5273(2)	22(1)
N(1)	5420(2)	5724(1)	5988(1)	20(1)
O(1)	6546(2)	6276(1)	8678(1)	20(1)
O(2)	8356(2)	9257(1)	8491(1)	27(1)
O(3)	4610(2)	10009(1)	7974(1)	25(1)
O(4)	3031(2)	8126(1)	7578(1)	21(1)
O(5)	6416(2)	4334(1)	8712(1)	26(1)

All esds (except the esd in the dihedral angle between two l.s. planes) are estimated using the full covariance matrix. The cell esds are taken into account individually in the estimation of esds in distances, angles and torsion angles; correlations between esds in cell parameters are only used when they are defined by crystal symmetry. An approximate (isotropic) treatment of cell esds is used for estimating esds involving l.s. planes.

Table 3. Bond lengths [Å] and angles [deg] for 08mz206_0m.

C(1)-O(4)	1.4101(18)	C(2)-H(2)	1.0000
C(1)-O(3)	1.419(2)	C(3)-O(1)	1.4479(19)
C(1)-C(2)	1.553(2)	C(3)-C(4)	1.530(2)
C(1)-H(1)	1.0000	C(3)-H(3)	1.0000
C(2)-O(2)	1.4175(19)	C(4)-O(4)	1.4326(18)
C(2)-C(3)	1.521(2)	C(4)-C(5)	1.521(2)
		C(4)-H(4)	1.0000

C(5)-N(1)	1.464(2)
C(5)-H(5A)	0.9900
C(5)-H(5B)	0.9900
C(6)-O(3)	1.4274(18)
C(6)-O(2)	1.430(2)
C(6)-C(8)	1.505(3)
C(6)-C(7)	1.517(2)
C(7)-H(7A)	0.9800
C(7)-H(7B)	0.9800
C(7)-H(7C)	0.9800
C(8)-H(8A)	0.9800
C(8)-H(8B)	0.9800
C(8)-H(8C)	0.9800
C(9)-O(5)	1.200(2)
C(9)-O(1)	1.348(2)
C(9)-C(10)	1.527(2)
C(10)-N(1)	1.275(2)
C(10)-C(11)	1.481(2)
C(11)-C(12)	1.391(2)
C(11)-C(16)	1.402(2)
C(12)-C(13)	1.389(2)
C(12)-H(12)	0.9500
C(13)-C(14)	1.384(3)
C(13)-H(13)	0.9500
C(14)-C(15)	1.395(3)
C(14)-H(14)	0.9500
C(15)-C(16)	1.383(2)
C(15)-H(15)	0.9500
C(16)-H(16)	0.9500

O(4)-C(1)-O(3)	110.63(13)
O(4)-C(1)-C(2)	106.42(12)
O(3)-C(1)-C(2)	104.19(12)
O(4)-C(1)-H(1)	111.7
O(3)-C(1)-H(1)	111.7
C(2)-C(1)-H(1)	111.7
O(2)-C(2)-C(3)	107.29(13)
O(2)-C(2)-C(1)	105.21(13)
C(3)-C(2)-C(1)	104.74(12)
O(2)-C(2)-H(2)	113.0
C(3)-C(2)-H(2)	113.0
C(1)-C(2)-H(2)	113.0
O(1)-C(3)-C(2)	107.69(12)
O(1)-C(3)-C(4)	111.26(12)
C(2)-C(3)-C(4)	102.47(12)
O(1)-C(3)-H(3)	111.7
C(2)-C(3)-H(3)	111.7
C(4)-C(3)-H(3)	111.7
O(4)-C(4)-C(5)	108.27(12)
O(4)-C(4)-C(3)	104.51(11)
C(5)-C(4)-C(3)	113.14(13)
O(4)-C(4)-H(4)	110.2
C(5)-C(4)-H(4)	110.2
C(3)-C(4)-H(4)	110.2
N(1)-C(5)-C(4)	109.54(12)
N(1)-C(5)-H(5A	109.8
C(4)-C(5)-H(5A)	109.8
N(1)-C(5)-H(5B)	109.8
C(4)-C(5)-H(5B)	109.8
H(5A)-C(5)-H(5B)	108.2
O(3)-C(6)-O(2)	105.41(13)
O(3)-C(6)-C(8)	109.15(14)
O(2)-C(6)-C(8)	107.81(14)
O(3)-C(6)-C(7)	110.76(14)
O(2)-C(6)-C(7)	109.77(14)
C(8)-C(6)-C(7)	113.58(16)
C(6)-C(7)-H(7A)	109.5
C(6)-C(7)-H(7B)	109.5
H(7A)-C(7)-H(7B)	109.5
C(6)-C(7)-H(7C)	109.5
H(7A)-C(7)-H(7C)	109.5
H(7B)-C(7)-H(7C)	109.5
C(6)-C(8)-H(8A)	109.5
C(6)-C(8)-H(8B)	109.5
H(8A)-C(8)-H(8B)	109.5
C(6)-C(8)-H(8C)	109.5
H(8A)-C(8)-H(8C)	109.5
H(8B)-C(8)-H(8C)	109.5
O(5)-C(9)-O(1)	119.52(14)
O(5)-C(9)-C(10)	122.34(15)
O(1)-C(9)-C(10)	118.07(13)
N(1)-C(10)-C(11)	120.64(13)
N(1)-C(10)-C(9)	121.24(14)
C(11)-C(10)-C(9)	117.96(12)
C(12)-C(11)-C(16)	119.10(14)
C(12)-C(11)-C(10)	122.16(14)
C(16)-C(11)-C(10)	118.73(13)
C(13)-C(12)-C(11)	120.46(15)
C(13)-C(12)-H(12)	119.8
C(11)-C(12)-H(12)	119.8
C(14)-C(13)-C(12)	120.22(16)
C(14)-C(13)-H(13)	119.9
C(12)-C(13)-H(13)	119.9
C(13)-C(14)-C(15)	119.75(16)
C(13)-C(14)-H(14)	120.1
C(15)-C(14)-H(14)	120.1
C(16)-C(15)-C(14)	20.21(16)
C(16)-C(15)-H(15)	119.9
C(14)-C(15)-H(15)	119.9
C(15)-C(16)-C(11)	20.22(14)
C(15)-C(16)-H(16)	119.9
C(11)-C(16)-H(16)	119.9
C(10)-N(1)-C(5)	117.53(13)
C(9)-O(1)-C(3)	118.96(11)
C(2)-O(2)-C(6)	108.74(12)
C(1)-O(3)-C(6)	109.57(12)
C(1)-O(4)-C(4)	107.86(11)

Table 4. Anisotropic displacement parameters [$Å^2 \times 10^3$] for 08mz206_0m. The anisotropic displacement factor exponent takes the form: $-2\pi^2$ [(h a*)^2 U11 + ... + 2 h k a* b* U12]

	U11	U22	U33	U23	U13	U12
C(1)	19(1)	23(1)	18(1)	-2(1)	2(1)	-1(1)
C(2)	20(1)	20(1)	19(1)	-2(1)	1(1)	-2(1)
C(3)	18(1)	17(1)	17(1)	1(1)	3(1)	-1(1)
C(4)	17(1)	20(1)	14(1)	-1(1)	3(1)	1(1)
C(5)	19(1)	23(1)	18(1)	-2(1)	0(1)	0(1)
C(6)	20(1)	19(1)	26(1)	-3(1)	3(1)	1(1)
C(7)	32(1)	27(1)	29(1)	-10(1)	-1(1)	4(1)
C(8)	36(1)	29(1)	35(1)	0(1)	9(1)	-6(1)
C(9)	21(1)	20(1)	17(1)	2(1)	2(1)	-3(1)
C(10)	22(1)	15(1)	16(1)	0(1)	3(1)	-4(1)
C(11)	20(1)	14(1)	21(1)	-2(1)	2(1)	-3(1)
C(12)	25(1)	20(1)	21(1)	1(1)	1(1)	-2(1)
C(13)	23(1)	22(1)	31(1)	2(1)	-1(1)	0(1)
C(14)	21(1)	25(1)	35(1)	-5(1)	4(1)	-1(1)
C(15)	24(1)	31(1)	24(1)	-8(1)	4(1)	-4(1)
C(16)	21(1)	23(1)	20(1)	-2(1)	1(1)	-3(1)
N(1)	22(1)	18(1)	18(1)	-2(1)	2(1)	-2(1)
O(1)	26(1)	19(1)	15(1)	1(1)	4(1)	-2(1)
O(2)	17(1)	18(1)	45(1)	-3(1)	6(1)	-1(1)
O(3)	20(1)	22(1)	31(1)	2(1)	1(1)	1(1)
O(4)	16(1)	27(1)	20(1)	-6(1)	4(1)	-1(1)
O(5)	35(1)	22(1)	20(1)	6(1)	5(1)	-4(1)

Table 5. Hydrogen coordinates ($\times 10^4$) and isotropic displacement parameters ($Å^2 \times 10^3$) for 08mz206_0m.

	x	y	z	U(eq)
H(1)	3522	8949	9199	24
H(2)	7325	8169	9725	24
H(3)	8388	7291	7683	21
H(4)	5159	8110	6358	21
H(5A)	2836	5998	6948	25
H(5B)	2338	6654	5651	25
H(7A)	6676	11819	9308	45
H(7B)	9255	11228	9696	45
H(7C)	7009	10636	10104	45
H(8A)	7170	10491	6479	49
H(8B)	9487	11020	7362	49
H(8C)	7035	11740	7128	49
H(12)	10316	3888	8217	27

H(13)	13195	2675	7651	31
H(14)	13392	2480	5599	32
H(15)	10790	3567	4111	31
H(16)	7877	4760	4665	26

Table 6. Torsion angles [deg] for 08mz206_0m.

O(4)-C(1)-C(2)-O(2)	116.16(14)
O(3)-C(1)-C(2)-O(2)	-0.81(16)
O(4)-C(1)-C(2)-C(3)	3.20(16)
O(3)-C(1)-C(2)-C(3)	-113.77(13)
O(2)-C(2)-C(3)-O(1)	149.62(12)
C(1)-C(2)-C(3)-O(1)	-98.90(14)
O(2)-C(2)-C(3)-C(4)	-92.97(13)
C(1)-C(2)-C(3)-C(4)	18.51(15)
O(1)-C(3)-C(4)-O(4)	80.62(14)
C(2)-C(3)-C(4)-O(4)	-34.22(15)
O(1)-C(3)-C(4)-C(5)	-36.95(16)
C(2)-C(3)-C(4)-C(5)	-151.79(13)
O(4)-C(4)-C(5)-N(1)	-167.39(12)
C(3)-C(4)-C(5)-N(1)	-52.04(16)
O(5)-C(9)-C(10)-N(1)	122.01(18)
O(1)-C(9)-C(10)-N(1)	-55.1(2)
O(5)-C(9)-C(10)-C(11)	-53.4(2)
O(1)-C(9)-C(10)-C(11)	129.48(14)
N(1)-C(10)-C(11)-C(12)	-179.34(15)
C(9)-C(10)-C(11)-C(12)	-3.9(2)
N(1)-C(10)-C(11)-C(16)	0.9(2)
C(9)-C(10)-C(11)-C(16)	176.34(14)
C(16)-C(11)-C(12)-C(13)	-1.7(2)
C(10)-C(11)-C(12)-C(13)	178.58(15)
C(11)-C(12)-C(13)-C(14)	0.4(3)
C(12)-C(13)-C(14)-C(15)	1.4(3)
C(13)-C(14)-C(15)-C(16)	-1.9(3)
C(14)-C(15)-C(16)-C(11)	0.6(2)
C(12)-C(11)-C(16)-C(15)	1.2(2)
C(10)-C(11)-C(16)-C(15)	-179.04(14)
C(11)-C(10)-N(1)-C(5)	179.63(13)
C(9)-C(10)-N(1)-C(5)	4.3(2)
C(4)-C(5)-N(1)-C(10)	73.65(17)
O(5)-C(9)-O(1)-C(3)	178.09(14)
C(10)-C(9)-O(1)-C(3)	-4.70(18)
C(2)-C(3)-O(1)-C(9)	-176.29(12)
C(4)-C(3)-O(1)-C(9)	72.16(16)
C(3)-C(2)-O(2)-C(6)	127.65(13)
C(1)-C(2)-O(2)-C(6)	16.50(16)
O(3)-C(6)-O(2)-C(2)	-26.08(17)
C(8)-C(6)-O(2)-C(2)	-142.56(14)
C(7)-C(6)-O(2)-C(2)	93.25(16)
O(4)-C(1)-O(3)-C(6)	-129.27(13)
C(2)-C(1)-O(3)-C(6)	-15.27(16)
O(2)-C(6)-O(3)-C(1)	25.73(16)
C(8)-C(6)-O(3)-C(1)	141.29(14)

C(7)-C(6)-O(3)-C(1)	-92.94(16)
O(3)-C(1)-O(4)-C(4)	86.79(14)
C(2)-C(1)-O(4)-C(4)	-25.80(16)
C(5)-C(4)-O(4)-C(1)	159.11(12)
C(3)-C(4)-O(4)-C(1)	38.25(15)

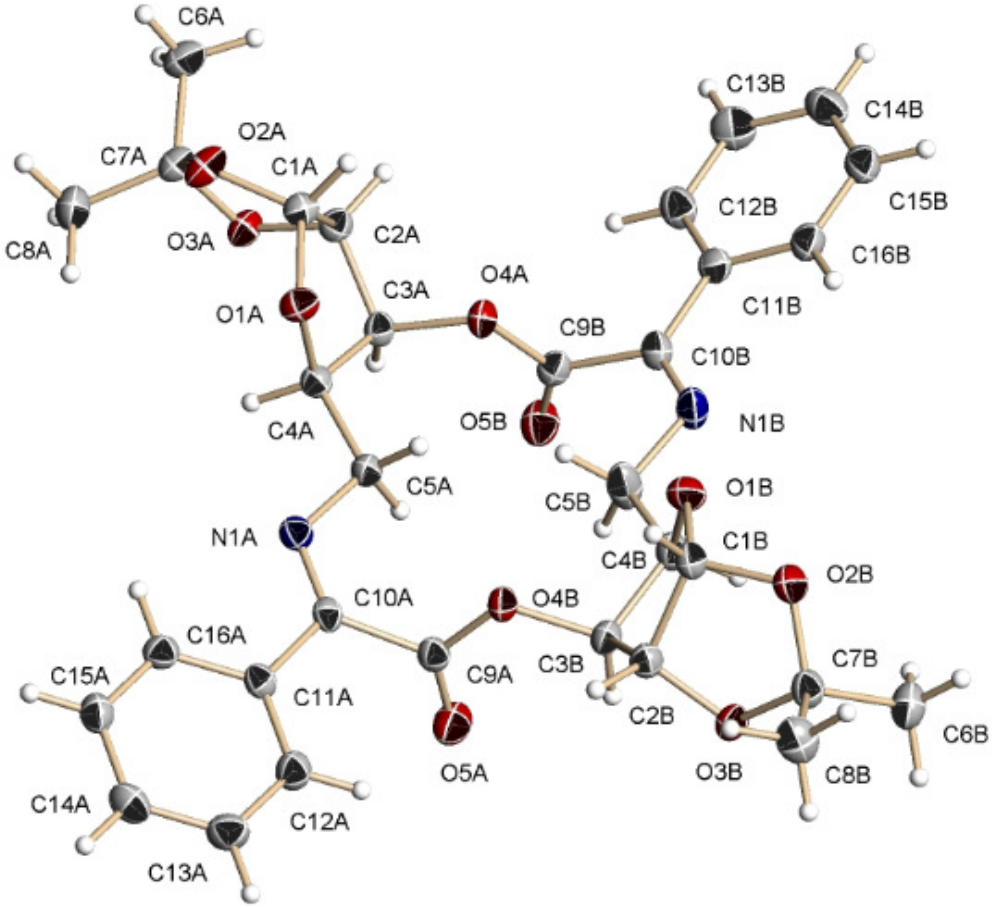

Figure 75: X-Ray crystal structure of macrocycle **9**.

Table 1. Crystal data and structure refinement for 07mz451m:

Identification code: 07mz451m
Empirical formula: C32 H34 N2 O10
Formula weight: 606.61
Temperature: 100(2) K
Wavelength: 0.71073 Å
Crystal system: Monoclinic
Space group: $P2_1$
Unit cell dimensions:
a = 12.2470(16) Å, α = 90°
b = 8.9617(12) Å, β = 92.672(2)°
c = 13.4118(17) Å, γ = 90°
Volume, *Z*: 1470.4(3) $Å^3$, 2
Density (calculated): 1.370 Mg/m^3
Absorption coefficient: 0.102 mm^{-1}
F(000): 640
Crystal size: 0.65 × 0.51 × 0.10 mm
Crystal shape, colour: plate, colourless
θ range for data collection: 1.52 to 28.28°
Limiting indices: $-16 \le h \le 16$, $-10 \le k \le 11$, $-17 \le l \le 15$
Reflections collected: 9956
Independent reflections: 3838 (*R*(int) = 0.0296)
Completeness to θ = 28.28°: 98.9 %
Absorption correction: multi-scan
Max. and min. transmission: 1.0000 and 0.7240
Refinement method: Full-matrix least-squares on F^2
Data / restraints / parameters: 3838 / 1 / 401
Goodness-of-fit on F^2: 1.092
Final *R* indices [$I>2\sigma(I)$]: R1 = 0.0463, wR2 = 0.1053
R indices (all data): R1 = 0.0521, wR2 = 0.1087
Largest diff. peak and hole: 0.379 and −0.181 e × $Å^{-3}$

Refinement of F^2 against ALL reflections. The weighted R-factor wR and goodness of fit are based on F^2, conventional R-factors R are based on *F*, with *F* set to zero for negative F^2. The threshold expression of $F^2 > 2\sigma(F^2)$ is used only for calculating R-factors

Treatment of hydrogen atoms:
All hydrogen atoms were placed in calculated positions and were refined with an isotropic displacement parameter 1.5 (methyl) or 1.2 times (all others) that of the adjacent carbon atom. Methyl H atoms were allowed to rotate to best fit the experimental electron density.

Table 2. Atomic coordinates [× 10^4] and equivalent isotropic displacement parameters [Å^2 × 10^3] for 07mz451m. U(eq) is defined as one third of the trace of the orthogonalized U_{ij} tensor.

	x	y	z	U(eq)
C(1A)	962(2)	1312(3)	−1217(2)	23(1)
C(2A)	1297(2)	−324(3)	−1349(2)	22(1)
C(3A)	1297(2)	−969(3)	−309(2)	21(1)
C(4A)	406(2)	−55(3)	162(2)	21(1)
C(5A)	519(2)	37(3)	1289(2)	24(1)
C(6A)	483(2)	243(4)	−3516(2)	32(1)
C(7A)	−62(2)	224(3)	−2529(2)	24(1)
C(8A)	−1286(2)	10(4)	−2631(2)	36(1)
C(9A)	385(2)	−48(3)	3377(2)	23(1)
C(10A)	−522(2)	571(3)	2670(2)	21(1)
C(11A)	−1511(2)	1109(3)	3162(2)	22(1)
C(12A)	−1571(2)	1118(3)	4194(2)	28(1)
C(13A)	−2515(2)	1612(4)	4631(2)	32(1)
C(14A)	−3393(2)	2118(3)	4038(2)	31(1)
C(15A)	−3329(2)	2144(3)	3011(2)	28(1)
C(16A)	−2398(2)	1643(3)	2570(2)	25(1)
C(1B)	3297(2)	2563(3)	4354(2)	26(1)
C(2B)	2442(2)	1593(3)	4864(2)	24(1)
C(3B)	2180(2)	362(3)	4112(2)	23(1)
C(4B)	3225(2)	283(3)	3549(2)	26(1)
C(5B)	3054(2)	−368(4)	2511(2)	37(1)
C(6B)	4898(2)	967(4)	6330(2)	34(1)
C(7B)	3930(2)	1894(3)	5961(2)	26(1)
C(8B)	3564(3)	3012(4)	6721(2)	36(1)
C(9B)	2905(2)	−1682(3)	679(2)	23(1)
C(10B)	3995(2)	−1123(3)	1126(2)	24(1)
C(11B)	4957(2)	−1301(3)	512(2)	24(1)
C(12B)	4867(2)	−1998(3)	−415(2)	31(1)
C(13B)	5776(3)	−2157(4)	−986(2)	36(1)
C(14B)	6784(2)	−1625(4)	−622(2)	34(1)
C(15B)	6875(2)	−921(3)	297(2)	30(1)
C(16B)	5978(2)	−751(3)	857(2)	26(1)
N(1A)	−486(2)	550(3)	1727(2)	23(1)
N(1B)	4081(2)	−569(3)	2006(2)	30(1)
O(1A)	520(2)	1422(2)	−259(1)	25(1)
O(2A)	175(2)	1585(2)	−1995(1)	30(1)

O(3A)	387(2)	-935(2)	-1904(1)	24(1)
O(4A)	2368(1)	-598(2)	161(1)	23(1)
O(5A)	310(2)	-1198(2)	3824(2)	34(1)
O(1B)	3567(2)	1819(2)	3474(1)	31(1)
O(2B)	4192(2)	2644(2)	5058(1)	30(1)
O(3B)	3053(2)	911(2)	5672(1)	26(1)
O(4B)	1268(1)	857(2)	3449(1)	23(1)
O(5B)	2562(2)	-2914(2)	810(2)	34(1)

All esds (except the esd in the dihedral angle between two l.s. planes) are estimated using the full covariance matrix. The cell esds are taken into account individually in the estimation of esds in distances, angles and torsion angles; correlations between esds in cell parameters are only used when they are defined by crystal symmetry. An approximate (isotropic) treatment of cell esds is used for estimating esds involving l.s. planes.

Table 3. Bond lengths [Å] and angles [deg] for 07mz451m.

C(1A)-O(2A)	1.408(3)	C(11A)-C(12A)	1.389(4)
C(1A)-O(1A)	1.420(3)	C(11A)-C(16A)	1.401(3)
C(1A)-C(2A)	1.535(4)	C(12A)-C(13A)	1.392(4)
C(1A)-H(1A)	1.0000	C(12A)-H(12A)	0.9500
C(2A)-O(3A)	1.421(3)	C(13A)-C(14A)	1.384(4)
C(2A)-C(3A)	1.511(3)	C(13A)-H(13A)	0.9500
C(2A)-H(2A)	1.0000	C(14A)-C(15A)	1.384(4)
C(3A)-O(4A)	1.466(3)	C(14A)-H(14A)	0.9500
C(3A)-C(4A)	1.525(4)	C(15A)-C(16A)	1.383(4)
C(3A)-H(3A)	1.0000	C(15A)-H(15A)	0.9500
C(4A)-O(1A)	1.448(3)	C(16A)-H(16A)	0.9500
C(4A)-C(5A)	1.514(3)	C(1B)-O(1B)	1.408(3)
C(4A)-H(4A)	1.0000	C(1B)-O(2B)	1.414(3)
C(5A)-N(1A)	1.462(3)	C(1B)-C(2B)	1.545(4)
C(5A)-H(5A1)	0.9900	C(1B)-H(1B)	1.0000
C(5A)-H(5A2)	0.9900	C(2B)-O(3B)	1.426(3)
C(6A)-C(7A)	1.510(4)	C(2B)-C(3B)	1.519(4)
C(6A)-H(6A1)	0.9800	C(2B)-H(2B)	1.0000
C(6A)-H(6A2)	0.9800	C(3B)-O(4B)	1.464(3)
C(6A)-H(6A3)	0.9800	C(3B)-C(4B)	1.518(4)
C(7A)-O(3A)	1.429(3)	C(3B)-H(3B)	1.0000
C(7A)-O(2A)	1.437(3)	C(4B)-O(1B)	1.443(4)
C(7A)-C(8A)	1.511(4)	C(4B)-C(5B)	1.514(4)
C(8A)-H(8A1)	0.9800	C(4B)-H(4B)	1.0000
C(8A)-H(8A2)	0.9800	C(5B)-N(1B)	1.468(4)
C(8A)-H(8A3)	0.9800	C(5B)-H(5B1)	0.9900
C(9A)-O(5A)	1.197(3)	C(5B)-H(5B2)	0.9900
C(9A)-O(4B)	1.352(3)	C(6B)-C(7B)	1.512(4)
C(9A)-C(10A)	1.531(3)	C(6B)-H(6B1)	0.9800
C(10A)-N(1A)	1.268(3)	C(6B)-H(6B2)	0.9800
C(10A)-C(11A)	1.486(3)	C(6B)-H(6B3)	0.9800

C(7B)-O(3B)	1.429(3)	H(6A1)-C(6A)-H(6A3)	109.5
C(7B)-O(2B)	1.435(3)	H(6A2)-C(6A)-H(6A3)	109.5
C(7B)-C(8B)	1.512(4)	O(3A)-C(7A)-O(2A)	105.17(18)
C(8B)-H(8B1)	0.9800	O(3A)-C(7A)-C(6A)	110.4(2)
C(8B)-H(8B2)	0.9800	O(2A)-C(7A)-C(6A)	109.8(2)
C(8B)-H(8B3)	0.9800	O(3A)-C(7A)-C(8A)	108.3(2)
C(9B)-O(5B)	1.197(3)	O(2A)-C(7A)-C(8A)	109.2(2)
C(9B)-O(4A)	1.348(3)	C(6A)-C(7A)-C(8A)	113.5(2)
C(9B)-C(10B)	1.523(3)	C(7A)-C(8A)-H(8A1)	109.5
C(10B)-N(1B)	1.281(3)	C(7A)-C(8A)-H(8A2)	109.5
C(10B)-C(11B)	1.477(4)	H(8A1)-C(8A)-H(8A2)	109.5
C(11B)-C(12B)	1.392(4)	C(7A)-C(8A)-H(8A3)	109.5
C(11B)-C(16B)	1.402(4)	H(8A1)-C(8A)-H(8A3)	109.5
C(12B)-C(13B)	1.387(4)	H(8A2)-C(8A)-H(8A3)	109.5
C(12B)-H(12B)	0.9500	O(5A)-C(9A)-O(4B)	124.1(2)
C(13B)-C(14B)	1.391(4)	O(5A)-C(9A)-C(10A)	123.5(2)
C(13B)-H(13B)	0.9500	O(4B)-C(9A)-C(10A)	112.4(2)
C(14B)-C(15B)	1.384(4)	N(1A)-C(10A)-C(11A)	121.0(2)
C(14B)-H(14B)	0.9500	N(1A)-C(10A)-C(9A)	123.7(2)
C(15B)-C(16B)	1.368(4)	C(11A)-C(10A)-C(9A)	115.1(2)
C(15B)-H(15B)	0.9500	C(12A)-C(11A)-C(16A)	119.2(2)
C(16B)-H(16B)	0.9500	C(12A)-C(11A)-C(10A)	121.8(2)
		C(16A)-C(11A)-C(10A)	119.0(2)
O(2A)-C(1A)-O(1A)	112.5(2)	C(11A)-C(12A)-C(13A)	120.3(2)
O(2A)-C(1A)-C(2A)	104.9(2)	C(11A)-C(12A)-H(12A)	119.9
O(1A)-C(1A)-C(2A)	106.6(2)	C(13A)-C(12A)-H(12A)	119.9
O(2A)-C(1A)-H(1A)	110.9	C(14A)-C(13A)-C(12A)	120.1(3)
O(1A)-C(1A)-H(1A)	110.9	C(14A)-C(13A)-H(13A)	120.0
C(2A)-C(1A)-H(1A)	110.9	C(12A)-C(13A)-H(13A)	120.0
O(3A)-C(2A)-C(3A)	107.6(2)	C(15A)-C(14A)-C(13A)	119.9(3)
O(3A)-C(2A)-C(1A)	102.80(19)	C(15A)-C(14A)-H(14A)	120.0
C(3A)-C(2A)-C(1A)	104.3(2)	C(13A)-C(14A)-H(14A)	120.0
O(3A)-C(2A)-H(2A)	113.7	C(16A)-C(15A)-C(14A)	120.5(2)
C(3A)-C(2A)-H(2A)	113.7	C(16A)-C(15A)-H(15A)	119.8
C(1A)-C(2A)-H(2A)	113.7	C(14A)-C(15A)-H(15A)	119.8
O(4A)-C(3A)-C(2A)	105.79(19)	C(15A)-C(16A)-C(11A)	120.0(2)
O(4A)-C(3A)-C(4A)	110.13(19)	C(15A)-C(16A)-H(16A)	120.0
C(2A)-C(3A)-C(4A)	101.9(2)	C(11A)-C(16A)-H(16A)	120.0
O(4A)-C(3A)-H(3A)	112.8	O(1B)-C(1B)-O(2B)	112.3(2)
C(2A)-C(3A)-H(3A)	112.8	O(1B)-C(1B)-C(2B)	107.2(2)
C(4A)-C(3A)-H(3A)	112.8	O(2B)-C(1B)-C(2B)	104.7(2)
O(1A)-C(4A)-C(5A)	109.5(2)	O(1B)-C(1B)-H(1B)	110.8
O(1A)-C(4A)-C(3A)	104.2(2)	O(2B)-C(1B)-H(1B)	110.8
C(5A)-C(4A)-C(3A)	114.1(2)	C(2B)-C(1B)-H(1B)	110.8
O(1A)-C(4A)-H(4A)	109.6	O(3B)-C(2B)-C(3B)	106.3(2)
C(5A)-C(4A)-H(4A)	109.6	O(3B)-C(2B)-C(1B)	103.62(19)
C(3A)-C(4A)-H(4A)	109.6	C(3B)-C(2B)-C(1B)	104.0(2)
N(1A)-C(5A)-C(4A)	112.25(19)	O(3B)-C(2B)-H(2B)	114.0
N(1A)-C(5A)-H(5A1)	109.2	C(3B)-C(2B)-H(2B)	114.0
C(4A)-C(5A)-H(5A1)	109.2	C(1B)-C(2B)-H(2B)	114.0
N(1A)-C(5A)-H(5A2)	109.2	O(4B)-C(3B)-C(4B)	110.4(2)
C(4A)-C(5A)-H(5A2)	109.2	O(4B)-C(3B)-C(2B)	108.3(2)
H(5A1)-C(5A)-H(5A2)	107.9	C(4B)-C(3B)-C(2B)	102.0(2)
C(7A)-C(6A)-H(6A1)	109.5	O(4B)-C(3B)-H(3B)	111.9
C(7A)-C(6A)-H(6A2)	109.5	C(4B)-C(3B)-H(3B)	111.9
H(6A1)-C(6A)-H(6A2)	109.5	C(2B)-C(3B)-H(3B)	111.9
C(7A)-C(6A)-H(6A3)	109.5	O(1B)-C(4B)-C(5B)	109.4(2)

O(1B)-C(4B)-C(3B) 104.1(2)
C(5B)-C(4B)-C(3B) 113.1(2)
O(1B)-C(4B)-H(4B) 110.0
C(5B)-C(4B)-H(4B) 110.0
C(3B)-C(4B)-H(4B) 110.0
N(1B)-C(5B)-C(4B) 112.7(2)
N(1B)-C(5B)-H(5B1) 109.0
C(4B)-C(5B)-H(5B1) 109.0
N(1B)-C(5B)-H(5B2) 109.0
C(4B)-C(5B)-H(5B2) 109.0
H(5B1)-C(5B)-H(5B2) 107.8
C(7B)-C(6B)-H(6B1) 109.5
C(7B)-C(6B)-H(6B2) 109.5
H(6B1)-C(6B)-H(6B2) 109.5
C(7B)-C(6B)-H(6B3) 109.5
H(6B1)-C(6B)-H(6B3) 109.5
H(6B2)-C(6B)-H(6B3) 109.5
O(3B)-C(7B)-O(2B) 104.78(18)
O(3B)-C(7B)-C(8B) 110.4(2)
O(2B)-C(7B)-C(8B) 110.1(2)
O(3B)-C(7B)-C(6B) 108.6(2)
O(2B)-C(7B)-C(6B) 109.3(2)
C(8B)-C(7B)-C(6B) 113.3(2)
C(7B)-C(8B)-H(8B1) 109.5
C(7B)-C(8B)-H(8B2) 109.5
H(8B1)-C(8B)-H(8B2) 109.5
C(7B)-C(8B)-H(8B3) 109.5
H(8B1)-C(8B)-H(8B3) 109.5
H(8B2)-C(8B)-H(8B3) 109.5
O(5B)-C(9B)-O(4A) 125.1(2)
O(5B)-C(9B)-C(10B) 123.5(2)
O(4A)-C(9B)-C(10B) 111.3(2)
N(1B)-C(10B)-C(11B) 121.5(2)
N(1B)-C(10B)-C(9B) 121.5(2)
C(11B)-C(10B)-C(9B) 117.0(2)
C(12B)-C(11B)-C(16B) 119.0(2)
C(12B)-C(11B)-C(10B) 120.9(2)
C(16B)-C(11B)-C(10B) 120.0(2)
C(13B)-C(12B)-C(11B) 120.4(3)
C(13B)-C(12B)-H(12B) 119.8
C(11B)-C(12B)-H(12B) 119.8
C(12B)-C(13B)-C(14B) 119.6(3)
C(12B)-C(13B)-H(13B) 120.2
C(14B)-C(13B)-H(13B) 120.2
C(15B)-C(14B)-C(13B) 120.1(3)
C(15B)-C(14B)-H(14B) 119.9
C(13B)-C(14B)-H(14B) 119.9
C(16B)-C(15B)-C(14B) 120.4(3)
C(16B)-C(15B)-H(15B) 119.8
C(14B)-C(15B)-H(15B) 119.8
C(15B)-C(16B)-C(11B) 120.4(3)
C(15B)-C(16B)-H(16B) 119.8
C(11B)-C(16B)-H(16B) 119.8
C(10A)-N(1A)-C(5A) 118.3(2)
C(10B)-N(1B)-C(5B) 116.0(2)
C(1A)-O(1A)-C(4A) 109.70(19)
C(1A)-O(2A)-C(7A) 109.69(19)
C(2A)-O(3A)-C(7A) 107.31(19)
C(9B)-O(4A)-C(3A) 117.6(2)
C(1B)-O(1B)-C(4B) 108.3(2)
C(1B)-O(2B)-C(7B) 110.02(19)
C(2B)-O(3B)-C(7B) 107.6(2)
C(9A)-O(4B)-C(3B) 116.5(2)

Table 4. Anisotropic displacement parameters [$Å^2 \times 10^3$] for 07mz451m. The anisotropic displacement factor exponent takes the form: $-2\pi^2$ [(h a*)^2 U11 + ... + 2 h k a* b* U12]

	U11	U22	U33	U23	U13	U12
C(1A)	25(1)	21(1)	21(1)	0(1)	1(1)	-1(1)
C(2A)	24(1)	23(1)	19(1)	-2(1)	0(1)	0(1)
C(3A)	19(1)	23(1)	21(1)	-2(1)	-2(1)	-2(1)
C(4A)	21(1)	23(1)	20(1)	-1(1)	1(1)	-1(1)
C(5A)	20(1)	31(1)	20(1)	1(1)	0(1)	1(1)
C(6A)	40(2)	34(2)	23(1)	3(1)	2(1)	5(1)
C(7A)	29(1)	24(1)	20(1)	1(1)	-2(1)	3(1)
C(8A)	28(1)	46(2)	34(2)	3(1)	-6(1)	2(1)
C(9A)	20(1)	27(1)	21(1)	-3(1)	1(1)	2(1)
C(10A)	17(1)	21(1)	25(1)	-1(1)	-1(1)	-3(1)
C(11A)	20(1)	23(1)	25(1)	-2(1)	1(1)	-3(1)
C(12A)	26(1)	33(1)	25(1)	-3(1)	-1(1)	0(1)
C(13A)	35(2)	37(2)	25(1)	-2(1)	6(1)	0(1)
C(14A)	27(1)	31(1)	36(2)	-4(1)	9(1)	2(1)
C(15A)	23(1)	29(1)	32(1)	1(1)	-1(1)	2(1)
C(16A)	26(1)	24(1)	24(1)	1(1)	1(1)	-2(1)
C(1B)	21(1)	30(1)	28(1)	1(1)	-1(1)	-1(1)
C(2B)	22(1)	28(1)	21(1)	-2(1)	1(1)	1(1)
C(3B)	21(1)	27(1)	20(1)	1(1)	-3(1)	1(1)
C(4B)	22(1)	33(1)	24(1)	-3(1)	-1(1)	1(1)
C(5B)	24(1)	62(2)	26(1)	-16(1)	0(1)	4(1)
C(6B)	29(1)	34(1)	39(2)	0(1)	-8(1)	3(1)
C(7B)	23(1)	30(1)	25(1)	-4(1)	-2(1)	-1(1)
C(8B)	34(2)	41(2)	34(2)	-14(1)	2(1)	0(1)
C(9B)	25(1)	24(1)	19(1)	-3(1)	0(1)	4(1)
C(10B)	20(1)	25(1)	27(1)	-1(1)	-1(1)	3(1)
C(11B)	22(1)	25(1)	25(1)	2(1)	2(1)	5(1)
C(12B)	26(1)	35(2)	31(1)	-7(1)	1(1)	0(1)
C(13B)	40(2)	39(2)	31(2)	-9(1)	5(1)	3(1)
C(14B)	30(2)	34(2)	38(2)	2(1)	10(1)	4(1)
C(15B)	25(1)	29(1)	34(1)	6(1)	0(1)	0(1)
C(16B)	26(1)	28(1)	26(1)	1(1)	-1(1)	3(1)
N(1A)	21(1)	24(1)	23(1)	-1(1)	1(1)	-1(1)
N(1B)	21(1)	43(1)	25(1)	-6(1)	-1(1)	6(1)
O(1A)	31(1)	23(1)	22(1)	-1(1)	4(1)	3(1)
O(2A)	44(1)	25(1)	22(1)	-1(1)	-6(1)	5(1)
O(3A)	28(1)	22(1)	22(1)	0(1)	-5(1)	0(1)
O(4A)	20(1)	24(1)	24(1)	-1(1)	-4(1)	0(1)
O(5A)	35(1)	29(1)	38(1)	7(1)	-8(1)	-7(1)
O(1B)	29(1)	39(1)	24(1)	1(1)	3(1)	-4(1)
O(2B)	24(1)	37(1)	29(1)	1(1)	-1(1)	-4(1)
O(3B)	25(1)	31(1)	21(1)	1(1)	-4(1)	-2(1)
O(4B)	19(1)	27(1)	24(1)	3(1)	-3(1)	-2(1)
O(5B)	33(1)	26(1)	43(1)	4(1)	-6(1)	0(1)

Table 5. Hydrogen coordinates ($\times 10^4$) and isotropic displacement parameters ($Å^2 \times 10^3$) for 07mz451m.

	x	y	z	U(eq)
H(1A)	1605	1990	−1270	27
H(2A)	2006	−450	−1679	26
H(3A)	1143	−2064	−306	25
H(4A)	−327	−472	−45	26
H(5A1)	712	−960	1561	28
H(5A2)	1121	730	1483	28
H(6A1)	246	1129	−3896	48
H(6A2)	279	−657	−3895	48
H(6A3)	1279	271	−3396	48
H(8A1)	−1599	117	−1975	54
H(8A2)	−1449	−988	−2896	54
H(8A3)	−1604	763	−3088	54
H(12A)	−965	786	4604	34
H(13A)	−2556	1601	5337	38
H(14A)	−4039	2448	4336	37
H(15A)	−3928	2508	2606	34
H(16A)	−2361	1662	1864	30
H(1B)	2999	3580	4200	31
H(2B)	1787	2160	5071	28
H(3B)	2017	−606	4446	28
H(4B)	3791	−305	3940	32
H(5B1)	2684	−1346	2559	45
H(5B2)	2568	300	2105	45
H(6B1)	4711	420	6931	51
H(6B2)	5523	1623	6487	51
H(6B3)	5089	257	5810	51
H(8B1)	2920	3548	6449	55
H(8B2)	4156	3724	6874	55
H(8B3)	3380	2488	7332	55
H(12B)	4178	−2369	−659	37
H(13B)	5710	−2625	−1621	44
H(14B)	7412	−1745	−1004	40
H(15B)	7565	−555	541	36
H(16B)	6047	−256	1483	32

Table 6. Torsion angles [deg] for 07mz451m

O(2A)-C(1A)-C(2A)-O(3A)	-22.5(3)
O(1A)-C(1A)-C(2A)-O(3A)	97.0(2)
O(2A)-C(1A)-C(2A)-C(3A)	-134.7(2)
O(1A)-C(1A)-C(2A)-C(3A)	-15.2(2)
O(3A)-C(2A)-C(3A)-O(4A)	167.11(19)
C(1A)-C(2A)-C(3A)-O(4A)	-84.2(2)
O(3A)-C(2A)-C(3A)-C(4A)	-77.7(2)
C(1A)-C(2A)-C(3A)-C(4A)	31.0(2)
O(4A)-C(3A)-C(4A)-O(1A)	75.7(2)
C(2A)-C(3A)-C(4A)-O(1A)	-36.3(2)
O(4A)-C(3A)-C(4A)-C(5A)	-43.7(3)
C(2A)-C(3A)-C(4A)-C(5A)	-155.6(2)
O(1A)-C(4A)-C(5A)-N(1A)	79.5(3)
C(3A)-C(4A)-C(5A)-N(1A)	-164.2(2)
O(5A)-C(9A)-C(10A)-N(1A)	-105.6(3)
O(4B)-C(9A)-C(10A)-N(1A)	75.2(3)
O(5A)-C(9A)-C(10A)-C(11A)	69.8(3)
O(4B)-C(9A)-C(10A)-C(11A)	-109.4(2)
N(1A)-C(10A)-C(11A)-C(12A)	179.0(3)
C(9A)-C(10A)-C(11A)-C(12A)	3.4(3)
N(1A)-C(10A)-C(11A)-C(16A)	-2.1(4)
C(9A)-C(10A)-C(11A)-C(16A)	-177.7(2)
C(16A)-C(11A)-C(12A)-C(13A)	1.9(4)
C(10A)-C(11A)-C(12A)-C(13A)	-179.2(3)
C(11A)-C(12A)-C(13A)-C(14A)	-1.0(5)
C(12A)-C(13A)-C(14A)-C(15A)	-0.5(5)
C(13A)-C(14A)-C(15A)-C(16A)	1.1(4)
C(14A)-C(15A)-C(16A)-C(11A)	-0.1(4)
C(12A)-C(11A)-C(16A)-C(15A)	-1.3(4)
C(10A)-C(11A)-C(16A)-C(15A)	179.8(2)
O(1B)-C(1B)-C(2B)-O(3B)	104.3(2)
O(2B)-C(1B)-C(2B)-O(3B)	-15.1(3)
O(1B)-C(1B)-C(2B)-C(3B)	-6.6(3)
O(2B)-C(1B)-C(2B)-C(3B)	-126.0(2)
O(3B)-C(2B)-C(3B)-O(4B)	161.10(19)
C(1B)-C(2B)-C(3B)-O(4B)	-89.9(2)
O(3B)-C(2B)-C(3B)-C(4B)	-82.4(2)
C(1B)-C(2B)-C(3B)-C(4B)	26.6(2)
O(4B)-C(3B)-C(4B)-O(1B)	77.2(2)
C(2B)-C(3B)-C(4B)-O(1B)	-37.7(2)
O(4B)-C(3B)-C(4B)-C(5B)	-41.4(3)
C(2B)-C(3B)-C(4B)-C(5B)	-156.4(2)
O(1B)-C(4B)-C(5B)-N(1B)	69.8(3)
C(3B)-C(4B)-C(5B)-N(1B)	-174.7(3)
O(5B)-C(9B)-C(10B)-N(1B)	-85.8(4)
O(4A)-C(9B)-C(10B)-N(1B)	91.7(3)
O(5B)-C(9B)-C(10B)-C(11B)	92.0(3)
O(4A)-C(9B)-C(10B)-C(11B)	-90.5(3)
N(1B)-C(10B)-C(11B)-C(12B)	175.5(3)
C(9B)-C(10B)-C(11B)-C(12B)	-2.3(4)
N(1B)-C(10B)-C(11B)-C(16B)	-5.1(4)
C(9B)-C(10B)-C(11B)-C(16B)	177.1(2)
C(16B)-C(11B)-C(12B)-C(13B)	0.5(4)
C(10B)-C(11B)-C(12B)-C(13B)	179.9(3)
C(11B)-C(12B)-C(13B)-C(14B)	0.6(5)
C(12B)-C(13B)-C(14B)-C(15B)	-1.1(5)
C(13B)-C(14B)-C(15B)-C(16B)	0.4(5)

C(14B)-C(15B)-C(16B)-C(11B)	0.7(4)
C(12B)-C(11B)-C(16B)-C(15B)	-1.2(4)
C(10B)-C(11B)-C(16B)-C(15B)	179.4(3)
C(11A)-C(10A)-N(1A)-C(5A)	178.8(2)
C(9A)-C(10A)-N(1A)-C(5A)	-6.0(4)
C(4A)-C(5A)-N(1A)-C(10A)	175.0(2)
C(11B)-C(10B)-N(1B)-C(5B)	176.3(3)
C(9B)-C(10B)-N(1B)-C(5B)	-6.0(4)
C(4B)-C(5B)-N(1B)-C(10B)	179.7(3)
O(2A)-C(1A)-O(1A)-C(4A)	106.3(2)
C(2A)-C(1A)-O(1A)-C(4A)	-8.2(2)
C(5A)-C(4A)-O(1A)-C(1A)	150.66(19)
C(3A)-C(4A)-O(1A)-C(1A)	28.2(2)
O(1A)-C(1A)-O(2A)-C(7A)	-110.4(2)
C(2A)-C(1A)-O(2A)-C(7A)	5.1(3)
O(3A)-C(7A)-O(2A)-C(1A)	14.3(3)
C(6A)-C(7A)-O(2A)-C(1A)	-104.5(2)
C(8A)-C(7A)-O(2A)-C(1A)	130.3(2)
C(3A)-C(2A)-O(3A)-C(7A)	141.7(2)
C(1A)-C(2A)-O(3A)-C(7A)	31.9(2)
O(2A)-C(7A)-O(3A)-C(2A)	-29.6(2)
C(6A)-C(7A)-O(3A)-C(2A)	88.9(2)
C(8A)-C(7A)-O(3A)-C(2A)	-146.3(2)
O(5B)-C(9B)-O(4A)-C(3A)	-2.2(4)
C(10B)-C(9B)-O(4A)-C(3A)	-179.6(2)
C(2A)-C(3A)-O(4A)-C(9B)	-135.3(2)
C(4A)-C(3A)-O(4A)-C(9B)	115.3(2)
O(2B)-C(1B)-O(1B)-C(4B)	96.7(2)
C(2B)-C(1B)-O(1B)-C(4B)	-17.7(3)
C(5B)-C(4B)-O(1B)-C(1B)	156.4(2)
C(3B)-C(4B)-O(1B)-C(1B)	35.2(2)
O(1B)-C(1B)-O(2B)-C(7B)	-119.4(2)
C(2B)-C(1B)-O(2B)-C(7B)	-3.5(3)
O(3B)-C(7B)-O(2B)-C(1B)	20.8(3)
C(8B)-C(7B)-O(2B)-C(1B)	-97.9(3)
C(6B)-C(7B)-O(2B)-C(1B)	137.0(2)
C(3B)-C(2B)-O(3B)-C(7B)	137.6(2)
C(1B)-C(2B)-O(3B)-C(7B)	28.4(3)
O(2B)-C(7B)-O(3B)-C(2B)	-31.0(3)
C(8B)-C(7B)-O(3B)-C(2B)	87.5(3)
C(6B)-C(7B)-O(3B)-C(2B)	-147.7(2)
O(5A)-C(9A)-O(4B)-C(3B)	0.6(4)
C(10A)-C(9A)-O(4B)-C(3B)	179.8(2)
C(4B)-C(3B)-O(4B)-C(9A)	124.2(2)
C(2B)-C(3B)-O(4B)-C(9A)	-125.0(2)

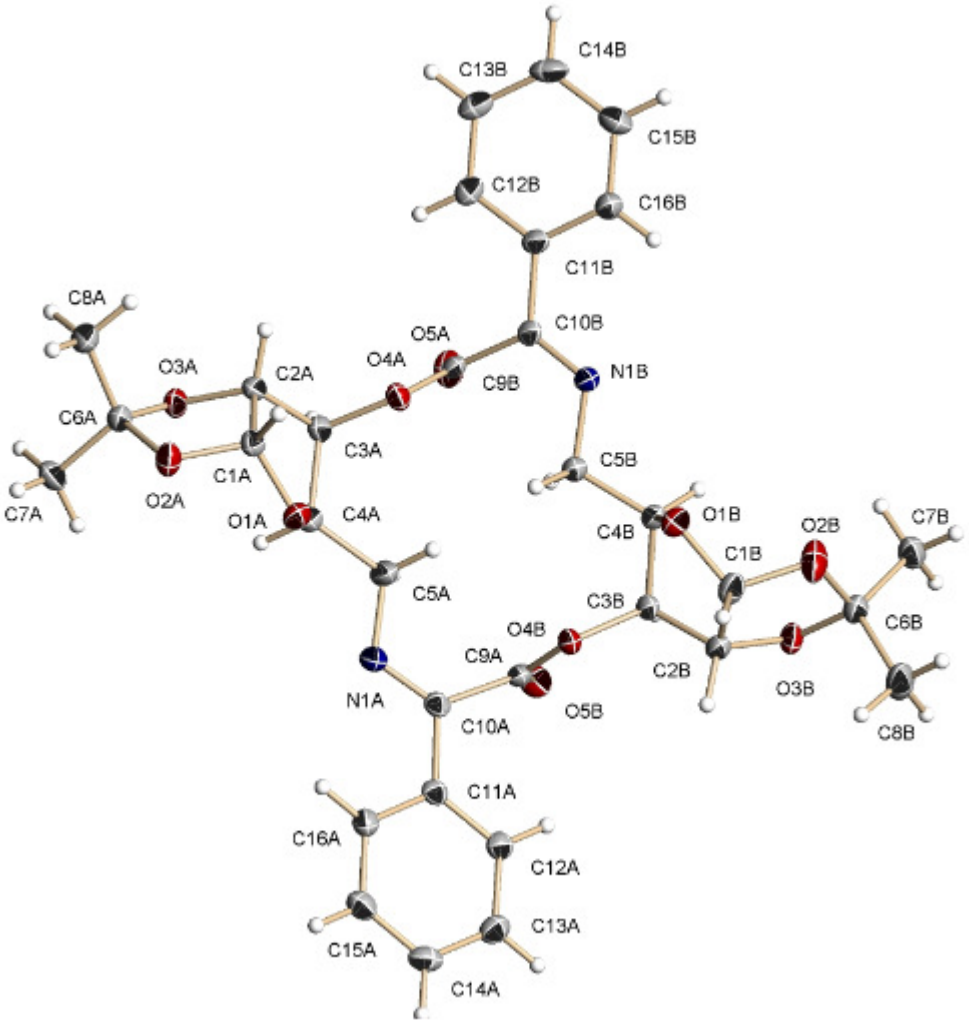

Figure 76: Alternate x-ray crystal structure of macrocycle **9**.

Table 1. Crystal data and structure refinement for 08mz038_0m:

Identification code: 08mz038_0m
Empirical formula: C32 H34 N2 O10
Formula weight: 606.61
Temperature: 100(2) K
Wavelength: 0.71073 Å
Crystal system: Monoclinic
Space group: $P2_1$
Unit cell dimensions:
a = 12.4039(12) Å, α = 90°
b = 9.5046(9) Å, β = 95.238(2)°
c = 12.4401(11) Å, γ = 90°
Volume, *Z*: 1460.5(2) $Å^3$, 2
Density (calculated): 1.379 Mg/m^3
Absorption coefficient: 0.103 mm^{-1}
F(000): 640
Crystal size: 0.50 × 0.45 × 0.40 mm
Crystal shape, colour: block, colourless
θ range for data collection: 1.65 to 28.28°
Limiting indices: $-16 \le h \le 16$, $-12 \le k \le 12$, $-16 \le l \le 11$
Reflections collected: 9799
Independent reflections: 3824 (*R*(int) = 0.0199)
Completeness to θ = 28.28°: 99.3 %
Absorption correction: multi-scan
Max. and min. transmission: 0.960 and 0.776
Refinement method: Full-matrix least-squares on F^2
Data / restraints / parameters: 3824 / 1 / 401
Goodness-of-fit on F^2: 1.061
Final *R* indices [$I>2\sigma(I)$]: R1 = 0.0322, wR2 = 0.0789
R indices (all data): R1 = 0.0352, wR2 = 0.0810
Largest diff. peak and hole: 0.253 and −0.161 e × $Å^{-3}$

Refinement of F^2 against ALL reflections. The weighted R-factor wR and goodness of fit are based on F^2, conventional R-factors R are based on *F*, with *F* set to zero for negative F^2. The threshold expression of $F^2 > 2\sigma(F^2)$ is used only for calculating R-factors

Treatment of hydrogen atoms:
All hydrogen atoms were placed in calculated positions and were refined with an isotropic displacement parameter 1.5 (methyl) or 1.2 times (all others) that of the adjacent carbon atom.

Table 2. Atomic coordinates [× 10^4] and equivalent isotropic displacement parameters [Å^2 × 10^3] for 08mz038_0m. U(eq) is defined as one third of the trace of the orthogonalized U_{ij} tensor.

	x	y	z	U(eq)
C(1A)	2922(1)	2257(2)	539(2)	22(1)
C(2A)	2596(1)	3685(2)	23(2)	22(1)
C(3A)	1825(1)	4288(2)	780(1)	22(1)
C(4A)	2296(1)	3680(2)	1861(2)	23(1)
C(5A)	1519(2)	3651(3)	2725(2)	33(1)
C(6A)	4434(1)	3481(2)	77(2)	23(1)
C(7A)	5422(2)	4018(3)	745(2)	30(1)
C(8A)	4651(2)	3199(3)	-1085(2)	37(1)
C(9A)	152(1)	3128(2)	4294(1)	20(1)
C(10A)	1345(1)	2687(2)	4431(1)	20(1)
C(11A)	1715(1)	2031(2)	5482(1)	20(1)
C(12A)	1053(1)	2038(2)	6327(2)	22(1)
C(13A)	1433(2)	1506(2)	7335(2)	26(1)
C(14A)	2465(2)	942(2)	7487(2)	28(1)
C(15A)	3118(2)	900(2)	6638(2)	28(1)
C(16A)	2752(1)	1451(2)	5639(2)	24(1)
C(1B)	-2551(2)	242(2)	3258(2)	26(1)
C(2B)	-2304(1)	1364(2)	4147(2)	24(1)
C(3B)	-1635(1)	2463(2)	3614(2)	20(1)
C(4B)	-1971(1)	2220(2)	2416(1)	20(1)
C(5B)	-1157(1)	2726(2)	1677(1)	21(1)
C(6B)	-4148(1)	990(2)	3911(2)	24(1)
C(7B)	-5121(2)	1768(3)	3409(2)	32(1)
C(8B)	-4398(2)	21(3)	4827(2)	44(1)
C(9B)	-98(1)	4410(2)	298(1)	19(1)
C(10B)	-1088(1)	3527(2)	-92(1)	19(1)
C(11B)	-1463(1)	3616(2)	-1258(1)	21(1)
C(12B)	-832(2)	4269(2)	-1986(2)	24(1)
C(13B)	-1194(2)	4341(2)	-3073(2)	29(1)
C(14B)	-2185(2)	3763(3)	-3438(2)	32(1)
C(15B)	-2813(2)	3108(3)	-2723(2)	35(1)
C(16B)	-2456(2)	3038(3)	-1633(2)	28(1)
N(1A)	1990(1)	2988(2)	3730(1)	26(1)
N(1B)	-1603(1)	2797(2)	545(1)	20(1)
O(1A)	2589(1)	2271(2)	1598(1)	25(1)
O(2A)	4060(1)	2211(2)	551(1)	27(1)
O(3A)	3575(1)	4468(2)	140(1)	24(1)
O(4A)	790(1)	3605(1)	451(1)	21(1)
O(5A)	-145(1)	5646(2)	475(1)	30(1)
O(1B)	-2091(1)	713(2)	2329(1)	24(1)
O(2B)	-3692(1)	207(2)	3089(1)	37(1)

O(3B)	−3328(1)	1979(2)	4282(1)	26(1)
O(4B)	−490(1)	2110(2)	3833(1)	20(1)
O(5B)	−134(1)	4264(2)	4559(1)	29(1)

All esds (except the esd in the dihedral angle between two l.s. planes) are estimated using the full covariance matrix. The cell esds are taken into account individually in the estimation of esds in distances, angles and torsion angles; correlations between esds in cell parameters are only used when they are defined by crystal symmetry. An approximate (isotropic) treatment of cell esds is used for estimating esds involving l.s. planes.

Table 3. Bond lengths [Å] and angles [deg] for 08mz038_0m.

C(1A)-O(2A)	1.412(2)	C(15A)-H(15A)	0.9300
C(1A)-O(1A)	1.416(2)	C(16A)-H(16A)	0.9300
C(1A)-C(2A)	1.540(3)	C(1B)-O(1B)	1.407(2)
C(1A)-H(1A)	0.9800	C(1B)-O(2B)	1.411(2)
C(2A)-O(3A)	1.420(2)	C(1B)-C(2B)	1.546(3)
C(2A)-C(3A)	1.514(3)	C(1B)-H(1B)	0.9800
C(2A)-H(2A)	0.9800	C(2B)-O(3B)	1.422(2)
C(3A)-O(4A)	1.463(2)	C(2B)-C(3B)	1.524(3)
C(3A)-C(4A)	1.530(2)	C(2B)-H(2B)	0.9800
C(3A)-H(3A)	0.9800	C(3B)-O(4B)	1.4608(19)
C(4A)-O(1A)	1.434(3)	C(3B)-C(4B)	1.528(2)
C(4A)-C(5A)	1.508(3)	C(3B)-H(3B)	0.9800
C(4A)-H(4A)	0.9800	C(4B)-O(1B)	1.443(2)
C(5A)-N(1A)	1.472(2)	C(4B)-C(5B)	1.505(2)
C(5A)-H(5A1)	0.9700	C(4B)-H(4B)	0.9800
C(5A)-H(5A2)	0.9700	C(5B)-N(1B)	1.466(2)
C(6A)-O(3A)	1.427(2)	C(5B)-H(5B1)	0.9700
C(6A)-O(2A)	1.438(2)	C(5B)-H(5B2)	0.9700
C(6A)-C(7A)	1.505(3)	C(6B)-O(2B)	1.423(2)
C(6A)-C(8A)	1.518(3)	C(6B)-O(3B)	1.430(2)
C(7A)-H(7A1)	0.9600	C(6B)-C(7B)	1.502(3)
C(7A)-H(7A2)	0.9600	C(6B)-C(8B)	1.519(3)
C(7A)-H(7A3)	0.9600	C(7B)-H(7B1)	0.9600
C(8A)-H(8A1)	0.9600	C(7B)-H(7B2)	0.9600
C(8A)-H(8A2)	0.9600	C(7B)-H(7B3)	0.9600
C(8A)-H(8A3)	0.9600	C(8B)-H(8B1)	0.9600
C(9A)-O(5B)	1.192(2)	C(8B)-H(8B2)	0.9600
C(9A)-O(4B)	1.347(2)	C(8B)-H(8B3)	0.9600
C(9A)-C(10A)	1.532(2)	C(9B)-O(5A)	1.198(2)
C(10A)-N(1A)	1.269(2)	C(9B)-O(4A)	1.341(2)
C(10A)-C(11A)	1.483(2)	C(9B)-C(10B)	1.529(2)
C(11A)-C(12A)	1.392(3)	C(10B)-N(1B)	1.269(2)
C(11A)-C(16A)	1.397(2)	C(10B)-C(11B)	1.484(2)
C(12A)-C(13A)	1.393(3)	C(11B)-C(16B)	1.390(3)
C(12A)-H(12A)	0.9300	C(11B)-C(12B)	1.396(3)
C(13A)-C(14A)	1.386(3)	C(12B)-C(13B)	1.387(3)
C(13A)-H(13A)	0.9300	C(12B)-H(12B)	0.9300
C(14A)-C(15A)	1.389(3)	C(13B)-C(14B)	1.385(3)
C(14A)-H(14A)	0.9300	C(13B)-H(13B)	0.9300
C(15A)-C(16A)	1.387(3)	C(14B)-C(15B)	1.383(3)

C(14B)-H(14B)	0.9300
C(15B)-C(16B)	1.389(3)
C(15B)-H(15B)	0.9300
C(16B)-H(16B)	0.9300
O(2A)-C(1A)-O(1A)	111.57(14)
O(2A)-C(1A)-C(2A)	104.81(14)
O(1A)-C(1A)-C(2A)	106.97(16)
O(2A)-C(1A)-H(1A)	111.1
O(1A)-C(1A)-H(1A)	111.1
C(2A)-C(1A)-H(1A)	111.1
O(3A)-C(2A)-C(3A)	108.72(15)
O(3A)-C(2A)-C(1A)	103.28(13)
C(3A)-C(2A)-C(1A)	103.34(15)
O(3A)-C(2A)-H(2A)	113.5
C(3A)-C(2A)-H(2A)	113.5
C(1A)-C(2A)-H(2A)	113.5
O(4A)-C(3A)-C(2A)	104.26(15)
O(4A)-C(3A)-C(4A)	109.47(15)
C(2A)-C(3A)-C(4A)	101.06(14)
O(4A)-C(3A)-H(3A)	113.7
C(2A)-C(3A)-H(3A)	113.7
C(4A)-C(3A)-H(3A)	113.7
O(1A)-C(4A)-C(5A)	109.74(18)
O(1A)-C(4A)-C(3A)	103.68(15)
C(5A)-C(4A)-C(3A)	114.60(15)
O(1A)-C(4A)-H(4A)	109.5
C(5A)-C(4A)-H(4A)	109.5
C(3A)-C(4A)-H(4A)	109.5
N(1A)-C(5A)-C(4A)	112.51(16)
N(1A)-C(5A)-H(5A1)	109.1
C(4A)-C(5A)-H(5A1)	109.1
N(1A)-C(5A)-H(5A2)	109.1
C(4A)-C(5A)-H(5A2)	109.1
H(5A1)-C(5A)-H(5A2)	107.8
O(3A)-C(6A)-O(2A)	105.01(14)
O(3A)-C(6A)-C(7A)	108.71(17)
O(2A)-C(6A)-C(7A)	109.59(16)
O(3A)-C(6A)-C(8A)	111.47(16)
O(2A)-C(6A)-C(8A)	109.46(18)
C(7A)-C(6A)-C(8A)	112.34(17)
C(6A)-C(7A)-H(7A1)	109.5
C(6A)-C(7A)-H(7A2)	109.5
H(7A1)-C(7A)-H(7A2)	109.5
C(6A)-C(7A)-H(7A3)	109.5
H(7A1)-C(7A)-H(7A3)	109.5
H(7A2)-C(7A)-H(7A3)	109.5
C(6A)-C(8A)-H(8A1)	109.5
C(6A)-C(8A)-H(8A2)	109.5
H(8A1)-C(8A)-H(8A2)	109.5
C(6A)-C(8A)-H(8A3)	109.5
H(8A1)-C(8A)-H(8A3)	109.5
H(8A2)-C(8A)-H(8A3)	109.5
O(5B)-C(9A)-O(4B)	126.13(17)
O(5B)-C(9A)-C(10A)	121.68(17)
O(4B)-C(9A)-C(10A)	112.17(16)
N(1A)-C(10A)-C(11A)	122.42(16)
N(1A)-C(10A)-C(9A)	121.76(17)
C(11A)-C(10A)-C(9A)	115.49(15)
C(12A)-C(11A)-C(16A)	119.64(17)
C(12A)-C(11A)-C(10A)	120.53(16)
C(16A)-C(11A)-C(10A)	119.78(16)
C(11A)-C(12A)-C(13A)	120.32(17)
C(11A)-C(12A)-H(12A)	119.8
C(13A)-C(12A)-H(12A)	119.8
C(14A)-C(13A)-C(12A)	119.67(18)
C(14A)-C(13A)-H(13A)	120.2
C(12A)-C(13A)-H(13A)	120.2
C(13A)-C(14A)-C(15A)	120.22(18)
C(13A)-C(14A)-H(14A)	119.9
C(15A)-C(14A)-H(14A)	119.9
C(16A)-C(15A)-C(14A)	120.34(18)
C(16A)-C(15A)-H(15A)	119.8
C(14A)-C(15A)-H(15A)	119.8
C(15A)-C(16A)-C(11A)	119.77(17)
C(15A)-C(16A)-H(16A)	120.1
C(11A)-C(16A)-H(16A)	120.1
O(1B)-C(1B)-O(2B)	111.23(16)
O(1B)-C(1B)-C(2B)	107.42(16)
O(2B)-C(1B)-C(2B)	104.66(15)
O(1B)-C(1B)-H(1B)	111.1
O(2B)-C(1B)-H(1B)	111.1
C(2B)-C(1B)-H(1B)	111.1
O(3B)-C(2B)-C(3B)	107.30(16)
O(3B)-C(2B)-C(1B)	104.29(14)
C(3B)-C(2B)-C(1B)	104.00(15)
O(3B)-C(2B)-H(2B)	113.5
C(3B)-C(2B)-H(2B)	113.5
C(1B)-C(2B)-H(2B)	113.5
O(4B)-C(3B)-C(2B)	108.65(14)
O(4B)-C(3B)-C(4B)	108.76(14)
C(2B)-C(3B)-C(4B)	102.07(15)
O(4B)-C(3B)-H(3B)	112.3
C(2B)-C(3B)-H(3B)	112.3
C(4B)-C(3B)-H(3B)	112.3
O(1B)-C(4B)-C(5B)	109.99(15)
O(1B)-C(4B)-C(3B)	103.89(15)
C(5B)-C(4B)-C(3B)	114.10(15)
O(1B)-C(4B)-H(4B)	109.6
C(5B)-C(4B)-H(4B)	109.6
C(3B)-C(4B)-H(4B)	109.6
N(1B)-C(5B)-C(4B)	112.71(14)
N(1B)-C(5B)-H(5B1)	109.0
C(4B)-C(5B)-H(5B1)	109.0
N(1B)-C(5B)-H(5B2)	109.0
C(4B)-C(5B)-H(5B2)	109.0
H(5B1)-C(5B)-H(5B2)	107.8
O(2B)-C(6B)-O(3B)	104.87(14)
O(2B)-C(6B)-C(7B)	108.41(17)
O(3B)-C(6B)-C(7B)	109.34(17)
O(2B)-C(6B)-C(8B)	110.1(2)
O(3B)-C(6B)-C(8B)	110.15(17)
C(7B)-C(6B)-C(8B)	113.56(16)

C(6B)-C(7B)-H(7B1) 109.5
C(6B)-C(7B)-H(7B2) 109.5
H(7B1)-C(7B)-H(7B2)109.5
C(6B)-C(7B)-H(7B3) 109.5
H(7B1)-C(7B)-H(7B3)109.5
H(7B2)-C(7B)-H(7B3)109.5
C(6B)-C(8B)-H(8B1) 109.5
C(6B)-C(8B)-H(8B2) 109.5
H(8B1)-C(8B)-H(8B2)109.5
C(6B)-C(8B)-H(8B3) 109.5
H(8B1)-C(8B)-H(8B3)109.5
H(8B2)-C(8B)-H(8B3)109.5
O(5A)-C(9B)-O(4A) 125.90(17)
O(5A)-C(9B)-C(10B) 123.07(16)
O(4A)-C(9B)-C(10B) 110.97(15)
N(1B)-C(10B)-C(11B)120.73(16)
N(1B)-C(10B)-C(9B) 122.46(16)
C(11B)-C(10B)-C(9B)116.74(15)
C(16B)-C(11B)-C(12B)119.30(17)
C(16B)-C(11B)-C(10B)119.67(17)
C(12B)-C(11B)-C(10B)121.03(16)
C(13B)-C(12B)-C(11B)120.29(18)
C(13B)-C(12B)-H(12B) 119.9
C(11B)-C(12B)-H(12B) 119.9
C(14B)-C(13B)-C(12B)119.93(19)
C(14B)-C(13B)-H(13B)120.0
C(12B)-C(13B)-H(13B)120.0
C(15B)-C(14B)-C(13B)120.18(18)
C(15B)-C(14B)-H(14B)119.9
C(13B)-C(14B)-H(14B)119.9
C(14B)-C(15B)-C(16B)120.1(2)
C(14B)-C(15B)-H(15B)120.0
C(16B)-C(15B)-H(15B)120.0
C(15B)-C(16B)-C(11B)120.25(19)
C(15B)-C(16B)-H(16B)119.9
C(11B)-C(16B)-H(16B)119.9
C(10A)-N(1A)-C(5A) 116.91(16)
C(10B)-N(1B)-C(5B) 117.27(15)
C(1A)-O(1A)-C(4A) 108.83(14)
C(1A)-O(2A)-C(6A) 109.25(14)
C(2A)-O(3A)-C(6A) 106.61(14)
C(9B)-O(4A)-C(3A) 118.42(15)
C(1B)-O(1B)-C(4B) 107.50(15)
C(1B)-O(2B)-C(6B) 109.90(15)
C(2B)-O(3B)-C(6B) 107.99(15)
C(9A)-O(4B)-C(3B) 116.12(14)

Table 4. Anisotropic displacement parameters [$Å^2 \times 10^3$] for 08mz038_0m. The anisotropic displacement factor exponent takes the form: $-2\pi^2$ [(h a*)^2 U11 + ... + 2 h k a* b* U12]

	U11	U22	U33	U23	U13	U12
C(1A)	19(1)	25(1)	20(1)	-1(1)	2(1)	-4(1)
C(2A)	18(1)	30(1)	17(1)	3(1)	-1(1)	-4(1)
C(3A)	17(1)	26(1)	21(1)	2(1)	1(1)	-3(1)
C(4A)	18(1)	33(1)	17(1)	1(1)	2(1)	-2(1)
C(5A)	22(1)	60(2)	18(1)	6(1)	4(1)	4(1)
C(6A)	18(1)	31(1)	21(1)	5(1)	2(1)	-1(1)
C(7A)	21(1)	40(1)	29(1)	7(1)	-5(1)	-6(1)
C(8A)	24(1)	63(2)	23(1)	-1(1)	5(1)	-3(1)
C(9A)	20(1)	26(1)	14(1)	2(1)	3(1)	0(1)
C(10A)	19(1)	23(1)	17(1)	-5(1)	0(1)	-1(1)
C(11A)	20(1)	20(1)	19(1)	-2(1)	-1(1)	-4(1)
C(12A)	21(1)	22(1)	22(1)	0(1)	1(1)	-3(1)
C(13A)	30(1)	26(1)	22(1)	1(1)	5(1)	-4(1)
C(14A)	33(1)	28(1)	21(1)	3(1)	-4(1)	-3(1)
C(15A)	23(1)	32(1)	27(1)	4(1)	-3(1)	1(1)
C(16A)	20(1)	29(1)	22(1)	-1(1)	2(1)	-1(1)
C(1B)	23(1)	25(1)	30(1)	8(1)	8(1)	2(1)
C(2B)	19(1)	35(1)	19(1)	7(1)	3(1)	2(1)
C(3B)	15(1)	27(1)	19(1)	3(1)	2(1)	4(1)
C(4B)	18(1)	23(1)	18(1)	3(1)	3(1)	2(1)
C(5B)	18(1)	27(1)	18(1)	3(1)	2(1)	0(1)
C(6B)	19(1)	29(1)	24(1)	4(1)	5(1)	-1(1)
C(7B)	21(1)	40(1)	34(1)	11(1)	1(1)	1(1)
C(8B)	26(1)	59(2)	47(1)	30(1)	5(1)	-3(1)
C(9B)	19(1)	25(1)	15(1)	4(1)	4(1)	1(1)
C(10B)	17(1)	23(1)	18(1)	2(1)	4(1)	5(1)
C(11B)	21(1)	25(1)	17(1)	3(1)	3(1)	5(1)
C(12B)	26(1)	24(1)	23(1)	0(1)	7(1)	1(1)
C(13B)	38(1)	28(1)	21(1)	3(1)	9(1)	5(1)
C(14B)	41(1)	38(1)	16(1)	3(1)	-1(1)	9(1)
C(15B)	29(1)	50(1)	24(1)	2(1)	-5(1)	1(1)
C(16B)	22(1)	40(1)	22(1)	7(1)	2(1)	0(1)
N(1A)	20(1)	40(1)	18(1)	-1(1)	0(1)	1(1)
N(1B)	18(1)	26(1)	17(1)	2(1)	2(1)	2(1)
O(1A)	24(1)	30(1)	21(1)	6(1)	4(1)	0(1)
O(2A)	19(1)	27(1)	35(1)	5(1)	7(1)	1(1)
O(3A)	17(1)	28(1)	26(1)	7(1)	3(1)	-3(1)
O(4A)	16(1)	23(1)	23(1)	2(1)	0(1)	0(1)
O(5A)	27(1)	25(1)	38(1)	-3(1)	7(1)	2(1)
O(1B)	26(1)	24(1)	24(1)	2(1)	5(1)	-1(1)
O(2B)	25(1)	42(1)	46(1)	-16(1)	12(1)	-9(1)
O(3B)	17(1)	37(1)	25(1)	-4(1)	6(1)	-3(1)
O(4B)	15(1)	25(1)	20(1)	1(1)	1(1)	1(1)
O(5B)	28(1)	28(1)	30(1)	-6(1)	1(1)	4(1)

Table 5. Hydrogen coordinates ($\times 10^4$) and isotropic displacement parameters ($Å^2 \times 10^3$) for 08mz038_0m.

	x	y	z	U(eq)
H(1A)	2584	1477	117	26
H(2A)	2280	3610	-726	26
H(3A)	1789	5317	770	26
H(4A)	2947	4207	2121	27
H(5A1)	1306	4607	2880	40
H(5A2)	873	3139	2459	40
H(7A1)	5665	4872	433	45
H(7A2)	5986	3325	762	45
H(7A3)	5244	4201	1467	45
H(8A1)	3991	2916	-1490	55
H(8A2)	5178	2463	-1104	55
H(8A3)	4920	4039	-1394	55
H(12A)	355	2398	6219	26
H(13A)	995	1530	7903	31
H(14A)	2722	590	8160	33
H(15A)	3805	501	6741	33
H(16A)	3196	1434	5075	28
H(1B)	-2260	-678	3491	31
H(2B)	-1941	981	4816	29
H(3B)	-1795	3422	3842	24
H(4B)	-2671	2672	2218	23
H(5B1)	-904	3653	1908	25
H(5B2)	-539	2096	1735	25
H(7B1)	-4921	2306	2805	48
H(7B2)	-5386	2390	3933	48
H(7B3)	-5676	1107	3169	48
H(8B1)	-4926	-664	4563	66
H(8B2)	-4679	564	5390	66
H(8B3)	-3748	-448	5109	66
H(12B)	-166	4657	-1742	29
H(13B)	-772	4778	-3556	34
H(14B)	-2429	3815	-4167	38
H(15B)	-3476	2713	-2972	42
H(16B)	-2882	2603	-1153	34

Table 6. Torsion angles [deg] for 07mz075m.

O(2A)-C(1A)-C(2A)-O(3A)	-19.17(18)
O(1A)-C(1A)-C(2A)-O(3A)	99.41(15)
O(2A)-C(1A)-C(2A)-C(3A)	-132.42(15)
O(1A)-C(1A)-C(2A)-C(3A)	-13.85(17)
O(3A)-C(2A)-C(3A)-O(4A)	169.34(14)
C(1A)-C(2A)-C(3A)-O(4A)	-81.42(15)
O(3A)-C(2A)-C(3A)-C(4A)	-77.07(17)

C(1A)-C(2A)-C(3A)-C(4A)	32.17(17)
O(4A)-C(3A)-C(4A)-O(1A)	69.40(17)
C(2A)-C(3A)-C(4A)-O(1A)	-40.20(17)
O(4A)-C(3A)-C(4A)-C(5A)	-50.2(2)
C(2A)-C(3A)-C(4A)-C(5A)	-159.78(18)
O(1A)-C(4A)-C(5A)-N(1A)	60.8(2)
C(3A)-C(4A)-C(5A)-N(1A)	176.90(18)
O(5B)-C(9A)-C(10A)-N(1A)	-84.5(2)
O(4B)-C(9A)-C(10A)-N(1A)	94.1(2)
O(5B)-C(9A)-C(10A)-C(11A)	89.1(2)
O(4B)-C(9A)-C(10A)-C(11A)	-92.33(19)
N(1A)-C(10A)-C(11A)-C(12A)	163.80(19)
C(9A)-C(10A)-C(11A)-C(12A)	-9.7(3)
N(1A)-C(10A)-C(11A)-C(16A)	-13.7(3)
C(9A)-C(10A)-C(11A)-C(16A)	172.81(17)
C(16A)-C(11A)-C(12A)-C(13A)	1.9(3)
C(10A)-C(11A)-C(12A)-C(13A)	-175.59(18)
C(11A)-C(12A)-C(13A)-C(14A)	-1.4(3)
C(12A)-C(13A)-C(14A)-C(15A)	-0.3(3)
C(13A)-C(14A)-C(15A)-C(16A)	1.4(3)
C(14A)-C(15A)-C(16A)-C(11A)	-1.0(3)
C(12A)-C(11A)-C(16A)-C(15A)	-0.7(3)
C(10A)-C(11A)-C(16A)-C(15A)	176.79(18)
O(1B)-C(1B)-C(2B)-O(3B)	110.68(16)
O(2B)-C(1B)-C(2B)-O(3B)	-7.64(19)
O(1B)-C(1B)-C(2B)-C(3B)	-1.65(18)
O(2B)-C(1B)-C(2B)-C(3B)	-119.97(16)
O(3B)-C(2B)-C(3B)-O(4B)	158.41(14)
C(1B)-C(2B)-C(3B)-O(4B)	-91.47(16)
O(3B)-C(2B)-C(3B)-C(4B)	-86.80(17)
C(1B)-C(2B)-C(3B)-C(4B)	23.33(17)
O(4B)-C(3B)-C(4B)-O(1B)	77.40(17)
C(2B)-C(3B)-C(4B)-O(1B)	-37.31(17)
O(4B)-C(3B)-C(4B)-C(5B)	-42.4(2)
C(2B)-C(3B)-C(4B)-C(5B)	-157.08(15)
O(1B)-C(4B)-C(5B)-N(1B)	77.69(19)
C(3B)-C(4B)-C(5B)-N(1B)	-166.04(16)
O(5A)-C(9B)-C(10B)-N(1B)	-97.5(2)
O(4A)-C(9B)-C(10B)-N(1B)	79.9(2)
O(5A)-C(9B)-C(10B)-C(11B)	79.4(2)
O(4A)-C(9B)-C(10B)-C(11B)	-103.20(18)
N(1B)-C(10B)-C(11B)-C(16B)	7.9(3)
C(9B)-C(10B)-C(11B)-C(16B)	-169.10(18)
N(1B)-C(10B)-C(11B)-C(12B)	-171.95(18)
C(9B)-C(10B)-C(11B)-C(12B)	11.1(3)
C(16B)-C(11B)-C(12B)-C(13B)	0.1(3)
C(10B)-C(11B)-C(12B)-C(13B)	179.91(18)
C(11B)-C(12B)-C(13B)-C(14B)	0.0(3)
C(12B)-C(13B)-C(14B)-C(15B)	-0.3(3)
C(13B)-C(14B)-C(15B)-C(16B)	0.5(4)
C(14B)-C(15B)-C(16B)-C(11B)	-0.5(4)
C(12B)-C(11B)-C(16B)-C(15B)	0.2(3)
C(10B)-C(11B)-C(16B)-C(15B)	-179.7(2)
C(11A)-C(10A)-N(1A)-C(5A)	-179.34(19)
C(9A)-C(10A)-N(1A)-C(5A)	-6.2(3)
C(4A)-C(5A)-N(1A)-C(10A)	-167.70(19)
C(11B)-C(10B)-N(1B)-C(5B)	177.95(16)

C(9B)-C(10B)-N(1B)-C(5B)	-5.2(3)
C(4B)-C(5B)-N(1B)-C(10B)	162.83(17)
O(2A)-C(1A)-O(1A)-C(4A)	101.97(17)
C(2A)-C(1A)-O(1A)-C(4A)	-12.12(17)
C(5A)-C(4A)-O(1A)-C(1A)	155.96(14)
C(3A)-C(4A)-O(1A)-C(1A)	33.11(17)
O(1A)-C(1A)-O(2A)-C(6A)	-115.94(17)
C(2A)-C(1A)-O(2A)-C(6A)	-0.52(19)
O(3A)-C(6A)-O(2A)-C(1A)	20.07(19)
C(7A)-C(6A)-O(2A)-C(1A)	136.68(17)
C(8A)-C(6A)-O(2A)-C(1A)	-99.70(17)
C(3A)-C(2A)-O(3A)-C(6A)	141.26(15)
C(1A)-C(2A)-O(3A)-C(6A)	31.97(17)
O(2A)-C(6A)-O(3A)-C(2A)	-32.98(18)
C(7A)-C(6A)-O(3A)-C(2A)	-150.19(16)
C(8A)-C(6A)-O(3A)-C(2A)	85.45(19)
O(5A)-C(9B)-O(4A)-C(3A)	-5.4(3)
C(10B)-C(9B)-O(4A)-C(3A)	177.33(14)
C(2A)-C(3A)-O(4A)-C(9B)	-131.77(16)
C(4A)-C(3A)-O(4A)-C(9B)	120.79(17)
O(2B)-C(1B)-O(1B)-C(4B)	91.30(18)
C(2B)-C(1B)-O(1B)-C(4B)	-22.68(18)
C(5B)-C(4B)-O(1B)-C(1B)	160.56(14)
C(3B)-C(4B)-O(1B)-C(1B)	38.04(17)
O(1B)-C(1B)-O(2B)-C(6B)	-126.27(18)
C(2B)-C(1B)-O(2B)-C(6B)	-10.6(2)
O(3B)-C(6B)-O(2B)-C(1B)	24.8(2)
C(7B)-C(6B)-O(2B)-C(1B)	141.55(17)
C(8B)-C(6B)-O(2B)-C(1B)	-93.65(19)
C(3B)-C(2B)-O(3B)-C(6B)	132.94(16)
C(1B)-C(2B)-O(3B)-C(6B)	23.01(18)
O(2B)-C(6B)-O(3B)-C(2B)	-29.84(19)
C(7B)-C(6B)-O(3B)-C(2B)	-145.91(16)
C(8B)-C(6B)-O(3B)-C(2B)	88.64(19)
O(5B)-C(9A)-O(4B)-C(3B)	1.9(3)
C(10A)-C(9A)-O(4B)-C(3B)	-176.62(14)
C(2B)-C(3B)-O(4B)-C(9A)	-125.23(17)
C(4B)-C(3B)-O(4B)-C(9A)	124.42(16)

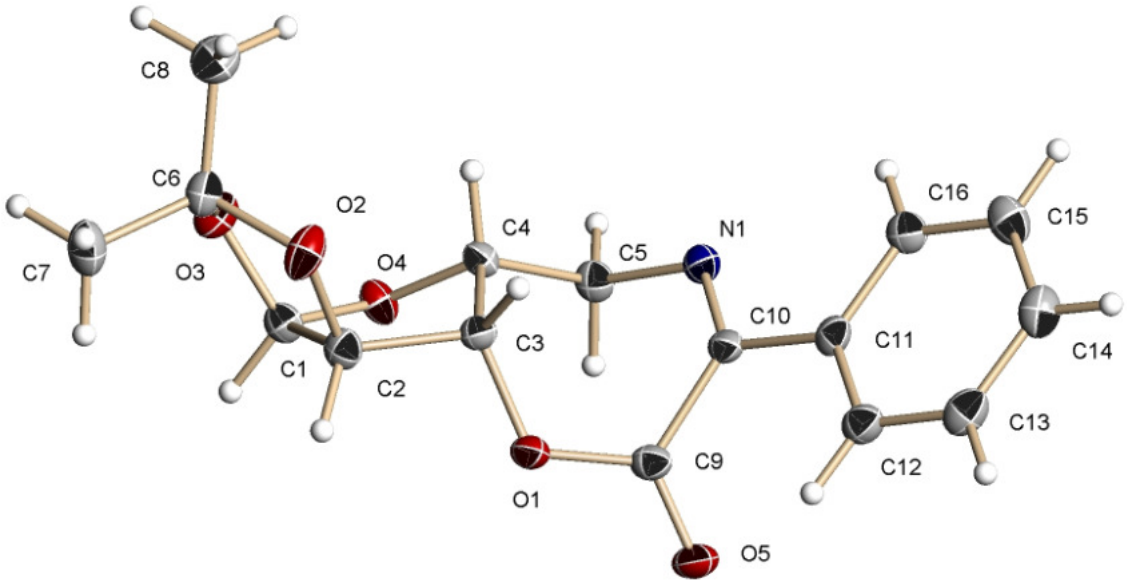

Figure 77: X-Ray crystal structure of oxazepine **10**.

Table 1. Crystal data and structure refinement for 08mz206_0m:

Identification code: 08mz206_0m
Empirical formula: C16 H17 O5
Formula weight: 303.31
Temperature: 100(2) K
Wavelength: 0.71073 Å
Crystal system: Monoclinic
Space group: P1
Unit cell dimensions:
a = 5.7348(5) Å, α = 90°
b = 11.3363(10) Å, β = 101.8530(10)°
c = 11.1977(10) Å, γ = 90°
Volume, *Z*: 712.46(11) Å^3, 2
Density (calculated): 1.414 Mg/m^3
Absorption coefficient: 0.106 mm^{-1}
F(000): 320
Crystal size: 0.55 × 0.40 × 0.24 mm
Crystal shape, colour: block, colourless
θ range for data collection: 1.86 to 28.28°
Limiting indices: $-7 \le h \le 7$, $-15 \le k \le 14$, $-11 \le l \le 14$
Reflections collected: 5290
Independent reflections: 1826 (*R*(int) = 0.0156)
Completeness to θ = 28.28°: 98.4 %
Absorption correction: multi-scan
Max. and min. transmission: 0.975 and 0.876
Refinement method: Full-matrix least-squares on F^2
Data / restraints / parameters: 1826 / 1 / 201
Goodness-of-fit on F^2: 1.098
Final *R* indices [$I>2\sigma(I)$]: R1 = 0.0270, wR2 = 0.0727
R indices (all data): R1 = 0.0278, wR2 = 0.0734
Largest diff. peak and hole: 0.228 and −0.184 e × Å^{-3}

Refinement of F^2 against ALL reflections. The weighted R-factor wR and goodness of fit are based on F^2, conventional R-factors R are based on *F*, with *F* set to zero for negative F^2. The threshold expression of $F^2 > 2\sigma(F^2)$ is used only for calculating R-factors

Treatment of hydrogen atoms:
All hydrogen atoms were placed in calculated positions and were refined with an isotropic displacement parameter 1.5 (methyl) or 1.2 times (all

others) that of the adjacent carbon or nitrogen atom.

Table 2. Atomic coordinates [× 10^4] and equivalent isotropic displacement parameters [$Å^2$ × 10^3] for 08mz206_0m. U(eq) is defined as one third of the trace of the orthogonalized U_{ij} tensor.

	x	y	z	U(eq)
C(1)	4299(3)	8887(1)	8479(1)	20(1)
C(2)	6864(3)	8381(1)	8841(2)	20(1)
C(3)	6882(3)	7328(1)	8001(1)	17(1)
C(4)	4717(3)	7567(1)	6979(1)	17(1)
C(5)	3589(3)	6448(2)	6370(1)	21(1)
C(6)	7060(3)	10341(2)	8293(2)	22(1)
C(7)	7543(3)	11071(2)	9453(2)	30(1)
C(8)	7748(4)	10951(2)	7222(2)	33(1)
C(9)	6631(3)	5214(2)	8148(1)	20(1)
C(10)	6885(3)	5182(1)	6817(1)	18(1)
C(11)	8777(3)	4427(1)	6500(1)	19(1)
C(12)	10390(3)	3814(2)	7380(2)	23(1)
C(13)	12107(3)	3094(2)	7045(2)	26(1)
C(14)	12239(3)	2986(2)	5829(2)	27(1)
C(15)	10672(3)	3623(2)	4943(2)	26(1)
C(16)	8948(3)	4334(2)	5273(2)	22(1)
N(1)	5420(2)	5724(1)	5988(1)	20(1)
O(1)	6546(2)	6276(1)	8678(1)	20(1)
O(2)	8356(2)	9257(1)	8491(1)	27(1)
O(3)	4610(2)	10009(1)	7974(1)	25(1)
O(4)	3031(2)	8126(1)	7578(1)	21(1)
O(5)	6416(2)	4334(1)	8712(1)	26(1)

All esds (except the esd in the dihedral angle between two l.s. planes)
are estimated using the full covariance matrix. The cell esds are taken into account individually in the estimation of esds in distances, angles and torsion angles; correlations between esds in cell parameters are only used when they are defined by crystal symmetry. An approximate (isotropic) treatment of cell esds is used for estimating esds involving l.s. planes.

Table 3. Bond lengths [Å] and angles [deg] for 08mz206_0m.

C(1)-O(4)	1.4101(18)	C(2)-H(2)	1.0000
C(1)-O(3)	1.419(2)	C(3)-O(1)	1.4479(19)
C(1)-C(2)	1.553(2)	C(3)-C(4)	1.530(2)
C(1)-H(1)	1.0000	C(3)-H(3)	1.0000
C(2)-O(2)	1.4175(19)	C(4)-O(4)	1.4326(18)
C(2)-C(3)	1.521(2)	C(4)-C(5)	1.521(2)

C(4)-H(4)	1.0000	N(1)-C(5)-H(5A)	109.8
C(5)-N(1)	1.464(2)	C(4)-C(5)-H(5A)	109.8
C(5)-H(5A)	0.9900	N(1)-C(5)-H(5B)	109.8
C(5)-H(5B)	0.9900	C(4)-C(5)-H(5B)	109.8
C(6)-O(3)	1.4274(18)	H(5A)-C(5)-H(5B)	108.2
C(6)-O(2)	1.430(2)	O(3)-C(6)-O(2)	105.41(13)
C(6)-C(8)	1.505(3)	O(3)-C(6)-C(8)	109.15(14)
C(6)-C(7)	1.517(2)	O(2)-C(6)-C(8)	107.81(14)
C(7)-H(7A)	0.9800	O(3)-C(6)-C(7)	110.76(14)
C(7)-H(7B)	0.9800	O(2)-C(6)-C(7)	109.77(14)
C(7)-H(7C)	0.9800	C(8)-C(6)-C(7)	113.58(16)
C(8)-H(8A)	0.9800	C(6)-C(7)-H(7A)	109.5
C(8)-H(8B)	0.9800	C(6)-C(7)-H(7B)	109.5
C(8)-H(8C)	0.9800	H(7A)-C(7)-H(7B)	109.5
C(9)-O(5)	1.200(2)	C(6)-C(7)-H(7C)	109.5
C(9)-O(1)	1.348(2)	H(7A)-C(7)-H(7C)	109.5
C(9)-C(10)	1.527(2)	H(7B)-C(7)-H(7C)	109.5
C(10)-N(1)	1.275(2)	C(6)-C(8)-H(8A)	109.5
C(10)-C(11)	1.481(2)	C(6)-C(8)-H(8B)	109.5
C(11)-C(12)	1.391(2)	H(8A)-C(8)-H(8B)	109.5
C(11)-C(16)	1.402(2)	C(6)-C(8)-H(8C)	109.5
C(12)-C(13)	1.389(2)	H(8A)-C(8)-H(8C)	109.5
C(12)-H(12)	0.9500	H(8B)-C(8)-H(8C)	109.5
C(13)-C(14)	1.384(3)	O(5)-C(9)-O(1)	119.52(14)
C(13)-H(13)	0.9500	O(5)-C(9)-C(10)	122.34(15)
C(14)-C(15)	1.395(3)	O(1)-C(9)-C(10)	118.07(13)
C(14)-H(14)	0.9500	N(1)-C(10)-C(11)	120.64(13)
C(15)-C(16)	1.383(2)	N(1)-C(10)-C(9)	121.24(14)
C(15)-H(15)	0.9500	C(11)-C(10)-C(9)	117.96(12)
C(16)-H(16)	0.9500	C(12)-C(11)-C(16)	119.10(14)
		C(12)-C(11)-C(10)	122.16(14)
O(4)-C(1)-O(3)	110.63(13)	C(16)-C(11)-C(10)	118.73(13)
O(4)-C(1)-C(2)	106.42(12)	C(13)-C(12)-C(11)	120.46(15)
O(3)-C(1)-C(2)	104.19(12)	C(13)-C(12)-H(12)	119.8
O(4)-C(1)-H(1)	111.7	C(11)-C(12)-H(12)	119.8
O(3)-C(1)-H(1)	111.7	C(14)-C(13)-C(12)	120.22(16)
C(2)-C(1)-H(1)	111.7	C(14)-C(13)-H(13)	119.9
O(2)-C(2)-C(3)	107.29(13)	C(12)-C(13)-H(13)	119.9
O(2)-C(2)-C(1)	105.21(13)	C(13)-C(14)-C(15)	119.75(16)
C(3)-C(2)-C(1)	104.74(12)	C(13)-C(14)-H(14)	120.1
O(2)-C(2)-H(2)	113.0	C(15)-C(14)-H(14)	120.1
C(3)-C(2)-H(2)	113.0	C(16)-C(15)-C(14)	120.21(16)
C(1)-C(2)-H(2)	113.0	C(16)-C(15)-H(15)	119.9
O(1)-C(3)-C(2)	107.69(12)	C(14)-C(15)-H(15)	119.9
O(1)-C(3)-C(4)	111.26(12)	C(15)-C(16)-C(11)	120.22(14)
C(2)-C(3)-C(4)	102.47(12)	C(15)-C(16)-H(16)	119.9
O(1)-C(3)-H(3)	111.7	C(11)-C(16)-H(16)	119.9
C(2)-C(3)-H(3)	111.7	C(10)-N(1)-C(5)	117.53(13)
C(4)-C(3)-H(3)	111.7	C(9)-O(1)-C(3)	118.96(11)
O(4)-C(4)-C(5)	108.27(12)	C(2)-O(2)-C(6)	108.74(12)
O(4)-C(4)-C(3)	104.51(11)	C(1)-O(3)-C(6)	109.57(12)
C(5)-C(4)-C(3)	113.14(13)	C(1)-O(4)-C(4)	107.86(11)
O(4)-C(4)-H(4)	110.2		
C(5)-C(4)-H(4)	110.2		
C(3)-C(4)-H(4)	110.2		
N(1)-C(5)-C(4)	109.54(12)		

Table 4. Anisotropic displacement parameters [$Å^2 \times 10^3$] for 08mz206_0m. The anisotropic displacement factor exponent takes the form: $-2\pi^2 [(h a^*)^2 U11 + ... + 2 h k a^* b^* U12]$

	U11	U22	U33	U23	U13	U12
C(1)	19(1)	23(1)	18(1)	-2(1)	2(1)	-1(1)
C(2)	20(1)	20(1)	19(1)	-2(1)	1(1)	-2(1)
C(3)	18(1)	17(1)	17(1)	1(1)	3(1)	-1(1)
C(4)	17(1)	20(1)	14(1)	-1(1)	3(1)	1(1)
C(5)	19(1)	23(1)	18(1)	-2(1)	0(1)	0(1)
C(6)	20(1)	19(1)	26(1)	-3(1)	3(1)	1(1)
C(7)	32(1)	27(1)	29(1)	-10(1)	-1(1)	4(1)
C(8)	36(1)	29(1)	35(1)	0(1)	9(1)	-6(1)
C(9)	21(1)	20(1)	17(1)	2(1)	2(1)	-3(1)
C(10)	22(1)	15(1)	16(1)	0(1)	3(1)	-4(1)
C(11)	20(1)	14(1)	21(1)	-2(1)	2(1)	-3(1)
C(12)	25(1)	20(1)	21(1)	1(1)	1(1)	-2(1)
C(13)	23(1)	22(1)	31(1)	2(1)	-1(1)	0(1)
C(14)	21(1)	25(1)	35(1)	-5(1)	4(1)	-1(1)
C(15)	24(1)	31(1)	24(1)	-8(1)	4(1)	-4(1)
C(16)	21(1)	23(1)	20(1)	-2(1)	1(1)	-3(1)
N(1)	22(1)	18(1)	18(1)	-2(1)	2(1)	-2(1)
O(1)	26(1)	19(1)	15(1)	1(1)	4(1)	-2(1)
O(2)	17(1)	18(1)	45(1)	-3(1)	6(1)	-1(1)
O(3)	20(1)	22(1)	31(1)	2(1)	1(1)	1(1)
O(4)	16(1)	27(1)	20(1)	-6(1)	4(1)	-1(1)
O(5)	35(1)	22(1)	20(1)	6(1)	5(1)	-4(1)

Table 5. Hydrogen coordinates ($\times 10^4$) and isotropic displacement parameters ($Å^2 \times 10^3$) for 08mz206_0m.

	x	y	z	U(eq)
H(1)	3522	8949	9199	24
H(2)	7325	8169	9725	24
H(3)	8388	7291	7683	21
H(4)	5159	8110	6358	21
H(5A)	2836	5998	6948	25
H(5B)	2338	6654	5651	25
H(7A)	6676	11819	9308	45
H(7B)	9255	11228	9696	45
H(7C)	7009	10636	10104	45
H(8A)	7170	10491	6479	49
H(8B)	9487	11020	7362	49
H(8C)	7035	11740	7128	49
H(12)	10316	3888	8217	27

H(13)	13195	2675	7651	31
H(14)	13392	2480	5599	32
H(15)	10790	3567	4111	31
H(16)	7877	4760	4665	26

Table 6. Torsion angles [deg] for 08mz206_0m.

O(4)-C(1)-C(2)-O(2)	116.16(14)
O(3)-C(1)-C(2)-O(2)	-0.81(16)
O(4)-C(1)-C(2)-C(3)	3.20(16)
O(3)-C(1)-C(2)-C(3)	-113.77(13)
O(2)-C(2)-C(3)-O(1)	149.62(12)
C(1)-C(2)-C(3)-O(1)	-98.90(14)
O(2)-C(2)-C(3)-C(4)	-92.97(13)
C(1)-C(2)-C(3)-C(4)	18.51(15)
O(1)-C(3)-C(4)-O(4)	80.62(14)
C(2)-C(3)-C(4)-O(4)	-34.22(15)
O(1)-C(3)-C(4)-C(5)	-36.95(16)
C(2)-C(3)-C(4)-C(5)	-151.79(13)
O(4)-C(4)-C(5)-N(1)	-167.39(12)
C(3)-C(4)-C(5)-N(1)	-52.04(16)
O(5)-C(9)-C(10)-N(1)	122.01(18)
O(1)-C(9)-C(10)-N(1)	-55.1(2)
O(5)-C(9)-C(10)-C(11)	-53.4(2)
O(1)-C(9)-C(10)-C(11)	129.48(14)
N(1)-C(10)-C(11)-C(12)	-179.34(15)
C(9)-C(10)-C(11)-C(12)	-3.9(2)
N(1)-C(10)-C(11)-C(16)	0.9(2)
C(9)-C(10)-C(11)-C(16)	176.34(14)
C(16)-C(11)-C(12)-C(13)	-1.7(2)
C(10)-C(11)-C(12)-C(13)	178.58(15)
C(11)-C(12)-C(13)-C(14)	0.4(3)
C(12)-C(13)-C(14)-C(15)	1.4(3)
C(13)-C(14)-C(15)-C(16)	-1.9(3)
C(14)-C(15)-C(16)-C(11)	0.6(2)
C(12)-C(11)-C(16)-C(15)	1.2(2)
C(10)-C(11)-C(16)-C(15)	-179.04(14)
C(11)-C(10)-N(1)-C(5)	179.63(13)
C(9)-C(10)-N(1)-C(5)	4.3(2)
C(4)-C(5)-N(1)-C(10)	73.65(17)
O(5)-C(9)-O(1)-C(3)	178.09(14)
C(10)-C(9)-O(1)-C(3)	-4.70(18)
C(2)-C(3)-O(1)-C(9)	-176.29(12)
C(4)-C(3)-O(1)-C(9)	72.16(16)
C(3)-C(2)-O(2)-C(6)	127.65(13)
C(1)-C(2)-O(2)-C(6)	16.50(16)
O(3)-C(6)-O(2)-C(2)	-26.08(17)
C(8)-C(6)-O(2)-C(2)	-142.56(14)
C(7)-C(6)-O(2)-C(2)	93.25(16)
O(4)-C(1)-O(3)-C(6)	-129.27(13)
C(2)-C(1)-O(3)-C(6)	-15.27(16)
O(2)-C(6)-O(3)-C(1)	25.73(16)
C(8)-C(6)-O(3)-C(1)	141.29(14)

C(7)-C(6)-O(3)-C(1)	-92.94(16)
O(3)-C(1)-O(4)-C(4)	86.79(14)
C(2)-C(1)-O(4)-C(4)	-25.80(16)
C(5)-C(4)-O(4)-C(1)	159.11(12)
C(3)-C(4)-O(4)-C(1)	38.25(15)